FROM BABY STEPS TO MATURE STRIDES

Maturation of drug metabolism and transport studied using innovative approaches

Bianca D. van Groen

From Baby Steps To Mature Strides

Maturation of drug metabolism and transport studied using innovative approaches

Bianca Dolinda van Groen

Printing of the thesis was financially supported by Health and Environmental Sciences Institute (HESI) and Netherlands Organization for Applied Scientific Research (TNO)

The studies described in this thesis were supported by:

- Netherlands Organization for Health Research and Development (ZonMw) – research grant 113202007
- Novartis – investigator grant
- Royal Netherlands Academy of Arts and Sciences - Ter Meulen Fund
- National Institute of Health grants R01GM117163, R01DK103729, N01HD90011 and N01DK70004
- Food and Drug Administration grant U01FD004979
- UC San Francisco-CTSI grant UL1TR000004
- U54 grant HD090258

Travel grants from: American Society of Clinical Pharmacology and Therapeutics, FIGON, Erasmus Trustfonds, Dutch Society of Pharmacology (NVT)

ISBN: 978-94-6361-396-5

Cover design: Erwin Timmerman
Layout and printing: Optima Grafische Communicatie, Rotterdam, the Netherlands

From Baby Steps To Mature Strides

Maturation of drug metabolism and transport studied using innovative approaches

Van babystapjes naar volgroeide sprongen

Maturatie van geneesmiddelmetabolisme en transport bestudeerd met behulp van innovatieve methodes

Proefschrift

ter verkrijging van de graad van doctor aan de

Erasmus Universiteit Rotterdam

op gezag van de

rector magnificus

Prof.dr. R.C.M.E. Engels

en volgens besluit van het College voor Promoties.

De openbare verdediging zal plaatsvinden op

woensdag 17 juni 2020 om 15:30 uur

door

Bianca Dolinda van Groen

geboren te Barendrecht

Erasmus University Rotterdam

PROMOTIECOMMISSIE

Promotoren:	Prof.dr. D. Tibboel
	Prof.dr. S.N. de Wildt
	Prof.dr. K. Allegaert
Overige leden:	Prof.dr. R.H.N. van Schaik
	Prof.dr. J. S. Leeder
	Prof.dr. C.A.J. Knibbe

CONTENTS

1 General introduction

The disposition of a drug is driven by various processes, such as drug metabolism, drug transport, glomerular filtration and body composition. We now know that these processes are subject to age-related changes, reflecting growth and maturation along the pediatric continuum.[1-3] It used to be common practice, however, to linearly adjust the dose for an adult to that of a child based on the child's bodyweight. This oversimplification of pediatric physiology commonly resulted in drug plasma concentrations either below or above adult reference concentrations. Then, a series of reports of children who experienced either severe drug toxicity or lack of effect raised awareness on this oversimplification. A classic example is the case of toxic exposure to chloramphenicol with fatal cardiovascular collapse (grey baby syndrome) in neonates as a result.[4] This was ascribed to underdevelopment of drug metabolism in neonates. But even recently there have been cases of serious adverse events in pediatric drug treatment partly explained by ontogeny. To illustrate this, in 2017 the US Food and Drug Administration (FDA) restricted the use of codeine and tramadol as the risk of apnea appears greater in children younger than 12 years.[5,6] Another example is the precipitation of ceftriaxone with calcium-containing products, which resulted in fatal cases in neonates only.[7]

Regulations on pediatric drug development

Well, why did we have limited information on drug therapy in pediatrics when the drug development processes carried out by pharmaceutical companies are extremely regulated? Wasn't there any pediatric data when the drugs entered the market? Pediatric drug development is challenged by ethical concerns and logistical issues. In the earlier days, pharmaceutical companies were not obliged to study their compounds in children, and excluded children from experimental trials because they were considered vulnerable as developing humans. Serious adverse event such as sketched above brought realization that it is actually unethical to not conduct studies in children. For example, the drugs that could be valuable for certain disease conditions in children were made available 'off-label', but an appropriate benefit-risk analysis, including dose finding, as is mandatory for adults, was lacking. Therefore, over the years, specific regulations for pediatric drug development have been established (see Table 1 for an overview of the key landmarks). These regulations mandated pediatric research and have greatly increased expertise and activity in pediatric drug development.

Ontogeny of drug metabolism and membrane transport

One of the major challenges in pediatric drug research is finding the right dose for children of different ages. We know now that most processes involved in drug disposition, including drug metabolism and membrane transport, are dependent on a child's growth and development.[3] Drug metabolizing enzymes are divided into phase 1 enzymes like Cytochrome P450s (CYPs) and phase 2 enzymes like UDP-glucuronosyltransferase

Table 1 Key landmarks in pediatric medicines regulation. Adapted from *Germovsek et al*.[8]

Year	Regulation	Impact
1997	US FDA Modernization Act (FDAMA)	This act presented the financial incentive of an additional 6 months of market exclusivity to companies undertaking required pediatric studies
1998	US FDA Pediatric Rule	This rule permitted companies to label medicines for use in children based on extrapolation of efficacy from adult trial data, together with pediatric PKPD and safety data
2002	US Best Pharmaceutical for Children Act (BPCA)	Framework for pediatric research in both on- and off-patent drugs
2003	US Pediatric Research Equity Act (PREA)	Sponsors required to undertake clinical studies in children for new medicines and biological products
2006	EU Pediatric Regulation	Introduction of new legislation in the European Union mandating pediatric medicines research for new medicinal products
2012	US Food and Drug Administration Safety and Innovation Act (FDASIA)	BPCA and PREA became permanent in US Law

(UGTs). These drug metabolizing enzymes biotransform the parent drug into active and/or inactive metabolites. Membrane transporters are capable of moving endogenous and exogenous substrates over cell membranes in and/or out the cell.[9] Dependent on the characteristics, a drug may be a substrate for one or more of these drug metabolizing enzymes or transporters. As such, they are critical determinants in drug disposition.

After birth, newborns become dependent on exogenous food sources for nutrition, and the diet expands as they grow into infanthood. During all changes in food exposure, the child must defend itself against potentially toxic dietary constituents, recruiting pathways not yet expressed or differentially expressed during fetal life. Hence ontogeny of drug metabolizing enzymes and transporters occurs, influencing the disposition of their endogenous and exogenous substrates over age.[2,3] Drug metabolizing enzymes work together with membrane transporters located in various organs to detoxify the body from exogenous compounds, like drugs and food toxins, and to maintain homeostasis of endogenous compounds. As each transporter or enzyme has its own developmental pattern, the metabolic profiles of drugs in children can significantly differ between age groups. Adjusting an adult dose based on bodyweight does not take these age-related changes into account. As such, one cannot simply perform linear size- or weight-based extrapolations from adult to pediatric doses, and dosing regimens specifically tailored to pediatrics are necessary.

Innovation in developmental pharmacology

Better understanding of the underlying processes involved in drug disposition may aid to better predict drug disposition and create age-appropriate dosing guidelines for use in

clinical trials, thereby reducing the risks and burdens of these trials. Innovative approaches have been developed to study these developmental changes in drug metabolism and transport. First, advances in analytical methods, including liquid chromatography–mass spectrometry (LC-MS/MS) for proteomic analyses, allow to quantify the expressions of a wide variety of proteins, e.g. membrane transporters, in a small piece of organ tissue. The latter is specifically important for pediatric research where tissues are scarcely available. Second, innovative study designs using radioactive labelled microtracers allowed to study – without risk for the child – the oral bioavailability of compounds used as a marker for certain drug metabolism pathways. Feasibility of these designs to assess age-associated changes metabolism was shown for paracetamol.[10,11] Third, the use of modeling and simulation to support dosing recommendations in a pediatric trial or even to substitute a pediatric trial in children is supported by both the EMA and the US FDA.[12,13] As a result, physiologically based PK (PBPK) models, that include age-specific physiologic information, are increasingly being used, not only to aid pediatric drug development but also to improve drug therapy of existing compounds.

Mind the gaps and try to close them

Although the knowledge on ontogeny of drug metabolism and transport has increased over time, important knowledge gaps remain, some of which are explained below.

Membrane transporter ontogeny in the liver and kidney

The importance of membrane transporters in drug disposition and effect has received increasing attention in recent years.[14-17] In light of this, *ex vivo* transporter gene and protein expression studies using pediatric tissues allow to learn whether there are age-related changes in the expression of these membrane transporters. These studies are dependent on the availability of pediatric tissues, which is rather an exception than the rule, but these tissues may be obtained from unique biobanks.

Recently, the hepatic protein expression levels of 10 clinically relevant transporters in 25 liver samples from fetuses, neonates and young infants have been explored using LC-MS/MS.[18] The age-related variation in transporter protein expression appeared both transporter and organ dependent. This exploratory study was clearly informative, but the sample size was too small, however, to define transporter specific maturational patterns. While liver data is scarce, data on the ontogeny of renal membrane transporters is even scarcer. Moreover, little is known of the underlying regulatory mechanisms of ontogeny.

CYP3A ontogeny in the intestine and liver

The drug metabolizing enzyme CYP3A is well known for its involvement in >50% of metabolized drugs, and is abundantly present in the intestine and liver. CYP3A consists

of the three main isoforms CYP3A4, -3A5 and -3A7, for which substrate specificity differs.[19,20] *In vitro* studies have shown that hepatic CYP3A7 abundance decreases rapidly after birth, and that hepatic and intestinal CYP3A4 abundance increases with increasing age.[21-23] CYP3A5 is polymorphically expressed with a stable expression from fetus to adult. This developmental pattern of CYP3A expression, established through *in vitro* studies, is supported by PK data of CYP3A substrate drugs. The benzodiazepine midazolam is a well-validated CYP3A probe with substrate specificity for CYP3A4/5 and almost no specificity for CYP3A7.[24-28] In preterm neonates, the intravenous midazolam clearance, reflecting hepatic CYP3A activity, was much lower (1.8 mL/kg/min) than that in infants and older children (9.1–16.7 mL/kg/min).[29-32] This was also seen for oral dosing, reflecting CYP3A in the intestine and liver. In preterm infants (gestational age 26-31 weeks and postnatal age 3-13 days), the oral midazolam clearance was markedly lower (0.16 L/h/kg vs 3.0 L/h/kg), and the oral bioavailability higher than those in children beyond 1 year of age (49-92% vs 21%) and in adults (49-92% vs 37%).[33-35] These findings suggest developmentally lower intestinal and/or hepatic CYP3A activity in preterm neonates.

Although the oral bioavailability of midazolam has been studied in children[31,33-36], there is a distinct knowledge gap for term neonates to children <1 year old. This knowledge gap hampers dose predictions for oral CYP3A substrates to be prescribed to this age group.

The classical study design to obtain data on oral bioavailability entails a cross-over study in which an oral and IV dose of a drug are administered alternately, with a wash-out period in between. This design is ethically and practically challenging as children are exposed twice to therapeutic drug doses with extensive blood sampling. An interesting alternative is a microtracer study with a [^{14}C]-labelled drug. A microdose is defined as '<1/100th of the no observed adverse effect level (NOAEL) or <100 μg'.[37,38] The [^{14}C]-label allows quantification of extremely low plasma concentrations by accelerator mass spectrometry (AMS) in only 10-15μl plasma.[39,40] A microdose can be used in an elegant design as a microtracer in which an oral [^{14}C]-labelled drug is administered simultaneously with therapeutic IV doses of the same unlabeled drug or *vice versa*. This allows simultaneous measurement of both the oral and IV disposition in the same subject and, with that, quantification of the oral bioavailability.[10,11] This approach has been shown practically and ethically feasible to study developmental changes in pharmacokinetics in children.[10,11,41]

Importantly, for direct extrapolation of exposure from microdose to therapeutic dose, the PK of the microdose must be linear to the PK of the therapeutic dose.[42,43] This may

not be the case, for example, when a therapeutic dose saturates drug metabolism pathways, plasma protein binding and/or active transporters.[43] Dose-linearity of the PK of a from a midazolam microdose to that of a therapeutic dose has been established in adults[42,44,45], but not in children. Yet, the results in adults cannot simply be extrapolated to children due to children's developmental changes in drug metabolism, hepatic blood flow, protein binding and membrane transport.

Pediatric metabolite in safety testing (MIST) study

Due to ontogeny of processes involved in drug disposition, predicting parent and metabolite exposure of compounds with a complex metabolism is challenging in children.[46] In adults, a general approach to study the parent and metabolite exposures of a drug during the drug development process, is performing a mass balance and metabolite in safety testing (MIST) study to create metabolite profiles.

Just recently, advances mainly in analytical technology have enabled new approaches to MIST studies with less radioactivity exposure.[47,48] By using [^{14}C]microtracers concurrently administered with a therapeutic dose, metabolites can be identified and quantified with a radioactivity exposure of even less than 0.1 μCi.[37,38] This approach not only justifies earlier radioactive exposure during drug development, but may also be used to derive metabolic profiles for vulnerable populations like children, for which higher radioactivity levels would not be ethically acceptable, even in a late stage of drug development. Yet, to the best of our knowledge, MIST microtracer studies with [^{14}C]-labelled compounds to create complete metabolic profiles have not yet been conducted in children.

Ontogeny data in literature

The accuracy of predicting pediatric drug exposure is highly dependent on the available ontogeny profiles of drug metabolizing enzymes and transporters. While increasing pediatric data become available in literature, results are often limited in age range and fragmented in several publications. Therefore, new data are needed, in combination with better accessibility of all the available *in vitro* and *ex vivo* data. Moreover, creating high-resolution quantitative ontogeny profiles will aid to improve existing models and to specify remaining information gaps.

AIMS AND OUTLINE OF THIS THESIS

Based on the above-mentioned knowledge gaps, the aims of this thesis are:

- To review the current literature and quantitatively describe ontogeny of hepatic membrane transporters and drug metabolizing enzymes.
- To study the ontogeny of relevant human membrane transporters gene and protein expression in pediatric hepatic and kidney tissues.
- To investigate alternative splicing as an underlying mechanism for the ontogeny of the OATP1B1 transporter
- To study the dose linearity of the pharmacokinetics of an intravenous [^{14}C]-labeled microdose of midazolam in children.
- To study the absolute oral bioavailability and metabolism of midazolam in children by an oral [^{14}C]-labeled microtracer study approach.
- To study the feasibility of a MIST study in children using a [^{14}C]-labeled microtracer study approach.

From literature to bench to clinical research

The outline of this thesis is tailored to the common approach in research; starting with literature research (Part I), going to fundamental (*ex vivo*) research on the bench (Part II), and taking it into clinical research (Part III).

First, in Part I the hepatic ontogeny of drug transporters and drug metabolizing enzymes is captured in a quantitative review in **chapter 2.** A review of the ontogeny of drug transporters in all major organs is presented in **chapter 3.**

Part II focuses on our *ex vivo* studies. **Chapter 4** and **chapter 5** address age-related changes in gene and protein expression of clinically relevant hepatic and renal transporters. To better understand observed age-related variation in transporter protein expression, in **chapter 6** alternative splicing of the OATP1B1 transporter as a mechanism for developmentally regulated expression is explored.

Part III presents the results of two clinical pediatric studies. **Chapter 7** shows the dose linearity of an intravenous [^{14}C]midazolam microdose in children. The oral bioavailability of midazolam in children 0-6 years as determined by a [^{14}C]midazolam microtracer study is described in **chapter 8**. **Chapter 9** presents the pilot results of the first pediatric MIST study with midazolam as an example compound.

Part IV puts the results of the studies in a broader perspective, and areas of current and future research are described in **chapter 10**. Results of the studies are summarized in **chapter 11**.

REFERENCES

1. van den Anker J, Reed MD, Allegaert K, Kearns GL. Developmental Changes in Pharmacokinetics and Pharmacodynamics. J Clin Pharmacol 2018;58 Suppl 10:S10-S25.
2. Brouwer KL, Aleksunes LM, Brandys B, et al. Human ontogeny of drug transporters: review and recommendations of the pediatric transporter working group. Clin Pharmacol Ther 2015;98(3):266-287.
3. Kearns GL, Abdel-Rahman SM, Alander SW, Blowey DL, Leeder JS, Kauffman RE. Developmental pharmacology--drug disposition, action, and therapy in infants and children. N Engl J Med 2003;349(12):1157-1167.
4. Weiss CF, Glazko AJ, Weston JK. Chloramphenicol in the newborn infant. A physiologic explanation of its toxicity when given in excessive doses. N Engl J Med 1960;262:787-794.
5. Food and Drug Administration. FDA Drug Safety Communication: FDA requires labeling changes for prescription opioid cough and cold medicines to limit their use to adults 18 years and older. 2018.
6. Food and Drug Administration. FDA Drug Safety Communication: FDA restricts use of prescription codeine pain and cough medicines and tramadol pain medicines in children; recommends against use in breastfeeding women. 2017.
7. Food and Drug Administration. Information for Healthcare Professionals: Ceftriaxone (marketed as Rocephin). 2007.
8. Germovsek E, Barker CIS, Sharland M, Standing JF. Pharmacokinetic-Pharmacodynamic Modeling in Pediatric Drug Development, and the Importance of Standardized Scaling of Clearance. Clin Pharmacokinet 2019;58(1):39-52.
9. Nigam SK. What do drug transporters really do? Nat Rev Drug Discov 2015;14(1):29-44.
10. Mooij MG, van Duijn E, Knibbe CA, et al. Successful Use of [14C]Paracetamol Microdosing to Elucidate Developmental Changes in Drug Metabolism. Clin Pharmacokinet 2017.
11. Mooij MG, van Duijn E, Knibbe CA, et al. Pediatric microdose study of [(14)C]paracetamol to study drug metabolism using accelerated mass spectrometry: proof of concept. Clin Pharmacokinet 2014;53(11):1045-1051.
12. Grimstein M, Yang Y, Zhang X, et al. Physiologically Based Pharmacokinetic Modeling in Regulatory Science: An Update From the U.S. Food and Drug Administration's Office of Clinical Pharmacology. J Pharm Sci 2019;108(1):21-25.
13. Committee for Human Medicinal Products EMA. ICH E11(R1) guideline on clinical investigation of medicinal products in the pediatric population. https://www.ema.europa.eu/en/documents/scientific-guideline/ich-e11r1-guideline-clinical-investigation-medicinal-products-pediatric-population-revision-1_en.pdf. Accessed June 12, 2019.
14. Food and Drug Administration. In vitro metabolism- and transporter-mediated drug-drug interaction Studies. https://www.fda.gov/Drugs/GuidanceComplianceRegulatoryInformation/Guidances/ucm064982.htm. Accessed September 24, 2018.
15. International Council for Harmonisation. Guidance for Industry. E11 Clinical investigation of medicinal products in the pediatric population. 2000.
16. European Medicines Agency. Guideline on the investigation of drug interactions. Committee for Human Medicinal Products. http://www.ema.europa.eu/docs/en_GB/document_library/Scientific_guideline/2012/07/WC500129606.pdf. Accessed April 3, 2018.
17. Pharmaceuticals Medical Devices Agency. Guideline on drug-drug interactions 2018;http://www.pmda.go.jp/files/000225191.pdf Accessed September 24, 2018.

18. Mooij MG, van de Steeg E, van Rosmalen J, et al. Proteomic analysis of the developmental trajectory of human hepatic membrane transporter proteins in the first three months of life. Drug Metab Dispos 2016;44(7):1005-1013.
19. de Wildt SN, Kearns GL, Leeder JS, van den Anker JN. Cytochrome P450 3A: ontogeny and drug disposition. Clin Pharmacokinet 1999;37(6):485-505.
20. Williams JA, Ring BJ, Cantrell VE, et al. Comparative metabolic capabilities of CYP3A4, CYP3A5, and CYP3A7. Drug Metab Dispos 2002;30(8):883-891.
21. Stevens JC, Hines RN, Gu C, et al. Developmental expression of the major human hepatic CYP3A enzymes. J Pharmacol Exp Ther 2003;307(2):573-582.
22. Fakhoury M, Litalien C, Medard Y, et al. Localization and mRNA expression of CYP3A and P-glycoprotein in human duodenum as a function of age. Drug Metab Dispos 2005;33(11):1603-1607.
23. Johnson TN, Tanner MS, Taylor CJ, Tucker GT. Enterocytic CYP3A4 in a paediatric population: developmental changes and the effect of coeliac disease and cystic fibrosis. Br J Clin Pharmacol 2001;51(5):451-460.
24. Watkins PB. Noninvasive tests of CYP3A enzymes. Pharmacogenetics 1994;4(4):171-184.
25. Streetman DS, Bertino JS, Jr., Nafziger AN. Phenotyping of drug-metabolizing enzymes in adults: a review of in-vivo cytochrome P450 phenotyping probes. Pharmacogenetics 2000;10(3):187-216.
26. Chainuvati S, Nafziger AN, Leeder JS, et al. Combined phenotypic assessment of cytochrome p450 1A2, 2C9, 2C19, 2D6, and 3A, N-acetyltransferase-2, and xanthine oxidase activities with the "Cooperstown 5+1 cocktail". Clin Pharmacol Ther 2003;74(5):437-447.
27. Fuhr U, Jetter A, Kirchheiner J. Appropriate phenotyping procedures for drug metabolizing enzymes and transporters in humans and their simultaneous use in the "cocktail" approach. Clin Pharmacol Ther 2007;81(2):270-283.
28. de Wildt SN, Ito S, Koren G. Challenges for drug studies in children: CYP3A phenotyping as example. Drug Discov Today 2009;14(1-2):6-15.
29. de Wildt SN, Kearns GL, Hop WC, Murry DJ, Abdel-Rahman SM, van den Anker JN. Pharmacokinetics and metabolism of intravenous midazolam in preterm infants. Clin Pharmacol Ther 2001;70(6):525-531.
30. Rey E, Delaunay L, Pons G, et al. Pharmacokinetics of midazolam in children: comparative study of intranasal and intravenous administration. Eur J Clin Pharmacol 1991;41(4):355-357.
31. Reed MD, Rodarte A, Blumer JL, et al. The single-dose pharmacokinetics of midazolam and its primary metabolite in pediatric patients after oral and intravenous administration. J Clin Pharmacol 2001;41(12):1359-1369.
32. Tolia V, Brennan S, Aravind MK, Kauffman RE. Pharmacokinetic and pharmacodynamic study of midazolam in children during esophagogastroduodenoscopy. J Pediatr 1991;119(3):467-471.
33. de Wildt SN, Kearns GL, Hop WC, Murry DJ, Abdel-Rahman SM, van den Anker JN. Pharmacokinetics and metabolism of oral midazolam in preterm infants. Br J Clin Pharmacol 2002;53(4):390-392.
34. Brussee JM, Yu H, Krekels EHJ, et al. First-Pass CYP3A-Mediated Metabolism of Midazolam in the Gut Wall and Liver in Preterm Neonates. CPT Pharmacometrics Syst Pharmacol 2018;7(6):374-383.
35. Brussee JM, Yu H, Krekels EHJ, et al. Characterization of Intestinal and Hepatic CYP3A-Mediated Metabolism of Midazolam in Children Using a Physiological Population Pharmacokinetic Modelling Approach. Pharm Res 2018;35(9):182.
36. Payne K, Mattheyse FJ, Liebenberg D, Dawes T. The pharmacokinetics of midazolam in paediatric patients. Eur J Clin Pharmacol 1989;37(3):267-272.

37. European Medicines Agency. ICH Topic M3 (R2) Non-Clinical Safety Studies for the Conduct of Human Clinical Trials and Marketing Authorization for Pharmaceuticals. 2008.
38. Food and Drug Administration US Department of Health and Human Services Guidance for Industry Investigators and Reviewers. Exploratory IND Studies. 2006.
39. Salehpour M, Possnert G, Bryhni H. Subattomole sensitivity in biological accelerator mass spectrometry. Anal Chem 2008;80(10):3515-3521.
40. Vuong LT, Blood AB, Vogel JS, Anderson ME, Goldstein B. Applications of accelerator MS in pediatric drug evaluation. Bioanalysis 2012;4(15):1871-1882.
41. Turner MA, Mooij MG, Vaes WH, et al. Pediatric microdose and microtracer studies using 14C in Europe. Clin Pharmacol Ther 2015;98(3):234-237.
42. Lappin G, Kuhnz W, Jochemsen R, et al. Use of microdosing to predict pharmacokinetics at the therapeutic dose: experience with 5 drugs. Clin Pharmacol Ther 2006;80(3):203-215.
43. Bosgra S, Vlaming ML, Vaes WH. To Apply Microdosing or Not? Recommendations to Single Out Compounds with Non-Linear Pharmacokinetics. Clin Pharmacokinet 2016;55(1):1-15.
44. Hohmann N, Kocheise F, Carls A, Burhenne J, Haefeli WE, Mikus G. Midazolam microdose to determine systemic and pre-systemic metabolic CYP3A activity in humans. Br J Clin Pharmacol 2015;79(2):278-285.
45. Halama B, Hohmann N, Burhenne J, Weiss J, Mikus G, Haefeli WE. A nanogram dose of the CYP3A probe substrate midazolam to evaluate drug interactions. Clin Pharmacol Ther 2013;93(6):564-571.
46. Leclercq L, Cuyckens F, Mannens GS, de Vries R, Timmerman P, Evans DC. Which human metabolites have we MIST? Retrospective analysis, practical aspects, and perspectives for metabolite identification and quantification in pharmaceutical development. Chem Res Toxicol 2009;22(2):280-293.
47. Schadt S, Bister B, Chowdhury SK, et al. A Decade in the MIST: Learnings from Investigations of Drug Metabolites in Drug Development Under the "Metabolites in Safety Testing" Regulatory Guidances. Drug Metab Dispos 2018.
48. Yu H, Bischoff D, Tweedie D. Challenges and solutions to metabolites in safety testing: impact of the International Conference on Harmonization M3(R2) guidance. Expert Opin Drug Metab Toxicol 2010;6(12):1539-1549.

PART I

From literature research –

3 Incorporating ontogeny in physiologically-based pharmacokinetic modeling to improve pediatric drug development: what we know about developmental changes in membrane transporters

Kit Wun Kathy Cheung, Bianca D van Groen, Gilbert J Burckart, Lei Zhang, Saskia N de Wildt, Shiew-Mei Huang

J Clin Pharmacol. 2019 Sep;59 Suppl 1:S56-S69. DOI: 10.1002/JCPH.1489

ABSTRACT

Developmental changes in the biological processes involved in the disposition of drugs, such as membrane transporter expression and activity, may alter the drug exposure and clearance in pediatric patients. Physiologically-based pharmacokinetic (PBPK) models take these age-dependent changes into account and may be used to predict drug exposure in children. As such, this mechanistic-based tool has increasingly been applied to improve pediatric drug development. Under the Prescription Drug User Fee Act VI, the U.S. Food and Drug Administration has committed to facilitate the advancement of PBPK modeling in the drug application review process. Yet, significant knowledge gaps on developmental biology still exist, which must be addressed to increase the confidence of prediction. Recently, more data on ontogeny of transporters have emerged and supplied a missing piece of the puzzle. This review highlights the recent findings on the ontogeny of transporters specifically in the intestine, liver and kidney. It also provides a case study, which illustrates the utility of incorporating this information in predicting drug exposure in children using a PBPK approach. Collaborative work has greatly improved the understanding of the interplay between developmental physiology and drug disposition. Such efforts will continually be needed to address the remaining knowledge gaps to enhance the application of PBPK modeling in drug development for children.

INTRODUCTION

The off-label use of drugs in doses that are insufficiently studied is extensive in pediatric medicine.[1] This is mainly because drug development for treatment in pediatric patients is challenged by ethical concerns and logistical issues.[2] As children widely differ from adults due to developmental changes in the biological processes involved in the disposition of drugs, this leaves them at risk for subtherapeutic or toxic exposures. [3] The establishment of the Best Pharmaceuticals for Children Act (BPCA) in 2002 and the Pediatric Research Equity Act (PREA) in 2003, which were made permanent under the Food and Drug Administration Safety and Innovation Act (FDASIA) in 2012, and the European 'Paediatric Regulation' (regulation no 1901-2/2006) in 2006 have highlighted the commitment of the U.S. Food and Drug Administration (FDA) and the European parliament and council to conduct studies in pediatric patients, and thereby fill the pediatric gaps in drug development to increase the safety and efficacy of pediatric drug therapy.[4-6]

With the advancement of *in silico* technologies, novel methodologies such as model-informed drug development (MIDD) can leverage our existing understanding of pediatric physiology, disease states and pharmacology. This provides quantitative information to streamline decision-making in drug development, such as clinical trial design and dose optimization, which can increase the success of pediatric clinical trials.[7] To support this, FDA has committed to advance MIDD under the Prescription Drug User Fee Act (PDUFA) VI, with approaches that include convening a series of workshops to identify best practices for MIDD, conducting a pilot meeting program for MIDD approaches, publishing or revising an existing draft guidance on MIDD and engaging in regulatory science research to develop expertise and capacity in MIDD approaches.[7,8]

Physiologically-based pharmacokinetic (PBPK) modeling is one of the mechanistic-based MIDD tools that has been increasingly incorporated into drug development programs to support submissions to the FDA and European Medicines Agency (EMA).[9,10] Of all the PBPK analyses that were included in the New Drug Application (NDA) submissions to the FDA between 2008 and 2017, 60% were utilized to assess enzyme-mediated drug-drug interactions (DDIs). This was followed by 15% of the submissions that supported the evaluation of pediatric-related issues such as initial dose recommendation for clinical trials, and 7% that analyzed transporter-mediated DDIs.[9] During the FDA Advisory Committee for Pharmaceutical Science and Clinical Pharmacology Meeting in March 2012, some experts expressed concerns regarding the routine use of PBPK modeling in pediatric drug development as pediatric PBPK models still had significant knowledge

gaps in areas such as the ontogeny of membrane transporters, and thereby may not predict drug exposure well.[11]

Given that new data on the ontogeny of membrane transporters has emerged since 2012, the objective of this article is to review findings from recent studies that have evaluated pediatric developmental changes in the membrane transporters.

ONTOGENY OF MEMBRANE TRANSPORTERS

Membrane transporters facilitate the active movement of drug molecules and endogenous compounds into and out of cells of various organs, affecting drug absorption, distribution and excretion.[12] Hence, they have a critical role in impacting pharmacokinetics (PK) and pharmacodynamics (PD) of drugs, and should be considered and assessed carefully during drug development. In the 2017 FDA's draft *in vitro* DDI guidance, FDA recommended the evaluation of DDI potential by studying whether a

Table 1. The full name, protein names and gene names of the membrane transporters that are discussed in this review

Full name	Protein name	Gene name
P-glycoprotein	P-gp	*ABCB1*
Breast Cancer Resistance Protein	BCRP	*ABCG2*
Multidrug and Toxin Extrusion 1	MATE1	*SLC47A1*
Multidrug and Toxin Extrusion 2-K	MATE2-K	*SLC47A2*
Organic Anion Transporting Polypeptide 1B1	OATP1B1	*SLCO1B1*
Organic Anion Transporting Polypeptide 1B3	OATP1B3	*SLCO1B3*
Organic Anion Transporter 1	OAT1	*SLC22A6*
Organic Anion Transporter 3	OAT3	*SLC22A8*
Organic Cation Transporter 2	OCT2	*SLC22A2*
Multidrug Resistance-Associated Protein 2	MRP2	*ABCC2*
Multidrug Resistance-Associated Protein 4	MRP4	*ABCC4*
Peptide Transporter 1	PEPT1	*SLC15A1*
Sodium/taurocholate Cotransporting Polypeptide	NTCP	*SLC10A1*
Bile salt export pump	BSEP	*ABCB11*
Glucose transporter 1	GLUT1	*SLC2A1*
Glucose transporter 2	GLUT2	*SLC2A2*
Monocarboxylate transporter 1	MCT1	*SLC16A1*
Uric acid transporter 1	URAT1	*SLC22A12*

new drug is a potential substrate or inhibitor of the following nine transporters (see Table 1 for full, protein and gene names): P-gp, BCRP, MATE1, MATE2-K, OATP1B1, OATP1B3, OAT1, OAT3, OCT2.[13]

There is a wealth of information on how alterations in the transporter activity, mainly due to genetic polymorphisms and DDIs, can lead to variability in drug safety and efficacy in adults. However, less is known about age-related changes in transporter expression levels and activities, and how that relates to the safety and efficacy of pediatric drug use. In 2015, the Pediatric Transporter Working Group performed a comprehensive review on the data available for the ontogeny of clinically relevant membrane transporters.[14] Further, the working group also provided recommendations to address and overcome some of the challenges in filling the pediatric knowledge.[14] These include building multidisciplinary and international collaborative networks to facilitate data sharing, increasing awareness of clinicians about the importance of transporters in pediatric drug disposition and identifying biomarkers for transporter activity in children. In the following discussion and in Table 2, human data presented in that review are highlighted, and updated information from recent literature is provided. Figure 1 also depicts the human membrane transporters in the intestine, liver and kidneys that are mentioned in this article.

Ontogeny of intestinal transporters

Most drugs prescribed to children are administered orally.[37] The intestine is a major absorption site of drugs that are administered via oral route. Transporters that are present in the enterocytes on the gut wall mucosa govern the initial access into the systemic circulation of molecules such as sugars, amino acids, vitamins, but also of drug substrates.[38,39] P-gp, multidrug resistance-associated protein (MRP2) and BCRP, for instance, are major efflux transporters that are responsible for limiting drug absorption. On the other hand, OATP1A2 and OATP2B1 have been suggested to participate in the intestinal absorption of drugs in human.[40] Further, peptide transporter (PEPT)1 is a major uptake transporter that facilitates absorption of peptide-like drugs in the systemic circulation such as β-lactam antibiotics.[38,41] Therefore, drug absorption in children will be highly dependent on the expression and activity of these intestinal transporters.

P-gp, BCRP, MRPs, OATP2B1 and PEPT1: In their review, Brouwer et al noted that ontogeny of intestinal transporters was mainly revealed by mRNA expression and localization data using immunohistochemistry.[14] P-gp and MRP2 mRNA expression levels in neonates and infants appeared to be comparable to adults.[17-24] Localization data suggested that BCRP and MRP1 distribution was similar in adult and fetal samples (5.5-28 weeks and 9-28 weeks of gestation, respectively).[24] In contrast to the other

Table 2. Human ontogeny data of membrane transporters in intestine, liver and kidney highlighted in this article.

Membrane transporter [protein name (gene name)]	Types of ontogeny data available	Reported ontogeny pattern	Reference
Intestinal transporters*			
P-gp (*ABCB1*)	Gene expression	mRNA level in neonates and infants was comparable to adults	17-23
BCRP (*ABCG2*)	Immunohistochemistry	BCRP distribution was similar in fetal (5.5-28 weeks of gestation) and adult samples	24
MRP1 (*ABCC1*)	Immunohistochemistry	MRP1 distribution was similar in adults and fetal samples (9-28 weeks of gestation)	24
MRP2 (*ABCC2*)	Gene expression	mRNA level was stable from neonates to adults	23
OATP2B1 (*SLCO2B1*)	Gene expression	mRNA level was higher in neonates than in adults	23
PEPT1 (*SLC15A1*)	Gene expression	mRNA was slightly lower in neonates than in older counterparts	25
	Immunohistochemistry	Tissue distribution was relatively stable from preterm neonates to adolescents	25
Liver transporters			
OCT1 (*SLC22A1*)	Gene expression	Transcript levels in pediatric livers was comparable to that in adults	26
	Western blot	Age-dependent increase in OCT1 protein expression from birth up to 8-12 years old	27
	Quantitative proteomics	Age-dependent increase in protein expression level; TM_{50} was approximately 6 months	28,29
OATP1B1 (*SLCO1B1*)	Gene expression	mRNA expression of OATP1B1 in fetal liver was 20-fold lower than that in adults. Neonates and infants have even lower levels than fetus (500-fold and 90-fold lower than adults, respectively)	23
	Quantitative proteomics	van Groen et al reported higher protein expression in fetal livers compared to that in term neonates. The protein expression in infants to adults were similar. Genetic polymorphism was not associated with expression levels in this study. Prasad et al reported that when all samples were considered, no age-dependent changes in the protein expression was found. Protein levels were higher in *1A/*1A >1-year-old cohort than the 0 to 12 months group	28,29
OATP1B3 (*SLCO1B3*)	Gene expression	mRNA levels in fetus, neonates and infants were lower than that in adults	23
	Quantitative proteomics	No age-dependent changes were found in van Groen et al; Age-dependent increase reported in Prasad et al with TM_{50} approximately 6-months	28,29
OATP2B1 (*SLCO2B1*)	Gene expression	mRNA level was significantly higher in adult livers compared to that in fetus (GA 18-23 weeks)	30
	Quantitative proteomics	Comparable protein expression levels in livers from fetus to adults	28,29,31

Table 2. Human ontogeny data of membrane transporters in intestine, liver and kidney highlighted in this article. (continued)

Membrane transporter [protein name (gene name)]	Types of ontogeny data available	Reported ontogeny pattern	Reference
NTCP (*SLC10A1*)	Gene expression	mRNA level was low in fetal liver compared to adults	30,32
	Western blot	Relative expression was stable in livers samples from neonates and adults	33
	Quantitative proteomics	Prasad et al reported stable protein expression from neonates to adults. van Groen showed that protein expression was significantly lower in fetuses than in term neonates, infants, children and adults	28,29
P-gp (*ABCB1*)	Gene expression	Detected in fetal liver; mRNA level increased rapidly during first 12 months of life in infants	23
	Western blot	No significant differences in the relative protein expression from 0.3 to 12 years old	34
	Quantitative proteomics	Protein level increase from fetus to adults with TM_{50} approximately 2.9 years old	28,29
MRP2 (*ABCC2*)	Gene expression	mRNA level increased; levels in fetal, neonatal and infant livers were substantially lower than that in older children up to 12 years old	23,35
	Quantitative proteomics	van Groen et al reported that MRP2 level was much lower in fetal and term newborn livers than that in adults. Prasad et al found no age-dependent changes	28,29
MRP3 (*ABCC3*)	Gene expression	mRNA level was lower in fetal livers than that in adults	30
	Quantitative proteomics	van Groen et al reported that protein abundance was lower in fetus and term neonates than in adults. In Prasad et al, lower protein abundance was found in infants and adolescents than adults.	28,29
MRP1 (*ABCC1*)	Quantitative proteomics	Protein levels were lower in fetus and term neonates than adults	28
MRP4 (*ABCC4*)	Gene expression	No age-dependent changes in mRNA level	30
MRP6 (*ABCC6*)	Gene expression	mRNA level increase from neonates to older children and adults	35
BCRP (*ABCG2*)	Immunohistochemistry	Detected in fetus as young as GA 5.5 weeks	24
	Gene expression	mRNA level was lower in fetal livers than in adults	30,35
	Quantitative proteomics	Stable across age groups from fetus to adults but age-dependent decrease observed in fetal and newborn cohorts	28,29
BSEP (*ABCB11*)	Quantitative proteomics	Significantly lower in fetal livers compared to that in adults; no age-dependent changes after birth	28,29
MATE1 (*SLC47A1*)	Gene expression	mRNA showed age-dependent increase	35
	Quantitative proteomics	No age-dependent changes in protein abundance	29
GLUT1 (*SLC2A1*)	Quantitative proteomics	Protein abundance was high in fetus and lower in other age groups	28
MCT1 (*SLC16A1*)	Quantitative proteomics	No age-dependent changes in protein abundance	28

Table 2. Human ontogeny data of membrane transporters in intestine, liver and kidney highlighted in this article. (continued)

Membrane transporter [protein name (gene name)]	Types of ontogeny data available	Reported ontogeny pattern	Reference
Kidney transporters			
BCRP (*ABCG2*)	Gene expression	mRNA level was higher in term neonates than older counterparts	36
	Quantitative proteomics	No age-dependent changes in protein abundance	36
MATE1 (*SLC47A1*)	Gene expression	No age-dependent changes in mRNA level	36
	Quantitative proteomics	No age-dependent changes in protein abundance	36
MATE2-K (*SLC47A2*)	Gene expression	mRNA level was lower in term newborns than adults	36
	Quantitative proteomics	No age-dependent changes in protein abundance	36
MRP2 (*ABCC2*)	Gene expression	No age-dependent changes in mRNA level	36
MRP4 (*ABCC4*)	Gene expression	No age-dependent changes in mRNA level	36
	Immunohistochemistry	Proper localization observed in renal cortical fetal sample as early as GA 27 weeks	36
URAT1 (*SLC22A12*)	Gene expression	mRNA levels increased with age from term newborn to adults	36
	Quantitative proteomics	Protein levels increased with age from term newborn to adults	36
P-gp (*ABCB1*)	Immunohistochemistry	Localization detected as early as end of first trimester of fetal life	22
	Gene expression	mRNA levels were lower in preterm newborn, term newborns and infants compared to older counterparts	36
	Quantitative proteomics	Protein levels increased with age with TM_{50} approximately 1 month	36
GLUT2 (*SLC2A2*)	Gene expression	No age-dependent changes in mRNA level	36
	Quantitative proteomics	No age-dependent changes in protein abundance	36
OAT1 (*SLC22A6*)	Gene expression	mRNA level increased with age	36
	Quantitative proteomics	Protein abundance increased with age. TM_{50} was approximately 5 months	36
OAT3 (*SLC22A8*)	Gene expression	mRNA level increased with age	36
	Quantitative proteomics	Protein abundance increased with age. TM_{50} was approximately 8 months	36
OCT2 (*SLC22A2*)	Gene expression	mRNA level increased with age	36
	Quantitative proteomics	Protein expression increased with age. TM_{50} was approximately 1 month	36

***** *See Brouwer et al for more detailed review.*[14]

Figure 1 Summary of the human membrane transporters in the intestine, liver and kidneys that are mentioned in this review.

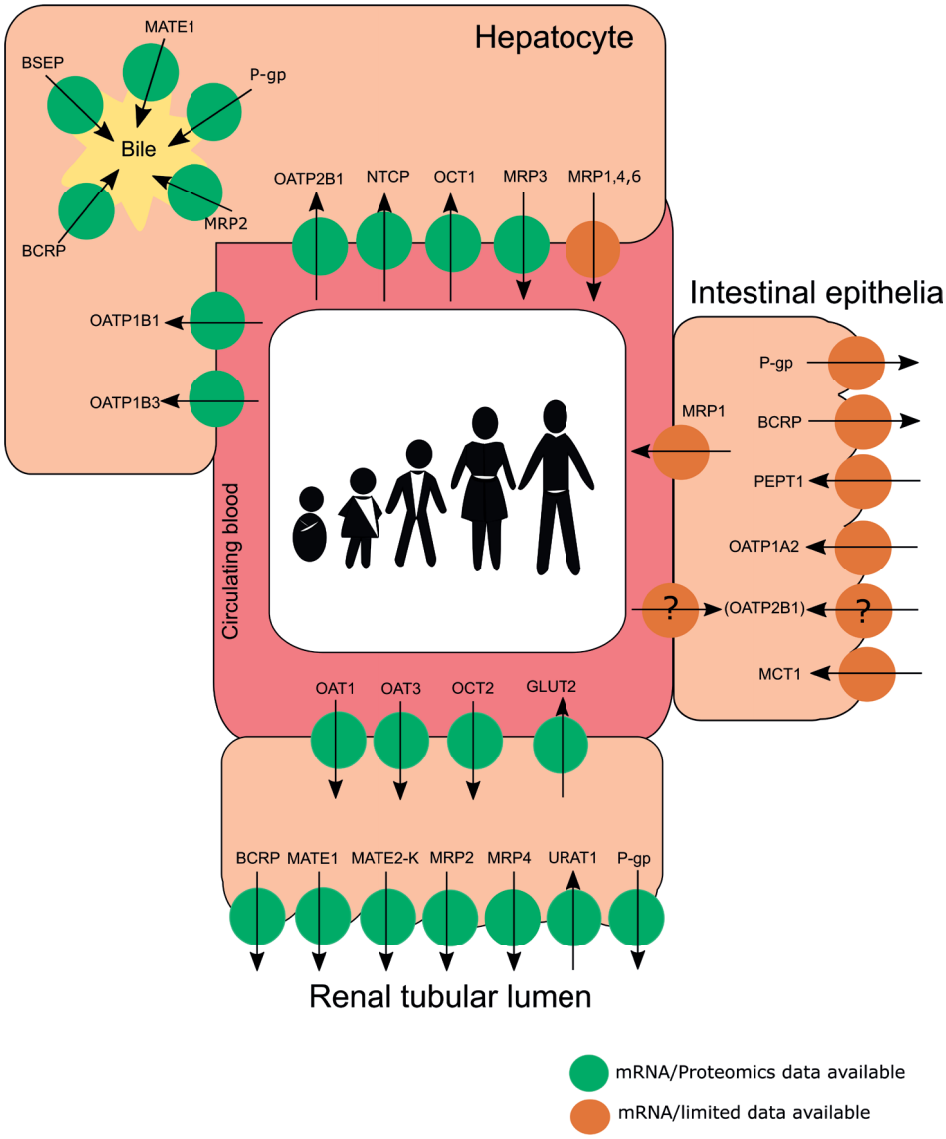

Transporters with only mRNA or limited data are depicted in brown circles; whereas those that have both gene expression and protein abundance data are depicted in green circles. (adapted/modified from Brouwer et al and Chu et al)[15,16] *Noteworthy, the localization of OATP2B1 remains questionable. Future investigation would also be needed to characterize if its localization is subject to developmental changes.*

intestinal transporters, OATP2B1 gene expression levels were much higher in neonates than in adults.[23] Noteworthy, the localization of OATP2B1 remains questionable; while two studies observed localization of the transporter to the apical membrane of human enterocytes, another research group, which studied mainly pediatric intestinal tissue samples, detected OATP2B1 in the basolateral membrane.[25,42-44] This basolateral localization was also reported by another independent group using six healthy human adult jejunal tissue samples.[45] Future studies are warranted to elucidate the localization of OATP2B1 and if it is subject to developmental changes. Using a total of 26 intestinal tissues samples, which included 19 preterm and term neonates, one infant 13.9 weeks old, two children and four adolescents, Mooij and colleagues studied the developmental changes in PEPT1 mRNA expression and localization.[25] While PEPT1 expression appeared to be slightly lower in neonates than in their older counterparts, the tissue distribution was relatively stable among all the samples studied.

While changes in the gene expression and localization of these transporters during development were stressed in various published studies, data on their protein expression levels are still missing. In addition, the ontogeny patterns of other human intestinal transporters, such as OATP1A2 and MCT1, remain uncertain. Since many drugs are administered orally, it is crucial to fill this knowledge gap in intestinal transporter ontogeny.

Ontogeny of liver transporters

In comparison to intestinal transporters, data on developmental changes in hepatic transporters have grown quite rapidly recently. Classic analytical approaches include quantitative real-time polymerase chain reaction (qRT-PCR), which measures gene expression levels, immunohistochemistry which visualizes localization and western blot which measures the relative protein expression. In addition, quantitative proteomics via liquid chromatography/tandem mass spectrometry (LC-MS/MS) has been increasingly utilized to measure the absolute protein abundance of these transporters, allowing the quantification of many transporters in only a small amount of tissue. Proteomics data generated from two independent laboratories complemented each other in terms of age range of the samples and provided a more complete picture of the developmental patterns of hepatic transporters with higher confidence than what was known previously.[28,29,46] In one study, the protein abundance of 11 hepatic transporters was measured in approximately 69 postmortem tissue samples that covered the whole pediatric age range (4 neonates, 19 infants, 32 children and 14 adolescents) and in 41 adult samples (> 16 years old).[29] In another study, the absolute protein expression of 13 liver transporters was quantified in a pediatric cohort with a focus on the fetus and newborn up to postnatal 18 weeks of age that consisted of 62 pediatric tissue samples

(36 fetuses, 12 premature newborns, 10 term newborns, 4 pediatric patients and 8 tissue samples from adults).[28] The findings in these two studies and other previous studies are discussed below.

OCT1: As previously reported, OCT1 mRNA levels in pediatric livers appeared to be comparable to that in adult livers.[14,26] Nonetheless, OCT1 protein levels have shown to undergo age-dependent increase.[27-29] This was supported by a recently published clinical study in neonates who were admitted to the neonatal intensive care unit where postmenstrual age as well as OCT1 genotype impacted the PK of the OCT1 substrate morphine.[47] Further, the age at which half of adult level is reached (TM_{50}) was also estimated using a sigmoidal Emax model and was reported to be about 6 months.

OATP1B1: mRNA expression of OATP1B1 in fetal liver was 20-fold lower than that in adults, and that in neonates and infants was even lower (500-fold and 90-fold, respectively).[14,23] Recent quantification of protein expression, nonetheless, revealed different findings. In their sample set, van Groen et al found that the OATP1B1 expression was significantly higher in the fetal livers compared to that term neonatal livers. The protein expressions in infants, children and adults were similar.[28] OATP1B1 is highly polymorphic. The impact of genetic variants on developmental changes in OATP1B1 expression was investigated in this cohort but no association was identified for the studied genotypes. When all tissue samples were considered, Prasad et al reported that OAPT1B1 did not show age-dependent changes in the protein expression.[29] Yet, when the analysis was performed on samples from donors with the OATP1B1 reference allele, *1A/*1A, samples from > 1 year old was found to have higher protein expression than the 0 to 12 months group. Notably, in the >1-year-old cohort, OATP1B1 expression was about 2.5-fold higher in samples from donors with *14/*1A than that with *15/*1A.

OATP1B3: Similar to OATP1B1, mRNA expression of OATP1B3 was reported to be much lower in fetuses, neonates and infants compared to adults.[14,23] While proteomics data in one study showed that OATP1B3 expression was not associated with age, the other illustrated that the expression of the transporter was subjected to age-dependent increase, and by 6 months of age, similar to OCT1, the protein expression would have reached 50% of the adult level.[28,29]

OATP2B1: mRNA levels of OAT2B1 was significantly higher in adult livers compared to that in livers from fetus at gestational age 18-23 weeks.[14,30] However, quantitative proteomics suggested that OATP2B1 expression in liver from fetus of median 23.4 (range 15.3-41.3) weeks was comparable to that from preterm neonates, term neonates,

children and adults.[28] This lack of correlation with age was supported by two other analyses.[29,31]

NTCP: Various studies suggested that maturation of NTCP starts during perinatal stage and the expression reaches adult levels at birth.[14,29,30,32,33] Protein expression of NTCP revealed similar trend where NTCP expression was significantly lower in fetuses than in term neonates, infants, children and adults and that in preterm neonates was lower than in adults.[28]

P-gp: Previously it has been reported that P-gp is subject to developmental changes in the mRNA expression.[14] The transcript level of P-gp was detected as early as 14 weeks gestational age and the level increased rapidly during the first 12 months of life in infants, which then reached a level comparable to adults.[22] Despite the developmental changes in gene expression, one study reported no age-related differences in the relative protein expression in patients from 0.3 to 12 years old.[34] Interestingly, however, the results from the two recent proteomic studies were in agreement with the mRNA data – P-gp protein expression was low in fetal liver tissues but increased with age.[28,29] Further, TM_{50} was also estimated to be 2.94 years old, suggesting that the P-gp expression continued to increase postnatally and would achieve adult level later on in children.[29]

MRP2: Using gene expression analysis, previous studies have shown that MRP2 mRNA levels were substantially lower in fetal, neonatal and infant livers compared to older children up to 12 years of age.[14,23,35] The result reported in one of the recent proteomic studies was in agreement with these findings, where MRP2 protein expression was approximately three-fold lower in fetal and term newborn livers compared to adults.[28] Yet, in another study, it was reported that MRP2 expression was not age-dependent in their cohort. [29]

MRP3: MRP3 mRNA was detected in fetal hepatocytes as early as 18 weeks gestational age, and was significantly lower than that found in adult livers.[30] Proteomic data from recent studies agree with this observation. The fetal MRP3 protein level was approximately 3-folder lower than the adult level.[28] Interestingly it was found in one study that the transporter expression appeared to be lower in adolescents compared to that in adults. [29]

MRP1, MRP4, MRP6: Developmental information on these three MRPs is scarce. In their study, van Groen et al showed that MRP1 levels in livers from fetus and term neonates were about two-fold lower than that in adults.[28] MRP4 mRNA did not change with age.[14,30] While MRP6 mRNA expression was shown to increase from neonates to older

children and adults, no proteomic data is currently available to determine if the actual protein expression shows similar age-dependent change.[35]

BCRP: Localization of BCRP in the hepatocytes was detected in fetus as young as 5.5 weeks gestational age.[24] BCRP mRNA expression was lower in fetal samples compared to adults.[30,35] BCRP protein levels appeared to be comparable in fetus and after birth in all age groups.[28,29] However, when data set was analyzed as continuous data by postnatal age and postmenstrual age within the fetal and newborn cohort, BCRP expression interestingly showed age-dependent decrease with a spearman correlation coefficients of -0.345 and -0.421, respectively.[28]

BSEP: Using sandwich-cultured fetal and adult hepatocytes, a functional study was conducted, which showed that the biliary excretion index for taurocholate, an endogenous BSEP substrate, was lower in the fetal liver cells compared to that in adults.[30] Results from quantitative proteomics studies coincide with this observation; the fetal liver tissues expressed significantly lower BSEP compared to term newborn and adults.[28] Maturation of BSEP appeared to occur mainly during perinatal period as no significant age-dependent changes were seen from neonates onwards.[28,29]

MATE1: In contrast to the age-dependent increase in mRNA reported previously, protein expression of MATE1 appeared to be independent of age.[14,28,29]

GLUT1: Developmental information for GLUT1 was previously lacking but recent proteomic study indicated that GLUT1 expression showed age-dependent decrease with fetal liver tissues expressing the highest protein abundance and lower expression in the other age groups.[28] This age-dependent decrease was more apparent when analyzing the expression levels in the youngest cohorts, fetus and newborn, based on the PNA and PMA with spearman correlation coefficient of -0.51 and -0.59, respectively.

MCT1: Similar to GLUT1, the ontogeny of MCT1 was missing. The absolute protein abundance of this transporter was found to be comparable in fetal liver and in other age groups after birth.[28]

Recent knowledge gain on liver transporters

Recent proteomics studies provided valuable ontogeny information for the liver transporters. Although gaps in the developmental changes in various liver transporters such as OAT2 and OAT7 still exist, the understanding in the association between transporter expression and age has been improved substantially, particularly for those

transporters that have been shown to be clinically important: BCRP, P-gp, MATE1 and OATP1B1/3.[13]

Ontogeny of renal transporters

The kidney is the major site for elimination of many drugs. Three major processes are involved in drug disposition: glomerular filtration, active secretion and reabsorption. Maturation of glomerular filtration has been studied quite extensively but information on ontogeny of renal membrane transporters, which are key players in the active secretion was relatively scarce.[14,48] Yet, information on the developmental changes in renal membrane transporters has emerged recently. Gene expression of 11 transporters was analyzed from a total of 184 frozen human renal cortical samples from preterm newborn to 75 years of age. The protein expression of 9 transporters and localization of MRP4 using immunohistochemistry were also studied using a subset of the kidney samples.[36]

BCRP: The mRNA level of BCRP was significantly higher in term neonates compared to other age groups but the protein abundance appeared to be comparable across all age groups from term neonates to adults. Further studies would be warranted to investigate this lack of gene-protein correlation as only one term neonate was included for the proteomic analysis in that study.[36]

MATE1 and **MATE2-K**: mRNA and protein levels of MATE1 were independent of age.[36] While transcript level of MATE2-K in term newborn was significantly lower than that in adults, the protein was found to be comparable across all the age groups studied from term newborn to adults. However, similar to BCRP, the cohort of term neonates for proteomic analysis would need to be expanded in order to better characterize the correlation between gene and protein expression.

MRP2 and **MRP4**: mRNA levels of MRP2 and MRP4 appeared to be stable in preterm newborn, term newborn, infants, children and their older counterparts. Interestingly, proper MRP4 localization was detected as early as GA 27 weeks, postnatal 9 day old. This result appeared to accompany the stable gene expression during development.[36]

URAT1: The mRNA and protein abundance of URAT1 increased with age from term newborn to adults.[36]

P-gp: Similar to the liver and intestine, the ontogeny of renal P-gp was studied relatively extensively. P-gp localization was detected as early as the end of first trimester of fetal life.[22] Results from gene expression analysis and quantitative proteomics expanded the

understanding of the developmental changes of P-gp in kidney. P-gp mRNA levels were significantly lower in preterm newborn, newborn and infants as compared to children, adolescents and adults. This observation appeared to be translated well to protein expressions. Sigmoidal Emax model described this age-dependent increase and the TM_{50} was approximately 1 month.[36]

GLUT2: An efficient carrier of glucose, GLUT2, did not show age-dependent changes in its mRNA expression and protein abundance.[36]

OAT1 and **OAT3:** The ontogeny of these two organic anion transporters were reflected in clinical data.[48] For instance, one study showed that the secretion capacity of *p*-aminohippurate (PAH), an OAT1/3 substrate, appeared to be about one-fifth of adult level at birth.[49-51] These observed age-related changes in pharmacokinetics of transporter substrates are likely due to a combination of maturation in both transporter expression and glomerular filtration. Yet, the changes in transcript levels and protein abundance aligned with the clinical observations. mRNA and protein expressions for both OAT1 and OAT3 increased with age with TM_{50} of approximately 5 months and 8 months, respectively. Further, inter-transporter correlation analysis also demonstrated that these two transporters were highly correlated in their gene and protein expression.[36]

OCT2: Similar to OATs and P-gp, the OCT2 mRNA levels and protein abundance are age-dependent with the levels in newborns being significantly lower compared to children and adults. Like P-gp, OCT2 would reach half of the adult level about one month after birth.[36]

Recent knowledge gain on renal transporters

The data from gene expression analysis, quantitative proteomics and immunohistochemistry have painted a more complete picture for the ontogeny of renal membrane transporters. Within the six transporters that are clinically important and should be carefully considered in drug development, four of them, P-gp, OAT1, OAT3 and OCT2, showed age-dependent increase in their expression levels. This implies that drug substrates of these transporters would also be subject to age-dependent changes and might impact the elimination of these drugs in pediatric patients. Despite this increase in knowledge, more studies on term and preterm neonates would be needed to better capture the variability in the age-related changes of transporter expression, and also the interplay with maturation of glomerular filtration, during this rapid developmental phase of life.[52,53]

APPLICATION OF ONTOGENY OF TRANSPORTERS TO MIDD IN CHILDREN

Overall, there has been a recent surge in data on the ontogeny of membrane transporters, which will greatly enhance our understanding in not only the disposition of drug substrates but the involvement of these transporters in developmental physiology in children. While scarce data in the ontogeny of intestinal transporters still limits their application to modeling and simulation of oral drugs, the wealth of data in the domain of hepatic and renal transporter ontogeny present an opportunity to be leveraged for pediatric PBPK modeling, especially for intravenous administrated drugs, to assist the prediction in drug disposition and clearance in children.

The workflow of pediatric PBPK model development has been previously described (see Figure 2).[54-57] In most cases, an adult PBPK model is first established, verified and refined. This model is comprised of the drug profile as well as the virtual adult population in

Figure 2 Workflow of the pediatric physiologically-based pharmacokinetic model (PBPK) establishment to simulate drug exposure in children.

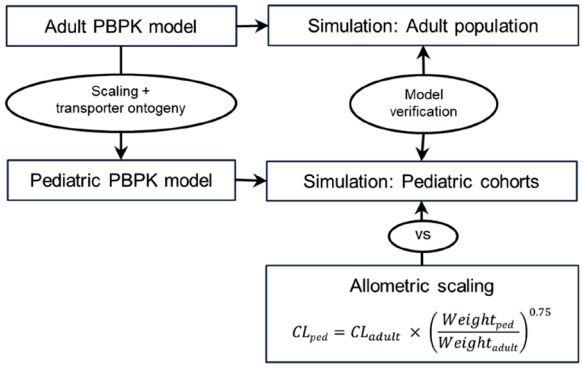

An adult PBPK model was first established and verified by comparing the output from the simulations to that in observed data. After ensuring that adult model was robust, the pediatric model was generated by scaling the anatomical and physiological parameters using default age-dependent algorithms, and incorporating ontogeny information for the transporters that are pertinent to this study. The pediatric PBPK model was verified, once again, by comparing the output from the simulation input with observed data from literature. Predictive performance of allometry and PBPK in estimating the clearance in children was also evaluated.

which transporter protein abundance data and kinetics parameters, such as Km and Vmax, can be incorporated to predict the organ-specific clearance (CL).[58] Following the finalization and verification of the robust adult PBPK model, pediatric models could be generated by modifying the population-specific inputs (e.g. blood flow to organs, organ weights and protein abundance of drug metabolizing enzymes and transporters) using algorithms or parameters such as ontogeny scaling factor for transporter abundance or

intrinsic clearance. These are expressed as a function of age and can be derived from the developmental changes in the expression data described in previous section. Of note, while pediatric PBPK models can also be established based on drug physiological properties and preclinical data alone, this approach could lead to a lower confidence in the prediction compared to a model that is verified with adult clinical data.

The success and confidence of PBPK modeling and simulation that involves transporter-mediated disposition using bottom-up approach are critically dependent on factors such as the quality and availability of transporter kinetic data and understanding in in vitro-in vivo correlation. The following case study illustrates that the utility of leveraging transporter ontogeny data in PBPK modeling, with sufficient information gathered, can be useful to simulate drug exposure in pediatric patients.[59]

Figure 3 The elimination pathway of tazobactam.

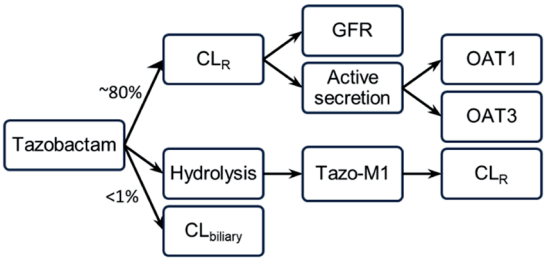

After intravenous administration, approximately 80% of tazobactam would be cleared renally by glomerular filtration and active secretion via OAT1 and OAT3. Majority of the rest of tazobactam would undergo hydrolysis to form the inactive metabolite, tazo-M1, which, similar to the parent drug, will be eliminated renally. A small amount (<1%) of tazobactam would undergo biliary excretion.

PBPK modeling with integrated transporter ontogeny reasonably predicted the exposure of an actively renally secreted drug in children

Tazobactam is a beta-lactamase inhibitor. Currently, it is formulated as an intravenously-administered combination product with either piperacillin, a beta-lactam, or ceftolozane, a cephalosporin, as a broad-spectrum antibiotic.[60,61] Tazobactam is prescribed for infections that could potentially be life threatening when left untreated. Hence sufficient exposure is needed to assure therapeutic action without adverse events. As much as 80% of tazobactam is renally cleared in adults.[61,62] In addition to glomerular filtration, tazobactam undergoes active tubular secretion that is mediated by OAT1 and OAT3.[62,63] The remaining tazobactam is either converted to the inactive metabolite, M1, via hydrolysis and then eliminated renally or undergoes biliary excretion (Figure 3).[62,64]

The workflow of the adult and pediatric PBPK model establishment is summarized in Figure 2. OAT1/ 3 protein abundance and transporter kinetics from *in vitro* studies are

obtained from literature.[36,63] The ontogeny scaling factors, which are the sigmoidal Emax functions, of OAT1/3 were incorporated.[36] To address the argument on whether PBPK modeling is preferred over an allometric scaling approach in predicting the PK for pediatric patients < 2 years old, the clearance in the pediatric cohorts were also estimated based on allometry and compared to that predicted using PBPK models.[9]

Figure 4 Simulation of tazobactam exposure in adult population (a) and three pediatric cohorts (b – d) using PBPK (PK-Sim v7.3).

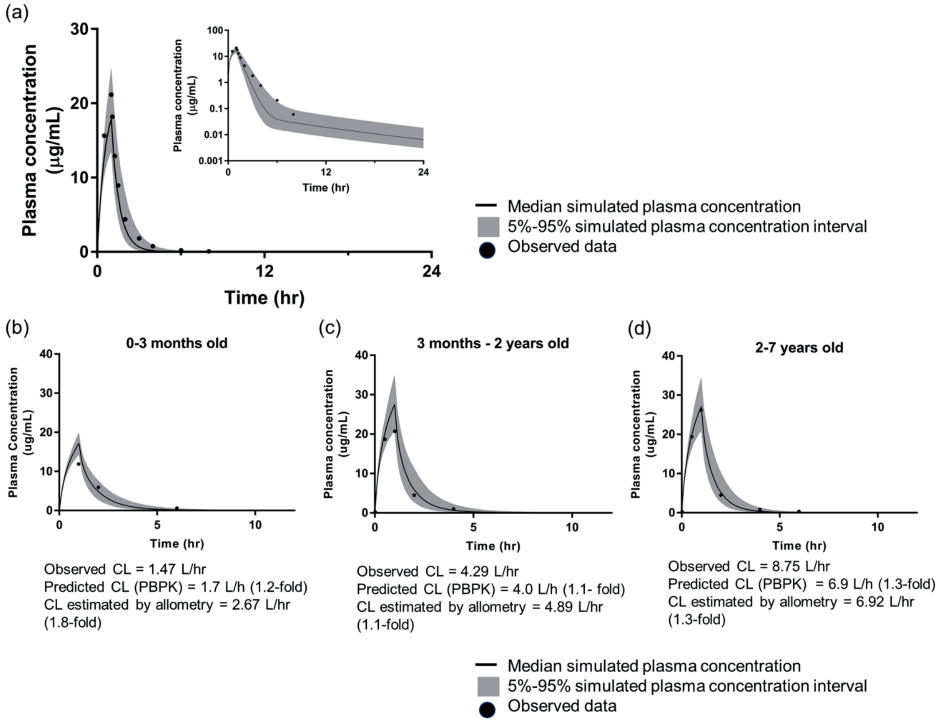

Following 500mg x 60min infusion in the virtual adult population, the predicted Cmax, AUC and CL were between 1.02-1.2-fold of the observed data.[65] Three pediatric cohorts were generated: 0-3 months old (b), 3 months-2 years old (c), and 2-7 years old (d). By taking into account the physiological and anatomical changes during development, and the ontogeny of transporters that are pertinent to the disposition of tazobactam, the tazobactam exposure was predicted reasonably well with Cmax, AUC and CL were all within 1.5-fold of observed data.[66] Allometric scaling approach resulted in CL estimation that were comparable to that predicted using PBPK. However, for the youngest age group, 0-3 months old (b), PBPK model performed slightly better as allometry slightly overpredicted the CL (1.2-fold vs 1.8-fold of observed CL).

The PBPK model captured the exposure of tazobactam after 500mg x 60min IV infusion in adults well with the predicted maximal concentration (C_{max}), area under the curve (AUC) and clearance (CL) between 1.02- to-1.2-fold of the observed data (Fig 4a).[65] After verifying and ensuring that the adult model was robust, three virtual pediatric populations were generated using the approach as outlined above: 0 to 3 months, 3 months to 2 years old, 2 to 7 years old. C_{max}, AUC and CL were all within 1.5-fold of observed data when the simulation was performed in these three cohorts, suggesting that the pediatric PBPK model predicted the exposure of tazobactam adequately in neonates, infants and children (Fig 4b).[66] Significantly, allometric scaling approach resulted in CL estimations that were comparable to that predicted using PBPK. However, for the youngest age group, 0-3 months old, PBPK model performed slightly better as allometry slightly overpredicted the CL (1.2-fold vs 1.8-fold of observed CL).

This case study illustrated the utility of a pediatric PBPK model with integrated renal transporter ontogeny function in simulating exposure of a drug that is actively renally secreted in pediatric patients. It exemplifies how this approach could be applied in pediatric drug development to support decision-making on dosing to limit unnecessary exposure in pediatric patients. Further, it also highlighted how a PBPK model can be used to complement allometric scaling approach by predicting the whole PK (concentration-time) profile, rather than just the drug clearance.

CONSIDERATIONS

The recent emergence of quantitative proteomics data on the expression and ontogeny of transporters substantially improves the predictive power of pediatric PBPK models for drug substrates. Nonetheless, there are important factors that need to be considered when incorporating protein abundance into PBPK models. While LC-MS/MS based quantitative proteomics is a powerful tool by using peptide sequences to measure the absolute abundance of transporter proteins, it could not acknowledge if the transporters are successfully localized to the membrane, nor could it distinguish truncated protein and splice variants from properly formed proteins, and glycosylated and not-glycosylated protein.[67] Consequently, these would undermine the assumed correlation between transporter expression and activity. Further, scaling from the protein abundance data per *crude membrane protein* or *per gram tissue* level to per *organ* level is the first step when integrating such data into PBPK. This should be done carefully as parameters that are used to scale, such as membrane protein yield per gram of tissue could also subject to age-related changes.[28] Lastly, it is important to reiterate that the success of PBPK simulation in children using bottom-up approach depends highly on the

knowledge in the drug disposition pathway and the data available for the ontogeny of the metabolic enzymes and transporter involved. For instance, with good understanding in the maturational differences between UGT enzymes and sulfotransferase, one study successfully predicted the exposure, as well as metabolic formation and elimination of acetaminophen, which is mainly glucuronidated in adults but almost exclusively sulfated in newborn due to age-dependent changes in the UGT enzymes expression and activity, in various pediatric age groups using PBPK.[68] Nonetheless, for drugs that are substrates of certain metabolic enzymes and transporters of which the developmental changes are not fully understood, results from the simulation should be interpreted carefully.

CONCLUSION/FUTURE DIRECTION

Collectively, international collaborative efforts have greatly improved the understanding of the role of transporters in drug PK, PD, safety and efficacy not only in adults but also in specific populations such as pediatrics. This understanding is supported by the expansion of knowledge in the ontogeny of membrane transporters, especially those in the liver and kidney. This increased knowledge has significant implications for PBPK modeling for drug substrates and therefore is of great importance for pediatric drug development. However, knowledge gaps in the ontogeny of transporters in the intestine and other important barrier tissues such as the blood-brain barrier remain, and are awaiting to be addressed through future collaborative work. Further investigation would also be required to elucidate how gene and protein expression relate to transporter activity. Lastly, as illustrated in the case study, in addition to ontogeny, a thorough understanding of the disposition of drugs and their interplay are critical in the application of PBPK to adequately predict drug exposure in children.

REFERENCES

1. 'T Jong GW, Eland IA, Sturkenboom MC, van den Anker JN, Stricker BH. Unlicensed and off label prescription of drugs to children: population based cohort study. BMJ 2002;324(7349):1313-1314.
2. Institute of Medicine (US) Forum on Drug Discovery D, and Translation,. Addressing the barriers to pediatric drug development: workshop summary. . In: The National Academies Collection: Reports Funded by National Institutes of Health Washington (DC): National Academies Press (US); 2008.
3. Rodieux F, Wilbaux M, van den Anker JN, Pfister M. Effect of Kidney Function on Drug Kinetics and Dosing in Neonates, Infants, and Children. Clin Pharmacokinet 2015;54(12):1183-1204.
4. U.S. Food and Drug Administration. Best Pharmaceuticals for Children Act and Pediatric Research Equity Act. https://www.fda.gov/science-research/pediatrics/best-pharmaceuticals-children-act-and-pediatric-research-equity-act. Accessed May 16, 2019.
5. European Medicines Agency. Paediatric Regulation. https://www.ema.europa.eu/en/human-regulatory/overview/paediatric-medicines/paediatric-regulation. Accessed June 13, 2019.
6. European Medicines Agency. 10-year Report to the European Commission: General report on the experience acquired as a result of the application of the Paediatric Regulation (EMA/231225/2015). 2016.
7. Wang Y, Zhu H, Madabushi R, Liu Q, Huang SM, Zineh I. Model-Informed Drug Development: Current US Regulatory Practice and Future Considerations. Clin Pharmacol Ther 2019;105(4):899-911.
8. US Food and Drug Administration. PDUFA reauthorization performance goals and procedures fiscal years 2018 through 2022. https://www.fda.gov/industry/prescription-drug-user-fee-amendments/pdufa-vi-fiscal-years-2018-2022. Accessed May 14, 2019.
9. Grimstein M, Yang Y, Zhang X, et al. Physiologically Based Pharmacokinetic Modeling in Regulatory Science: An Update From the U.S. Food and Drug Administration's Office of Clinical Pharmacology. J Pharm Sci 2019;108(1):21-25.
10. Committee for Human Medicinal Products EMA. ICH E11(R1) guideline on clinical investigation of medicinal products in the pediatric population. https://www.ema.europa.eu/en/documents/scientific-guideline/ich-e11r1-guideline-clinical-investigation-medicinal-products-pediatric-population-revision-1_en.pdf. Accessed June 12, 2019.
11. US Food and Drug Administration. 2012 Meeting Materials, Pharmaceutical Science and Clinical Pharmacology Advisory Committee. http://wayback.archive-it.org/7993/20170111202603/http://www.fda.gov/AdvisoryCommittees/CommitteesMeetingMaterials/Drugs/AdvisoryCommitteeforPharmaceuticalScienceandClinicalPharmacology/ucm286697.htm. Accessed May 19, 2019.
12. Zhang L, Huang SM, Reynolds K, Madabushi R, Zineh I. Transporters in Drug Development: Scientific and Regulatory Considerations. Clin Pharmacol Ther 2018;104(5):793-796.
13. US Food and Drug Administration. In Vitro Metabolism- and Transporter- Mediated Drug-Drug Interaction Studies Guidance for Industry. 2017;https://www.fda.gov/regulatory-information/search-fda-guidance-documents/vitro-metabolism-and-transporter-mediated-drug-drug-interaction-studies-guidance-industry. Accessed May 15, 2019.
14. Brouwer KL, Aleksunes LM, Brandys B, et al. Human ontogeny of drug transporters: review and recommendations of the pediatric transporter working group. Clin Pharmacol Ther 2015;98(3):266-287.

15. Prasad B, Johnson K, Billington S, et al. Abundance of Drug Transporters in the Human Kidney Cortex as Quantified by Quantitative Targeted Proteomics. Drug Metab Dispos 2016;44(12):1920-1924.
16. Chu X, Liao M, Shen H, et al. Clinical Probes and Endogenous Biomarkers as Substrates for Transporter Drug-Drug Interaction Evaluation: Perspectives From the International Transporter Consortium. Clin Pharmacol Ther 2018;104(5):836-864.
17. Mizuno T, Fukuda T, Masuda S, et al. Developmental trajectory of intestinal MDR1/ABCB1 mRNA expression in children. Br J Clin Pharmacol 2014;77(5):910-912.
18. Fakhoury M, de Beaumais T, Guimiot F, et al. mRNA expression of MDR1 and major metabolising enzymes in human fetal tissues. Drug Metab Pharmacokinet 2009;24(6):529-536.
19. Fakhoury M, Lecordier J, Medard Y, Peuchmaur M, Jacqz-Agrain E. Impact of inflammation on the duodenal mRNA expression of CYP3A and P-glycoprotein in children with Crohn's disease. Inflamm Bowel Dis 2006;12(8):745-749.
20. Fakhoury M, Litalien C, Medard Y, et al. Localization and mRNA expression of CYP3A and P-glycoprotein in human duodenum as a function of age. Drug Metab Dispos 2005;33(11):1603-1607.
21. Miki Y, Suzuki T, Tazawa C, Blumberg B, Sasano H. Steroid and xenobiotic receptor (SXR), cytochrome P450 3A4 and multidrug resistance gene 1 in human adult and fetal tissues. Mol Cell Endocrinol 2005;231(1-2):75-85.
22. van Kalken CK, Giaccone G, van der Valk P, et al. Multidrug resistance gene (P-glycoprotein) expression in the human fetus. Am J Pathol 1992;141(5):1063-1072.
23. Mooij MG, Schwarz UI, de Koning BA, et al. Ontogeny of human hepatic and intestinal transporter gene expression during childhood: age matters. Drug Metab Dispos 2014;42(8):1268-1274.
24. Konieczna A, Erdosova B, Lichnovska R, Jandl M, Cizkova K, Ehrmann J. Differential expression of ABC transporters (MDR1, MRP1, BCRP) in developing human embryos. J Mol Histol 2011;42(6):567-574.
25. Mooij MG, de Koning BE, Lindenbergh-Kortleve DJ, et al. Human Intestinal PEPT1 Transporter Expression and Localization in Preterm and Term Infants. Drug Metab Dispos 2016;44(7):1014-1019.
26. Hayashi M, Hui A, DeKeyser J, Louie S, Shou M, Xu L. Evaluation Of Uptake Transporters In Human Adult And Pediatric Hepatocytes. Abstracts of the 17th North American Regional ISSXInternational Society for the Study of Xenobiotics. Drug Metab Rev;43:198.
27. Hahn D, Emoto C, Vinks AA, Fukuda T. Developmental Changes in Hepatic Organic Cation Transporter OCT1 Protein Expression from Neonates to Children. Drug Metab Dispos 2017;45(1):23-26.
28. van Groen BD, van de Steeg E, Mooij MG, et al. Proteomics of human liver membrane transporters: a focus on fetuses and newborn infants. Eur J Pharm Sci 2018;124:217-227.
29. Prasad B, Gaedigk A, Vrana M, et al. Ontogeny of hepatic drug transporters as quantified by LC-MS/MS proteomics. Clin Pharmacol Ther 2016;100(4):362-370.
30. Sharma S, Ellis EC, Gramignoli R, et al. Hepatobiliary disposition of 17-OHPC and taurocholate in fetal human hepatocytes: a comparison with adult human hepatocytes. Drug Metab Dispos 2013;41(2):296-304.
31. Prasad B, Evers R, Gupta A, et al. Interindividual variability in hepatic organic anion-transporting polypeptides and P-glycoprotein (ABCB1) protein expression: quantification by liquid chromatography tandem mass spectroscopy and influence of genotype, age, and sex. Drug Metab Dispos 2014;42(1):78-88.

32. Chen HL, Chen HL, Liu YJ, et al. Developmental expression of canalicular transporter genes in human liver. J Hepatol 2005;43(3):472-477.
33. Yanni SB, Smith PB, Benjamin DK, Jr., Augustijns PF, Thakker DR, Annaert PP. Higher clearance of micafungin in neonates compared with adults: role of age-dependent micafungin serum binding. Biopharm Drug Dispos 2011;32(4):222-232.
34. Tang L. Age-Associated Hepatic Drug Transporter Expression and Its Implication. Theses and Dissertations (ETD). Paper 260. 2007;http://dx.doi.org/10.21007/etd.cghs.2007.0312.
35. Klaassen CD, Aleksunes LM. Xenobiotic, bile acid, and cholesterol transporters: function and regulation. Pharmacol Rev 2010;62(1):1-96.
36. Wun Kathy Cheung K, van Groen BD, Spaans E, et al. A comprehensive analysis of ontogeny of renal drug transporters: mRNA analyses, quantitative proteomics and localization. Clin Pharmacol Ther 2019.
37. Mooij MG, de Koning BA, Huijsman ML, de Wildt SN. Ontogeny of oral drug absorption processes in children. Expert Opin Drug Metab Toxicol 2012;8(10):1293-1303.
38. Muller J, Keiser M, Drozdzik M, Oswald S. Expression, regulation and function of intestinal drug transporters: an update. Biol Chem 2017;398(2):175-192.
39. Estudante M, Morais JG, Soveral G, Benet LZ. Intestinal drug transporters: an overview. Adv Drug Deliv Rev 2013;65(10):1340-1356.
40. Tamai I. Oral drug delivery utilizing intestinal OATP transporters. Adv Drug Deliv Rev 2012;64(6):508-514.
41. Kramer W. Transporters, Trojan horses and therapeutics: suitability of bile acid and peptide transporters for drug delivery. Biol Chem 2011;392(1-2):77-94.
42. Kobayashi D, Nozawa T, Imai K, Nezu J, Tsuji A, Tamai I. Involvement of human organic anion transporting polypeptide OATP-B (SLC21A9) in pH-dependent transport across intestinal apical membrane. J Pharmacol Exp Ther 2003;306(2):703-708.
43. Sai Y, Kaneko Y, Ito S, et al. Predominant contribution of organic anion transporting polypeptide OATP-B (OATP2B1) to apical uptake of estrone-3-sulfate by human intestinal Caco-2 cells. Drug Metab Dispos 2006;34(8):1423-1431.
44. Oswald S. Organic Anion Transporting Polypeptide (OATP) transporter expression, localization and function in the human intestine. Pharmacol Ther 2019;195:39-53.
45. Keiser M, Kaltheuner L, Wildberg C, et al. The Organic Anion-Transporting Peptide 2B1 Is Localized in the Basolateral Membrane of the Human Jejunum and Caco-2 Monolayers. J Pharm Sci 2017;106(9):2657-2663.
46. Mooij MG, van de Steeg E, van Rosmalen J, et al. Proteomic analysis of the developmental trajectory of human hepatic membrane transporter proteins in the first three months of life. Drug Metab Dispos 2016;44(7):1005-1013.
47. Hahn D, Emoto C, Euteneuer JC, Mizuno T, Vinks AA, Fukuda T. Influence of OCT1 Ontogeny and Genetic Variation on Morphine Disposition in Critically Ill Neonates: Lessons From PBPK Modeling and Clinical Study. Clin Pharmacol Ther 2019;105(3):761-768.
48. Fernandez E, Perez R, Hernandez A, Tejada P, Arteta M, Ramos JT. Factors and Mechanisms for Pharmacokinetic Differences between Pediatric Population and Adults. Pharmaceutics 2011;3(1):53-72.
49. Alcorn J, McNamara PJ. Ontogeny of hepatic and renal systemic clearance pathways in infants: part II. Clin Pharmacokinet 2002;41(13):1077-1094.
50. Burckhardt G, Bahn A, Wolff NA. Molecular physiology of renal p-aminohippurate secretion. News Physiol Sci 2001;16:114-118.

51. Cha SH, Sekine T, Fukushima JI, et al. Identification and characterization of human organic anion transporter 3 expressing predominantly in the kidney. Mol Pharmacol 2001;59(5):1277-1286.
52. Rhodin MM, Anderson BJ, Peters AM, et al. Human renal function maturation: a quantitative description using weight and postmenstrual age. Pediatr Nephrol 2009;24(1):67-76.
53. Faa G, Gerosa C, Fanni D, et al. Morphogenesis and molecular mechanisms involved in human kidney development. J Cell Physiol 2012;227(3):1257-1268.
54. Maharaj AR, Edginton AN. Physiologically based pharmacokinetic modeling and simulation in pediatric drug development. CPT Pharmacometrics Syst Pharmacol 2014;3:e150.
55. Hornik CP, Wu H, Edginton AN, Watt K, Cohen-Wolkowiez M, Gonzalez D. Development of a Pediatric Physiologically-Based Pharmacokinetic Model of Clindamycin Using Opportunistic Pharmacokinetic Data. Clin Pharmacokinet 2017;56(11):1343-1353.
56. Leong R, Vieira ML, Zhao P, et al. Regulatory experience with physiologically based pharmacokinetic modeling for pediatric drug trials. Clin Pharmacol Ther 2012;91(5):926-931.
57. Salerno SN, Burckart GJ, Huang SM, Gonzalez D. Pediatric Drug-Drug Interaction Studies: Barriers and Opportunities. Clin Pharmacol Ther 2019;105(5):1067-1070.
58. Guo Y, Chu X, Parrott NJ, et al. Advancing Predictions of Tissue and Intracellular Drug Concentrations Using In Vitro, Imaging and Physiologically Based Pharmacokinetic Modeling Approaches. Clin Pharmacol Ther 2018;104(5):865-889.
59. Cheung K, Zhang L, S-M. H, Giacomini KM. PBPK models with integrated renal transporter ontogeny predict systemic exposure to tazobactam, oseltamivir and oseltamivir carboxylate in children. Clin Pharmacol Ther 2019;105(S1):S8.
60. Zosyn [Package insert]. 2017.
61. Zerbaxa [Package insert]. 2014.
62. Sorgel F, Kinzig M. The chemistry, pharmacokinetics and tissue distribution of piperacillin/tazobactam. J Antimicrob Chemother 1993;31 Suppl A:39-60.
63. Wen S, Wang C, Duan Y, et al. OAT1 and OAT3 also mediate the drug-drug interaction between piperacillin and tazobactam. Int J Pharm 2018;537(1-2):172-182.
64. Westphal JF, Brogard JM, Caro-Sampara F, et al. Assessment of biliary excretion of piperacillin-tazobactam in humans. Antimicrob Agents Chemother 1997;41(8):1636-1640.
65. Miller B, Hershberger E, Benziger D, Trinh M, Friedland I. Pharmacokinetics and safety of intravenous ceftolozane-tazobactam in healthy adult subjects following single and multiple ascending doses. Antimicrob Agents Chemother 2012;56(6):3086-3091.
66. Bradley JS, Ang JY, Arrieta AC, et al. Pharmacokinetics and Safety of Single Intravenous Doses of Ceftolozane/Tazobactam in Children With Proven or Suspected Gram-Negative Infection. Pediatr Infect Dis J 2018;37(11):1130-1136.
67. Achour B, Dantonio A, Niosi M, et al. Data Generated by Quantitative Liquid Chromatography-Mass Spectrometry Proteomics Are Only the Start and Not the Endpoint: Optimization of Quantitative Concatemer-Based Measurement of Hepatic Uridine-5′-Diphosphate-Glucuronosyltransferase Enzymes with Reference to Catalytic Activity. Drug Metab Dispos 2018;46(6):805-812.
68. Jiang XL, Zhao P, Barrett JS, Lesko LJ, Schmidt S. Application of physiologically based pharmacokinetic modeling to predict acetaminophen metabolism and pharmacokinetics in children. CPT Pharmacometrics Syst Pharmacol 2013;2:e80.

PART II

– to bench –

4 Proteomics of human liver membrane transporters: a focus on fetuses and newborn infants

Bianca D van Groen, Evita van de Steeg, Miriam G Mooij, Marola MH van Lipzig, Barbara AE de Koning, Robert M Verdijk, Heleen M Wortelboer, Roger Gaedigk, Chengpeng Bi, J Steven Leeder, Ron HN van Schaik, Joost van Rosmalen, Dick Tibboel, Wouter H Vaes, Saskia N de Wildt

Eur J Pharm Sci. 2018 Nov 1;124:217-227. DOI: 10.1016/J.EJPS.2018.08.042.

ABSTRACT

Background: Hepatic membrane transporters are involved in the transport of many endogenous and exogenous compounds, including drugs. We aimed to study the relation of age with absolute transporter protein expression in a cohort of 62 mainly fetus and newborn samples.

Methods: Protein expressions of BCRP, BSEP, GLUT1, MCT1, MDR1, MRP1, MRP2, MRP3, NTCP, OCT1, OATP1B1, OATP1B3, OATP2B1 and ATP1A1 were quantified with LC-MS/MS in isolated crude membrane fractions of snap-frozen post mortem fetal and pediatric, and surgical adult liver samples. mRNA expression was quantified using RNA sequencing, and genetic variants with TaqMan assays. We explored relationships between protein expression and age (gestational age [GA], postnatal age [PNA], and postmenstrual age); between protein and mRNA expression; and between protein expression and genotype.

Results: We analyzed 36 fetal (median GA 23.4 weeks [range 15.3-41.3]), 12 premature newborn (GA 30.2 weeks [24.9-36.7], PNA 1.0 weeks [0.14-11.4]), 10 term newborn (GA 40.0 weeks [39.7-41.3], PNA 3.9 weeks [0.3-18.1]), 4 pediatric (PNA 4.1 years [1.1-7.4]) and 8 adult liver samples. A relationship with age was found for BSEP, BCRP, GLUT1, MDR1, MRP1, MRP2, MRP3, NTCP and OATP1B1, with the strongest relationship for postmenstrual age. For most transporters mRNA and protein expression were not correlated. No genotype-protein expression relationship was detected.

Discussion and conclusion: Various developmental patterns of protein expression of 13 hepatic transporters emerged in fetuses and newborns up to four months of age. Postmenstrual age was the most robust factor predicting transporter expression in this cohort. Our data fill an important gap in current pediatric transporter ontogeny knowledge.

INTRODUCTION

Membrane-embedded transporter proteins are crucial in handling endogenous and exogenous compounds. More specifically, hepatic transporters are critical determinants in drug distribution, metabolism and biliary secretion, as they facilitate influx and efflux of substrates from hepatocytes, where metabolism takes place.[1]

Children admitted to a neonatal or pediatric intensive care unit may receive many drugs. Earlier it was shown that infants with normal weight received on average four different drugs, and infants with an extreme low birth weight, often prematurely born, up to 17 drugs.[2] Many of these drugs are substrates for transporters[3], and the expression and activity of certain transporters are known to be subject to age-related changes.[1] An example of a transporter substrate is morphine, which is widely used in newborns and children. Morphine is taken up into the hepatocyte by the transporter OCT1, where it is glucuronidated mainly by UGT2B7.[4] Data suggest lower protein expression of hepatic OCT1 in younger age groups[5,6], leading to elevated plasma levels and therefore posing a higher risk of adverse events like respiratory depression. However, the exact developmental pattern of OCT1 in fetuses and premature newborns is not known, while data for other transporters are also scarce or even lacking.[1,3]

In neonates and young infants, age can be defined in various ways: gestational age (GA) - reflecting duration of pregnancy at birth; postnatal age (PNA) – the age after birth; and postmenstrual age (PMA) – the combination of gestational age and postnatal age. Both GA and birth are important determinants of postnatal gene expression of drug metabolizing enzymes.[7] We hypothesize that this also accounts for drug transporters. More insight in the relative importance of these determinants could help personalize drug dosing in this young vulnerable population.

Previously, we explored the hepatic protein expressions of 10 clinically relevant transporters in 25 liver samples from fetuses, neonates and young infants.[8] Protein expression of a number of these transporters was related to age, and important transporter-specific differences were found. While this exploratory study was clearly informative, the sample size was too small to define transporter-specific maturational patterns. A recent publication from Prasad et al. describes the postnatal ontogeny of hepatic drug transporters in a wider cohort, but the younger ages (<four months) were not well represented.[6] Data on gene expression of transporters in the younger ages are richer[1,8], but lack of correlation between gene and protein expression restricts us from extrapolating these findings. Thus, knowledge of transporter protein expression is lacking for fetuses and ages up to 18 weeks PNA.

Besides ontogeny, drug transporter expression and activity can be influenced by genetic variants, as described in adults.[9] For *SLC22A1*/OCT1 a relationship with genotype was suggested by variation in the pharmacokinetics of tramadol, an OCT1 substrate, in preterm infants, even when *in vitro* data suggested developmentally low expression.[10] This is interesting as for some drug metabolizing enzymes the interplay between development and genetics obscures an effect of genetic variation. But pediatric clinical data for transporters substrates are scarce.

In the current study we aimed to elucidate the developmental expression patterns of various hepatic drug transporters in an expanded cohort of mainly fetal and newborn samples up to 18 weeks PNA, also including the samples from our previous pilot study. The large variation in GA and PNA in this cohort enabled us to analyze whether PNA or PMA correlates strongest with transporter expression. We also investigated correlation between protein expression and mRNA expression in a subset of this cohort, and analyzed whether genotype, in addition to age, explains the variability in expression of hepatic drug transporters. Expression patterns were compared to hepatic transporter proteins in stably transfected cell lines (HEK293 cells expressing OATP1B1, OATP1B3, or OCT1 and MDCKII cells expressing MDR1, MRP2 or BCRP) in order to be used for future PBPK modeling.

MATERIAL AND METHODS

Tissue samples

Post-mortem liver tissue samples from autopsy of fetuses (from therapeutic abortions or stillbirths) and infants were provided by the Erasmus MC Tissue Bank. Tissue was procured at the time of autopsy within 24 hours after death and snap-frozen at -80^{0}C for later research use. The Erasmus MC Research Ethics Board waived the need for formal ethics approval according to the Dutch Law on Medical Research in Humans. Tissue was collected when parental written informed consent for both autopsy and the explicit use of the tissue for research was present. The samples were selected when the clinical diagnosis of the patient was not related to hepatic problems and the tissue was histologically normal (Supplemental Table 1).

Human adult liver tissue samples were a gift from Prof. G.M.M. Groothuis (University of Groningen, Groningen, the Netherlands) (n=3) and Prof. P. Artursson (Uppsala University, Uppsala, Sweden) (n=5). These had been collected anonymously as surgical waste material after partial hepatectomy because of liver metastasis. For these samples, a no-

objection clause permitted use for research purposes in line with the Dutch guidelines on secondary use of human tissue.

Selection of hepatic transporters

Thirteen clinically relevant hepatic transporters were selected (*gene name*/protein name): breast cancer resistance protein (*ABCG2*/BCRP), bile salt export pump (*ABCB11*/BSEP), glucose transporter 1 (*SLC2A1*/GLUT1), monocarboxylate transporter 1 (*SLC16A1*/MCT1), multidrug resistance protein 1 (*ABCB1*/MDR1), multidrug resistance associated protein (*ABCC*/MRP) 1, 2 and 3, sodium-taurocholate cotransporting polypeptide (*SLC10A1*/NTCP), organic anion-transporting polypeptide (*SLCO*/OATP) 1B1, 1B3 and 2B1, and organic cation transporter 1 (*SLC22A1*/OCT1). Analysis on the transporters MRP1, NTCP, OATP1B3 and OCT1 was lacking in our pilot study[8], but was added in this expanded study because of their clinical relevance. We also selected ATP1A1, which is often used as a housekeeping protein.[6]

Protein expression

Absolute transporter protein expression of the selected hepatic drug transporters was quantified in crude membrane fractions in all samples, including the samples from our pilot-study, using LC-MS/MS as previously described[11], with some minor modifications regarding isolation of the membrane fractions (see below). Crude membrane fractions include nuclei, mitochondria as well as the microsomal and plasma membranes. Absolute transporter expression was also determined in cell pellets of HEK-OATP1B1, -OATP1B3, -OCT1, MDCKII-MDR1, -MRP2, and –BCRP cells.

Isolation of crude membrane fractions from tissue samples was conducted as follows. Approximately 10 mg liver tissue or approximately 20 x 10^6 cells was homogenized in a hypotonic buffer (0.5 mM sodium phosphate, 0.1 mM EDTA, and a cocktail of protease inhibitors containing 2 mM phenylmethylsulfonylfluoride, aprotinin, leupeptin, and pepstatin) using a Potter-Elvehjem homogenizer. The homogenate was centrifuged at 100,000 g for 30 min at 4°C using a LE-80k Centrifuge with an SW28 rotor (Beckman Coulter, Fullerton, CA, USA). This step was repeated, and the remaining pellet containing the crude membrane fraction was resuspended in 200 µL of isotonic buffer (10 mM Tris-HEPES and 250 mM sucrose (pH 7.4)). A maximum of 100 µg of crude membrane protein was used for tryptic digestion. Samples were diluted with 2 volumes of 90% methanol. The proteins were subsequently reduced with 0.01 M dithiothreitol at 37°C for 60 minutes and alkylated with 0.04 M iodoacetamide for 20 minutes at room temperature in the dark. Digestion was performed after addition of $CaCl_2$ (final concentration 1 nM) and 0.5 mg trypsin in 17% methanol by diluting the solution with 50 mM NH_4HCO_3. After overnight incubation the samples were incubated for another 2 hours with 0.5

mg trypsin to ensure complete digestion of the protein sample. The efficiency of the tryptic digestion using this protocol was previously checked using SDS-PAGE followed by silver stain, confirming complete digestion.[11] Finally the protein digests were evaporated by vacuum centrifugation (Scanvac, Ballerup, DK) and dissolved in 100 ml 15% acetonitrile containing 0.1% formic acid and 5 ng ml^{-1} internal standard (AQUA peptide mix, Supplemental Table 2). Samples were analyzed using an ultraperformance liquid chromatography coupled to a 6500 QTrap mass spectrometer (AB Sciex, Nieuwerkerk aan den IJssel, the Netherlands). Multiple reaction monitoring transitions were determined from tandem mass spectra, obtained by direct infusion of 0.5 mg mL^{-1}. Per peptide, three transitions were chosen (Q3-1, Q3-2, and Q3-3) for quantification and confirmation. A peptide labeled with ^{15}N and ^{13}C (AQUA peptide) was synthesized (Sigma-Aldrich, Steinheim, DE) and used as an internal standard for quantification (Supplemental Table 2). Peak identification and quantification were performed using Analyst software version 1.6.

mRNA expression

mRNA expression of the selected drug transporters was determined in a subset of 31 samples using RNA-Sequencing (RNA-Seq). RNA was isolated from hepatic tissue using QiaSchredder column and RNeasy Mini kit (both Qiagen, Valencia, CA) as described by Mooij et al [12]. Samples with an RNA integrity number of <5 were excluded. The RNA-Seq experiments were performed according to the Illumina RNA-Seq protocol (San Diego, CA). In brief, a population of poly$(A)^+$ mRNA was selected and converted to a library of cDNA fragments (220–450 bp) with adaptors attached to both ends, using an Illumina mRNA-Seq sample preparation kit. The quality of the library preparation was confirmed by analysis on a 2100 Bioanalyzer (Agilent Technologies, Santa Clara, CA). The cDNA fragments were then sequenced on an Illumina HiSeq 2000 to obtain 100-bp sequences from both ends (paired end). The resulting reads were mapped by Bowtie 2[13] to the transcriptome constructed through annotated genes/transcripts according to the reference human genome GRCh37.61/hg19. The mapped reads were then assigned to transcripts from which the expression of each transcript is estimated by RSEM.[14] The counts of RNA-Seq fragments were used to indicate the amount of identified mRNA transcripts, presented in transcripts per million (TPM).[14]

For each transporter we calculated the total TPM values of all mRNA transcripts, and the TPM values of only the mRNA transcripts coding for a full functioning protein (Ensembl genome database). Correlation with protein levels as determined in the same sample was tested with Spearman's rank correlation coefficient.

Genetics

Single nucleotide polymorphisms (SNPs) were only selected when mRNA and/or protein expression of our selection of transporters was expected to be influenced, based on information in the PharmGKB database.[15] Liver samples of children were genotyped for these SNPs (Supplemental Table 3). Next, within a particular genotype the effect of age was studied. Adult samples were not genotyped for logistic reasons. Because previously the influence of diplotypes of *SLCO1B1* on protein expression was shown[9], we studied relationships between *SLCO1B1* *1A, *1B, *4, *5, *14 and *15 and protein expression.

DNA was isolated from liver tissue according to protocol using the DNeasy® Blood and Tissue Kit (Qiagen, Valencia, CA). DNA concentrations were measured on the Nanodrop® 1000 Spectrophotometer (Thermo Fisher Scientific®). The DNA isolates were diluted in 1X TE Buffer to a 10 ng μL^{-1} solution for SNP analysis. The SNPs were genotyped according to the TaqMan® allelic discrimination assays. The PCR program consisted of an initial denaturation and DNA polymerase activation step at 92°C for 20 s, followed by 40 cycles at 95°C for 3 s and 60°C for 30 s. All PCR reactions and post-PCR detection were performed on a 7500 Fast Real-Time PCR System (software version 2.3; Applied Biosystems).

Cell lines

HEK293 cells overexpressing *SLCO1B1* *1A (NM_006446.4 referring to wild-type; hereafter named *SLCO1B1*) or *SLCO1B3* (NM_019844.3) were generated as previously described by our group[11,16]. HEK293 cells, stably overexpressing *SLC22A1* (NM_003057.2), were generated in a similar way, by transfection with pIRES puro-OCT1 (internally designed, produced by Baseclear, Leiden, NL), applying puromycin selection pressure and selecting colonies for further analysis. MDCKII cells stably overexpressing MDR1, MRP2 or BCRP were licensed from The Netherlands Cancer Institute (NKI, Amsterdam).[17-19]

Data and statistical analysis

Data are expressed as median (range), unless otherwise stated. The relationship of age with protein expression levels was studied as follows: first, differences in expression between age groups were explored. We distinguished five age groups: fetal, premature newborn (GA <37 weeks; PNA 0 – 18 weeks), term newborn (GA >37 weeks, PNA 0 – 18 weeks), pediatric (1.5 – 18 year) and adult liver samples. Next, in the combined first three age groups (further referred to as fetal/newborn cohort) the correlation between age on a continuous scale (GA, PNA and PMA) and protein levels was assessed. Within a particular genotype the effect of age on transporter protein expression was studied as above. Relationship between mRNA expression and protein expression were studied with correlation.

Kruskal-Wallis tests with Dunn's post-hoc test were used for multiple comparisons between age groups, and Spearman's rank correlation coefficient was used for testing correlations. Influence of gender on transporter protein expression was tested with a Mann-Whitney U test. A two-sided significance level of $p<0.05$ is used throughout the paper. For Dunn's post-hoc test for multiple comparisons the adjusted p-values are reported, in which a correction for multiple testing for age groups is applied. Statistical analyses were performed using IBM SPSS Statistics software (SPSS Statistics for Windows, version 21.0; IBM, Armonk, NY).

RESULTS

Descriptive results

In total 71 hepatic tissue samples were available for the study, including 25 samples of our pilot study.[8] One sample was detected as an outlier due to inexplicably high transporter expression and was excluded. See Table 1 for the age distribution. Gender was known for the pediatric samples only: 35 male and 27 female. The Tissue Bank provided only the following clinical data: GA, PNA, gender, and main clinical diagnosis. The adult tissue was histologically normal tissue and no additional clinical data were available, due to the anonymous sample collection.

Table 1 Age distribution of study samples in each age group.

		All	Fetuses	Preterm newborns	Term newborns	Pediatrics	Adults
Age distribution	GA	NA	23.4 (15.3-41.3) weeks	30.2 (24.9-36.7) weeks	40.0 (39.7-41.3) weeks	NA	NA
	PNA	NA	NA	1.0 (0.14-11.4) weeks	3.86 (0.29-18.1) weeks	4.13 (1.08-7.44) years	NA

GA=gestational age, PNA=postnatal age, NA=not available.

Protein expression

The selected hepatic transporter proteins were detected in nearly all samples; in two samples MRP2 could not be detected. There was high variability in expression between transporters and between individual samples (Supplemental Table 4). Protein expression in males and females was similar (Supplemental Table 5). Crude membrane protein yield per mg tissue was higher in fetuses than in term newborns (Figure 1A). Moreover, it was negatively correlated with PNA and PMA in the fetal/newborn cohort (Figure 1B and 1C, respectively).

Figure 1 Crude membrane protein (CMP) yield per amount of hepatic tissue, presented for various age groups (A), and, for the fetal/newborn cohort, for postnatal age (PNA) (B) and postmenstrual age (PMA) (C). ρ=Spearmans rho.

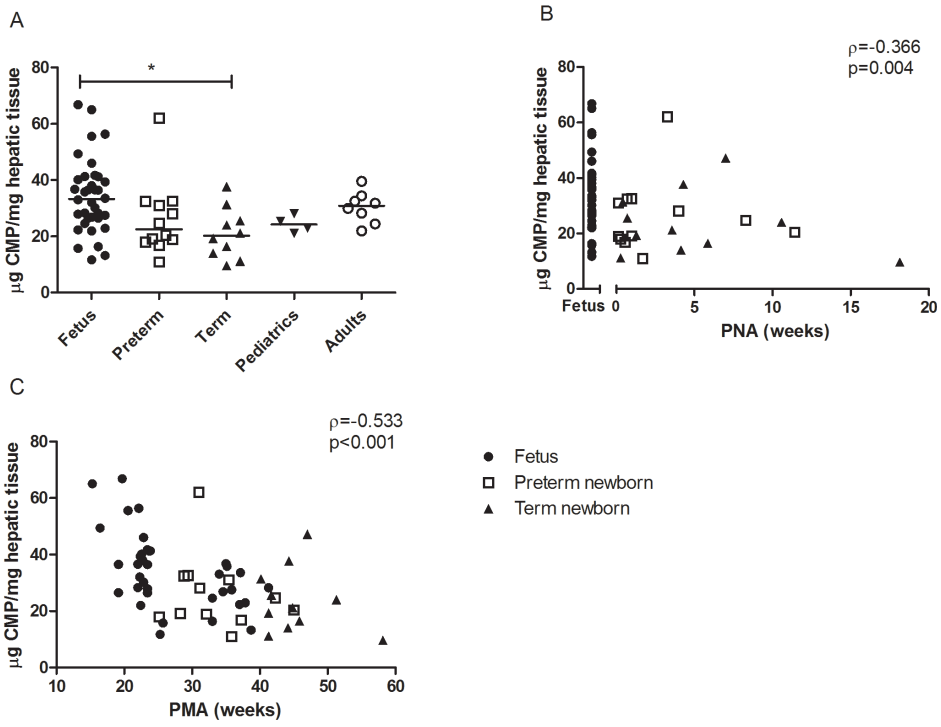

**Significant after Dunn's test (*p<0.05)*

Age-related transporter protein expression

Overall, protein expression was highly variable within age groups (Figure 2 and Supplemental table 4). More specifically, in fetal samples, BSEP and MDR1 protein expression was lower than in adult samples, and for BSEP also lower than in term newborn samples. MRP1, MRP2, MRP3 and OCT1 showed a similar developmental pattern with a lower protein expression in fetuses and newborns than in adults. NTCP levels increased over the whole age range. In contrast, GLUT1 protein levels were high in fetuses, with lower expression in term newborns, pediatrics and adults. Similarly, OATP1B1 showed high expression in the fetal age group and low expression in the term newborn age group, with stable protein levels further on. Protein expression levels of ATP1A1, BCRP, MCT1, OATP1B3 and OATP2B1 were similar in samples from all age groups.

Next, we analyzed whether GA, PNA and PMA within the fetal/newborn cohort could partly explain the observed variability (Table 2, Figure 3 and Figure 4). BCRP, BSEP and

Figure 2 Protein expression of hepatic transporters in fetuses (n=36), preterm newborns (n=12), term newborns (n=10), pediatrics (n=4) and adults (n=8).

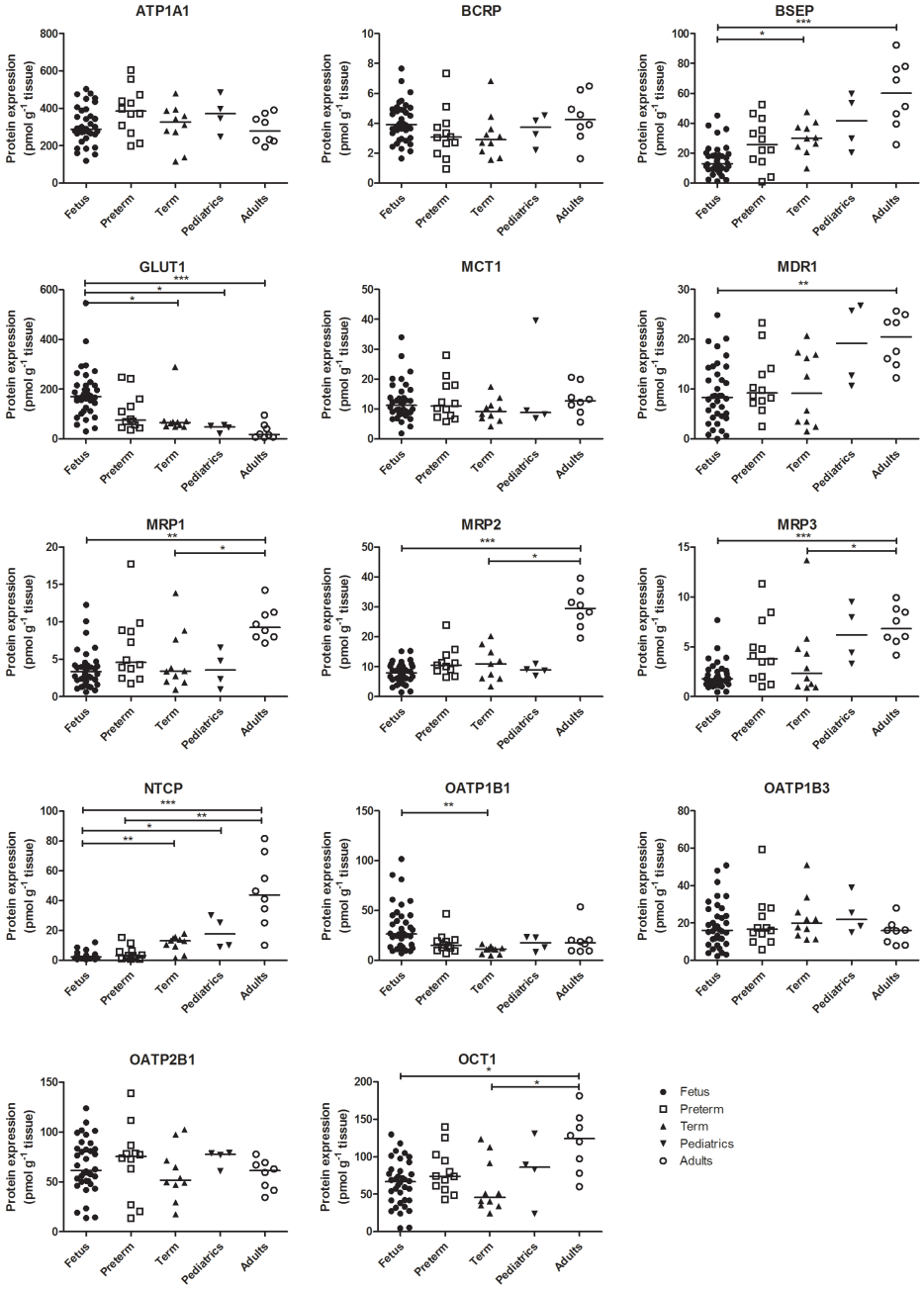

*Significant after Dunn's test (*p<0.05, **p<0.01, ***p<0.001)

NTCP expression significantly increased with increasing GA, PNA and PMA, whereas GLUT1 and OATP1B1 decreased. For these transporters the strongest correlation was shown for with PMA. MRP2 and MRP3 were only positively correlated with PNA, and MCT1 only with PMA. When only fetal samples (postnatal age = 0) are included, the relationship between GA and transporter expression remains statistically significant for GLUT1 and OATP1B1. For the other transporters no relationship between GA, PNA or PMA and expression was found.

Correlation mRNA- and protein expression

RNA-Seq data were generated from a representative subpopulation of 31 out of the 62 pediatric patients: 12 fetal (GA 29.7 weeks [15.3 – 41.3], no PNA), 8 premature newborn (GA 34.1 weeks [24.9 – 36.7], PNA 0.43 [0 – 8.29]), 7 term newborn (GA 40.0 weeks [39.7 – 41.3], PNA 3.57 [0.29 – 18.1]) and 4 pediatrics (PNA 4.13 years [1.08-7.44]). The mRNA expression levels and protein expression of ABCB11/BSEP, SLC16A1/MCT1, ABCC2/MRP2 and SLC10A1/NTCP were significantly correlated when using total TPM values of all mRNA transcripts (Supplemental Table 6). When only taking into account the mRNA transcripts actually known to be coding for protein, the correlation between mRNA expression and protein expression was lost for SLC16A1/MCT1, but appeared for ABCB1/MDR1 (Supplemental Table 6).

Table 2 Correlation of hepatic protein expression of transporters with age in fetal/newborn cohort.

Protein expression of	GA (n=58)†	GA (fetal) (n=36)‡	PNA (n=58)†	PMA (n=58)†
ATP1A1	ρ=0.120, p=0.371	ρ=0.113, p=0.513	ρ=0.145, p=0.278	ρ=0.069, p=0.605
BCRP	**ρ=-0.367, p=0.005**	ρ=-0.301, p=0.074	**ρ=-0.345, p=0.008**	**ρ=-0.421, p=0.001**
BSEP	**ρ=0.484, p<0.001**	ρ=0.230, p=0.178	**ρ=0.485, p<0.001**	**ρ=0.513, p<0.001**
GLUT1	**ρ=-0.536, p<0.001**	**ρ=-0.365, p=0.028**	**ρ=-0.512, p<0.001**	**ρ=-0.585, p<0.001**
MCT1	**ρ=-0.342, p=0.009**	ρ=-0.327, p=0.052	ρ=-0.096, p=0.473	**ρ=-0.345, p=0.008**
MDR1	ρ=-0.047, p=0.728	ρ=-0.119, p=0.489	ρ=0.064, p=0.634	ρ=-0.046, p=0.733
MRP1	ρ=0.069, p=0.608	ρ=-0.039, p=0.822	ρ=0.176, p=0.187	ρ=0.100, p=0.453
MRP2	ρ=0.202, p=0.136	ρ=0.084, p=0.625	**ρ=0.306, p=0.022**	ρ=0.214, p=0.114
MRP3	ρ=0.010, p=0.942	ρ=-0.218, p=0.202	**ρ=0.273, p=0.038**	ρ=0.032, p=0.812
NTCP	**ρ=0.502, p<0.001**	ρ=0.223, p=0.190	**ρ=0.453, p<0.001**	**ρ=0.567, p<0.001**
OATP1B1	**ρ=-0.557, p<0.001**	**ρ=-0.343, p=0.041**	**ρ=-0.481, p<0.001**	**ρ=-0.604, p<0.001**
OATP1B3	ρ=0.089, p=0.508	ρ=-0.043, p=0.804	ρ=0.090, p=0.499	ρ=0.072, p=0.589
OATP2B1	ρ=-0.135, p=0.312	ρ=-0.102, p=0.554	ρ=0.005, p=0.970	ρ=-0.092, p=0.494
OCT1	ρ=-0.206, p=0.121	ρ=-0.278, p=0.101	ρ=0.055, p=0.684	ρ=-0.175, p=0.188

ρ= Spearman Correlation Coefficient. Bold=statistically significant (p<0.05). GA: gestational age, PNA: postnatal age, PMA: post menstrual age. †fetal/newborn cohort. ‡only fetal samples.

Figure 3 Transporter-specific postnatal maturation of hepatic protein expression in the fetal/newborn cohort (n=58).

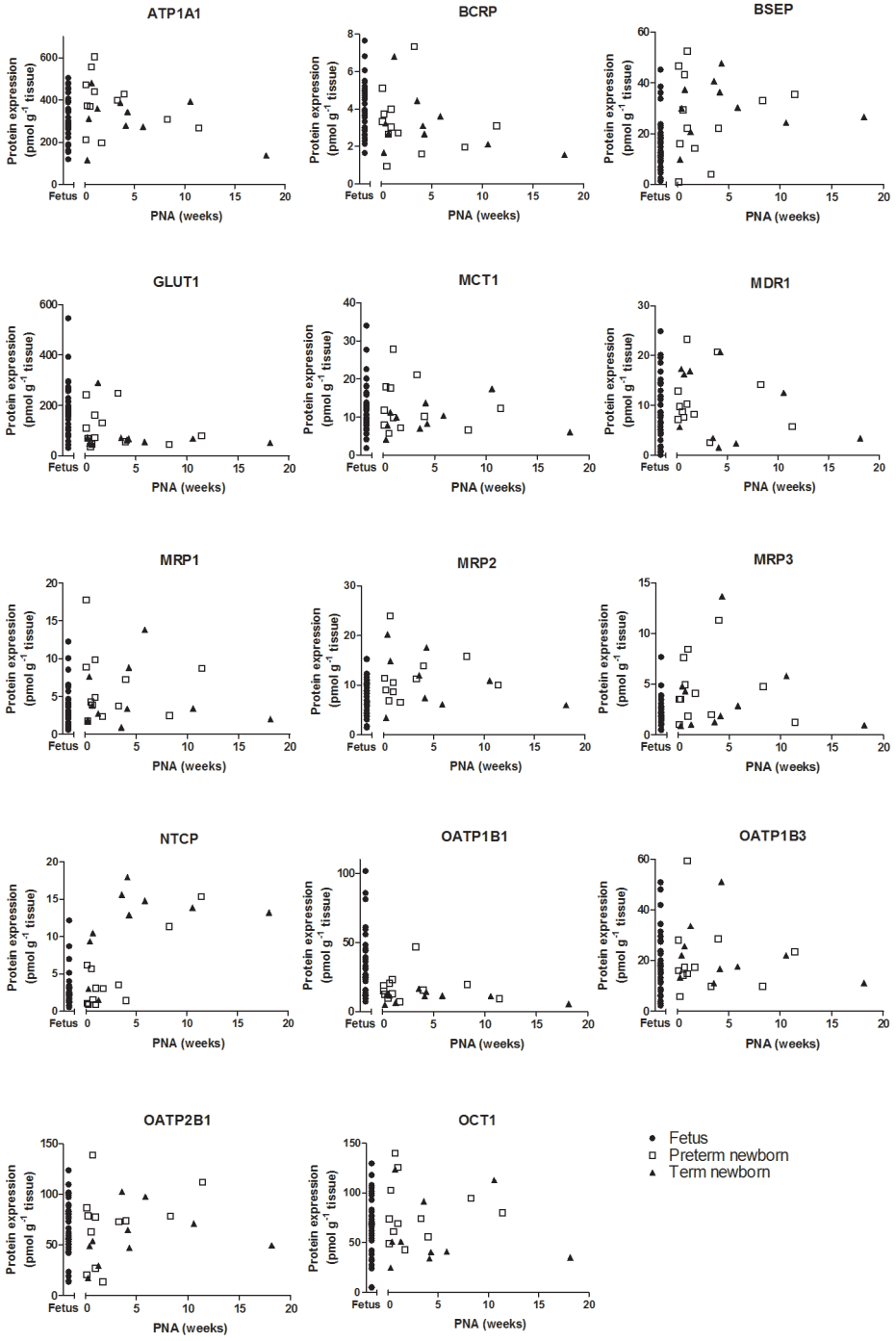

PNA=postnatal age

Figure 4 Transporter-specific post-menstrual maturation of hepatic protein expression in the fetal/newborn cohort (n=58).

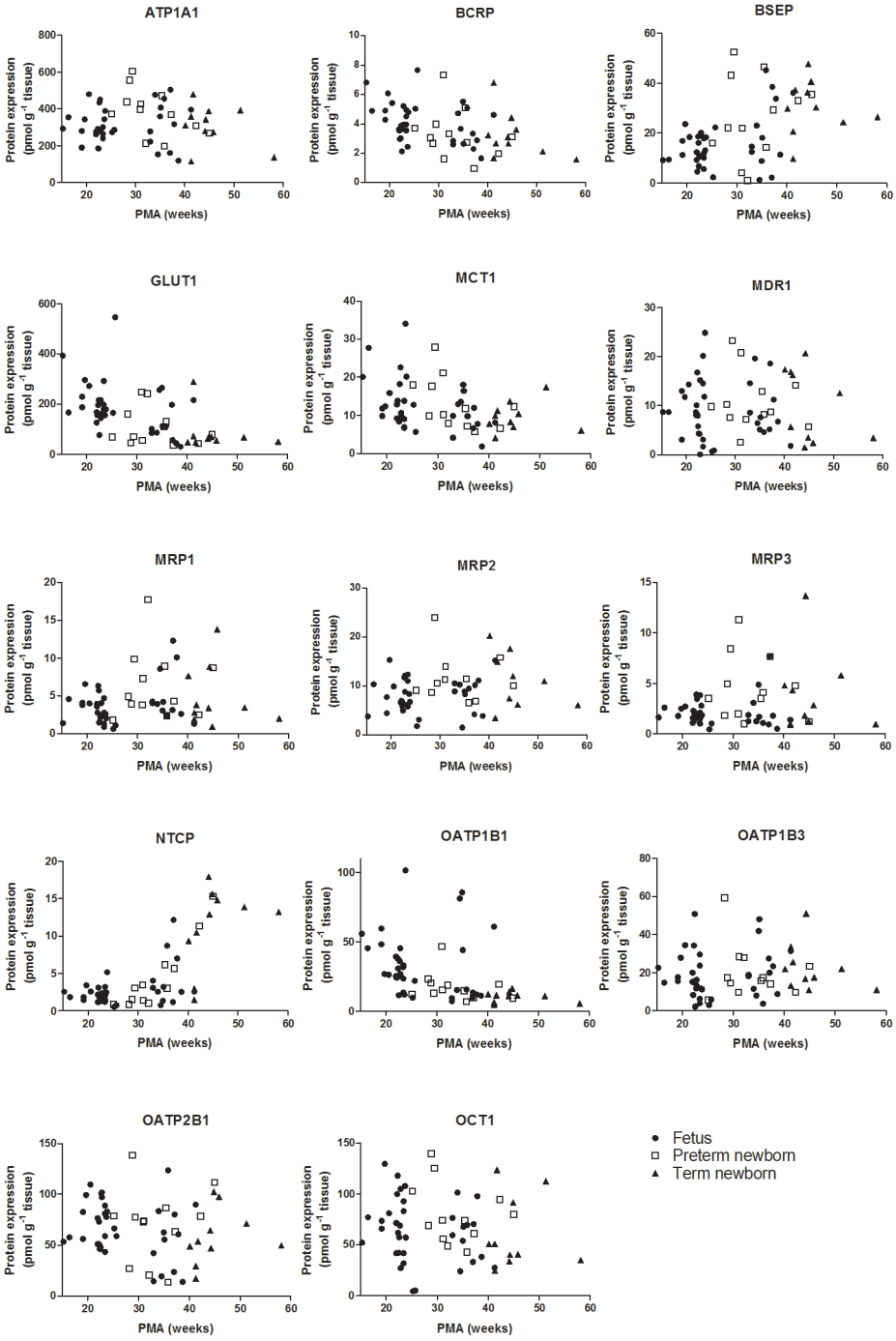

PMA=post menstrual age

Table 3 Age-related changes in hepatic transporter expression: literature data versus our current data. See also Brouwer et al.[1]

Transporter *gene*/protein	Literature data: age vs. hepatic mRNA expression	Literature data: age vs. hepatic protein expression	Current data: age vs hepatic protein expression		
			Age groups (fetuses– preterm – term – pediatrics – adults)	PNA (between 0 – 18 weeks)	PMA (between 15.3-58.1 weeks)
ATP1A1/ ATP1A1	-	Low in neonates and increasing up to adult age.[6]†	Stable	Stable	Stable
ABCG2/BCRP	Increased levels from fetuses vs 0-4 year and >7 year [31]. Stable expression in fetal, pediatric and adult samples [32,33].	Stable from neonate to adult age [6]†. Stable in neonates and adults (n=10, western blotting) [34], and in 7-70 yr (n=56, LC-MS/MS) [22].	Stable	Decrease	Decrease
ABCB11/BSEP	3 fold lower in fetuses (n=3) than in adults (n=3) [32]. Lower in neonates than in children >7yr [31].	Stable from neonate to adult age [6]†. Detected in second trimester fetuses with immune-histochemistry [35].	Lower in fetuses than in term newborns and adults.	Increase	Increase
SLC2A1/ GLUT1	-	-	Higher in fetuses than in term newborns, pediatrics and adults.	Decrease	Decrease
SLC16A1/ MCT1	-	-	Stable	Stable	Decrease
ABCB1/MDR1	Increase in first year of life [12,33,36-38].	Low expression up to infant age and increasing to adult age [6]†. Lower in S9 liver fractions from children (7d-18yr old, n=12) than in adults [39]. Stable in a cohort from 7-70 yr (LC-MS/MS) [9].	Lower in fetuses than in adults.	Stable	Stable
ABCC1/MRP1	-	Detected in fetuses with immune-histochemistry [40].	Lower in fetuses and term newborns than in adults.	Stable	Stable
ABCC2/MRP2	Lower in fetuses, neonates and infants <1yr old than in adults [12]. Lower in fetuses compared to pediatrics from 1-17yr old [33].	Stable expression from neonate to adult age [6] and in a cohort from 7 years onward [41].	Lower in fetuses and term newborns than in adults.	Increase	Stable

Table 3 Age-related changes in hepatic transporter expression: literature data versus our current data. See also Brouwer et al.[1] *(continued)*

Transporter *gene*/protein	Literature data: age vs. hepatic mRNA expression	Literature data: age vs. hepatic protein expression	Current data: age vs hepatic protein expression		
			Age groups (fetuses– preterm – term – pediatrics – adults)	PNA (between 0 – 18 weeks)	PMA (between 15.3-58.1 weeks)
ABCC3/MRP3	Lower expression in fetuses (n=3) than in adults (n=3) [32].	Lower in infants and adolescents than in adults [6]†. Similar expression in 5 neonates and 5 adults (Western Blot) [34].	Lower in fetuses and term newborns than in adults.	Increase	Stable
SLC10A1/ NTCP	Lower in perinatal (n =6) than in 0 to 4 years (n=8), and in >7yr old (n=6) [31].	Similar in 5 neonates and 5 adults (Western Blot) [34] .	Lower in fetuses than in term newborns, pediatrics and adults. Lower in preterm newborns than in adults.	Increase	Increase
SLCO1B1/ OATP1B1	Higher in adults (n=11) than in fetuses (n=6), neonates (n=19), infants (n=7) and children (n=2) [12]. Lower in fetuses than in pediatric and adults (all n=30) [33], and lower in fetuses (n=3) than adults (n=3) [32].	Similar expression in 5 neonates and 5 adults (Western Blot) [34]. Stable in a cohort from 7-70 yr (LC-MS/MS) [9]. OATP1B1 *1/*1 showed increase in children >0 - 1 year of age [6].	High in fetuses, low in term newborns.	Decrease	Decrease
SLCO1B3/ OATP1B3	Higher in adults (n=11) than in fetuses (n=6), neonates (n=19), infants (n=7) and children (n=2) [12].	High at birth, a decline over the first months of life and an increase in preadolescent period [25]. Lower in neonates than in adults [6]†.	Stable	Stable	Stable
SLCO2B1/ OATP2B1	Lower in second trimester fetuses (n=3) than adults (n=3) [32].	Stable from neonate to adult age [6]†. Stable in a cohort from 7-70yr (LC-MS/MS) [9].	Stable	Stable	Stable
SLC22A1/ OCT1	-	Low expression from neonate up to infant age and increasing to adult age [6]†. Increase between 1-2 days (n=7) and 3-4 weeks of age (n=5) (Western Blot) [5].	Lower in fetuses and term newborns than in adults.	Stable	Stable

†Prasad et al: studied protein expression of various transporters with LC-MS/MS in the following hepatic post-mortem samples; 4 neonates (0-28 days), 19 infants (29 days – 1 year), 32 children (1-12 year), 14 adolescents (12-16 year) and 41 adults (>16 year) [6]

Genetic variants

Genotype results are presented in Supplemental Table 3. For *SLC22A1* 1222A>G, the TaqMan assay failed for two patients, presumably due to poor quality of the DNA. All patients were successfully genotyped for other SNPs. Protein expression was neither associated with the selected SNPs, nor with diplotypes of *SLCO1B1* (Supplemental Table 3), also when taking into consideration age within genotype-groups.

Cell lines

The absolute protein expression of OATP1B1, OATP1B3, OCT1, MDR1, MRP2 and BCRP was determined in the crude membrane fractions of HEK-OATP1B1, -OATP1B3, -OCT1 and MDCKII-MDR1, -MRP2, and -BCRP cells, showing good expression profiles (Supplemental Table 7).

DISCUSSION

Our study expands and presents data on human hepatic transporter protein expression in a pediatric cohort with a focus on fetal and newborn patients up to 18 weeks of postnatal age. Together with findings on gene expression and genetic variants in the same patient subcohort, this study is a comprehensive analysis of ontogeny of human hepatic drug transport in the age range where knowledge was still lacking. Below we will discuss the main findings.

Age-related changes in protein expression were transporter dependent. The results with existing data from literature are summarized in Table 3. Apart from our previous exploratory study, the only other published LC-MS/MS proteomics study we could identify included four neonates.[6] At this time, due to a lack of biological data, drug dosing in preterm and term infants is left with uncertainty regarding the level of exposure. Similarly, in pregnant women, the level of exposure to the fetus remains unknown. Our data may aid to optimize dosing of transporter substrates in these patient populations. Interestingly, when looking at age groups, most differences in transporter expression were found between the fetal and adult age groups, indicating that major changes in transporter protein expression occur in early life. For example, previously was shown that OCT1 increased from neonatal to adult age.[5,6] Our data adds that also in fetal and preterm newborns the OCT1 levels are lower than in adults. While the expression of most transporters, like OCT1, is lower in the perinatal period than at adult age, the expression of GLUT1 is significantly higher in the perinatal period. This likely reflects the physiological high need of glucose early after conception. Moreover, we did not study the transporter GLUT2, which is highly expressed in the adult liver.[20] This transporter

could be subject to age-related changes, possibly explaining our findings on GLUT1. Subsequently, OATP1B1 is also higher in the perinatal period, and is important for the hepatic uptake of hormones like estrogens.[3] Importantly, the decrease in GLUT1 and OATP1B1 may also be explained by the observed negative correlation between crude membrane yield and age. Not surprisingly, ontogeny patterns are not similar when describing transporter protein expression per membrane yield instead of per amount of tissue. However, in literature these units are used inconsistent. As transporter proteomic data is often used for PBPK modelling, coming from various sources, a correction factor should be applied when describing protein expression results per crude membrane protein in young age groups.

Both gestational age and postnatal age may impact transporter activity differently and independently. However, the combined effect, i.e. postmenstrual age, needs to be considered as well. Our data suggest that dosing of transporter substrates for BCRP, BSEP, GLUT1 and OATP1B1 is best guided by PMA in the first months of life. Using linear correlation is problematic in wide age ranges because this implies continuously increasing or decreasing expression up to adult age.[21] But as we were dealing with a limited age range (<18 weeks PNA), we considered linear correlation the most suitable to describe our data within this subpopulation.

Considerably more literature data on pediatric transporter mRNA expression is available than protein expression data.[1] However, adults studies have shown that mRNA levels do not always correlate well with transporter protein expression[22-24], which was also shown in a subpopulation of our cohort (n=31). Interestingly, the earlier found ABCB1 mRNA ontogeny pattern[12] is similar to that for the MDR1 protein in the present study, but with a much higher fold change, possibly explaining the lack of correlation. Also, post-translational changes may occur introducing differences between protein expression and protein activity. For example, a previous study found that the fraction of highly glycosylated OATP1B3 increased with age[25]. Unfortunately, because we used crude membrane fractions to measure protein expression with LC-MS/MS we could not distinguish between glycosylated and un-glycosylated transporter protein. Other techniques, e.g. Western Blot, could enable this, but this is challenging in pediatrics as much more tissue is needed.

We could not identify a relationship between protein expression and the selected genetic variants in our cohort, although these have been shown earlier to impact mRNA and/or protein expression. This finding may be explained by our low sample size, but could also partly explained by the interplay between development and genetics. For example, in a previous study *SLC22A1* 181C>T in adult samples correlated with OCT1

protein expression[26] but this was not confirmed in our cohort. OCT1 expression was low in fetuses, potentially obscuring a possible effect of genetic variants. OATP1B1 protein expression was stable within *SLCO1B1* diplotypes. In contrast, Prasad et al. showed higher protein expression in neonates versus older children/adults with the *SLCO1B1* *1A/*1A haplotype.[6] Moreover, our group previously showed that the *SLC22A1* genotype is related to tramadol disposition in preterm infants, similar to adults.[10] This suggests that, although protein levels are low, the *SLC22A1* genotype can result in significant differences in protein activity in neonates. Thus, although we did not find a correlation between interrogated SNPs and protein expression, it remains important to include genotype when analyzing developmental patterns.

Some potential limitations of our study should be addressed. First, our results show high inter-individual variation in transporter protein expression, which in part remained unexplained by age, gender and genotype. It is well possible that inflammation[27], disease, nutrition and drugs influenced transporter expression in our cohort. Healthy infants do not require medications like ill newborns do, thus our cohort represents the relevant population for our intended purpose. The relative impact of these factors, however, deserves further study. Also, samples were snap-frozen at -80°C for later research use at the time of autopsy within 24 hours after death, which might have introduced differences in quality of tissue. These limitations warrant careful interpretation of our data.

Nevertheless, our data help improve our understanding of drugs and endogenous processes in human populations of different ages. Moreover, our data could be integrated in PBPK modeling, which might improve prediction of pediatric drug clearance. Because differences might exist between protein expression and protein activity, future perspectives will be to validate these models with clinical data from transporter substrates. Previously, we have shown the value of determining absolute transporter protein expressions in transfected cell lines for application in PBPK modelling: *in vivo* hepatic disposition of rosuvastatin was predicted by scaling from individually transfected cell lines by correcting for absolute transporter protein expression levels.[28] In the current study we therefore determined the absolute expression levels of the transporter protein in selected relevant cell lines, frequently applied in *in vitro* drug metabolism PK studies. Hence, the obtained results can be incorporated into PBPK modeling to extrapolate existing adult PK data to pediatric PK data[29,30], or used as appropriate scaling factors to scale between in vitro cell lines and human hepatic expression in adults or pediatric patients.

CONCLUSIONS

In conclusion, we observed various patterns in the maturation of protein expression of a number of hepatic transporter proteins in children up to four months. This strongly suggests that disposition of drugs and endogenous transporter substrates is subject to age-related changes and impacts the efficacy and safety of drugs in the first months of life. Postmenstrual age may present the most robust method to incorporate age-related variation in transporter protein expression in dosing guidelines. mRNA expression as surrogate marker of transporter activity should be carefully interpreted as correlation with protein expression is mostly lacking. Moreover, adult pharmacogenetic data cannot be directly extrapolated to neonates and young infants. Further study is needed to delineate the effect on *in vivo* drug disposition and effect.

REFERENCES

1. Brouwer KL, Aleksunes LM, Brandys B, et al. Human ontogeny of drug transporters: review and recommendations of the pediatric transporter working group. Clin Pharmacol Ther 2015;98(3):266-287.
2. Hsieh EM, Hornik CP, Clark RH, et al. Medication use in the neonatal intensive care unit. Am J Perinatol 2014;31(9):811-821.
3. Mooij MG, Nies AT, Knibbe CA, et al. Development of human membrane transporters: drug disposition and pharmacogenetics. Clin Pharmacokinet 2016;55(5):507-524.
4. Tzvetkov MV, dos Santos Pereira JN, Meineke I, Saadatmand AR, Stingl JC, Brockmoller J. Morphine is a substrate of the organic cation transporter OCT1 and polymorphisms in OCT1 gene affect morphine pharmacokinetics after codeine administration. Biochem Pharmacol 2013;86(5):666-678.
5. Hahn D, Emoto C, Vinks AA, Fukuda T. Developmental Changes in Hepatic Organic Cation Transporter OCT1 Protein Expression from Neonates to Children. Drug Metab Dispos 2017;45(1):23-26.
6. Prasad B, Gaedigk A, Vrana M, et al. Ontogeny of hepatic drug transporters as quantified by LC-MS/MS proteomics. Clin Pharmacol Ther 2016;100(4):362-370.
7. Hines RN. The ontogeny of drug metabolism enzymes and implications for adverse drug events. Pharmacol Ther 2008;118(2):250-267.
8. Mooij MG, van de Steeg E, van Rosmalen J, et al. Proteomic analysis of the developmental trajectory of human hepatic membrane transporter proteins in the first three months of life. Drug Metab Dispos 2016;44(7):1005-1013.
9. Prasad B, Evers R, Gupta A, et al. Interindividual variability in hepatic organic anion-transporting polypeptides and P-glycoprotein (ABCB1) protein expression: quantification by liquid chromatography tandem mass spectroscopy and influence of genotype, age, and sex. Drug Metab Dispos 2014;42(1):78-88.
10. Matic M, de Wildt SN, Elens L, et al. SLC22A1/OCT1 Genotype Affects O-desmethyltramadol Exposure in Newborn Infants. Ther Drug Monit 2016;38(4):487-492.
11. van de Steeg E, Greupink R, Schreurs M, et al. Drug-drug interactions between rosuvastatin and oral antidiabetic drugs occurring at the level of OATP1B1. Drug Metab Dispos 2013;41(3):592-601.
12. Mooij MG, Schwarz UI, de Koning BA, et al. Ontogeny of human hepatic and intestinal transporter gene expression during childhood: age matters. Drug Metab Dispos 2014;42(8):1268-1274.
13. Langmead B, Salzberg SL. Fast gapped-read alignment with Bowtie 2. Nat Methods 2012;9(4):357-359.
14. Li B, Dewey CN. RSEM: accurate transcript quantification from RNA-Seq data with or without a reference genome. BMC Bioinformatics 2011;12:323.
15. PharmGKB database. www.pharmgkb.org. Accessed 16-06, 2016.
16. van de Steeg E, Venhorst J, Jansen HT, et al. Generation of Bayesian prediction models for OATP-mediated drug-drug interactions based on inhibition screen of OATP1B1, OATP1B1 *15 and OATP1B3. Eur J Pharm Sci 2015;70:29-36.
17. Evers R, Kool M, van Deemter L, et al. Drug export activity of the human canalicular multispecific organic anion transporter in polarized kidney MDCK cells expressing cMOAT (MRP2) cDNA. J Clin Invest 1998;101(7):1310-1319.

18. Jonker JW, Wagenaar E, van Deemter L, et al. Role of blood-brain barrier P-glycoprotein in limiting brain accumulation and sedative side-effects of asimadoline, a peripherally acting analgaesic drug. Br J Pharmacol 1999;127(1):43-50.
19. Jonker JW, Buitelaar M, Wagenaar E, et al. The breast cancer resistance protein protects against a major chlorophyll-derived dietary phototoxin and protoporphyria. Proc Natl Acad Sci U S A 2002;99(24):15649-15654.
20. Karim S, Adams DH, Lalor PF. Hepatic expression and cellular distribution of the glucose transporter family. World J Gastroenterol 2012;18(46):6771-6781.
21. Leeder JS, Meibohm B. Challenges and Opportunities for Increasing the Knowledge Base Related to Drug Biotransformation and Pharmacokinetics during Growth and Development. Drug Metab Dispos 2016;44(7):916-923.
22. Prasad B, Lai Y, Lin Y, Unadkat JD. Interindividual variability in the hepatic expression of the human breast cancer resistance protein (BCRP/ABCG2): effect of age, sex, and genotype. J Pharm Sci 2013;102(3):787-793.
23. Ulvestad M, Skottheim IB, Jakobsen GS, et al. Impact of OATP1B1, MDR1, and CYP3A4 expression in liver and intestine on interpatient pharmacokinetic variability of atorvastatin in obese subjects. Clin Pharmacol Ther 2013;93(3):275-282.
24. Maier T, Guell M, Serrano L. Correlation of mRNA and protein in complex biological samples. FEBS Lett 2009;583(24):3966-3973.
25. Thomson MM, Hines RN, Schuetz EG, Meibohm B. Expression Patterns of Organic Anion Transporting Polypeptides 1B1 and 1B3 Protein in Human Pediatric Liver. Drug Metab Dispos 2016;44(7):999-1004.
26. Nies AT, Koepsell H, Winter S, et al. Expression of organic cation transporters OCT1 (SLC22A1) and OCT3 (SLC22A3) is affected by genetic factors and cholestasis in human liver. Hepatology 2009;50(4):1227-1240.
27. Le Vee M, Jouan E, Moreau A, Fardel O. Regulation of drug transporter mRNA expression by interferon-gamma in primary human hepatocytes. Fundam Clin Pharmacol 2011;25(1):99-103.
28. Bosgra S, van de Steeg E, Vlaming ML, et al. Predicting carrier-mediated hepatic disposition of rosuvastatin in man by scaling from individual transfected cell-lines in vitro using absolute transporter protein quantification and PBPK modeling. Eur J Pharm Sci 2014;65:156-166.
29. Barrett JS, Della Casa Alberighi O, Laer S, Meibohm B. Physiologically based pharmacokinetic (PBPK) modeling in children. Clin Pharmacol Ther 2012;92(1):40-49.
30. Hartmanshenn C, Scherholz M, Androulakis IP. Physiologically-based pharmacokinetic models: approaches for enabling personalized medicine. J Pharmacokinet Pharmacodyn 2016;43(5):481-504.
31. Klaassen CD, Aleksunes LM. Xenobiotic, bile acid, and cholesterol transporters: function and regulation. Pharmacol Rev 2010;62(1):1-96.
32. Sharma S, Ellis EC, Gramignoli R, et al. Hepatobiliary disposition of 17-OHPC and taurocholate in fetal human hepatocytes: a comparison with adult human hepatocytes. Drug Metab Dispos 2013;41(2):296-304.
33. Burgess KS, Philips S, Benson EA, et al. Age-Related Changes in MicroRNA Expression and Pharmacogenes in Human Liver. Clin Pharmacol Ther 2015;98(2):205-215.
34. Yanni SB, Smith PB, Benjamin DK, Jr., Augustijns PF, Thakker DR, Annaert PP. Higher clearance of micafungin in neonates compared with adults: role of age-dependent micafungin serum binding. Biopharm Drug Dispos 2011;32(4):222-232.

35. Chen HL, Chen HL, Liu YJ, et al. Developmental expression of canalicular transporter genes in human liver. J Hepatol 2005;43(3):472-477.
36. van Kalken CK, Giaccone G, van der Valk P, et al. Multidrug resistance gene (P-glycoprotein) expression in the human fetus. Am J Pathol 1992;141(5):1063-1072.
37. Miki Y, Suzuki T, Tazawa C, Blumberg B, Sasano H. Steroid and xenobiotic receptor (SXR), cytochrome P450 3A4 and multidrug resistance gene 1 in human adult and fetal tissues. Mol Cell Endocrinol 2005;231(1-2):75-85.
38. Fakhoury M, de Beaumais T, Guimiot F, et al. mRNA expression of MDR1 and major metabolising enzymes in human fetal tissues. Drug Metab Pharmacokinet 2009;24(6):529-536.
39. Abanda NN, Riches Z, Collier AC. Lobular Distribution and Variability in Hepatic ATP Binding Cassette Protein B1 (ABCB1, P-gp): Ontogenetic Differences and Potential for Toxicity. Pharmaceutics 2017;9(1).
40. Konieczna A, Erdosova B, Lichnovska R, Jandl M, Cizkova K, Ehrmann J. Differential expression of ABC transporters (MDR1, MRP1, BCRP) in developing human embryos. J Mol Histol 2011;42(6):567-574.
41. Deo AK, Prasad B, Balogh L, Lai Y, Unadkat JD. Interindividual variability in hepatic expression of the multidrug resistance-associated protein 2 (MRP2/ABCC2): quantification by liquid chromatography/tandem mass spectrometry. Drug Metab Dispos 2012;40(5):852-855.

SUPPLEMENTAL INFORMATION

Supplemental Table 1 Clinical diagnoses pediatric patients

Clinical diagnosis	Number of patients
Congenital malformations (cardiac, otolaryngeal, chromosomal, abdominal, unknown)	32
Intrauterine death	5
Hydrops fetalis	2
Viral/bacterial infections	7
Cardiac failure	5
Necrotizing enterocolitis	3
Hemangioendothelioma	1
Sudden infant death syndrome	2
Intracranial bleeding	1
Meconium aspiration	1
Pulmonary hypertension	1
Neurologic abnormality	1
Hernia incarcerate	1

Supplemental Table 2 Multiple reaction monitoring (MRM) transitions of the used peptides and the corresponding internal standards (AQUA)

Name	Labelled	Peptide sequence[a]	Molecular weight	Q1	Q3-1	Q3-2	Q3-3	Q3-4
ATP1A1	unlabeled	AAVPDAVGK	827.0	414.2	586.3	685.4	242.1	
	AQUA	AAVPDA***V***GK	833.0	417.5	592.3			
BCRP	unlabeled	SSLLDVLAAR	1.044.2	522.8	644.3	757.5	529.4	
	AQUA	SSLLDV***L***AAR	1.060.2	526.3	651.3			
BSEP	unlabeled	STALQLIQR	1.029.2	515.3	657.4	841.6	529.4	
	AQUA	STALQ***L***IQR	1.045.2	518.8	664.3			
GLUT1	unlabeled	VTILELFR	990.2	495.8	790.5	677.4	201.2	
	AQUA	VTILEL***F***R	1.000.2	500.8	800.5			
MCT1	unlabeled	SITVFFK	841.0	421.2	173.2	641.3	201.1	
	AQUA	SITVF***F***K	851.0	426.2	651.3			
MDR1	unlabeled	NTTGALTTR	934.0	467.7	719.4	216.1	618.4	
	AQUA	NTTGA***L***TTR	950.0	471.2	726.5			
MRP2	unlabeled	VLGPNGLLK	910.1	455.8	698.5	185.3	213.3	
	AQUA	VLGPNGL***L***K	926.1	459.2	705.4			
MRP3	unlabeled	ALVITNSVK	944.1	472.8	760.4	661.4	548.4	
	AQUA	ALVITNS***V***K	950.1	475.8	766.5			
NTCP	unlabeled	GIYDGDLK	880.44	440.7	710.3	143.2	171.2	
	AQUA	GIYDGD***L***K	896.44	444.2	717.3			
OATP1B1	unlabeled	LNTVGIAK	815.0	408.2	399.4	588.3	228.2	702.3
	AQUA	LNTVG***I***AK	831.0	411.7	402.9			
OATP1B3	unlabeled	IYNSVFFGR	1101.3	551.8	826.5	249.1	526.2	
	AQUA	IYNSVF***F***GR	1111.6	556.8	836.4			
OATP2B1	unlabeled	SSISTVEK	849.9	425.7	563.3	676.3	175.1	
	AQUA	SSIST***V***EK	855.9	428.7	569.3			
OCT1	unlabeled	LPPADLK	752.9	377.2	543.3	183.3	260.3	
	AQUA	LPPAD***L***K	768.9	380.7	550.4			

*[a] AQUA: Amino acid presented in **italic bold** is labelled with ^{13}C and ^{15}N.*

Supplemental Table 3 Overview selection of SNPs known to influence mRNA- or protein expression. Number of livers from carriers of various SNPs present in the studied cohort. *Kruskal-Wallis test

Gene	Gene SNP ID	Variant	SNP class	Genotype			Distribution protein expression across genotype groups*
				Wildtype (n=)	Hetero-zygous (n=)	Homo-zygous (n=)	
ABCG2	rs2231142	421C>A	Missense	50	10	0	p=0.132
ABCB1	rs1045642	3435C>T	Synonymous	15	27	18	p=0.883
ABCC1	rs45511401	16079375G>T	Missense	56	4	0	p=0.155
ABCC2	rs2273697	1249G>A	Missense	35	19	6	p=0.197
ABCC3	rs4793665	-211C>T	5 Flanking	15	22	23	p=0.792
SLCO1B1	rs4149056	521T>C	Missense	44	16	0	p=0.132
	rs2306283	388A>G	Missense	10	33	17	p= 0.821
	rs11045819	463C>A	Missense	45	12	3	p= 0.324
SLCO1B3	rs4149117	334T>G	Missense	1	19	40	p=0.459
	rs7311358	699G>A	Missense	1	19	40	p=0.459
SLCO2B1	rs2306168	1457C>T	Missense	54	4	1	p=0.132
	rs12422149	935G>A	Missense	49	10	1	p=0.682
SLC22A1	rs12208357	181C>T	Missense	55	5	0	p=0.841
	rs628031	1222A>G	Missense	9	25	24	p=0.206

Supplemental Table 4 hepatic protein expression of transporters in each age group. Data is presented as median (range).

	Transporter	All n=70	Fetuses n=36	Preterm newborns n=12	Term newborns n=10	Pediatrics n=4	Adults n=8	Expression difference across age groups ‡
Hepatic protein expression (pmol g^{-1} tissue)	ATP1A1	309.8 (115.7-604.3)	288.2 (119.3-503.6)	384.9 (197.6-604.3)	327.3 (115.7-479.6)	371.5 (247.3-484.1)	279.3 (193.8-391.2)	p=0.236
	BCRP	3.7 (0.9-7.7)	3.9 (1.7-7.7)	3.1 (0.9-7.3)	2.9 (1.6-6.8)	3.7 (2.2-4.5)	4.2 (1.6-6.5)	p=0.120
	BSEP	20.5 (0.9-92.4)	12.8 (1.3-45.2)	25.7 (0.9-52.4)	30.1 (9.8-47.7)	41.7 (20.4-59.7)	60.1 (25.7-92.4)	p<0.001
	GLUT1	105.5 (6.3-546.2)	170.4 (30.3-546.2)	75.2 (35.2-247.9)	65.0 (48.1-290.0)	48.8 (21.4-55.3)	17.8 (6.3-95.0)	p<0.001
	MCT1	10.5 (1.9-39.5)	11.2 (1.9-34.0)	11.0 (5.8-27.9)	9.2 (4.2-17.5)	8.9 (6.9-39.5)	12.8 (5.7-20.6)	p=0.598
	MDR1	10.2 (0.04-26.7)	8.3 (0.04-24.9)	9.2 (2.5-23.3)	9.1 (1.5-20.7)	19.2 (10.6-26.7)	20.5 (12.3-25.7)	p=0.002
	MRP1	3.9 (0.6-17.7)	3.4 (0.6-12.3)	4.6 (1.8-17.7)	3.4 (0.9-13.8)	3.6 (1.0-6.6)	9.3 (7.2-14.2)	p=0.001
	MRP2	9.3 (1.5-39.6)	8.0 (1.5-15.3)	10.5 (6.5-23.9)	10.9 (3.4-20.23)	8.9 (7.0-11.0)	29.5 (19.6-39.6)	p<0.001
	MRP3	2.4 (0.5-13.7)	1.8 (0.5-7.7)	3.8 (1-11.3)	2.4 (0.9-13.7)	6.2 (3.3-9.5)	6.8 (4.2-9.9)	p<0.001
	NTCP	3.1 (0.6-81.6)	2.3 (0.6-12.2)	3.1 (0.9-15.3)	13.1 (1.5-18.0)	17.7 (8.8-30.1)	43.8 (10.2-81.6)	p<0.001
	OATP1B1	17.7 (4.9-101.7)	26.6 (7.1-101.7)	15.0 (7.0-46.8)	11.3 (4.9-16.5)	17.9 (8.2-23.2)	17.7 (9.1-53.7)	p=0.001
	OATP1B3	16.6 (2.3-59.3)	16.0 (2.3-50.9)	16.7 (5.8-59.3)	19.9 (11.1-51.1)	21.9 (15.1-38.9)	16.0 (7.9-28.1)	p=0.566
	OATP2B1	63.9 (13.5-138.7)	61.6 (13.8-123.8)	75.5 (13.5-138.7)	51.9 (17.5-102.6)	77.7 (60.8-79.1)	61.3 (34.5-77.8)	p=0.503
	OCT1	70.0 (4.6-181.4)	66.7 (4.6-129.7)	73.9 (42.7-139.7)	45.9 (24.6-123.8)	86.1 (23.9-131.2)	124.3 (60.1-181.4)	p=0.010

GA=gestational age, PNA=postnatal age, NA=not available. ‡Kruskal-Wallis test.

Supplemental Table 5 Hepatic protein expression of transporters in males and females. Data is presented as median (range).* Mann Whitney U test.

Transporter	Hepatic expression (pmol/g tissue)		Distribution over groups*
	Male (n=35)	Female (n=27)	
ATP1A1	292.5 (115.7-604.9)	342.9 (137.6-471.9)	p=0.848
BCRP	3.5 (1.6-6.8)	4.0 (0.9-7.7)	p=0.122
BSEP	18.0 (0.9-59.7)	20.4 (4.0-47.7)	p=0.324
GLUT1	112.0 (21.4-393.0)	144.3 (35.2-546.2)	p=0.804
MCT1	12.0 (1.9-39.5)	9.8 (5.7-34.0)	p=0.189
MDR1	8.1 (0.7-24.9)	11.2 (0.1-26.7)	p=0.456
MRP1	3.8 (0.6-17.7)	3.8 (0.9-13.8)	p=0.609
MRP2	8.8 (1.5-23.9)	8.8 (3.1-20.2)	p=0.633
MRP3	1.8 (0.5-11.3)	2.5 (1.0-13.7)	p=0.138
NTCP	2.6 (0.6-30.1)	3.2 (0.8-15.6)	p=0.284
OATP1B1	20.4 (4.9-101.7)	14.7 (5.7-85.8)	p=0.624
OATP1B3	18.2 (2.3-59.3)	16.4 (3.9-51.1)	p=0.537
OATP2B1	64.6 (13.8-138.7)	72.9 (13.5-123.8)	p=0.189
OCT1	67.6 (4.6-139.7)	69.6 (5.2-129.7)	p=0.771

Supplemental Table 6 Correlation of mRNA- and protein expression of hepatic transporters. mRNA expression is presented as median (range). ρ= Spearman Correlation Coefficient. Bold=statistically significant (p<0.05)

Transporter	mRNA expression all transcripts (TPM)	Correlation protein expression and all mRNA transcripts	mRNA expression coding transcripts (TPM)	Correlation protein expression and coding mRNA transcripts
ATP1A1	20.9 (4.4-168.5)	ρ=-0.123, p=0.510	12.1 (0.6-105.7)	ρ=0.144, p=0.441
ABCG2/BCRP	1.8 (0.0-7.7)	ρ=-0.080, p=0.670	1.8 (0.0-7.7)	ρ=-0.080, p=0.670
ABCB11/BSEP	8.3 (0.0-41.8)	**ρ=0.533, p=0.002**	7.5 (0.0-27.3)	**ρ=0.525, p=0.002**
SLC2A1/GLUT1	9.0 (0.0-125.7)	ρ=0.293, p=0.110	6.2 (0.0-92.9)	ρ=0.313, p=0.087
SLC16A1/MCT1	9.1 (0.0-77.0)	**ρ=0.517, p=0.003**	4.3 (0.0-19.7)	ρ=0.342, p=0.060
ABCB1/MDR1	1.9 (0.0-8.6)	ρ=0.150, p=0.419	0.9 (0.0-5.0)	**ρ=0.394, p=0.028**
ABCC1/MRP1	2.6 (0.0-17.5)	ρ=0.118, p=0.527	0.6 (0.0-6.2)	ρ=0.104, p=0.577
ABCC2/MRP2	15.9 (0.4-70.6)	**ρ=0.467, p=0.011**	14.7 (0.4-61.8)	**ρ=0.512, p=0.005**
ABCC3/MRP3	11.1 (0.0-128.7)	ρ=0.096, p=0.606	1.4 (0.0-5.6)	ρ=0.260, p=0.158
SLC10A1/NTCP	1.4 (0.0-26.0)	**ρ=0.584, p=0.001**	1.4 (0.0-26.0)	**ρ=0.584, p=0.001**
SLCO1B1/OATP1B1	26.1 (0.0-69.4)	ρ=0.182, p=0.328	26.1 (0.0-69.4)	ρ=0.182, p=0.328
SLCO1B3/OATP1B3	10.6 (0.0-56.8)	ρ=-0.093, p=0.620	9.2 (0.0-49.6)	ρ=-0.114, p=0.541
SLCO2B1/OATP2B1	24.7 (0.4-84.0)	ρ=0.296, p=0.106	17.6 (0.3-72.6)	ρ=0.313, p=0.087
SLC22A1/OCT1	2.4 (0.0-122.1)	ρ=-0.032, p=0.865	1.4 (0.0-57.6)	ρ=-0.090, p=0.629

Supplemental Table 7 Absolute transporter expression in selected cell-lines

	Absolute transporter expression (fmol/106 cells)	
	Mean	**SD**
HEK-OATP1B1	143.5	8.8
HEK-OATP1B3	400.2	31.2
HEK-OCT1	667.0	174.2
MDCKII-MDR1	832.4	42.9
MDCKII-MRP2	54.8	1.9
MDCKII-BCRP	301.6	4.5

5 A comprehensive analysis of ontogeny of renal drug transporters: mRNA analyses, quantitative proteomics and localization

Bianca D van Groen*, Kit Wun Kathy Cheung*, Edwin Spaans, Marjolein D van Borselen, Adrianus CJM de Bruijn, Ytje Simons-Oosterhuis, Dick Tibboel, Janneke N Samsom, Robert M Verdijk, Bart Smeets, Lei Zhang, Shiew-Mei Huang, Kathleen M Giacomini**, Saskia N de Wildt**

*Contributed equally **Contributed equally

Clin Pharmacol Ther. 2019 Nov; 1083-1092. DOI: 10.1002/CPT.1516

ABSTRACT

Human renal membrane transporters play key roles in the disposition of renally cleared drugs and endogenous substrates but their ontogeny is largely unknown. Using 184 human postmortem frozen renal cortical tissues (preterm newborns – adults) and a subset of 62 tissue samples, we measured the mRNA levels of 11 renal transporters and the transcription factor PXR with RT-qPCR, and protein abundance of 9 transporters using LC-MS/MS SRM, respectively. Expression levels of P-gp, URAT1, OAT1, OAT3, and OCT2 increased with age. Protein levels of MATE2-K and BCRP showed no difference from newborns to adults despite age-related changes in mRNA expression. MATE1, GLUT2, MRP2, MRP4 and PXR expression levels were stable. Using immunohistochemistry, we found that MRP4 localization in pediatric samples was similar to that in adult samples. Collectively, our study revealed that renal drug transporters exhibited different rates and patterns of maturation, suggesting that renal handling of substrates may change with age.

INTRODUCTION

Renal membrane transporters, which are located on the apical and basolateral sides of the tubular epithelium, are key players in tubular secretion and reabsorption of a plethora of endogenous and exogenous compounds in the kidney.[1,2] Because of their role in renal elimination, many transporters in the kidney play critical roles in the disposition, efficacy and toxicity of drugs. Notably, renal drug transporters have received increasing regulatory attention in recent years, highlighting their significance in drug disposition.[3-6]

Interindividual variation in expression levels and functional activities of membrane transporters can affect the homeostasis of endogenous substrates, as well as the pharmacokinetics and pharmacodynamics of drugs.[1] As a result of developmental changes in key transporters and enzymes, levels of endogenous substrates, such as metabolites, nutrients, antioxidants and hormones, change as children grow.[7] Reduced hepatic clearance of the opioid morphine in newborns and young infants was reported.[8] This was suggested due to significantly lower hepatic levels of both the drug metabolizing enzyme uridine 5-diphosphoglucuronic acid glucuronyl transferase (UGT) 2B7 and the organic cation transporter (OCT) 1 in young pediatric populations compared to adults.[9,10] In contrast to the liver, less is known about the maturation and ontogeny pattern of renal membrane transporters. This knowledge gap limits the ability to predict the pharmacokinetics of renally eliminated drugs in children, which may be critical for rational dosing and drug efficacy and safety. Thus, there is an urgent need to understand the ontogeny of human drug transporters in the kidney.

The current study aimed to identify age-related differences in gene expression and protein abundance of renal transporters. We chose to focus on renal transporters with demonstrated clinical relevance in drug disposition, and those that handle various endogenous and exogenous substances important for developing children,[11,12] i.e., breast cancer resistance protein (gene name/protein name *ABCG2*/BCRP), multidrug and toxin extrusion protein (*SLC47A*/MATE) 1 and 2-K, multidrug resistance protein 1 (*ABCB1*/MDR1/P-gp), multidrug resistance-associated protein (*ABCC*/MRP) 2 and 4, and urate transporter 1 (*SLC22A12* /URAT1) on the apical site of the membrane and glucose transporter 2 (*SLC2A2*/GLUT2), organic anion transporter 1 (*SLC22A6*/OAT1) and 3 (*SLC22A8*/OAT3), and *SLC22A2*/OCT2 located on the basolateral site. In an effort to explore a regulatory mechanism for maturation of transporter expression, we also studied renal gene expression of the nuclear pregnane X receptor (PXR*)* in relation to the transporter expression levels.[13]

In addition, altered localization of a transporter may introduce variation in pharmacokinetics of transporter substrates. However, little is known about the localization of transporters during development of the kidney. MRP4 is an apical efflux transporter involved in transport of a range of endogenous molecules, including cyclic nucleotides, urate and conjugated steroid hormones, and drugs that are used in children, including antivirals and diuretics.[14] We performed immunohistochemistry, as a proof-of-concept, to visualize the location of MRP4 in our pediatric kidney tissues.

METHODS

Tissue procurement and sample characteristics

Two sample sets were analyzed and the demographic information of donors is reported in Table 1. Age groups were predefined based on the International Council for Harmonisation guidelines: preterm newborns (0-28 days PNA, <37 weeks GA), newborns (0-28 days PNA), infants (1-24 months old), children (2-12 years old), adolescents (12-16 years old) and adults (>16 years old)[4]. Sample set 1 consisted of postmortem autopsy kidney samples and surgical adult kidney samples from the Erasmus MC Tissue Bank, Rotterdam, the Netherlands. Sample set 2 consisted of 122 human postmortem frozen renal cortical tissues (donors aged 1 day to 30 years old), which were obtained from NIH NeuroBioBank at the University of Maryland, Baltimore, MD, United States. Tissues, which were selected for having no renal abnormalities in pathology and primary diagnosis, were procured at the time of autopsy within 48 hours after death and were stored at -196 ^{o}C (Sample set 1) and -80^{o}C (sample set 2) for later use. The quantitative proteomic analysis was done completely in the United States on the subset of samples from Sample set 2 and the immunohistochemistry was performed entirely in the Netherlands on Sample set 1. Gene expression analysis was conducted in both laboratories, and the data from the two sources were first analyzed separately, followed by a combined analysis. Combined analysis was deemed appropriate as no significant differences were observed between the expression levels of six transporter genes (MATE1, MATE2, P-gp, OAT1, OAT3 and OCT2) in adult samples obtained in the United States and in the Netherlands. Further, developmental patterns in expression of the transporters in the two sample sets showed comparable results.

mRNA expression

Figure 1 illustrates the sample analysis scheme. For sample set 1, the protocol on real-time reverse transcription polymerase chain reaction (RT-PCR) is described in Material S1 and Table S6. For sample set 2, the protocol described in Chen et al. was followed with slight modifications (Material S1).[15]

Table 1 Overview of sample size and age range of sample sets 1 and 2

	Number of samples				Age range	
	Sample set 1	Sample set 2				
Age group	Race unknown	Caucasian	African American	Total	Gestational age	Postnatal age
Preterm newborns	9	-	-	9	34.00 (24.00-36.71) wks	1.29 (0.14-4.00) wks
Term newborns	8	10	1	19	NA	1.29 (0.14-3.86) wks
Infants	21	30	30	81	NA	17.86 (4.14-103.00) wks
Children	7	15	16	38	NA	4.74 (2.00-11.56) yr
Adolescents	-	5	5	10	NA	13.38 (12.48-15.26) yr
Adults	17	5	5	27	NA	45.00 (16.75-75.00) yr
Total	62	65	57	184		
		122				

Figure 1 Sample analysis scheme.

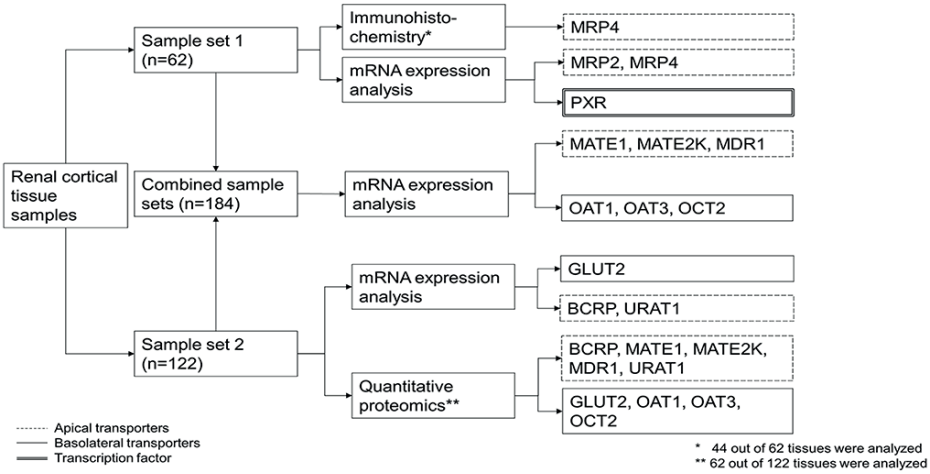

The subset of 62 samples from sample set 2 for quantitative proteomics consisted of the 57 African American samples and 5 adult Caucasian samples (See Table 1).

Quantitative proteomics using LC-MS/MS with Selective Reaction Monitoring (SRM)

Quantitative proteomics was only performed in sample set 2 (Figure 1). Unless otherwise stated, reagents from MyOmicsDx, Inc (Towson, MD) were used. Details of the LC and MS method and parameters are described in the supplemental documents (Material S2). Briefly, membrane proteins were extracted from the renal cortical tissues using

MyPro-MembraneEx buffer. The total extracted membrane protein concentration was determined using BCA protein assay kit. The membrane protein samples were then processed by MyOmicsDx, Inc (Towson, MD) using Filter-aided Sample Preparation method.[16]

Five peptides were chosen for each transporter as SRM quantifying targets and six best transitions per peptide precursors were selected for SRM quantification (Table S7). Peptide samples that were previously reconstituted in MyPro-Buffer 3 were spiked with MyPro-SRM Internal Control Mixture and were subjected to SRM analysis. The peptide samples were eluted through an online Agilent 1290 HPLC system into the Jet Stream ESI source of an Agilent 6495 Triple Quadrupole Mass Spectrometer (Agilent, Santa Clara, CA).

Quantitative data were imported into Skyline 3.1.[17] The abundance of a target peptide was represented by the area under the curve (AUC) of all its transitions normalized to the total AUC of all transitions from the most nearby (sharing a similar hydrophobicity) heavy isotope-labeled peptide from MyPro-SRM Internal Control Mixture spiked in before the SRM analysis. Absolute quantification of each protein is performed through applying AQUA^{TM} Peptides (Sigma-Aldrich, St. Louis, MO).

Immunohistochemistry

Localization of MRP4 was explored in a representative subpopulation of sample set 1. Immunohistochemistry was performed using an immunoperoxidase staining method for amplified antigen detection. Sections of 4 µm thick cortex were gained from formalin fixed, paraffin-embedded post-mortem kidney tissue blocks, and were mounted on glass slides. They were heated at 60°C for 30 min, deparaffinized in xylene, and rehydrated with a series of graded ethanol. Enhanced antigen retrieval was performed by treating slides in TRIS-EDTA (10mM Tris Base, 1mM EDTA Solution, 0.05% Tween 20, pH 9.0) for 15 min at 98°C. Endogenous peroxidase activity was quenched by incubating slides in 3% H_2O_2 for 30 min at room temperature. The sections were blocked with Avidin/Biotin blocking solution (Vector Laboratories, Burlingame, CA) 15 min each.

Primary antibodies rat anti-MRP4 (ab15598 Abcam) at dilution of 1:20 were incubated over night at 4°C in 1% BSA. A biotinylated secondary rabbit anti-rat serum (Acris Antibodies GmbH, R1371B) at dilution of 1:1000 was then applied for 30 min. Immunoreactive sides were detected using the ABC kit (Vector Laboratories, Burlingame, CA) for 30 min, and 3,3 diaminobenzidine tetrahydrochloride (Sigma-Aldrich, St. Louis, MO) solution staining for 15 min. The nuclei were counterstained with Mayers Hematoxylin Solution (Sigma-Aldrich, St. Louis, MO). One negative control staining lacking the primary antibody was performed for every age group.

Data analysis and statistics

Data were expressed as median (range). Kruskal-Wallis tests with Dunn's post-hoc test were used for multiple comparisons of expression levels between age groups, using the p-values adjusted for multiple testing. If no difference in expression was found between age groups, the ontogeny would be referred to as "stable". Sigmoidal Emax models are used often for maturational processes as it allows gradual maturation of clearance in early life and a "mature" clearance to be achieved at a later age.[18] Therefore, Emax models were used to fit the protein abundance data on a continuous scale of age for those transporters that showed between-group differences. The data point from the term newborn in this set of data was excluded prior to fitting to eliminate bias, as it was the only sample quantified for that age group. We first set the median of adult data to be 100%, and then normalized the data points from pediatric samples towards the median of adult data. Potential outliers were assessed and excluded using the Robust Regression followed by Outlier Identification method (ROUT) during the model fit process.[19] The age at which 50% maturation was reached (TM_{50}) was determined from the Emax model. Visual inspection and 95% CI of the Emax parameter estimates were used to assess the goodness of fit of the Sigmoidal model. Spearman's correlation analysis was used to evaluate the relationship between mRNA and protein abundances within the same and among other transporters.

For the analysis of staining intensity after immunohistochemistry, a semi-quantitative scoring system was used, graded by two observers (BG, MB) who independently confirmed cell staining intensity as negative (0), low staining (+1) or high staining (+2). Simultaneously, the localization of MRP4 in the kidney tissue was determined for each sample by the same observers.

Statistical analysis was performed using IBM SPSS Statistics software (version 21.0; Armonk, NY) and a significance level of $p<0.05$ was used throughout the study. Graphical exploration was performed using GraphPad Prism software (version 5.00; La Jolla, CA).

RESULTS

Two sample sets, which provided a total of 184 postmortem renal cortical tissues, were analyzed in this study (Figure 1 and Table 1). Sample set 1 represented 62 samples from individuals of different ages ranging from preterm newborns (gestational age (GA) > 24 weeks, postnatal age (PNA) 1 day) to adult donors (oldest 75 years). The 122 tissues in sample set 2 were from African American and Caucasian term newborns to adults. No statistical difference was observed in gene or protein abundance levels for any of

the transporters between males and females, and between African Americans and Caucasians (Table S1, Table S2 and Table S3); hence subsequent analyses were performed by combining both sexes and all ethnic groups.

Relative mRNA quantitation

All 184 tissues were processed for mRNA quantitation (Figure 2 and Table S4). mRNA levels of the selected transporters were detected successfully in all samples, with the exception of MATE1 in two samples. GAPDH mRNA expression did not change with age (r_s = -0.12, p=0.119).

Overall, a large variability in the developmental changes in transporter mRNA level was observed (Figure 2 and Table S4). MATE2-K, P-gp, URAT1, OAT1, OAT3 and OCT2 levels in premature and/or term newborns were significantly lower than in the older age groups. In contrast, term newborns showed significantly higher BCRP mRNA levels than children and adolescents. MATE1, MRP2, MRP4, GLUT2 and PXR levels were not different between all age groups (preterm newborn, term newborn, infants, children, adolescents and adults).

Figure 2 Relative mRNA expression of 11 renal membrane transporters and PXR in different age groups.

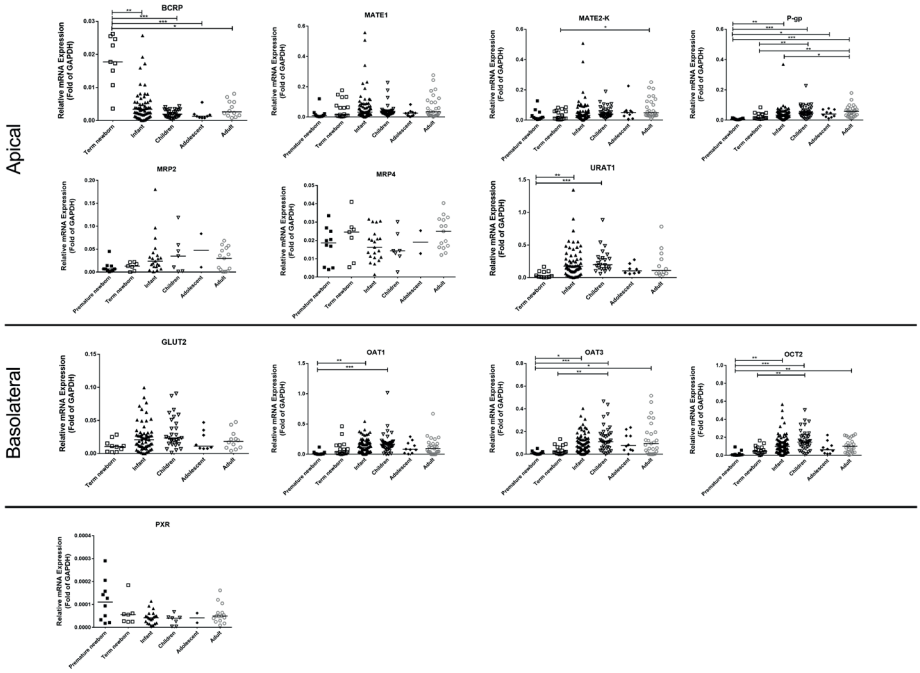

*Transporters are grouped according to their primary localization in the kidney (basolateral or apical). The bar represents the median for each age group. *p<0.05, **p<0.01, ***p<0.001*

Proteomics

62 samples were assessed for transporter protein levels (Figure 3 and Table S5). The median total membrane protein yield for all samples was 49.5 mg/g (range 41.7-62.1 mg/g) renal cortical tissue. All nine transporters were detected and quantified in our samples. P-gp was found to be the most abundant transporter, whereas MATE2-K was the least abundant (Table S5).

P-gp, URAT1, OAT1, OAT3 and OCT2 protein abundance levels were significantly lower in term newborn and infants than in the older age groups (Figure 3). Sigmoidal Emax models were used to fit the protein abundance levels of these five transporters, and all but URAT1 expression data conformed to the model (Figure 4a). OCT2 and P-gp expression increased at a faster rate than OAT1 and OAT3 as evidenced by the younger age at which half of the adult expression was reached (TM_{50}). Moreover, the transporters OCT2 and P-gp, shared a similar maturation pattern, as well as the transporters OAT1 and OAT3 (Figure 4b). No difference in protein abundance levels was found between age groups for BCRP, MATE1, MATE2-K and GLUT2.

Figure 3 Protein abundance levels of nine renal membrane transporters in different age groups.

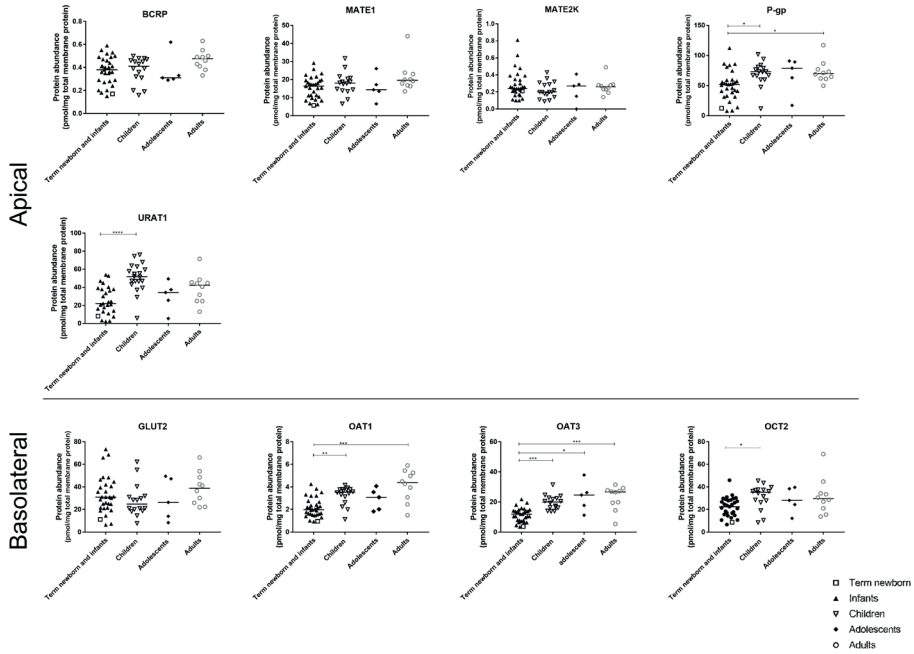

*The bar represents the median for each age group. Term newborn and infants were combined here for analysis since there was only one term newborn included for this part of the study. *p<0.05, **p<0.01, ***p<0.001*

Figure 4 a) Ontogeny of protein abundance of P-gp, OAT1, OAT3 and OCT2 as described by Sigmoidal Emax model (solid black lines). Dashed lines represent the 95% confidence bands; b) Superimposing the Sigmoidal curves showed that the pair transporters, P-gp /OCT2 and OAT1/OAT3, shared similar maturation patterns.

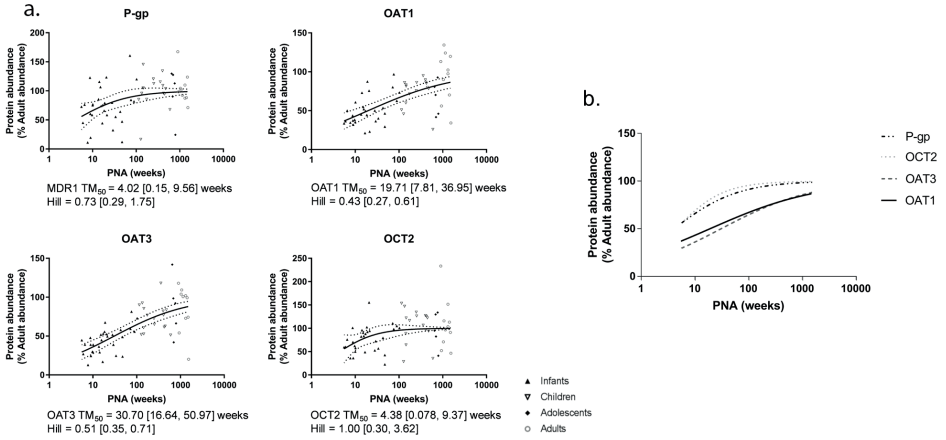

Table 2 Inter-transporter Spearman correlations

		Apical						Basolateral				
		BCRP	MATE1	MATE2-K	MDR1	MRP2	MRP4	URAT1	GLUT2	OAT1	OAT3	OCT2
Apical	BCRP	-	**0.69**		**0.44**	NA	NA			**0.59**		**0.43**
	MATE1		-	*0.63*	*0.36* **0.57**	*0.74*		*0.50* **0.57**	*0.44*	*0.53* **0.61**	*0.54* **0.54**	*0.62* **0.57**
	MATE2-K			-	*0.39*	*0.57*		*0.51*	*0.47*	*0.59*	*0.56*	*0.49*
	MDR1				-	0.47		*0.32* **0.56**	*0.37*	*0.52* **0.72**	*0.49* **0.60**	*0.57* **0.67**
	MRP2					-		NA	NA	*0.79*	*0.83*	*0.67*
	MRP4						-	NA	NA			
	URAT1							-	*0.42*	*0.54* **0.49**	*0.50* **0.49**	*0.46* **0.52**
Basolateral	GLUT2								-	*0.64*	*0.64*	*0.49*
	OAT1									-	*0.85* **0.83**	*0.74* **0.70**
	OAT3										-	*0.73* ***0.72***
	OCT2											-

Italic: mRNA expression; Bold: protein expression; NA=not available. All reached $p < 0.0001$. Data not presented if $p > 0.001$

Correlation between mRNA expression and protein abundance levels

Potential correlation between mRNA expression and protein abundance levels of the transporters was investigated (Figure S1). Significant correlation was found for MATE1, P-gp, URAT1, OAT3 and OCT2.

Inter-transporter correlation

To assess the potential shared expression regulation, we studied the correlation of mRNA expression and protein abundance levels between transporters (Table 2). Levels of OAT1 and OAT3 were the most significantly correlated.

Correlation between PXR and transporter mRNA expression

Weak negative correlations with PXR were found for MATE1 (r_s= -0.27, p = 0.035), MRP2 (r_s = -0.29, p = 0.021) and OCT2 (r_s = -0.26, p = 0.043), whereas no correlation was found for MATE2, P-gp, MRP4, OAT1 and OAT3.

Localization of MRP4 in pediatric kidney tissue

As a proof-of-concept, postmortem kidney tissues of 43 pediatric patients (GA > 24 weeks, PNA 2 days – 14 years old) and 1 adult were analyzed. Positive MRP4 immunostaining was detected as early as 27 weeks of gestation (PNA 9 days) despite negative staining found in 3 tissues from 1 child and 2 adolescents. For all the positive stained samples, MRP4 was found to be located at the apical side of the proximal tubule (Figure 5a and

Figure 5 Apical proximal tubule localization of MRP4 (arrow) by immunohistochemically staining in post mortem tissue of samples with a) GA of 27.7 weeks; PNA age 3.3 weeks, and b) GA of 40.0 weeks; PNA 3.1 year c) represents the negative control, and d) the semi quantification of MRP4 staining in various age groups: negative (0), low staining (+1) or high staining (+2).

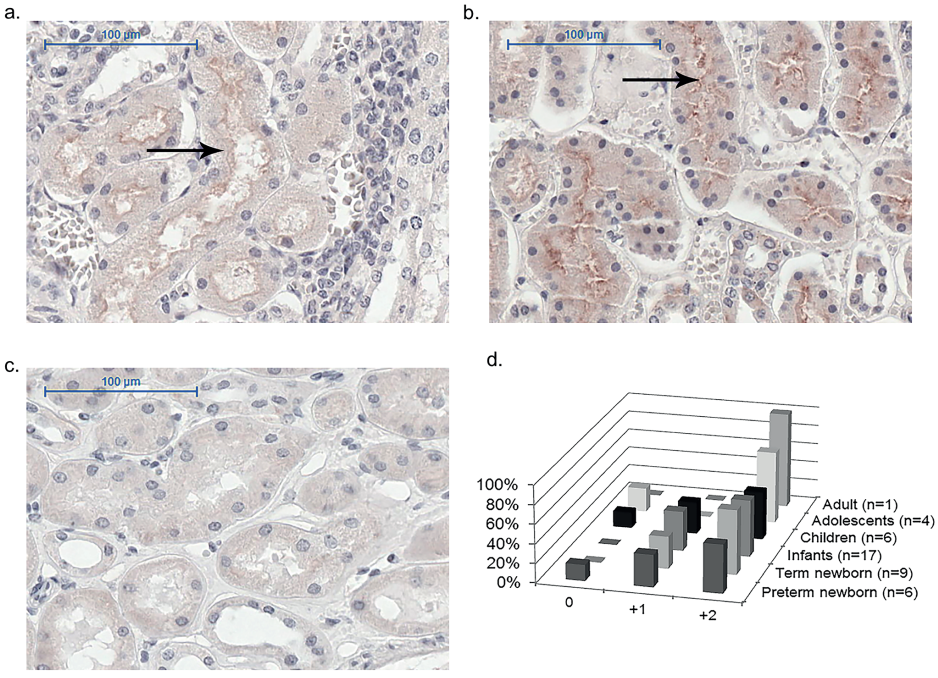

Figure 5b). See Figure 5c for the negative control. Although the examples showed lower staining at 3.3 weeks (Figure 5a) than 3.1 years old (Figure 5b), no statistically significant age-related changes were detected in the semi-quantification of the staining in the whole sample set (Figure 5d).

DISCUSSION

This study, to our best knowledge, is the first to comprehensively describe the ontogeny of human renal membrane transporters via mRNA expression analysis and quantitative proteomics in tissues representing a large span of ages. Albeit data on developmental changes in transporter mRNA expression in animals were reported previously,[20-24] cross species differences limit extrapolation, especially concerning the rates of maturation.[25]

Our study revealed two major findings with respect to the developmental maturation of renal transporters: (i) the expression of most of the transporters characterized in this study increased with age during the earliest developmental periods (< 2 years old); and (ii) maturation pattern was transporter-dependent. Additionally, we observed that: (a) there were maturational differences between mRNA expression and protein abundance; (b) there were correlations between the expression levels of various transporters; (c) PXR seems to play a minimal role in regulating mRNA expression of transporters in the kidney; and (d) stable MRP4 mRNA expression was accompanied by proper apical localization during development.

Transporter-dependent maturation patterns during the earliest developmental periods

The findings that most of the studied transporters showed a transporter-dependent age-related increase in their expression levels, especially during the earliest years of life were expected. Renal membrane transporters play critical roles in elimination and detoxification pathways in the body. They work in concert with enzymes in the kidney, as well as enzymes and transporters in other organs such as the intestine and liver to mediate the removal of ingested potential harmful compounds such as toxins derived from food, environmental toxins, drugs and their metabolites.[7] During infancy, dietary exposure to potential toxins is limited and begins to increase as infants are switched from an exclusively milk diet, to foods that may contain more toxins.[26,27] Thus, detoxification pathways are increasingly needed as the diet of infants expands and diversifies into childhood.

Further, besides changes in dietary intake and nutritional requirement, ontogeny of renal transporters can alter the disposition of endogenous compounds, suggesting important developmental roles for these renal transporters. Both BCRP and URAT1 are thought to play a clear role in uric acid (UA) homeostasis.[28,29] It was previously reported that the fractional excretion of UA (FEUA: the % of filtered UA not reabsorbed by the tubules), was 30-40% in term newborns <5 days old, which then decreased to 8-10% in children of 3 years old.[30-32] Our transporter maturation data, in addition to age-related physiological changes, *e.g.,* urinary acidification and concentration ability, may explain this observation: the decreasing BCRP mRNA expression from birth is accompanied by an increased expression of URAT1, a reabsorptive transporter, from birth till childhood, resulting in a net decrease in UA excretion.[30,32] Interestingly, sex-related differences in FEUA especially during adolescence were reported, which could be due to differences in proximal tubular secretion of UA.[32] Yet, no significant sex-related differences were found in our study consisting mainly of pediatric samples. As the influence of sex appears to be transporter-specific in adults,[33] follow-up studies with more samples and also with other transporters that handle UA, such as GLUT9, would be needed to fully understand the changes in FEUA.

In vivo pharmacokinetic data of drugs that are transporter substrates may be used to support our expression data. However, renal elimination of these drugs is accomplished not only by active tubular secretion facilitated by various transporters, but also by glomerular filtration, which is also subjected to age-dependent changes. As children grow and develop, the glomerular filtration rate (GFR) matures and is predicted to reach 50% of adult values by 2 months PNA and 90% of adult values by 1 year of age.[34] Though the full complement of nephrons in each kidney is complete around GA 36 weeks,[35] GFR continues to develop as a result of increases in kidney blood flow, improvements in filtration coefficients, and maturation of the tubules. Our findings that there are age-related changes in transporter expression early in life (<2 years) support the notion that active tubular secretion matures in parallel with GFR maturation. Thus, observed age-related changes in pharmacokinetics of transporter substrates are likely due to a combination of both maturation in transporter expression and GFR. For instance, after hepatic metabolism, the antiviral drug valacyclovir undergoes renal elimination via glomerular filtration and active tubular secretion likely by OAT1/3.[36] Apparent clearance of valacyclovir in infants < 3 months old is 50% lower than that in young children.[36] The GFR in infants <3 months old is expected to be >50%[34], and therefore this discrepancy may be explained by our findings that the TM_{50} of OAT1 and OAT3 were approximately 4 and 8 months (Figure 4a). Famotidine, an OAT3 substrate used in the treatment of gastritis, provides another example of maturational changes in both GFR and secretory transporters.[37] Given the complex developmental changes in renal elimination processes,

our data could be integrated into physiologically-based pharmacokinetic models to improve prediction of pediatric drug clearance. When doing so, scaling factors should be used to correct for membrane protein yield and total organ weight.

Other observations from data analysis

The abundance pattern of the transporters in our adult samples were assessed. P-gp has the highest abundance, followed by URAT1, GLUT2, OCT2, OAT3, MATE1, OAT1, BCRP and MATE2K. This abundance pattern is different from that reported in Prasad et al [38], where OCT2 was the most abundant transporter, followed by OAT1, MATE1, OAT3 and P-gp. This discrepancy could be due to actual inter-sample variation in expression levels of the transporters, or to differences in the inclusion criteria and quality of the tissue samples used in the studies. In addition, our study also showed much higher absolute abundance for most proteins in our adult samples compared to other studies [39]. As Li et al suggested[40], such inter-laboratory difference may, in part, be explained by different instrumental performance and varying tissue handling techniques.

Differences in the patterns and rates of change among mRNA expression and protein abundance levels of various transporters were noticed. For example, age-related changes were found in BCRP, GLUT2 and MATE2-K mRNA levels but not in protein abundance levels. This may suggest maturational differences in the regulation of gene transcription and post-translational processing. For gene transcription, alternative splicing is suggested to occur due to developmental signals.[41] Some of the alternatively spliced mRNA transcripts may not be translated into the protein of interest but will be quantified by qRT-PCR as the total mRNA expression could be derived from a mixture of different transcripts of the targeted gene. [42] Quantitative proteomics overcomes this challenge by measuring the actual expression of the protein of interest. This process could explain the lack of correlation between mRNA and protein expression.

Our data showed that transporter expression is correlated among various transporters. The strong correlation between expression of OAT1 and OAT3 is not surprising as they are located in adjacent regions on chromosome 11.[43] Moreover, they are both regulated by the transcription factors hepatocyte nuclear factor (HNF) 1α and 1β, which increase their transcription.[44] Our study of transcription factors was confined to PXR, and in agreement with previously reported findings; PXR mRNA levels in kidney were low in all age groups compared to the mRNA levels of the studied transporters.[33,45,46] Thus, PXR seems to have a minor role in regulating transporter gene expression in the kidney than in other organs. This is supported by findings in mice, where the potent rodent PXR activator pregnenolone-16α-carbonitrile induced transporter expression in liver and intestine, but not in kidney.[45] More research is needed to identify the developmental

triggers by which transcription of transporters increase and decrease. Moreover, the relationship between transcription factors maintaining basal expression level, like the HNF family, and renal transporter expression, should be studied.

Detoxification involves the interplay between enzymes and transporters that are ubiquitously expressed in tissues throughout the human body. P-gp expression levels in the liver only reached 50% of adult expression levels at 2.9 years of age[9] whereas our results suggested that full adult levels were achieved in the kidney by that age. For BCRP, our results for mRNA expression in the kidney were consistent with that in the liver, which showed a decline from newborns to adults.[47] As more transporter ontogenetic data in different organs become available, more reliable prediction in transporter-mediated substrate disposition on the whole-body level during development will be achieved.

Potential limitations

Certain limitations are present in this study. In addition to age, there are other potential factors, such as the use of co-medications and inflammation that can influence transporter expression and thereby contribute to the expression variability.[48] The impact of acute and chronic inflammation on transporter expression and activity is related to the activity of multiple proinflammatory cytokines. [49] The exact mechanism remains unknown, and may be related to various nuclear receptors and transcription factors. Similarly, certain medications and environmental toxins could lead to activation of nuclear receptor pathway, and could therefore influence the transporter expression.[49,50] The underlying reason for death of our tissue donors is heterogeneous, and so as the exposure of drugs and environmental toxins. Yet, despite all these inevitable differences, significant changes in the expression levels by age were still observed. However, due to the lack of detailed clinical data available for our samples, these factors could not be explored. Though protein and mRNA levels in the post-mortem samples used in our study were excellent, the amount of degradation in these levels from death to freezing is not known. Degradation may vary among samples, and may result in reduced absolute levels and increased variability in expression level measurements. Moreover, with the exception of PXR, we did not study the ontogeny of other transcription factors and proteins involved in gene and protein regulation; therefore, the mechanisms underlying the ontogeny of transporters observed in this study are not known. Finally, mRNA expression, protein abundance and transporter activity *ex-vivo* and *in-vivo* studies are needed to confirm the implications of our results to drug disposition in the kidney.

CONCLUSIONS

These results showed that the ontogeny of certain renal membrane transporters displayed an age-dependent pattern, suggesting that the clearance of exogenous and endogenous substrates for these kidney transporters are subject to transporter-specific age-related changes. Though future work is clearly needed in refining predictive models for pediatric drug disposition, leveraging our expression data in modeling and simulation strategies may improve predictability of pediatric drug disposition and exposure models. Importantly, our findings set the stage for future research in understanding the mechanisms of developmental changes in renal drug transporters.

REFERENCES

1. Morrissey KM, Stocker SL, Wittwer MB, Xu L, Giacomini KM. Renal transporters in drug development. Annu Rev Pharmacol Toxicol 2013;53:503-529.
2. Motohashi H, Nakao Y, Masuda S, et al. Precise comparison of protein localization among OCT, OAT, and MATE in human kidney. J Pharm Sci 2013;102(9):3302-3308.
3. Food and Drug Administration. In vitro metabolism- and transporter-mediated drug-drug interaction Studies. https://www.fda.gov/Drugs/GuidanceComplianceRegulatoryInformation/Guidances/ucm064982.htm. Accessed September 24, 2018.
4. International Council for Harmonisation. Guidance for Industry. E11 Clinical investigation of medicinal products in the pediatric population. 2000.
5. European Medicines Agency. Guideline on the investigation of drug interactions. Committee for Human Medicinal Products. http://www.ema.europa.eu/docs/en_GB/document_library/Scientific_guideline/2012/07/WC500129606.pdf. Accessed April 3, 2018.
6. Pharmaceuticals Medical Devices Agency. Guideline on drug-drug interactions 2018; http://www.pmda.go.jp/files/000225191.pdf Accessed September 24, 2018.
7. Nigam SK. What do drug transporters really do? Nat Rev Drug Discov 2015;14(1):29-44.
8. Knibbe CA, Krekels EH, van den Anker JN, et al. Morphine glucuronidation in preterm neonates, infants and children younger than 3 years. Clin Pharmacokinet 2009;48(6):371-385.
9. Prasad B, Gaedigk A, Vrana M, et al. Ontogeny of hepatic drug transporters as quantified by LC-MS/MS proteomics. Clin Pharmacol Ther 2016;100(4):362-370.
10. Lu H, Rosenbaum S. Developmental pharmacokinetics in pediatric populations. J Pediatr Pharmacol Ther 2014;19(4):262-276.
11. Giacomini KM, Huang SM, Tweedie DJ, et al. Membrane transporters in drug development. Nat Rev Drug Discov 2010;9(3):215-236.
12. Brouwer KL, Aleksunes LM, Brandys B, et al. Human ontogeny of drug transporters: review and recommendations of the pediatric transporter working group. Clin Pharmacol Ther 2015;98(3):266-287.
13. Zhang B, Xie W, Krasowski MD. PXR: a xenobiotic receptor of diverse function implicated in pharmacogenetics. Pharmacogenomics 2008;9(11):1695-1709.
14. Ritter CA, Jedlitschky G, Meyer zu Schwabedissen H, Grube M, Kock K, Kroemer HK. Cellular export of drugs and signaling molecules by the ATP-binding cassette transporters MRP4 (ABCC4) and MRP5 (ABCC5). Drug Metab Rev 2005;37(1):253-278.
15. Chen EC, Liang X, Yee SW, et al. Targeted disruption of organic cation transporter 3 attenuates the pharmacologic response to metformin. Mol Pharmacol 2015;88(1):75-83.
16. Wisniewski JR, Zougman A, Nagaraj N, Mann M. Universal sample preparation method for proteome analysis. Nat Methods 2009;6(5):359-362.
17. MacLean B, Tomazela DM, Shulman N, et al. Skyline: an open source document editor for creating and analyzing targeted proteomics experiments. Bioinformatics 2010;26(7):966-968.
18. Anderson BJ, Holford NH. Mechanism-based concepts of size and maturity in pharmacokinetics. Annu Rev Pharmacol Toxicol 2008;48:303-332.
19. Motulsky HJ, Brown RE. Detecting outliers when fitting data with nonlinear regression - a new method based on robust nonlinear regression and the false discovery rate. BMC Bioinformatics 2006;7:123.

20. Sweeney DE, Vallon V, Rieg T, Wu W, Gallegos TF, Nigam SK. Functional maturation of drug transporters in the developing, neonatal, and postnatal kidney. Mol Pharmacol 2011;80(1):147-154.
21. Pinto N, Halachmi N, Verjee Z, Woodland C, Klein J, Koren G. Ontogeny of renal P-glycoprotein expression in mice: correlation with digoxin renal clearance. Pediatr Res 2005;58(6):1284-1289.
22. Maher JM, Slitt AL, Cherrington NJ, Cheng X, Klaassen CD. Tissue distribution and hepatic and renal ontogeny of the multidrug resistance-associated protein (MRP) family in mice. Drug Metabolism and Disposition 2005;33(7):947-955.
23. Nakajima N, Sekine T, Cha SH, et al. Developmental changes in multispecific organic anion transporter 1 expression in the rat kidney. Kidney Int 2000;57(4):1608-1616.
24. Slitt AL, Cherrington NJ, Hartley DP, Leazer TM, Klaassen CD. Tissue distribution and renal developmental changes in rat organic cation transporter mRNA levels. Drug Metab Dispos 2002;30(2):212-219.
25. Chu X, Bleasby K, Evers R. Species differences in drug transporters and implications for translating preclinical findings to humans. Expert Opin Drug Metab Toxicol 2013;9(3):237-252.
26. Nicklaus S. The role of dietary experience in the development of eating behavior during the first years of life. Ann Nutr Metab 2017;70(3):241-245.
27. Bearer CF. Environmental health hazards: how children are different from adults. Future Child 1995;5(2):11-26.
28. Brackman DJ, Giacomini KM. Reverse translational research of ABCG2 (BCRP) in human disease and drug response. Clin Pharmacol Ther 2018;103(2):233-242.
29. Xu L, Shi Y, Zhuang S, Liu N. Recent advances on uric acid transporters. Oncotarget 2017;8(59):100852-100862.
30. Passwell JH, Modan M, Brish M, Orda S, Boichis H. Fractional excretion of uric acid in infancy and childhood. Index of tubular maturation. Arch Dis Child 1974;49(11):878-882.
31. Baldree LA, Stapleton FB. Uric acid metabolism in children. Pediatr Clin North Am 1990;37(2):391-418.
32. Stiburkova B, Bleyer AJ. Changes in serum urate and urate excretion with age. Adv Chronic Kidney Dis 2012;19(6):372-376.
33. Benson EA, Eadon MT, Desta Z, et al. Rifampin regulation of drug transporters gene expression and the association of microRNAs in human hepatocytes. Front Pharmacol 2016;7:111.
34. Rhodin MM, Anderson BJ, Peters AM, et al. Human renal function maturation: a quantitative description using weight and postmenstrual age. Pediatr Nephrol 2009;24(1):67-76.
35. Faa G, Gerosa C, Fanni D, et al. Morphogenesis and molecular mechanisms involved in human kidney development. J Cell Physiol 2012;227(3):1257-1268.
36. Mooij MG, Nies AT, Knibbe CA, et al. Development of human membrane transporters: drug disposition and pharmacogenetics. Clin Pharmacokinet 2016;55(5):507-524.
37. Motohashi H, Uwai Y, Hiramoto K, Okuda M, Inui K. Different transport properties between famotidine and cimetidine by human renal organic ion transporters (SLC22A). Eur J Pharmacol 2004;503(1-3):25-30.
38. Prasad B, Johnson K, Billington S, et al. Abundance of Drug Transporters in the Human Kidney Cortex as Quantified by Quantitative Targeted Proteomics. Drug Metab Dispos 2016;44(12):1920-1924.
39. Fallon JK, Smith PC, Xia CQ, Kim MS. Quantification of Four Efflux Drug Transporters in Liver and Kidney Across Species Using Targeted Quantitative Proteomics by Isotope Dilution NanoLC-MS/MS. Pharm Res 2016;33(9):2280-2288.

40. Li H, Han J, Pan J, Liu T, Parker CE, Borchers CH. Current trends in quantitative proteomics - an update. J Mass Spectrom 2017;52(5):319-341.
41. Baralle FE, Giudice J. Alternative splicing as a regulator of development and tissue identity. Nat Rev Mol Cell Biol 2017;18(7):437-451.
42. Zhang M, Liu YH, Chang CS, et al. Quantification of gene expression while taking into account RNA alternative splicing. Genomics 2018:DOI: 10.1016/j.ygeno.2018.1010.1009.
43. Kent WJ, Sugnet CW, Furey TS, et al. The human genome browser at UCSC. Genome Res 2002;12(6):996-1006.
44. Wang L, Sweet DH. Renal organic anion transporters (SLC22 family): expression, regulation, roles in toxicity, and impact on injury and disease. AAPS J 2013;15(1):53-69.
45. Cheng X, Klaassen CD. Regulation of mRNA expression of xenobiotic transporters by the pregnane x receptor in mouse liver, kidney, and intestine. Drug Metab Dispos 2006;34(11):1863-1867.
46. Miki Y, Suzuki T, Tazawa C, Blumberg B, Sasano H. Steroid and xenobiotic receptor (SXR), cytochrome P450 3A4 and multidrug resistance gene 1 in human adult and fetal tissues. Mol Cell Endocrinol 2005;231(1-2):75-85.
47. Mooij MG, van de Steeg E, van Rosmalen J, et al. Proteomic analysis of the developmental trajectory of human hepatic membrane transporter proteins in the first three months of life. Drug Metab Dispos 2016;44(7):1005-1013.
48. Vet NJ, Brussee JM, de Hoog M, et al. Inflammation and organ failure severely affect midazolam clearance in critically ill children. Am J Respir Crit Care Med 2016;194(1):58-66.
49. Evers R, Piquette-Miller M, Polli JW, et al. Disease-Associated Changes in Drug Transporters May Impact the Pharmacokinetics and/or Toxicity of Drugs: A White Paper From the International Transporter Consortium. Clin Pharmacol Ther 2018;104(5):900-915.
50. Prakash C, Zuniga B, Song CS, et al. Nuclear Receptors in Drug Metabolism, Drug Response and Drug Interactions. Nuclear Receptor Res 2015;2:101178.

SUPPLEMENTAL INFORMATION

Material S1 RT-PCR protocol sample set 1 and sample set 2

mRNA isolation and cDNA synthesis

Total RNA was isolated from the tissue using a Nucleospin® RNA II kit (Machery-Nagel, Düren, Germany) for sample set 1 and RNeasy Mini Kit (Qiagen, Valencia, CA) for sample set 2, according to the manufacturer's instructions. Approximately 5-30 mg of frozen tissue was manually homogenized on ice in an Eppendorf tube using pellet pestles to yield 22 – 570 ng/Ul (range) RNA. Quality Control standards were applied to all RNA samples in this study. Purity was assessed both with A260nm/A280nm 1.9-2.1. Absorbance measurements at 260 nm in water were used to adjust the stock concentrations of all RNA samples to 1 Ug/Ul.

For reverse transcription, samples were treated with DNAse to digest contaminating DNA. For sample set 1 cDNA was obtained following local protocol, and for sample set 2 using SuperScript VILO cDNA Synthesis Kit (Life Technologies) per manufacturer's protocol.

Quantitative RT-PCR

For sample set 1, expression was measured by a SYBR green (SensiMix SYBR Hi-ROX kit; Bioline) quantitative RT-PCR using a 7900 Sequence detector (Applied Biosystems) on a 96 well optical reaction plate (Applied Biosystems). In house designed primer sequences, with confirmed specificity in appropriate melting curves for each PCR, can be found in Table S1 and were derived from Eurogentec (Eurogentec Netherlands, Maastricht, Netherlands). PCR efficiency of each primer pair was determined using serial dilutions of cDNA from the Caco-2 (colon carcinoma) cell line and from peripheral blood mononuclear cells. Non template controls confirmed the absence of exogenous contaminated DNA.

For sample set 2 RT-PCR was carried out in 384-well reaction plates using 2X Taqman Fast Universal Master Mix (Applied Biosystems, Foster City, CA), 20X Taqman specific gene expression probes and 10ng of the cDNA template. The reactions were carried out on an Applied Biosystems 7500 Fast Real-Time Polymerase Chain Reaction System (Applied Biosystems).

Transporter mRNA expression levels for all samples were normalized to GAPDH mRNA expression levels (ratio transporter/GAPDH) and relative expression was compared across the age range. Quality was assessed by measuring the RNA integrity number (RIN)

by microfluidic capillary electrophoresis on a 2100 Bioanalyzer (Agilent Technologies, Santa Clara, USA), whereby RIN's below 5 were to be excluded from the analysis.

Material S2 Detail description of LC-MS sample preparation and method parameters for quantitative proteomics

Quantitative proteomics was only performed in sample set 2 (Figure 1). Unless otherwise stated, reagents from MyOmicsDx, Inc (Towson, MD) were used. Membrane proteins were extracted from the renal cortical tissues using MyPro-MembraneEx buffer. The total extracted membrane protein concentration was determined using BCA protein assay kit. The membrane protein samples were then processed by MyOmicsDx, Inc (Towson, MD) using Filter-aided Sample Preparation method.[16] Briefly, protein samples in 9M urea were reduced with 5mM TCEP at 37°C for 45 min and reduced cysteines were blocked using 50mM iodoacetamide at 25°C for 15min. Protein samples were then cleaned using 10kDa Amicon Filter (UFC 501096, Millipore) three times using 9M urea and two times using MyPro-Buffer 1 (MyOmicsDx, Inc., Towson, MD). Samples were then proteolyzed with trypsin (V5111, Promega) for 12 hours at 37°C. The peptide solution was acidified by adding 1% trifluoroacetic acid (TFA) and was incubated at room temperature for 15 min. A Sep-Pak light C18 cartridge (Waters Corporation) was activated by loading 5mL 100% (vol/vol) acetonitrile and was washed by 3.5mL 0.1% TFA solution two times. Acidified digested protein solution was centrifuged at 1,800 x g for 5 min and the supernatant was loaded into the cartridge. To desalt the peptide bound to the cartridge, 1mL, 3mL, and 4mL of 0.1% TFA were added sequentially. 2mL of 40% (vol/vol) acetonitrile with 0.1% TFA was used to elute the peptides from the cartridge. The eluted peptides were lyophilized overnight and reconstituted in 37 µL MyPro-Buffer 3 (MyOmicsDx, Inc., Towson, MD).

Five peptides were chosen for each transporter as SRM quantifying targets from MyOmicsDx's SRM target peptide database, MyPro-SRM Map, based on their performance in documented experiments. Transition parameters and retention times of the 45 peptides were established individually using an Agilent 6495 Triple Quadrapole Mass Spectrometer for 1+, 2+, 3+ and 4+ charged precursor ions. Six best transitions per peptide precursor were selected for SRM quantification (Table S2).

Peptide samples previously reconstituted in MyPro-Buffer 3 were spiked with MyPro-SRM Internal Control Mixture which composed of a pool of 1 femto mole heavy isotope labeled peptides covering a large hydrophobicity window and a large M/z range of 200~1300, and were subject to SRM analysis. The peptide samples were eluted through

an online Agilent 1290 HPLC system into the Jet Stream ESI source of an Agilent 6495 Triple Quadrupole Mass Spectrometer (Agilent, Santa Clara, CA).

The Agilent 6495 Triple Quadrupole Mass Spectrometer was tuned using the manufacturer's tuning mixture by MyPro-SRM Tuning Booster after every preventive maintenance. Before and after each batch of SRM analysis, to ensure the stable and consistent performance of the mass spectrometer throughout the entire study, MyPro-SRM Performance Standard, a mixture of standard peptides across a wide range of mass (M/Z 100-1400) and a broad range of hydrophobicity were analyzed.

Figure S1 Correlations between mRNA expressions and protein expressions (Spearman's correlation coefficient, r_s)

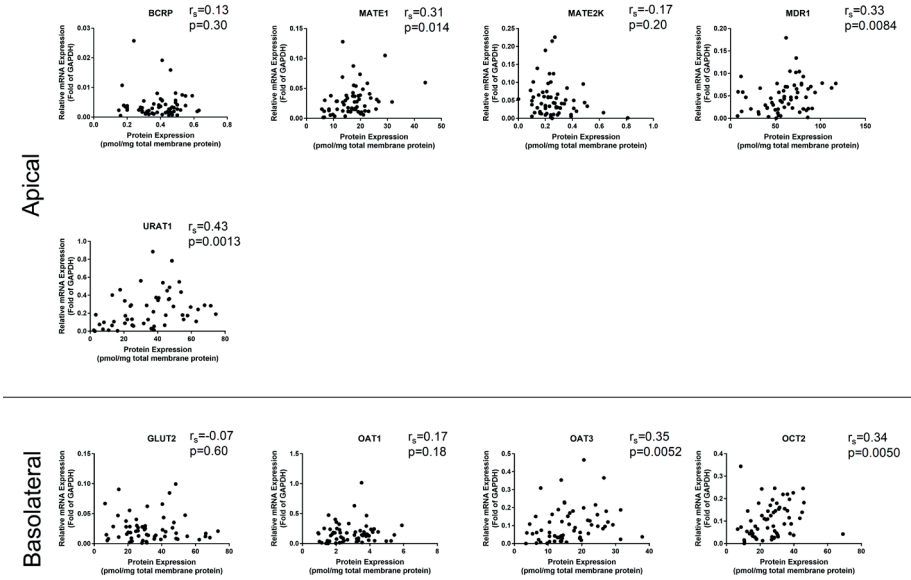

Table S1 Mann-Whitney U test to examine the differences in mRNA and protein expression between female and male

	mRNA Expression Analysis			Quantitative Proteomics		
	Median (range)		Mann-Whitney U test p-value	Median (range)		Mann-Whitney U test p-value
	Female	Male		Female	Male	
BCRP	0.00304 (0.00012-0.12)	0.0031 (0.00014-0.026)	0.71	0.41 (0.18-0.62)	0.37 (0.15-0.63)	0.52
MATE1	0.028 (0.0012-0.56)	0.032 (0-0.51)	0.44	17.24 (6.211-29.13)	16.12 (5.72-31.72)	0.4
MATE2-K	0.032 (0.0032-0.39)	0.034 (0.0022-0.51)	0.89	0.25 (0.14-0.81)	0.24 (0.00-0.31)	0.27
MRP2	0.013 (6.32E-5 - 0.083)	0.018 (0.00089 - 0.18)	0.32	NA	NA	NA
MRP4	0.019 (0.0042-0.031)	0.017 (0.0014-0.041)	0.91	NA	NA	NA
MDR1	0.031 (0.00032-0.37)	0.034 (0.0016-0.23)	0.52	66.12 (11.68-102)	54.6 (7.84-112.4)	0.2
URAT1	0.14 (0.0082-0.7204)	0.1582 (5.65E-5 - 1.35)	0.89	39.1 (2.17-76.05)	35.26 (2.79-74.50)	0.54
GLUT2	0.017 (0.0012-0.50)	0.024 (0.0012-0.099)	0.35	32.01 (7.21-73.94)	26.12 (6.41-68.55)	0.39
OAT1	0.076 (2.3E-5 - 0.36)	0.11 (0.00037-0.67)	0.18	3.14 (0.93 - 4.49)	2.35 (0.96 - 5.45)	0.87
OAT3	0.052 (0-0.40)	0.071 (0.00039-0.44)	0.21	13.91 (4.54-27.23)	15.17 (3.43-37.92)	0.6
OCT2	0.087 (3.37E-5 - 0.57)	0.094 (0.00061-0.50)	0.54	27.82 (8.48-45.94)	26.62 (6.66-45.44)	0.78
PXR	4.84E-5 (1.51E-5 - 0.00018)	4.34E-5 (4.58E-6 - 0.00029)	0.64	NA	NA	NA

Table S2 Kruskal Wallis followed by multiple comparisons to examine the differences in mRNA expression between African American and Caucasians in different age groups. All p-values > 0.9999, suggesting no statistical differences in the mRNA expression between these two ethnic groups in all age groups.

	Preterm to term newborn*	Infant*	Children*	Adolescent*	Adults*
BCRP	-6.7	5.68	11.32	26.00	-29.40
MATE1	16.07	35.92	11.98	1.00	23.20
MATE2-K	-76.09	20.14	3.00	-36.70	20.40
MDR1	5.08	17.25	-30.64	-38.4	62.60
URAT1	20.4	-0.87	27.52	9.30	22.80
GLUT2	51.17	11.15	-20.51	14.00	2.60
OAT1	61.50	-1.39	23.31	22.58	23.00
OAT3	-34.70	19.54	-6.32	16.60	18.00
OCT2	-27.98	14.69	1.44	-16.28	24.60

** mean rank differences*

Table S3 Mann-Whitney U test to examine the differences in protein expression levels between African American adults and Caucasian adults

	Median (range)		Mann-Whitney U test p-value
	African American	Caucasian	
BCRP	0.49 (0.33-0.63)	0.46 (0.38-0.5)	0.60
MATE1	16.8 (13.47-20.08)	23.01 (17.83-44.01)	0.095
MATE2-K	0.28 (0.14-0.49)	0.23 (0.19-0.27)	0.14
MDR1	64.57 (49.76-86.57)	70.98 (61.82-117.00)	0.55
URAT1	31.72 (24.79-45.64)	44.2 (12.95-71.51)	0.55
GLUT2	36.47 (22.02-42.34)	48.5 (22.37=66.12)	0.31
OAT1	4.49 (1.5-5.45)	3.95 (2.46-5.9)	0.84
OAT3	19.84 (5.39-27.23)	27.75 (14.43-31.51)	0.22
OCT2	28.6 (13.76)	33.52 (15.47-69.08)	0.69

Table S4 Relative mRNA expression of 11 transporters and PXR in age-groups

	Apical						Basolateral					
	BCRP	MATE1	MATE2-K	MDR1	MRP2	MRP4	URAT1	GLUT2	OAT1	OAT3	OCT2	PXR
All samples												
Median	0.0028	0.029	0.034	0.037	0.016	0.020	0.15	0.020	0.11	0.067	0.096	4.57E-05
Minimum	0.00	0.00	1.78E-05	2.91E-04	6.32E-05	0.0014	0.0001	0.0012	2.30E-05	0.00	3.37E-05	4.58E-06
Maximum	0.026	0.56	0.51	0.37	0.18	0.041	1.35	0.099	1.02	0.68	0.88	2.90E-04
Preterm newborns												
Median		0.010	0.019	0.0062	0.0065	0.020			0.0055	0.0072	0.0062	9.39E-05
Minimum		0.0012	0.0052	3.16E-04	8.59E-04	0.0042			2.30E-05	2.51E-05	3.37E-05	1.79E-05
Maximum		0.12	0.13	0.015	0.045	0.034			0.12	0.052	0.094	2.90E-04
Term newborn												
Median	0.018	0.015	0.017	0.014	0.013	0.023	0.026	0.011	0.038	0.023	0.049	5.56E-05
Minimum	0.0036	0.0023	0.0032	0.0023	6.32E-05	0.0053	0.0024	0.0022	4.37E-04	2.59E-04	1.11E-04	2.47E-05
Maximum	0.026	0.18	0.085	0.20	0.022	0.041	0.17	0.029	0.46	0.13	0.16	1.84E-04
Infants												
Median	0.0034	0.032	0.032	0.033	0.024	0.016	0.18	0.022	0.11	0.071	0.10	4.15E-05
Minimum	0.00	0.0001	1.78E-05	2.91E-04	8.85E-04	0.0014	5.65E-05	0.0012	4.71E-05	0.00	1.85E-04	7.69E-06
Maximum	0.026	0.56	0.51	0.37	0.18	0.032	1.35	0.099	0.47	0.42	0.88	1.14E-04
Children												
Median	0.0019	0.028	0.040	0.047	0.035	0.014	0.20	0.024	0.17	0.11	0.15	3.99E-05
Minimum	5.16E-04	0.0018	0.010	0.0057	0.0013	0.0028	0.058	0.0012	5.63E-04	3.87E-04	0.015	4.58E-06
Maximum	0.0043	0.23	0.19	0.23	0.12	0.030	0.89	0.091	1.02	0.68	0.50	6.75E-05
Adolescents												
Median	0.0013	0.025	0.051	0.041	0.047	0.019	0.10	0.011	0.081	0.077	0.062	4.12E-05
Minimum	7.96E-04	0.0037	0.0070	0.011	0.011	0.013	0.058	0.0074	0.0041	0.0015	0.017	2.01E-05

Table S4 Relative mRNA expression of 11 transporters and PXR in age-groups (continued)

	Apical						Basolateral					
	BCRP	MATE1	MATE2-K	MDR1	MRP2	MRP4	URAT1	GLUT2	OAT1	OAT3	OCT2	PXR
Maximum	0.0055	0.083	0.23	0.078	0.084	0.025	0.28	0.047	0.29	0.24	0.23	6.23E-05
Adults												
Median	0.0026	0.034	0.048	0.057	0.030	0.025	0.11	0.018	0.10	0.10	0.10	4.96E-05
Minimum	8.22E-04	0.0011	0.0062	0.014	6.69E-04	0.012	0.042	0.0041	2.66E-05	8.45E-05	0.0029	8.97E-06
Maximum	0.0081	0.28	0.25	0.18	0.069	0.040	0.78	0.048	0.67	0.52	0.24	1.61E-04

Table S5 Absolute abundance of nine selected renal membrane transporters[+]

	Apical				Basolateral				
	BCRP	MATE1	MATE2-K	MDR1	URAT1	GLUT2	OAT1	OAT3	OCT2
All samples									
median^	0.40	17.31	0.24	60.51	37.84	30.02	2.65	14.86	27.14
Range	0.15-0.63	5.72-44.01	0-0.81	7.84-117.00	2.17-76.05	6.41-73.34	0.93-5.90	3.43-37.92	6.66-69.08
Term newborn and infants									
median^	0.38	16.35	0.24	51.79	24.35	30.97	1.98	11.92	22.48
Range	0.15-0.59	5.72-29.13	0.10-0.81	7.84-112.4	2.17-63.98	6.41-73.34	0.93-4.25	3.43-21.76	6.66-45.94
Children									
median^	0.41	18.00	0.20	73.01	47.09	24.74	3.55	19.96	35.32
Range	0.16-0.50	6.59-31.72	0.090-0.43	11.68-102.00	5.86-76.05	7.76-62.25	1.14-4.17	13.71-31.53	8.48-45.44
Adolescents									
median^	0.31	14.36	0.27	78.91	34.33	26.27	3.08	24.61	28.09
Range	0.29-0.62	6.56-26.05	0.00-0.41	17.03-90.75	5.48-49.34	8.38-49.50	1.83-4.07	11.21-37.92	12.15-39.61
Adults*									
median^	0.48	19.56	0.26	69.92	42.42	38.81	4.39	26.71	29.59
Range	0.33-0.63	13.47-44.01	0.14-0.49	49.76-117.00	12.95-71.51	22.02-66.12	1.50-5.90	5.39-31.51	13.76-69.08

[+]*Term newborn and infants were combined for analysis because there was only one term newborn included in this part of the study. Levels of significance are shown in Figure 3.*

*^pmol/mg total membrane protein *African American and Caucasian adults*

Table S6 Primer sequences sample set 1

Transporter	Sequence
MDR1	Forward: 5'TTGCCACCACGATAGC 3' Reverse: 5'GCCAAGGGGTCGTAGA 3'
MRP2	Forward: 5'TGGGACCAAAAAAGATGTT 3' Reverse: 5'CCAGGGATTTGTAGCAGTT 3'
MRP4	Forward: 5' CGGTTTGGTCTCAACAAT 3' Reverse: 5'CCTCCTCCATTTACAGTGAC 3'
MATE1	Forward: 5'CCTGCAACCTTTCTTTATATG 3' Reverse: 5'CGAGGGCATTGACAAG 3'
MATE2-K	Forward: 5'GCCCAGGCTGTCATCT 3' Reverse: 5'CTTGGCCTGCACAGTATC 3'
PXR	Forward: 5'TCTCCCATTTCAAGAATTTC 3' Reverse: 5'ATGCCTTTGAACATGTAGGT 3'
OAT1	Forward: 5'GCCGGAAGGTACTCATCT 3' Reverse: 5'ATCCACTCCACATTCAGTGT 3'
OAT3	Forward: 5'CGTGCTTGGAGACCTGT 3' Reverse: 5'GGTCCGTGAGGCTGTAG 3'
OCT2	Forward: 5'ATCATTAAGCACATCGCAA 3' Reverse: 5'AGCTCGTGAACCAGTTGTAC 3'

Table S7 Surrogate peptides for each of the renal membrane transporters studied and their corresponding MS/MS parameters

Transporter	Surrogate peptide	Precursor Ion	Product Ion	Fragmentor	Collision Energy	Cell Accelerator Voltage	Polarity
OCT2	VSLQLLR.light	414.7687	729.4618	380	6	5	Positive
OCT2	VSLQLLR.light	414.7687	642.4297	380	10	5	Positive
OCT2	VSLQLLR.light	414.7687	529.3457	380	10	5	Positive
OCT2	VSLQLLR.light	414.7687	401.2871	380	10	5	Positive
OCT2	VSLQLLR.light	414.7687	321.7185	380	8	5	Positive
OCT2	LNPSFLDLVR.light	587.335	946.5356	380	12	5	Positive
OCT2	LNPSFLDLVR.light	587.335	849.4829	380	24	5	Positive
OCT2	LNPSFLDLVR.light	587.335	762.4509	380	24	5	Positive
OCT2	LNPSFLDLVR.light	587.335	530.7929	380	12	5	Positive
OCT2	LNPSFLDLVR.light	587.335	473.7715	380	8	5	Positive
OCT2	LNPSFLDLVR.light	587.335	228.1343	380	8	5	Positive
OCT2	LNPSFLDLVR.light	391.8924	559.2875	380	1	5	Positive
OCT2	LNPSFLDLVR.light	391.8924	502.2984	380	1	5	Positive
OCT2	LNPSFLDLVR.light	391.8924	473.7715	380	1	5	Positive
OCT2	LNPSFLDLVR.light	391.8924	387.2714	380	5	5	Positive
OCT2	LNPSFLDLVR.light	391.8924	336.6894	380	1	5	Positive
OCT2	SPGVAELSLR.light	514.7904	844.4887	380	18	5	Positive
OCT2	SPGVAELSLR.light	514.7904	688.3988	380	14	5	Positive
OCT2	SPGVAELSLR.light	514.7904	471.2744	380	18	5	Positive
OCT2	SPGVAELSLR.light	514.7904	341.1819	380	14	5	Positive
OCT2	SPGVAELSLR.light	514.7904	242.1135	380	18	5	Positive
OCT2	SPGVAELSLR.light	343.5293	541.2617	380	4	5	Positive
OCT2	SPGVAELSLR.light	343.5293	488.3191	380	4	5	Positive
OCT2	SPGVAELSLR.light	343.5293	412.2191	380	8	5	Positive
OCT2	SPGVAELSLR.light	343.5293	375.235	380	8	5	Positive
OCT2	SPGVAELSLR.light	343.5293	309.1845	380	8	5	Positive
OCT2	KLNPSFLDLVR.light	434.5907	687.3824	380	3	5	Positive
OCT2	KLNPSFLDLVR.light	434.5907	615.3824	380	3	5	Positive
OCT2	KLNPSFLDLVR.light	434.5907	502.2984	380	3	5	Positive
OCT2	KLNPSFLDLVR.light	434.5907	400.7369	380	3	5	Positive
OCT2	KLNPSFLDLVR.light	434.5907	308.1949	380	3	5	Positive
OCT2	VVAGVADAL.light	407.7371	683.3723	380	2	5	Positive
OCT2	VVAGVADAL.light	407.7371	612.3352	380	2	5	Positive
OCT2	VVAGVADAL.light	407.7371	426.2711	380	2	5	Positive
OCT2	VVAGVADAL.light	407.7371	389.2031	380	2	5	Positive
OCT2	VVAGVADAL.light	407.7371	342.1898	380	2	5	Positive
OCT2	VVAGVADAL.light	407.7371	203.139	380	2	5	Positive
OAT1	IYLTLLR.light	446.2867	778.4822	380	11	5	Positive

Table S7 Surrogate peptides for each of the renal membrane transporters studied and their corresponding MS/MS parameters (continued)

Transporter	Surrogate peptide	Precursor Ion	Product Ion	Fragmentor	Collision Energy	Cell Accelerator Voltage	Polarity
OAT1	IYLTLLR.light	446.2867	615.4188	380	11	5	Positive
OAT1	IYLTLLR.light	446.2867	502.3348	380	7	5	Positive
OAT1	IYLTLLR.light	446.2867	390.2387	380	7	5	Positive
OAT1	IYLTLLR.light	446.2867	277.1547	380	7	5	Positive
OAT1	LVGFLVINSLGR.light	644.3928	1075.626	380	18	5	Positive
OAT1	LVGFLVINSLGR.light	644.3928	871.536	380	22	5	Positive
OAT1	LVGFLVINSLGR.light	644.3928	758.4519	380	14	5	Positive
OAT1	LVGFLVINSLGR.light	644.3928	659.3835	380	18	5	Positive
OAT1	LVGFLVINSLGR.light	644.3928	417.2496	380	10	5	Positive
OAT1	LVGFLVINSLGR.light	644.3928	213.1598	380	22	5	Positive
OAT1	NGGLEVWLPR.light	570.8116	799.4461	380	20	5	Positive
OAT1	NGGLEVWLPR.light	570.8116	670.4035	380	8	5	Positive
OAT1	NGGLEVWLPR.light	570.8116	385.2558	380	12	5	Positive
OAT1	NGGLEVWLPR.light	570.8116	342.1772	380	8	5	Positive
OAT1	NGGLEVWLPR.light	570.8116	272.1717	380	12	5	Positive
OAT1	NGGLEVWLPR.light	570.8116	229.0931	380	24	5	Positive
OAT1	GQASAMELLR.light	538.2819	890.4764	380	11	5	Positive
OAT1	GQASAMELLR.light	538.2819	819.4393	380	15	5	Positive
OAT1	GQASAMELLR.light	538.2819	732.4073	380	11	5	Positive
OAT1	GQASAMELLR.light	538.2819	661.3702	380	11	5	Positive
OAT1	GQASAMELLR.light	538.2819	257.1244	380	11	5	Positive
OAT1	TSLAVLGK.light	394.7475	600.4079	380	9	5	Positive
OAT1	TSLAVLGK.light	394.7475	487.3239	380	9	5	Positive
OAT1	TSLAVLGK.light	394.7475	416.2867	380	13	5	Positive
OAT1	TSLAVLGK.light	394.7475	317.2183	380	13	5	Positive
OAT1	TSLAVLGK.light	394.7475	204.1343	380	17	5	Positive
OAT3	TFSEILNR.light	490.264	731.4046	380	13	5	Positive
OAT3	TFSEILNR.light	490.264	644.3726	380	13	5	Positive
OAT3	TFSEILNR.light	490.264	515.33	380	13	5	Positive
OAT3	TFSEILNR.light	490.264	402.2459	380	13	5	Positive
OAT3	TFSEILNR.light	490.264	289.1619	380	13	5	Positive
OAT3	TFSEILNR.light	490.264	249.1234	380	9	5	Positive
OAT3	INLQKEI.light	429.2582	744.425	380	7	5	Positive
OAT3	INLQKEI.light	429.2582	726.4145	380	11	5	Positive
OAT3	INLQKEI.light	429.2582	630.3821	380	11	5	Positive
OAT3	INLQKEI.light	429.2582	517.298	380	7	5	Positive
OAT3	INLQKEI.light	429.2582	228.1343	380	7	5	Positive
OAT3	VAVLDGK.light	351.2132	602.3508	380	8	5	Positive

Table S7 Surrogate peptides for each of the renal membrane transporters studied and their corresponding MS/MS parameters (continued)

Transporter	Surrogate peptide	Precursor Ion	Product Ion	Fragmentor	Collision Energy	Cell Accelerator Voltage	Polarity
OAT3	VAVLDGK.light	351.2132	531.3137	380	8	5	Positive
OAT3	VAVLDGK.light	351.2132	432.2453	380	8	5	Positive
OAT3	VAVLDGK.light	351.2132	319.1612	380	16	5	Positive
OAT3	VAVLDGK.light	351.2132	204.1343	380	16	5	Positive
OAT3	YTASDLFR.light	486.7429	809.4152	380	13	5	Positive
OAT3	YTASDLFR.light	486.7429	708.3675	380	9	5	Positive
OAT3	YTASDLFR.light	486.7429	637.3304	380	13	5	Positive
OAT3	YTASDLFR.light	486.7429	435.2714	380	21	5	Positive
OAT3	YTASDLFR.light	486.7429	265.1183	380	5	5	Positive
OAT3	TVLAVFGK.light	417.7578	634.3923	380	6	5	Positive
OAT3	TVLAVFGK.light	417.7578	521.3082	380	10	5	Positive
OAT3	TVLAVFGK.light	417.7578	450.2711	380	14	5	Positive
OAT3	TVLAVFGK.light	417.7578	351.2027	380	18	5	Positive
OAT3	TVLAVFGK.light	417.7578	201.1234	380	6	5	Positive
MATE1	QEEPLPEHPQDGAK.light	525.5864	659.3253	380	10	5	Positive
MATE1	QEEPLPEHPQDGAK.light	525.5864	594.804	380	10	5	Positive
MATE1	QEEPLPEHPQDGAK.light	525.5864	546.2776	380	10	5	Positive
MATE1	QEEPLPEHPQDGAK.light	525.5864	489.7356	380	6	5	Positive
MATE1	QEEPLPEHPQDGAK.light	525.5864	439.886	380	6	5	Positive
MATE1	QEEPLPEHPQDGAK.light	525.5864	396.8718	380	10	5	Positive
MATE1	TGEPQSDQQMR.light	638.783	989.4469	380	18	5	Positive
MATE1	TGEPQSDQQMR.light	638.783	559.7484	380	10	5	Positive
MATE1	TGEPQSDQQMR.light	638.783	495.2271	380	18	5	Positive
MATE1	TGEPQSDQQMR.light	638.783	486.2069	380	22	5	Positive
MATE1	TGEPQSDQQMR.light	638.783	288.119	380	18	5	Positive
MATE1	VGNALGAGDMEQAR.light	694.833	1047.489	380	20	5	Positive
MATE1	VGNALGAGDMEQAR.light	694.833	934.4047	380	20	5	Positive
MATE1	VGNALGAGDMEQAR.light	694.833	806.3461	380	20	5	Positive
MATE1	VGNALGAGDMEQAR.light	694.833	455.2613	380	16	5	Positive
MATE1	VGNALGAGDMEQAR.light	694.833	342.1772	380	24	5	Positive
MATE1	VGNALGAGDMEQAR.light	463.5577	467.706	380	4	5	Positive
MATE1	VGNALGAGDMEQAR.light	463.5577	455.2613	380	4	5	Positive
MATE1	VGNALGAGDMEQAR.light	463.5577	439.1953	380	4	5	Positive
MATE1	VGNALGAGDMEQAR.light	463.5577	411.5278	380	4	5	Positive
MATE1	VGNALGAGDMEQAR.light	463.5577	374.2146	380	4	5	Positive
MATE1	VGNALGAGDMEQAR.light	463.5577	246.1561	380	4	5	Positive
MATE1	GGPEATLEVR.light	514.7722	688.3988	380	14	5	Positive
MATE1	GGPEATLEVR.light	514.7722	617.3617	380	18	5	Positive

Table S7 Surrogate peptides for each of the renal membrane transporters studied and their corresponding MS/MS parameters (continued)

Transporter	Surrogate peptide	Precursor Ion	Product Ion	Fragmentor	Collision Energy	Cell Accelerator Voltage	Polarity
MATE1	GGPEATLEVR.light	514.7722	516.314	380	14	5	Positive
MATE1	GGPEATLEVR.light	514.7722	457.7507	380	10	5	Positive
MATE1	GGPEATLEVR.light	514.7722	412.1827	380	14	5	Positive
MATE1	MEAPEEPAPVR.light	613.2977	894.468	380	21	5	Positive
MATE1	MEAPEEPAPVR.light	613.2977	539.33	380	25	5	Positive
MATE1	MEAPEEPAPVR.light	613.2977	483.2562	380	13	5	Positive
MATE1	MEAPEEPAPVR.light	613.2977	447.7376	380	17	5	Positive
MATE1	MEAPEEPAPVR.light	613.2977	332.1275	380	9	5	Positive
MATE1	MEAPEEPAPVR.light	613.2977	261.0904	380	17	5	Positive
MATE2-K	SFGSPNR.light	382.6879	530.2681	380	5	5	Positive
MATE2-K	SFGSPNR.light	382.6879	473.2467	380	9	5	Positive
MATE2-K	SFGSPNR.light	382.6879	386.2146	380	9	5	Positive
MATE2-K	SFGSPNR.light	382.6879	379.1612	380	5	5	Positive
MATE2-K	SFGSPNR.light	382.6879	339.1719	380	9	5	Positive
MATE2-K	SFGSPNR.light	382.6879	235.1077	380	5	5	Positive
MATE2-K	AAEEAKK.light	373.7058	675.3672	380	13	5	Positive
MATE2-K	AAEEAKK.light	373.7058	604.3301	380	9	5	Positive
MATE2-K	AAEEAKK.light	373.7058	475.2875	380	9	5	Positive
MATE2-K	AAEEAKK.light	373.7058	338.1872	380	9	5	Positive
MATE2-K	AAEEAKK.light	249.4729	475.2875	380	4	5	Positive
MATE2-K	AAEEAKK.light	249.4729	346.2449	380	4	5	Positive
MATE2-K	AAEEAKK.light	249.4729	338.1872	380	4	5	Positive
MATE2-K	AAEEAKK.light	249.4729	302.6687	380	0	5	Positive
MATE2-K	AAEEAKK.light	249.4729	201.087	380	4	5	Positive
MATE2-K	AAEEAKK.light	249.4729	200.7711	380	4	5	Positive
MATE2-K	FSIAVSR.light	390.2241	632.3726	380	13	5	Positive
MATE2-K	FSIAVSR.light	390.2241	545.3406	380	9	5	Positive
MATE2-K	FSIAVSR.light	390.2241	432.2565	380	9	5	Positive
MATE2-K	FSIAVSR.light	390.2241	361.2194	380	9	5	Positive
MATE2-K	FSIAVSR.light	390.2241	235.1077	380	9	5	Positive
MATE2-K	TPEEAHALSAPTSR.light	489.5793	683.3415	380	13	5	Positive
MATE2-K	TPEEAHALSAPTSR.light	489.5793	634.8151	380	9	5	Positive
MATE2-K	TPEEAHALSAPTSR.light	489.5793	618.3206	380	17	5	Positive
MATE2-K	TPEEAHALSAPTSR.light	489.5793	460.2514	380	13	5	Positive
MATE2-K	TPEEAHALSAPTSR.light	489.5793	455.8968	380	13	5	Positive
MATE2-K	VGMALGAADTVQAK.light	666.353	973.5313	380	19	5	Positive
MATE2-K	VGMALGAADTVQAK.light	666.353	860.4472	380	23	5	Positive
MATE2-K	VGMALGAADTVQAK.light	666.353	803.4258	380	15	5	Positive

Table S7 Surrogate peptides for each of the renal membrane transporters studied and their corresponding MS/MS parameters (continued)

Transporter	Surrogate peptide	Precursor Ion	Product Ion	Fragmentor	Collision Energy	Cell Accelerator Voltage	Polarity
MATE2-K	VGMALGAADTVQAK.light	666.353	732.3886	380	15	5	Positive
MATE2-K	VGMALGAADTVQAK.light	666.353	472.2588	380	15	5	Positive
MATE2-K	VGMALGAADTVQAK.light	444.5711	616.8188	380	7	5	Positive
MATE2-K	VGMALGAADTVQAK.light	444.5711	588.3081	380	7	5	Positive
MATE2-K	VGMALGAADTVQAK.light	444.5711	546.3246	380	11	5	Positive
MATE2-K	VGMALGAADTVQAK.light	444.5711	392.5411	380	3	5	Positive
MATE2-K	VGMALGAADTVQAK.light	444.5711	218.1499	380	11	5	Positive
MDR1	EIIGVVSQEPVLFATTIAENIR.light	800.4442	917.5051	380	16	5	Positive
MDR1	EIIGVVSQEPVLFATTIAENIR.light	800.4442	816.4574	380	16	5	Positive
MDR1	EIIGVVSQEPVLFATTIAENIR.light	800.4442	715.4097	380	24	5	Positive
MDR1	EIIGVVSQEPVLFATTIAENIR.light	800.4442	531.2885	380	16	5	Positive
MDR1	EIIGVVSQEPVLFATTIAENIR.light	800.4442	512.3079	380	16	5	Positive
MDR1	EIIGVVSQEPVLFATTIAENIR.light	800.4442	955.5095	380	16	5	Positive
MDR1	AGAVAEEVLAAIR.light	635.3617	971.552	380	18	5	Positive
MDR1	AGAVAEEVLAAIR.light	635.3617	900.5149	380	18	5	Positive
MDR1	AGAVAEEVLAAIR.light	635.3617	430.2772	380	10	5	Positive
MDR1	AGAVAEEVLAAIR.light	635.3617	359.2401	380	10	5	Positive
MDR1	AGAVAEEVLAAIR.light	635.3617	299.1714	380	18	5	Positive
MDR1	AGAVAEEVLAAIR.light	423.9102	543.3613	380	6	5	Positive
MDR1	AGAVAEEVLAAIR.light	423.9102	430.2772	380	2	5	Positive
MDR1	AGAVAEEVLAAIR.light	423.9102	420.7267	380	2	5	Positive
MDR1	AGAVAEEVLAAIR.light	423.9102	359.2401	380	2	5	Positive
MDR1	AGAVAEEVLAAIR.light	423.9102	272.1843	380	2	5	Positive
MDR1	IATEAIENFR.light	582.3064	979.4843	380	16	5	Positive
MDR1	IATEAIENFR.light	582.3064	749.3941	380	16	5	Positive
MDR1	IATEAIENFR.light	582.3064	678.357	380	24	5	Positive
MDR1	IATEAIENFR.light	582.3064	565.2729	380	24	5	Positive
MDR1	IATEAIENFR.light	582.3064	490.2458	380	12	5	Positive
MDR1	IATEAIENFR.light	388.54	565.2729	380	1	5	Positive
MDR1	IATEAIENFR.light	388.54	486.2558	380	5	5	Positive
MDR1	IATEAIENFR.light	388.54	436.2303	380	5	5	Positive
MDR1	IATEAIENFR.light	388.54	283.1401	380	1	5	Positive
MDR1	STVVQLLER.light	522.806	856.5251	380	10	5	Positive
MDR1	STVVQLLER.light	522.806	757.4567	380	18	5	Positive
MDR1	STVVQLLER.light	522.806	658.3883	380	14	5	Positive
MDR1	STVVQLLER.light	522.806	530.3297	380	18	5	Positive
MDR1	STVVQLLER.light	522.806	428.7662	380	10	5	Positive
MDR1	TTIVIAHR.light	455.7771	708.4515	380	12	5	Positive

Table S7 Surrogate peptides for each of the renal membrane transporters studied and their corresponding MS/MS parameters (continued)

Transporter	Surrogate peptide	Precursor Ion	Product Ion	Fragmentor	Collision Energy	Cell Accelerator Voltage	Polarity
MDR1	TTIVIAHR.light	455.7771	595.3675	380	12	5	Positive
MDR1	TTIVIAHR.light	455.7771	496.299	380	16	5	Positive
MDR1	TTIVIAHR.light	455.7771	354.7294	380	12	5	Positive
MDR1	TTIVIAHR.light	455.7771	298.1874	380	12	5	Positive
MDR1	TTIVIAHR.light	304.1871	496.299	380	8	5	Positive
MDR1	TTIVIAHR.light	304.1871	405.2532	380	4	5	Positive
MDR1	TTIVIAHR.light	304.1871	354.7294	380	0	5	Positive
MDR1	TTIVIAHR.light	304.1871	298.1874	380	0	5	Positive
MDR1	TTIVIAHR.light	304.1871	203.1026	380	0	5	Positive
BCRP	SSLLDVLAAR.light	522.806	757.4567	380	18	5	Positive
BCRP	SSLLDVLAAR.light	522.806	644.3726	380	10	5	Positive
BCRP	SSLLDVLAAR.light	522.806	435.774	380	14	5	Positive
BCRP	SSLLDVLAAR.light	522.806	430.2772	380	14	5	Positive
BCRP	SSLLDVLAAR.light	522.806	317.1932	380	6	5	Positive
BCRP	LAEIYVNSSFYK.light	717.3692	1007.483	380	21	5	Positive
BCRP	LAEIYVNSSFYK.light	717.3692	844.4199	380	17	5	Positive
BCRP	LAEIYVNSSFYK.light	717.3692	745.3515	380	13	5	Positive
BCRP	LAEIYVNSSFYK.light	717.3692	427.2551	380	17	5	Positive
BCRP	LAEIYVNSSFYK.light	717.3692	314.171	380	21	5	Positive
BCRP	LFDSLTLLASGR.light	646.8641	1032.568	380	18	5	Positive
BCRP	LFDSLTLLASGR.light	646.8641	717.4254	380	14	5	Positive
BCRP	LFDSLTLLASGR.light	646.8641	503.2936	380	14	5	Positive
BCRP	LFDSLTLLASGR.light	646.8641	390.2096	380	18	5	Positive
BCRP	LFDSLTLLASGR.light	646.8641	319.1724	380	10	5	Positive
BCRP	TIIFSIHQPR.light	404.568	737.4053	380	10	5	Positive
BCRP	TIIFSIHQPR.light	404.568	499.2825	380	2	5	Positive
BCRP	TIIFSIHQPR.light	404.568	442.7405	380	10	5	Positive
BCRP	TIIFSIHQPR.light	404.568	369.2063	380	10	5	Positive
BCRP	TIIFSIHQPR.light	404.568	215.139	380	2	5	Positive
BCRP	VIQELGLDK.light	507.7951	802.4305	380	9	5	Positive
BCRP	VIQELGLDK.light	507.7951	674.3719	380	9	5	Positive
BCRP	VIQELGLDK.light	507.7951	432.2453	380	17	5	Positive
BCRP	VIQELGLDK.light	507.7951	401.7189	380	9	5	Positive
BCRP	VIQELGLDK.light	507.7951	213.1598	380	9	5	Positive
URAT1	AFSELLDLVGGLGR.light	723.9012	899.5309	380	25	5	Positive
URAT1	AFSELLDLVGGLGR.light	723.9012	786.4468	380	25	5	Positive
URAT1	AFSELLDLVGGLGR.light	723.9012	459.2674	380	21	5	Positive
URAT1	AFSELLDLVGGLGR.light	723.9012	402.2459	380	13	5	Positive

Table S7 Surrogate peptides for each of the renal membrane transporters studied and their corresponding MS/MS parameters (continued)

Transporter	Surrogate peptide	Precursor Ion	Product Ion	Fragmentor	Collision Energy	Cell Accelerator Voltage	Polarity
URAT1	AFSELLDLVGGLGR.light	723.9012	232.1404	380	13	5	Positive
URAT1	AFSELLDLVGGLGR.light	482.9366	889.4666	380	5	5	Positive
URAT1	AFSELLDLVGGLGR.light	482.9366	558.3358	380	5	5	Positive
URAT1	AFSELLDLVGGLGR.light	482.9366	459.2674	380	5	5	Positive
URAT1	AFSELLDLVGGLGR.light	482.9366	459.2575	380	5	5	Positive
URAT1	AFSELLDLVGGLGR.light	482.9366	402.2459	380	5	5	Positive
URAT1	AFSELLDLVGGLGR.light	482.9366	279.6715	380	5	5	Positive
URAT1	GAVQDTLTPEVLLSAMR.light	600.989	836.9506	380	9	5	Positive
URAT1	GAVQDTLTPEVLLSAMR.light	600.989	787.4163	380	13	5	Positive
URAT1	GAVQDTLTPEVLLSAMR.light	600.989	786.3992	380	9	5	Positive
URAT1	GAVQDTLTPEVLLSAMR.light	600.989	723.3871	380	9	5	Positive
URAT1	GAVQDTLTPEVLLSAMR.light	600.989	558.3028	380	9	5	Positive
URAT1	MGALLLLSHLGR.light	640.879	908.5676	380	26	5	Positive
URAT1	MGALLLLSHLGR.light	640.879	795.4835	380	22	5	Positive
URAT1	MGALLLLSHLGR.light	640.879	682.3995	380	22	5	Positive
URAT1	MGALLLLSHLGR.light	640.879	569.3154	380	18	5	Positive
URAT1	MGALLLLSHLGR.light	640.879	260.1063	380	26	5	Positive
URAT1	GGAILGPLVR.light	476.8006	654.4297	380	16	5	Positive
URAT1	GGAILGPLVR.light	476.8006	541.3457	380	8	5	Positive
URAT1	GGAILGPLVR.light	476.8006	484.3242	380	12	5	Positive
URAT1	GGAILGPLVR.light	476.8006	412.2554	380	4	5	Positive
URAT1	GGAILGPLVR.light	476.8006	299.1714	380	12	5	Positive
URAT1	GGAILGPLVR.light	476.8006	271.1765	380	20	5	Positive
URAT1	GGAILGPLVR.light	318.2028	484.3242	380	4	5	Positive
URAT1	GGAILGPLVR.light	318.2028	387.2714	380	8	5	Positive
URAT1	GGAILGPLVR.light	318.2028	274.1874	380	4	5	Positive
URAT1	GGAILGPLVR.light	318.2028	271.1765	380	0	5	Positive
URAT1	GGAILGPLVR.light	318.2028	242.6657	380	4	5	Positive
GLUT2	SFEEIAAEFQK.light	649.8168	1064.526	380	15	5	Positive
GLUT2	SFEEIAAEFQK.light	649.8168	693.3566	380	15	5	Positive
GLUT2	SFEEIAAEFQK.light	649.8168	622.3195	380	11	5	Positive
GLUT2	SFEEIAAEFQK.light	649.8168	235.1077	380	27	5	Positive
GLUT2	SFEEIAAEFQK.light	433.547	1211.594	380	15	5	Positive
GLUT2	SFEEIAAEFQK.light	433.547	1064.526	380	15	5	Positive
GLUT2	SFEEIAAEFQK.light	433.547	622.3195	380	11	5	Positive
GLUT2	SFEEIAAEFQK.light	433.547	606.277	380	3	5	Positive
GLUT2	SFEEIAAEFQK.light	433.547	551.2824	380	7	5	Positive
GLUT2	SFEEIAAEFQK.light	433.547	339.1607	380	3	5	Positive

Table S7 Surrogate peptides for each of the renal membrane transporters studied and their corresponding MS/MS parameters (continued)

Transporter	Surrogate peptide	Precursor Ion	Product Ion	Fragmentor	Collision Energy	Cell Accelerator Voltage	Polarity
GLUT2	VSIIQLFTNSSYR.light	764.4119	1115.548	380	19	5	Positive
GLUT2	VSIIQLFTNSSYR.light	764.4119	987.4894	380	23	5	Positive
GLUT2	VSIIQLFTNSSYR.light	764.4119	874.4054	380	19	5	Positive
GLUT2	VSIIQLFTNSSYR.light	764.4119	727.3369	380	15	5	Positive
GLUT2	VSIIQLFTNSSYR.light	764.4119	413.2758	380	15	5	Positive
GLUT2	VSIIQLFTNSSYR.light	509.9437	727.3369	380	10	5	Positive
GLUT2	VSIIQLFTNSSYR.light	509.9437	654.4185	380	6	5	Positive
GLUT2	VSIIQLFTNSSYR.light	509.9437	626.2893	380	10	5	Positive
GLUT2	VSIIQLFTNSSYR.light	509.9437	512.2463	380	14	5	Positive
GLUT2	VSIIQLFTNSSYR.light	509.9437	437.7063	380	6	5	Positive
GLUT2	VSIIQLFTNSSYR.light	509.9437	364.1721	380	6	5	Positive
GLUT2	HVLGVPLDDR.light	374.2085	615.3097	380	5	5	Positive
GLUT2	HVLGVPLDDR.light	374.2085	506.3085	380	1	5	Positive
GLUT2	HVLGVPLDDR.light	374.2085	407.2401	380	9	5	Positive
GLUT2	HVLGVPLDDR.light	374.2085	405.1728	380	9	5	Positive
GLUT2	HVLGVPLDDR.light	374.2085	308.1585	380	1	5	Positive
GLUT2	HVLGVPLDDRK.light	416.9068	533.2678	380	10	5	Positive
GLUT2	HVLGVPLDDRK.light	416.9068	506.3085	380	10	5	Positive
GLUT2	HVLGVPLDDRK.light	416.9068	416.2398	380	2	5	Positive
GLUT2	HVLGVPLDDRK.light	416.9068	407.2401	380	10	5	Positive
GLUT2	HVLGVPLDDRK.light	416.9068	372.206	380	10	5	Positive
GLUT2	HVLGVPLDDRK.light	416.9068	237.1346	380	14	5	Positive
GLUT2	LGPSHILIIAGR.light	416.2592	567.3431	380	10	5	Positive
GLUT2	LGPSHILIIAGR.light	416.2592	538.8324	380	6	5	Positive
GLUT2	LGPSHILIIAGR.light	416.2592	359.716	380	6	5	Positive
GLUT2	LGPSHILIIAGR.light	416.2592	359.5573	380	6	5	Positive
GLUT2	LGPSHILIIAGR.light	416.2592	303.1775	380	10	5	Positive
GLUT2	LGPSHILIIAGR.light	416.2592	303.1739	380	10	5	Positive

6 Alternative splicing of the *SLCO1B1* gene: an exploratory analysis of isoform diversity in pediatric liver

Bianca D van Groen, Chengpeng Bi, Roger Gaedigk, Vincent S Staggs, Dick Tibboel, Saskia N de Wildt, J Steven Leeder

Clin Transl Sci. 2020 Jan 9. DOI: 10.1111/cts.12733.

ABSTRACT

The hepatic influx transporter OATP1B1 (SLCO1B1) plays an important role in the disposition of endogenous substrates and drugs prescribed to children. Alternative splicing increases the diversity of protein products from >90% of human genes and may be triggered by developmental signals. As concentrations of several endogenous OATP1B1 substrates change during growth and development, with this exploratory study we investigated age-dependent alternative splicing of SLCO1B1 mRNA in 97 post-mortem livers (fetus-adolescents). Twenty-seven splice variants were detected; ten were confirmed by additional bioinformatic analyses and verified by qPCR, and selected for detailed analysis based on relative abundance, association with age and overlap with an adjacent gene. Two splice variants code for reference OATP1B1 protein, and eight code for truncated proteins. The expression of eight isoforms was associated with age. We conclude that alternative splicing of SLCO1B1 occurs frequently in children; although the functional consequences remain unknown, the data raise the possibility of a regulatory role for alternative splicing in mediating developmental changes in drug disposition.

INTRODUCTION

Transporters are membrane-bound proteins that are present in the apical and basolateral membranes of organs, such as the liver.[1] Their biological role is the trafficking of substrates across membranes, making them critical determinants of tissue and cellular substrate disposition. Moreover, they act in concert with drug-metabolizing enzymes (DMEs) to maintain homeostatic balance for endogenous substrates and to facilitate the detoxification and elimination of exogenous substrates, such as drugs and food toxins.[2]

This latter is important for newborns, as after birth they become dependent on exogenous food sources for nutrition, and the diet expands as they grow into infanthood. During all these changes in food exposure, the child must defend itself against potentially toxic dietary constituents, recruiting pathways not or differentially expressed during fetal life. Hence ontogeny of DMEs and transporters occurs, influencing the disposition of their endogenous and exogenous substrates over age. Moreover, ontogeny may well be driven by developmental homeostatic changes in endogenous substrates.[3]

A classic example of age-related changes in a DME that plays an important physiological role is hepatic cytochrome P450 (CYP) 3A7. CYP3A7 is highly expressed in fetal liver but steadily declines throughout the last trimester of pregnancy and first year of postnatal life to low levels characteristic of adult liver.[4,5] From a functional perspective, CYP3A7 catalyzes the 16α-hydroxylation of dehydroepiandosteron 3-sulfate (DHEA-S), to form 16α-DHEA-S, a precursor for estriol synthesis by placental syncytiotrophoblasts.[6] DHEA-S concentrations are high during the fetal and neonatal periods and decline postnatally.[7,8] DHEA-S has been reported to activate CYP3A7 activity, which explains the high expression of CYP3A7 in fetal liver.[9] DHEA-S also provides an example of the interplay between DMEs and transporters in a developmental context as prior to biotransformation by CYP3A7 in fetal liver, DHEA-S needs to cross the hepatocyte membrane, using the solute carrier organic anion transporter (gene name *SLCO1B1*, protein name OATP1B1) located on the basolateral membrane.[10] Consistent with CYP3A7, the OATP1B1 expression also has been demonstrated to decline directly after birth[11], followed by age-dependent increases in mRNA expression throughout childhood.[12] Data are conflicting regarding developmental patterns of OATP1B1 protein, with expression increased around age eight years, compared to younger children in one study, using immunoblotting techniques[13], and no apparent statistically significant relationship with age, using a quantitative proteomic approach.[14]

Whereas the contribution of CYP3A7 to drug clearance postnatally is relatively minor, OATP1B1 plays an important role in the clearance of potentially toxic endogenous

molecules. One example illustrating the importance of transporter function early after birth involves bilirubin; an association has been demonstrated between the *SLCO1B1* 388G>A allele, a variant associated with reduced function of the transporter, and unconjugated hyperbilirubinemia in newborns, which is associated with neurotoxicity.[15,16] Moreover, OATP1B1 is not only involved in the disposition of endogenous substrates but also of drugs that are used in pediatrics, such as statins, methotrexate and bosentan.[10] Malfunctioning of the OATP1B1 transporter may put children at risk of toxic or sub therapeutic effects of these drugs. Thus, understanding the regulatory mechanisms of the gene *SLCO1B1* in response to developmental signals is critical to understand physiological changes in endogenous substrates and to provide safe and effective drug therapy in children.

To date, ontogeny studies have generally focused on mRNA expression and, more recently, have expanded to protein abundance targeting specific regions of the reference gene and/or protein sequence. Recently, it has become increasingly apparent that alternative splicing, a process that increases the diversity of products from a single gene, may have functional consequences. Due to alternative splicing events, more than 90% of our genes give rise to more than one mRNA transcript, varying with respect to numbers of exons, different length of exons, and varying lengths of untranslated regions.[17] Not all products of alternative splicing necessarily result in the production of functional proteins. Alternative splicing may be the result of developmental signals expressed during the course of growth and development.[17-19] For example, developmentally regulated alternative splicing has been demonstrated for neuronal sodium channels genes *SCN1A, SCN2A, SCN3A, SCN8A* and *SCN9A* in brain tissue; the alternative exon 5N predominates in the neonatal period whereas 5A predominates in the adult.[20-25] In the case of *SCN1A,* a gene implicated in the pathogenesis of febrile seizures in newborns[26], an allelic variant *SCN1A* IVS5–91 G>A disrupts the 5′ splice donor site of exon 5N and potentially influences the relative expression of exons 5N and 5A. Although the *SCN1A* IVS5–91 G>A variant does not appear to be associated with febrile seizures *per se*[27], studies suggest that presence of the variant allele may affect dose requirements for phenytoin and carbamazepine.[25,28] Thus, alternative splicing and genetic variants affecting alternative splicing, may have therapeutic consequences.

The *SLCO1B1* gene, consisting of 14 coding and one non-coding exons, codes for the protein OATP1B1 that is composed of 691 amino acids, and consists of 12 transmembrane (TM) regions.[10] It is part of the *SLCO1B* family, for which splice variants have been described. For example, five mRNA transcripts for *SLCO1B3* have been deposited in Ensembl, of which four represent full-length or truncated protein-coding sequences.[29] Furthermore, the splice variant LST-3TM12 is a hybrid transcript with sequences derived

from *SLCO1B3* and *SLCO1B7*, and has functional transporter properties.[30] In contrast, for *SLCO1B1* there is only one reported mRNA transcript, ENST00000256958.2, encoding the functional 691 amino acid OATP1B1 protein; referred to hereafter as the "reference isoform".[10]

Given these considerations, the purpose of this exploratory study was to investigate alternative splicing of *SLCO1B1* in post-mortem pediatric liver tissue over a wide age range from fetal to adolescent ages. Using RNA sequencing (RNA-seq) data, we created a process involving computational software integrating our bioinformatics pipelines and an in-house developed RNA-seq database query system to perform a structured analysis of the RNA-seq data *in silico*. Using this data analysis pipeline, we aimed (1) to predict splice variants for *SLCO1B1*, (2) to identify potential hybrid splice variants overlapping *SLCO1B1* and *SCLO1B7* (another member of the *SLCO1B* family), and (3) to study age-related changes in expression of *SLCO1B1* splice variants.

MATERIALS AND METHODS

See Figure 1 for the workflow of the methods, and the explanation underneath.

Tissue samples

Post-mortem liver tissue samples from autopsies of fetuses (therapeutic abortions or stillbirths) and infants were provided by the Erasmus MC Tissue Bank (Rotterdam, NL) and the repository of the Division of Clinical Pharmacology, Toxicology, and Therapeutic Innovation at Children's Mercy Kansas City (Kansas City, MO, USA). Tissue was procured at the time of autopsy within 24 hours after death and snap-frozen at -80^{0}C for later research use. For the tissues provided by the Erasmus MC tissue bank, the Erasmus MC Research Ethics Board waived the need for formal ethics approval according to the Dutch Law on Medical Research in Humans. Tissue was collected when parental written informed consent for both autopsy and the explicit use of the tissue for research was present. The samples were selected when the clinical diagnosis of the patient was not related to hepatic problems and the tissue was histologically normal (as estimated by a pathologist based on hematoxylin and eosin staining). Postmortem pediatric liver tissues in the repository of the Division of Clinical Pharmacology, Toxicology, and Therapeutic Innovation at Children's Mercy Kansas City (Kansas City, MO, USA) were obtained from multiple sources, including the Brain and Tissue Bank for Developmental Disorders at the University of Maryland (Baltimore, MD), the Liver Tissue Cell Distribution System (LTCDS; University of Pittsburgh and University of Minnesota), University of Washington Center for Birth Defects Research (Seattle, WA) and XenoTech LLC (Lenexa, KS). The use of

these tissues was declared nonhuman subject research by the Children's Mercy Hospital Pediatric Institutional Review Board.

Figure 1 Flow of methods predicting splice variants of SLCO1B1

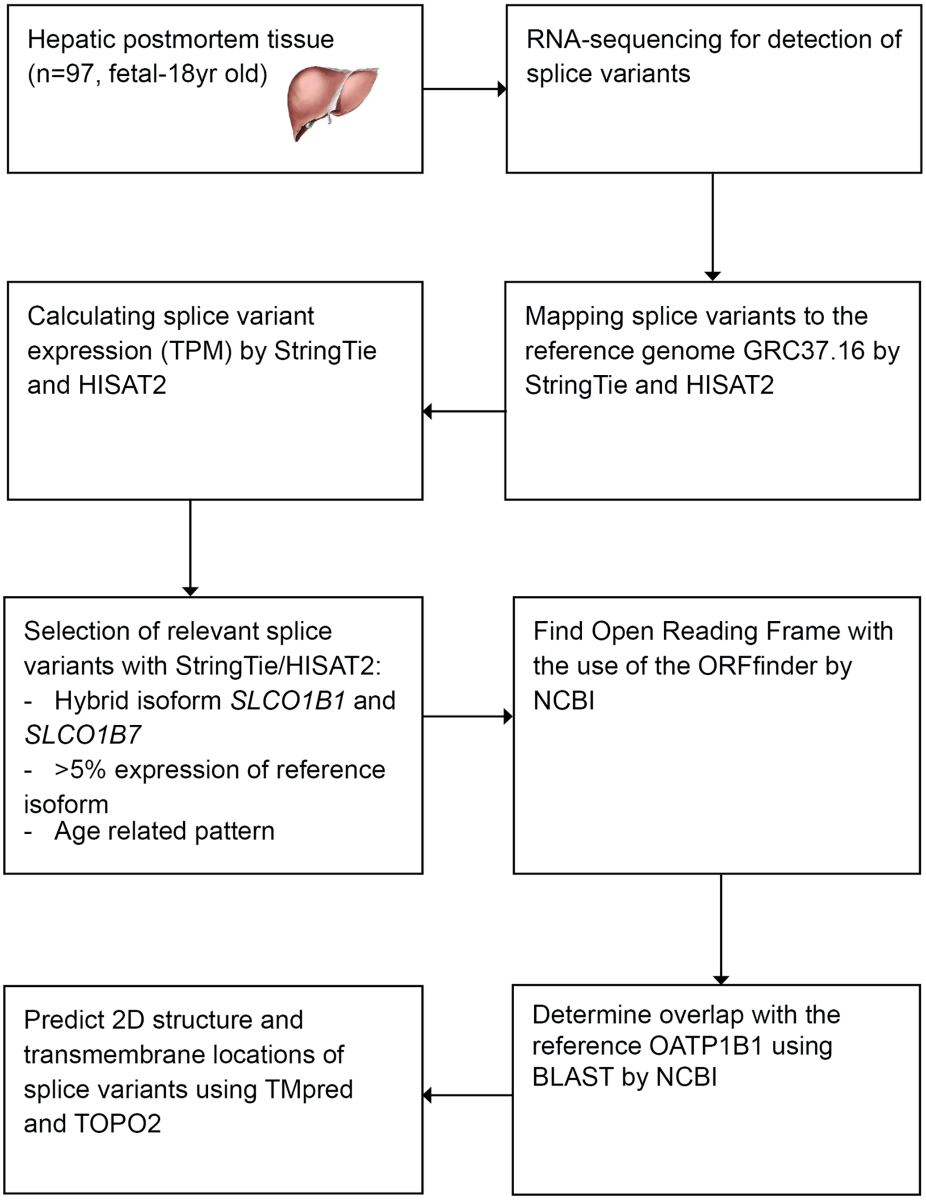

RNA sequencing

mRNA expression of SLCO1B1 was determined using RNA-seq. RNA was isolated from hepatic tissue according to the manufacturer's instructions using the RNeasy Mini kit (Qiagen, Valencia, CA). Samples with an RNA integrity number of <5 were excluded. The RNA-seq experiments were performed according to the Illumina RNA-seq protocol (San Diego, CA). In brief, a population of poly(A)$^+$ mRNA was selected and converted to a library of cDNA fragments (220–450 bp) with adaptors attached to both ends, using an Illumina mRNA-Seq sample preparation kit. The quality of the library preparation was confirmed by analysis on a 2100 Bioanalyzer (Agilent Technologies, Santa Clara, CA). The cDNA fragments were then sequenced on an Illumina HiSeq 2000 to obtain 100-bp sequences from both ends (paired end). The resulting reads were mapped by Bowtie2 and StringTie[31-33] to the transcriptome constructed through reference genes/transcripts according to the reference human genome GRCh37.61/hg19.[34] The mapped reads were then assigned to transcripts from which the abundance of the reference transcript is estimated by RSEM[35] and for the splice variants with HISAT2.[36] The counts of RNA-seq fragments were used to indicate the amount of identified mRNA transcripts, presented in transcripts per million transcripts (TPM).[35]

Validation dataset

To validate the RNA-seq results, the presence of the reference transcript was confirmed (Ensembl transcript ID ENST00000256958.3). Moreover, to further validate the results, the presence of the alternatively spliced transcript LST-3TM12[30] was detected using the algorithm RSEM combined with Bowtie2 and the assembly GRCh37.

Protein prediction

Sequence alignment and overlap of splice variants with consensus coding sequences (CCDS)[37] for *SLCO1B1* and the adjacent gene *SLCO1B7* was performed using Basic Local Alignment Search Tool (BLAST).[38] Splice variants were prioritized for further investigation when one of the following criteria was met and when the presence of the splice variant was verified with RT-PCR:

- the expression of the splice variant was >5% of the expression of the reference isoform,
- the splice variant was a *SLCO1B7* and *SLCO1B1* hybrid transcript, or
- the expression of the splice variant was associated with age (see 'Data and Statistical analysis')

Next, the open reading frame (ORF) of >600 nt of the relevant splice variants was predicted with ORF-Finder by NCBI.[39] Prediction of transmembrane (TM) regions and orientation was done with TMpred based on the TMbase database.[40] Two dimensional protein structures were generated with TOPO2.[41]

To provide additional bioinformatic confirmation that candidate novel alternatively spliced products represent coding transcripts, sequencing data were analyzed using two additional tools: the Coding Potential Calculator Algorithm (CPC2) and the Coding-Potential Assessment Tool (CPAT).[42,43] These algorithms both use logistic regression to distinguish between coding and non-coding transcripts based on four intrinsic features: the Fickett testcode score (both), ORF length (both), ORF integrity (CPC2), isoelectric point (CPC2), ORF coverage defined as the ratio of ORF to transcript lengths (CPAT) and hexamer usage bias (CPAT).

Verification of splice variants by RT-PCR and sequencing

The presence of the splice variants selected for further investigation was verified by RT-PCR and sequencing. Primers were designed to be specific for each splice variant (Figure S1 and Table S1). In addition, a universal primer pair was designed to amplify all splice variants and to function as a positive control. Due to the low abundance of some of the variants, a nested forward primer was also designed.

RNA was extracted from frozen liver tissue, utilizing the Qiagen RNeasy Mini Kit (Qiagen, Valencia, CA). One µg of total RNA was DNase treated and reverse transcribed with the Maxima H Minus First Strand cDNA Synthesis Kit, following the manufacturer's instructions (Thermo Scientific, Waltham, MA). The cDNA equivalent to 10 ng of total RNA was used per PCR reaction (2G Fast ReadyMix, KAPA Biosystems, Wilmington, MA). The cycling conditions were: 94°C, 3 min, followed by 40 cycles of 94°C for 15 sec, 60°C for 15 sec and 72°C for 5 sec. The primary PCR amplicons were diluted 1:4000 and a nested PCR was performed with the same KAPA mix and the same cycling conditions. The PCR reactions were column purified up with the QIAquick PCR Purification Kit (Qiagen). One ng was used in subsequent sequencing reactions with BigDye v.3.1 and run on a 3730xl DNA Analyzer (Thermo Fisher). The results were analyzed with Sequencher software (Gene Codes, Ann Arbor, MI).

Data and Statistical analysis

Because of non-normal distribution, the data are presented as median (range). First, the relative abundance of the expression of each transcript compared to the reference isoform was calculated. Also, the relationship of age with expression levels (TPM) was studied by comparing expression levels between age groups. Samples were assigned to one of five age groups: fetal, 0-1.5 years, 1.5-6 years, 6-12 years and 12-18 years. Kruskal-Wallis test with Dunn's post-hoc test were used for multiple comparisons of expression levels between age groups. For Dunn's post-hoc test for multiple comparisons the adjusted p-values are reported, in which a correction for multiple testing for age groups is applied. Second, Spearman correlations between age (on a continuous scale)

and expression levels of splice variants were examined. To control for the number of correlations tested (54), p-values were considered statistically significant only if their corresponding q-value was less than .05 after Benjamini-Hochberg adjustment to control the false discovery rate. Statistical analyses were performed using IBM SPSS Statistics software (SPSS Statistics for Windows, version 21.0; IBM, Armonk, NY) and graphical exploration was done with GraphPad Prism. We explored negative binomial and zero-inflated negative binomial models in SAS 9.4, but the former did not fit well, and we were unable to identify predictors of excess zeros for the latter.

RESULTS

Descriptive results

mRNA expression of the reference isoform and splice variants of SLCO1B1 was quantified in 97 post-mortem liver tissues of humans of various ages, of which the age distribution can be found in Table 1. The reference isoform of SLCO1B1 was detected in all but one sample with a median expression of 33.4 (range 0-134.2) TPM. The transcript consisted of 2791 nucleotides (nt) of which 95 nt comprise the 5'-UTR and 621 nt the '3-UTR, resulting in a protein of 691 amino acids. This is in accordance with Niemi *et al*.[10] In Figure 2A the expression of this transcript in various age groups is presented and did not show any age-related changes when binned in age groups. On the other hand, on a continuous scale, postnatal age was related to transcript expression (ρ=0.316, p=0.002) (Figure 2D). Twenty-seven splice variants of SLCO1B1 were identified using RNA-seq, representing a total expression of 18.8 (0.2-105.0) TPM (Figure 2B). These are numbered randomly between 21 and 55. The ratio of the total expression of the splice variants versus the reference isoform is presented in Figure 2C and was not different between age groups. Thirteen splice variants met the selection criteria for further analysis, and ten of these were subsequently verified by RT-PCR (Table 2), as described below.

Table 1 Median (range) age by group for post-mortem liver samples

Age groups	Number of samples	Gestational age (weeks)	Postnatal age (years)
Fetus	22	16.4 (14.7-41.3)	-
0 – 1.5 yr	35	-	0.1 (0-1.2)
1.5 – 6 yr	16	-	3 (1.8-6)
6 – 12 yr	15	-	9 (7-12)
12 – 18 yr	9	-	15 (13-17)
Total	97		

Figure 2 TPM expression of (A) the reference isoform of SLCO1B1 (B) the total TPM values of splice variants and (C) the ratio of total TPM values of splice variants to TPM values of the reference isoform in various age groups; and (D) the relationship of the reference isoform of SLCO1B1 with postnatal age (ρ=0.316, p=0.002).

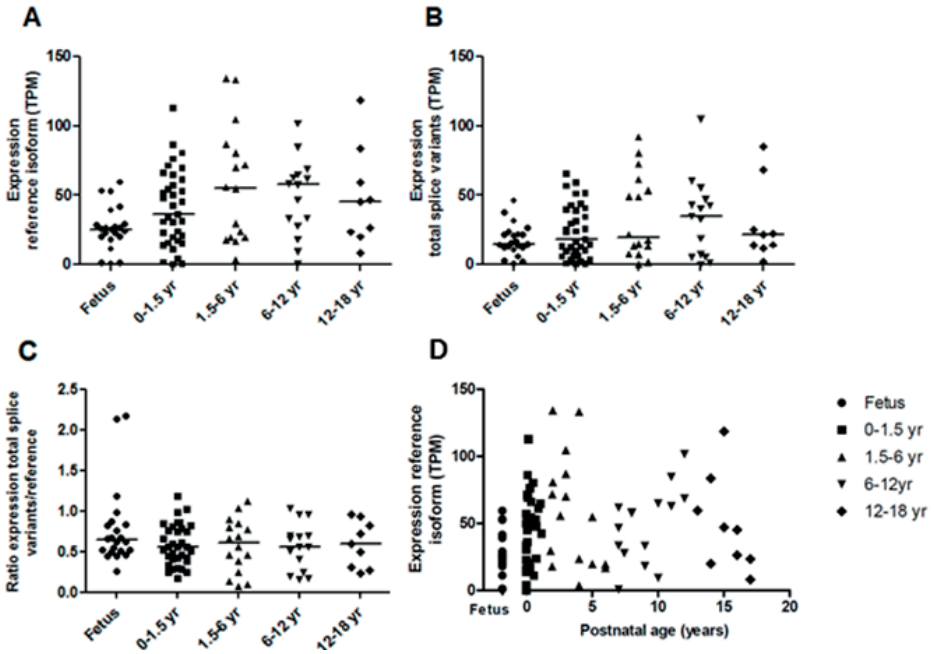

Verification splice variants by RT-PCR and sequencing

The presence of the splice variants meeting one or more criteria of 1) expression level >5% of the expression of the reference isoform, 2) a hybrid *SLCO1B7* and *SLCO1B1* transcript, or 3) expression was associated with age, were verified for 10/13 samples; splice variants 21, 37 and 48 could not be verified by RT-PCR (see Figure S2). Splice variants 21 and 37 had sizes different than expected. Splice variant 48 could not be amplified. Further analysis of variants 21, 37 and 48 by sequencing was also unable to confirm the presence of the 21, 37 and 48 splice variants, and thus these transcripts were excluded from further analysis. The splice junctions of variant 46 were not sufficiently unique to design primers that would amplify only this variant or to generate a product with a size that could resolved on an agarose gel from amplicons generated from other transcripts as templates. The results for splice variant 46 should therefore be interpreted with caution.

Validation dataset

To further validate our RNA-seq results, we confirmed the presence of the LST-3TM12 transcript[30] in our samples. The transcript emerged in 3 of the 97 samples with a low abundance of 0.11, 0.18 and 0.30 TPM.

Table 2 Relevant splice variants of SLCO1B1 in 97 pediatric liver samples for which the presence in the samples is confirmed by RT-PCR

Splice variant	Abundance of all novel isoforms (%)	Abundance compared to reference isoform (%)	Found in number of samples	Number of exons	Length (nt)	ORF (n AA)	Overlapping number of AA with locus:					Number of TM helices
							ORF SLCO1B1 (% of reference SLCO1B1)	Intron SLCO1B1	ORF SLCO1B7	In between SLCO1B1 and SLCO1A2†	SLCO-1A2†	
46‡*	26.55	16.48	63	10	4638	284	274 (40%)	10	-	-	-	6
50‡	14.26	8.85	93	17	34388	453	444 (65%)	9	-	-	-	10
34‡	9.24	5.73	46	18	4156	625	622 (90%)	-	-	3	-	11
24◊*	0.32	0.20	77	25	3151	659	622 (90%)	-	0	-	37	11
26◊*	1.80	1.12	81	24	13158	691	691 (100%)	-	0	-	-	12
28◊*	1.21	0.75	96	20	14577	691	691 (100%)	-	0	-	-	12
						210	-	-	-	-	210	0
						881	-	-	-	-	881	1
30◊*	0.34	0.21	54	20	5684	484	453 (66%)	-	0	-	31	8
38*	0.52	0.33	95	15	22310	453	444 (65%)	9	-	-	-	10
44*	7.86	4.88	65	3	7364	98	98 (14%)	-	-	-	-	2
51*	0.73	0.46	76	17	15407	522	522 (75%)	-	-	-	-	8

*AA=amino acid nt=nucleotides TM=transmembrane, †SLCO1A2 is on the reverse strand ‡Abundant splice variant ◊ Hybrid SLCO1B1 and -1B7 *Age related changes in expression*

Splice variants meeting the abundance criterion

Three splice variants had an abundance of >5% of the expression of the reference isoform (Table 2). They had 40-90% overlap with the ORF from the reference amino acid sequence for OATP1B1, resulting in a prediction of a number of TM helices ranging from 6 to 11. These three splice variants are therefore predicted to result in truncated versions of OATP1B1.

Splice variants overlapping with SLCO1B7 and SLCO1B1

Four splice variants were identified with exons overlapping the *SLCO1B1* as well as the *SLCO1B7* gene region (Table 2). They all had an ORF overlapping >40% of the amino acid sequence of OATP1B1. However, the ORF of none of them was overlapping the *SLCO1B7* region. Two of these isoforms are predicted to translate into similar protein versions of OATP1B1, as they have 100% overlap with the reference isoform. All four splice variants have longer untranslated regions than the reference isoform.

One isoform, sv28, overlapped with *SLCO1A2*. This hybrid isoform contains an intron-less complete coding sequence, which is officially located in intron 13 of *SLCO1A2*.

Figure 3 Expression (A) and expression in relation to the reference isoform (B) of developmentally regulated splice variants of SLCO1B1 in various age groups. Counts of tissues with isoform expressed out of total counts by age group are provided in parentheses. *p<0.05; **p<0.01

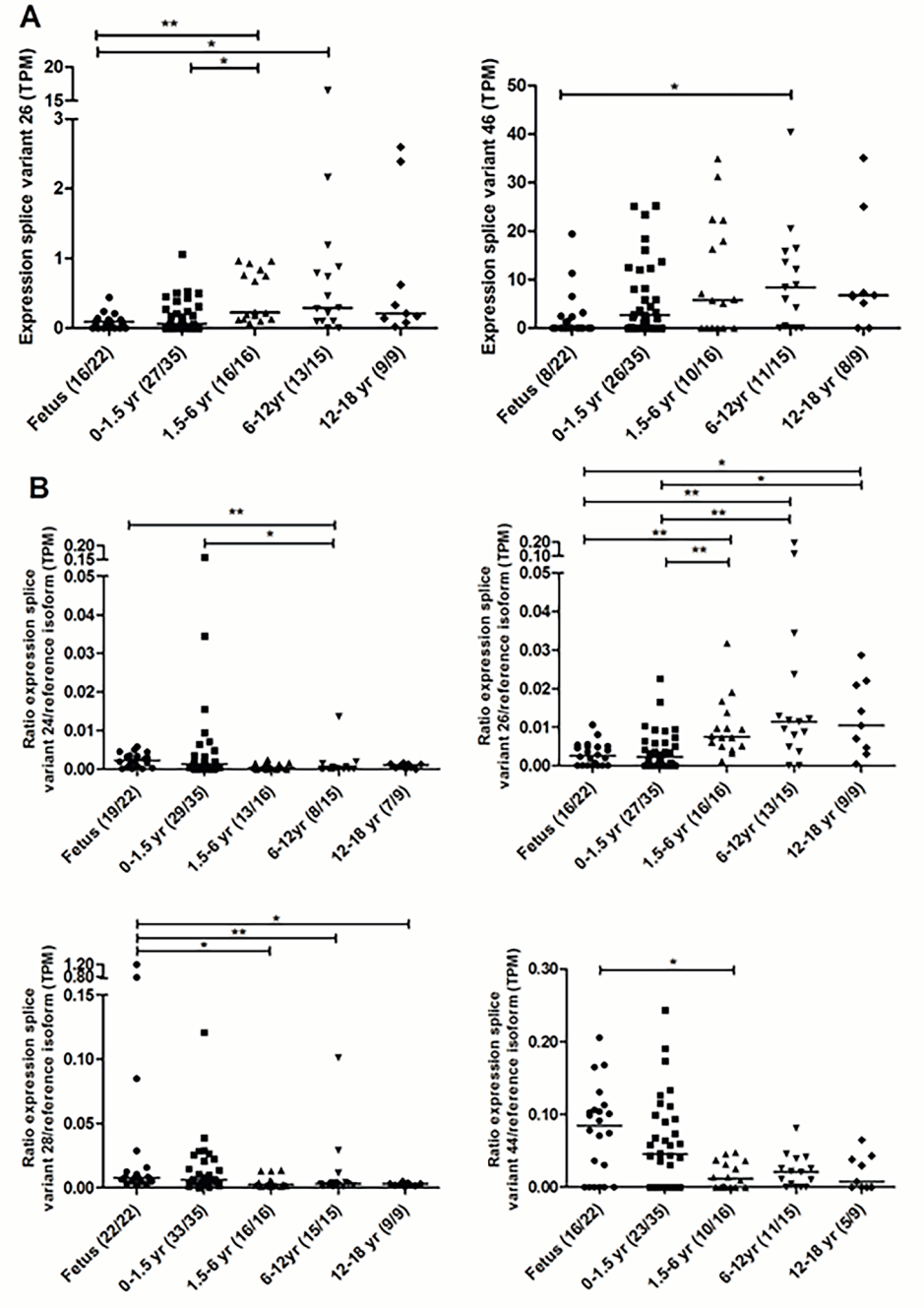

Splice variants with age-related expression

Age groups

The splice variants 26 and 46 showed age-related changes in their expression with lower expression in fetal tissue than in tissue from older children (see Figure 3A for specific changes and Table 2 for splice variant information). When analyzed as a ratio to the expression of the reference isoform, for one splice variant (26) the ratio variant/reference isoform increased with age, while three splice variants decreased with age: isoforms 24, 28 and 44 (see Figure 3B for specific changes and Table 2 for splice variant information). This latter observation reflects that for the individual samples either the expression of the splice variant was lower, or the expression of reference isoform was higher. As the expression of the reference isoform was shown to be similar when binned in age groups (Figure 3A), it is therefore likely that the expression of the splice variants that decreased with age was lower.

Age on continuous scale

The expression of four of the five hybrid SLCO1B7 and SLCO1B1 splice variants (24, 26, 28, 30) and the abundant splice variant 46 are significantly correlated with age (see Table 3). More specifically, the expression of the splice variants 24 and 28 decreased with increasing age, and the expression of 26, 30 and 46 increased with increasing age. When splice variant expression is analyzed as a ratio to the expression of the reference isoform, correlation with age was found for the same and for four additional splice variants (see Table 3). The expression of splice variant 48 was correlated with age, but was excluded for further analysis as their presence was not verified by RT-PCR (see 5.2).

Predicted protein structure

In Table S3 the coding-potential prediction results using the CPAT and CPC2 tool are depicted. Splice variant 44 has a low coding probability, hence will likely not result in a protein product. This can be explained by the fact that the ORF length was small compared to the size of the splice variant or because of a high hexamer-score.[42,43] The hexamer-score is a feature dependent on adjacent amino acids in proteins and is based on a log-likelihood ratio to measure differential hexamer usage between coding and noncoding sequences.[44] All other splice variants have a very high probability to be translated into a protein product. In Figure 4A the 2D structure of OATP1B1 is presented, consisting of 12 TM helices. In Figure 4B the predicted 2D structure of the splice variants with an ORF with high probability to be translated in a protein product are presented.

Figure 4 (A) Predicted 2D structure of reference OATP1B1 (1: extracellular, 2: transmembrane, 3: intracellular) and (B) the predicted 2D structure of splice variants of OATP1B1, centered on the 4th intracellular loop (dashed line) of the reference structure for OATP1B1.

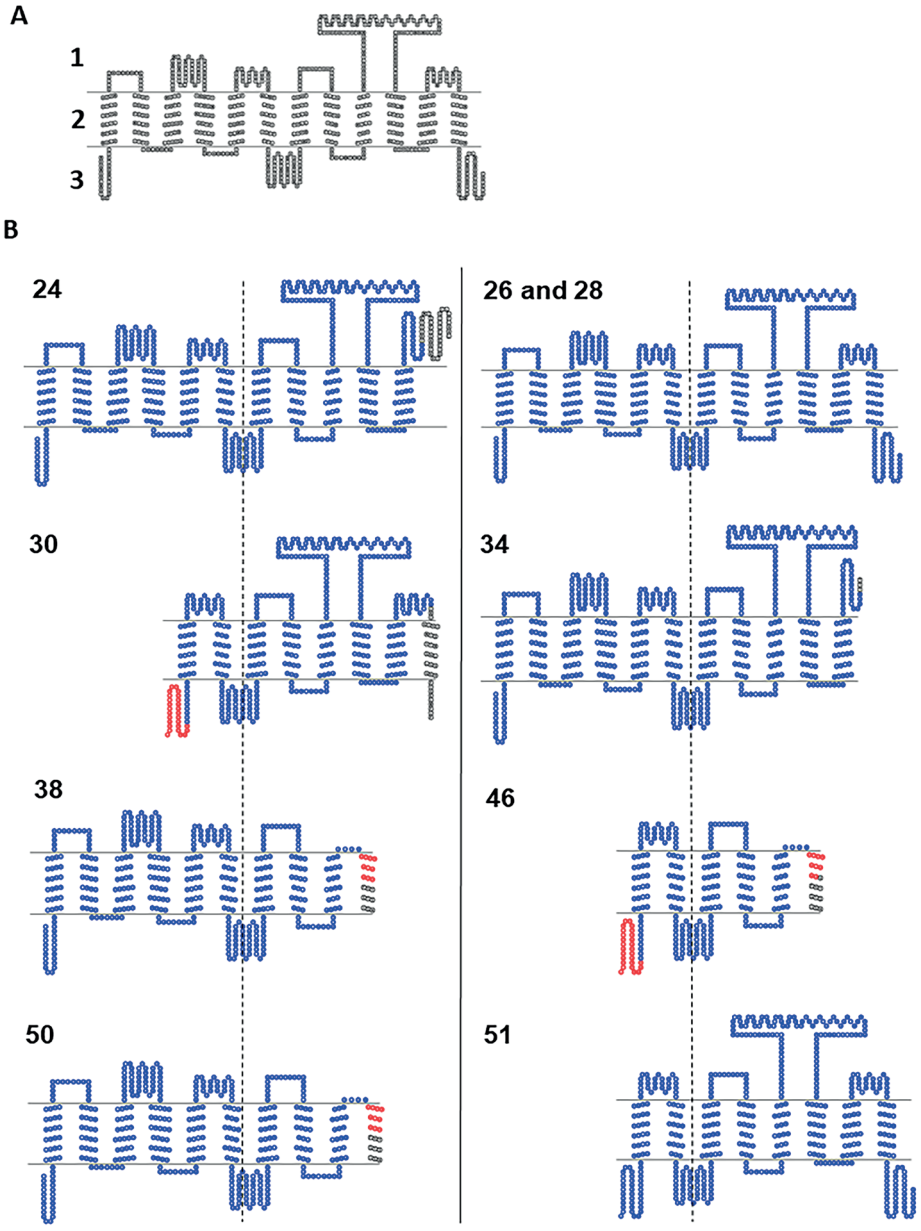

The number of the splice variant is presented in the upper left corner of each structure. Red and blue: overlapping amino acid sequence with OATP1B1. Blue: overlapping structure OATP1B1.

Table 3 Spearman correlations expression splice variant vs. postnatal age

Splice variant	Expression splice variant (TPM) vs. postnatal age (weeks)		Ratio expression splice variant/reference isoform vs. postnatal age (weeks)	
	r_s	p value	r_s	p value
21	0.231	0.023	0.194	0.057
24	-0.330	0.001*	-0.392	0.000*
26	0.489	0.000*	0.518	0.000*
28	-0.263	0.009*	-0.433	0.000*
30	0.290	0.004*	0.296	0.003*
33	0.142	0.166	0.143	0.163
34	0.133	0.193	0.110	0.285
35	-0.035	0.734	-0.222	0.029
36	0.063	0.539	0.058	0.575
37	0.069	0.501	0.006	0.955
38	-0.070	0.496	-0.271	0.007*
39	-0.141	0.167	-0.188	0.065
40	-0.017	0.869	-0.092	0.371
41	0.003	0.977	-0.001	0.990
42	0.055	0.591	-0.059	0.566
43	0.065	0.528	0.063	0.542
44	-0.121	0.240	-0.259	0.010*
45	-0.017	0.867	-0.020	0.843
46	0.386	0.000*	0.343	0.001*
47	-0.023	0.825	-0.106	0.299
48†	-0.243	0.016	-0.463	0.000*
49	-0.117	0.253	-0.146	0.152
50	0.204	0.045	-0.202	0.047
51	-0.177	0.083	-0.308	0.002*
53	-0.029	0.779	-0.043	0.678
54	-0.155	0.129	-0.169	0.097
55	-0.173	0.091	-0.203	0.046

** Significant after adjustment to control false discovery rate at .05 †excluded from further analysis because the presence was not confirmed by RT-PCR*

DISCUSSION

In the current study we have developed a data analysis pipeline that allowed a structured analysis of a large amount of RNA-seq data generated from pediatric liver samples and used this to investigate alternative splicing of the *SLCO1B1* gene that could potentially translate into functional OATP1B1 proteins. More specifically, we report three major findings from the ten relevant splice variants that we identified: (1) two splice variants are predicted to translate into the same amino acid sequence as the reference isoform for OATP1B1; (2) eight splice variants may translate into truncated versions of the OATP1B1 protein because of an altered length of amino acid sequence, and (3) the expression of eight splice variants was associated with age. None of the splice variants had an ORF that covered the *SLCO1B7* region.

Our results show that the *SLCO1B1* gene locus is subject to alternative splicing, as supported by the major findings presented above. More specifically, the fact that eight splice variants of SLCO1B1 showed a developmental pattern is consistent with developmentally regulated alternative splicing as a mechanism for altered SLCO1B1/OATP1B1 expression during growth and maturation. This finding may have implications for the functionality of the transporter in children, and with that the disposition of its endogenous and exogenous substrates, as most of these splice variants were predicted to result in truncated OATP1B1 isoforms with fewer TM regions compared to the reference OATP1B1 protein. Available evidence suggests that *SLCO1B7* is a pseudogene resulting in a non-functional protein product with only 11 TM regions, whereas the *SLCO1B1* gene, the *SLCO1B3* gene and the hybrid transcript LST-3TM12 give rise to at least one mRNA transcript that translates into functional transporters with 12 TM regions.[30] Moreover, the truncated proteins encoded by the transcripts we observed may lack one or more of the N-glycosylation sites Asn134, Asn503 and Asn516, located at the extracellular loop 2 and 5 of OATP1B1.[45] Glycosylation is a post-translational modification that is suggested to be essential for the proper function of OATP1B1. Disruption of all these sites led to lower protein stability with reduced total protein levels, and non-glycosylated OATP1B1 was retained within the endoplasmic reticulum, e.g. was not present on the cell membrane.[45]

Some of the alternative proteins of OATP1B1 reported in this study therefore are likely to result in non-functional protein products incapable of cellular transport, but could possibly possess alternative functional properties, such as regulating the activity of the functional OATP1B1 transporter protein. A precedent for this type of regulatory role is illustrated by the DME *UGT1A*, a complex gene with 3 major mRNA variants created by splicing events involving an alternative 5a or 5b exon. The classic variant (i1) with exon 5a has transferase activity, whereas the alternative proteins (i2), with either exon 5b or with both exon 5a and

5b, lack transferase activity.[46] The relative glucuronidation of SN-38, a substrate for UGT1A, was decreased in the presence of i2 proteins despite the same amount of i1 enzyme.[47] This phenomenon is explained by oligomerization of UGT1A enzyme; i2 proteins can form dimers with i1 enzymes, inhibiting the activity of i1 enzymes.[48] Interestingly, OATP1B transporters not only form homo-oligomers, but can also form hetero-oligomers, even with transporters from another family, *e.g.* with Na+/taurocholate co-transporting polypeptide (NTCP).[49,50] It has been demonstrated that a non-functional unit of OATP1B3, containing a lysine at position 41 in place of the wild-type cysteine in the homodimer did not affect normal substrate transport by the functional, cysteine-containing OATP1B3 component of the homodimer, suggesting that each unit within the dimer works as an independent functional unit.[49] However, each splice variant may have its own function and so we hypothesize that those resulting in truncated proteins may influence the transporter activity of the reference protein OATP1B1 and other transporters.

The specific *SLCO1B1* region is part of the wider *SLCO1B*-family region, which gives rise to the SLCO1B3/SLCO1B7 hybrid transcript LST-3TM12 that results in a functional transporter.[30] The four SLCO1B1 splice variants found in this study that contained exons covering the region of *SLCO1B7* did not contain the start codon from the *SLCO1B7* locus, thus we conclude that the *SLCO1B1* gene is not subject to hybridization with adjacent genes. However, the length of the untranslated region (UTR) of these and other transcripts could well be influencing the function of the transporter, even when the ORF of the splice variant is the same as the reference sequence. We note that a transcript of CYP3A4 with a shorter 3'-UTR than the canonical transcript due to an additional polyadenylation site was more stable and generated more protein[51] than an alternative transcript with a longer 3'-UTR. Interestingly, this shorter transcript showed developmental regulation as it was higher expressed in adult livers than in pediatric livers. Nevertheless, it remains to be seen whether this is also the case for the splice variants presented in this study.

Another consequence of these truncated versions of OATP1B1 is that they may interfere with the estimation of OATP1B1 content using LC-MS/MS-based proteomic methods. This quantitative proteomic approach utilizes short peptides to target the protein of interest. All truncated versions of OATP1B1 presented in this manuscript contained the amino acid sequences NVTGFFQSFK[14] and of LNTVGIAK[11] that have been used in studies presenting results on expression of OATP1B1 protein in pediatric liver tissue. The latter refers to our previous study, where a poor correlation was seen between total mRNA expression of SLCO1B1 as measured with RNA-seq and protein abundance of OATP1B1 in a subset of the samples presented in the current study.[11] This lack of correlation can be explained by the fact that not all mRNA transcripts translate into protein. Moreover, potential translation of splice variants into non-functional proteins that are nevertheless

detected by the peptide sequences used to quantitate OATP1B1 content, could also result in poor correlations between abundance and activity. Thus, care may be needed when extrapolating mRNA expression to protein abundance, protein abundance to actual activity, and ultimately the prediction of disposition of transporter substrates.

We recognize that a limitation of our study is that our results are based on *in silico* predictions, and the presence of the corresponding truncated proteins must be confirmed by protein abundance studies before any of the implications we propose above can be assessed, including investigations of a dominant-negative regulatory role analogous to the UGT1A situation. Developmental regulation of alternative splicing is a commonly recognized phenomenon during tissue development and cell differentiation. In fact, level of expression, localization within the cell, mRNA stability, translation efficiency and splicing of specific RNA binding proteins (RBPs) is finely regulated. RBPs bind to cis-elements and promote or inhibit splice site recognition, and therefore RBP expression coordinates alternative splicing networks during development.[18] Further work is necessary to characterize the specific developmental signals responsible for the observed changes in expression of the SLCO1B1 splice variants.

These exploratory data imply that the complexity of processes involved with growth and development throughout childhood may have influences on transporter expression and subsequent substrate disposition, as yet unrecognized. The observed age-related changes in expression of splice variants in the context of age-related changes in concentrations of endogenous OATP1B1 substrates, such as DHEA-S and 16alpha-hydroxylated metabolites, makes it tempting to speculate that additional regulatory mechanisms may be in play, with implications for the disposition of exogenous substrates used in pediatrics. Most importantly, the data analysis pipeline we have developed allows the analyses described in this manuscript for SLCO1B1 to be applied to any other gene of interest and will be repeated for other transporters and genes involved in drug disposition or growth of children in the future.

In conclusion, we have shown that SLCO1B1 splice variants with an ORF could potentially translate into proteins with unknown function; they are unlikely to code for functional, transporters, but may have other roles, such as regulatory activity. Moreover, as the expression of particular SLCO1B1 splice variants showed age-related changes, the data raise the possibility of a regulatory role for alternative splicing in mediating developmental changes of SLCO1B1/OATP1B1 in drug disposition. These data can contribute to improved understanding of age-related changes in expression of SLCO1B1, and possibly other enzymes and transporters involved in the disposition of endogenous and exogenous substrates throughout growth and development.

REFERENCES

1. Brouwer KL, Aleksunes LM, Brandys B, et al. Human ontogeny of drug transporters: review and recommendations of the pediatric transporter working group. Clin Pharmacol Ther 2015;98(3):266-287.
2. Nigam SK. What do drug transporters really do? Nat Rev Drug Discov 2015;14(1):29-44.
3. Mooij MG, Nies AT, Knibbe CA, et al. Development of human membrane transporters: drug disposition and pharmacogenetics. Clin Pharmacokinet 2016;55(5):507-524.
4. Stevens JC, Hines RN, Gu C, et al. Developmental expression of the major human hepatic CYP3A enzymes. J Pharmacol Exp Ther 2003;307(2):573-582.
5. Leeder JS, Gaedigk R, Marcucci KA, et al. Variability of CYP3A7 expression in human fetal liver. J Pharmacol Exp Ther 2005;314(2):626-635.
6. Oshiro C, Mangravite L, Klein T, Altman R. PharmGKB very important pharmacogene: SLCO1B1. Pharmacogenet Genomics 2010;20(3):211-216.
7. Kojima S, Yanaihara T, Nakayama T. Serum steroid levels in children at birth and in early neonatal period. Am J Obstet Gynecol 1981;140(8):961-965.
8. France JT. Levels of 16-alpha-hydroxydehydroepiandrosterone, dehydroepiandrosterone and pregnenolone in cord plasma of human normal and anencephalic fetuses. Steroids 1971;17(6):697-719.
9. Nakamura H, Torimoto N, Ishii I, et al. CYP3A4 and CYP3A7-mediated carbamazepine 10,11-epoxidation are activated by differential endogenous steroids. Drug Metab Dispos 2003;31(4):432-438.
10. Niemi M, Pasanen MK, Neuvonen PJ. Organic anion transporting polypeptide 1B1: a genetically polymorphic transporter of major importance for hepatic drug uptake. Pharmacol Rev 2011;63(1):157-181.
11. van Groen BD, van de Steeg E, Mooij MG, et al. Proteomics of human liver membrane transporters: a focus on fetuses and newborn infants. Eur J Pharm Sci 2018;124:217-227.
12. Mooij MG, Schwarz UI, de Koning BA, et al. Ontogeny of human hepatic and intestinal transporter gene expression during childhood: age matters. Drug Metab Dispos 2014;42(8):1268-1274.
13. Thomson MM, Hines RN, Schuetz EG, Meibohm B. Expression Patterns of Organic Anion Transporting Polypeptides 1B1 and 1B3 Protein in Human Pediatric Liver. Drug Metab Dispos 2016;44(7):999-1004.
14. Prasad B, Gaedigk A, Vrana M, et al. Ontogeny of hepatic drug transporters as quantified by LC-MS/MS proteomics. Clin Pharmacol Ther 2016;100(4):362-370.
15. Dennery PA, Seidman DS, Stevenson DK. Neonatal hyperbilirubinemia. N Engl J Med 2001;344(8):581-590.
16. Huang MJ, Kua KE, Teng HC, Tang KS, Weng HW, Huang CS. Risk factors for severe hyperbilirubinemia in neonates. Pediatr Res 2004;56(5):682-689.
17. Wang ET, Sandberg R, Luo S, et al. Alternative isoform regulation in human tissue transcriptomes. Nature 2008;456(7221):470-476.
18. Baralle FE, Giudice J. Alternative splicing as a regulator of development and tissue identity. Nat Rev Mol Cell Biol 2017;18(7):437-451.
19. Castle JC, Zhang C, Shah JK, et al. Expression of 24,426 human alternative splicing events and predicted cis regulation in 48 tissues and cell lines. Nat Genet 2008;40(12):1416-1425.
20. Plummer NW, Meisler MH. Evolution and diversity of mammalian sodium channel genes. Genomics 1999;57(2):323-331.

21. Plummer NW, McBurney MW, Meisler MH. Alternative splicing of the sodium channel SCN8A predicts a truncated two-domain protein in fetal brain and non-neuronal cells. J Biol Chem 1997;272(38):24008-24015.
22. Gustafson TA, Clevinger EC, O'Neill TJ, Yarowsky PJ, Krueger BK. Mutually exclusive exon splicing of type III brain sodium channel alpha subunit RNA generates developmentally regulated isoforms in rat brain. J Biol Chem 1993;268(25):18648-18653.
23. Sarao R, Gupta SK, Auld VJ, Dunn RJ. Developmentally regulated alternative RNA splicing of rat brain sodium channel mRNAs. Nucleic Acids Res 1991;19(20):5673-5679.
24. Belcher SM, Zerillo CA, Levenson R, Ritchie JM, Howe JR. Cloning of a sodium channel alpha subunit from rabbit Schwann cells. Proc Natl Acad Sci U S A 1995;92(24):11034-11038.
25. Tate SK, Depondt C, Sisodiya SM, et al. Genetic predictors of the maximum doses patients receive during clinical use of the anti-epileptic drugs carbamazepine and phenytoin. Proc Natl Acad Sci U S A 2005;102(15):5507-5512.
26. Mulley JC, Scheffer IE, Petrou S, Dibbens LM, Berkovic SF, Harkin LA. SCN1A mutations and epilepsy. Hum Mutat 2005;25(6):535-542.
27. Petrovski S, Scheffer IE, Sisodiya SM, O'Brien TJ, Berkovic SF, Consortium E. Lack of replication of association between scn1a SNP and febrile seizures. Neurology 2009;73(22):1928-1930.
28. Tate SK, Singh R, Hung CC, et al. A common polymorphism in the SCN1A gene associates with phenytoin serum levels at maintenance dose. Pharmacogenet Genomics 2006;16(10):721-726.
29. Hunt SE, McLaren W, Gil L, et al. Ensembl variation resources. Database 2018.
30. Malagnino V, Hussner J, Seibert I, Stolzenburg A, Sager CP, Meyer Zu Schwabedissen HE. LST-3TM12 is a member of the OATP1B family and a functional transporter. Biochem Pharmacol 2018;148:75-87.
31. Pertea M, Kim D, Pertea GM, Leek JT, Salzberg SL. Transcript-level expression analysis of RNA-seq experiments with HISAT, StringTie and Ballgown. Nat Protoc 2016;11:1650.
32. Langmead B, Salzberg SL. Fast gapped-read alignment with Bowtie 2. Nat Methods 2012;9(4):357-359.
33. Pertea M, Pertea GM, Antonescu CM, Chang T-C, Mendell JT, Salzberg SL. StringTie enables improved reconstruction of a transcriptome from RNA-seq reads. Nat Biotechnol 2015;33:290.
34. Genome Reference Consortium. Genome Reference Consortium Human Build 37. https://www.ncbi.nlm.nih.gov/assembly/GCF_000001405.13/. Accessed May, 2018.
35. Li B, Dewey CN. RSEM: accurate transcript quantification from RNA-Seq data with or without a reference genome. BMC Bioinformatics 2011;12:323.
36. Kim D, Langmead B, Salzberg SL. HISAT: a fast spliced aligner with low memory requirements. Nature Methods 2015;12:357.
37. Farrell CM, O'Leary NA, Harte RA, et al. Current status and new features of the Consensus Coding Sequence database. Nucleic Acids Res 2014;42(Database issue):D865-872.
38. Boratyn GM, Thierry-Mieg J, Thierry-Mieg D, Busby B, Madden TL. Magic-BLAST, an accurate DNA and RNA-seq aligner for long and short reads. bioRxiv 2018.
39. NCBI. ORFfinder. https://www.ncbi.nlm.nih.gov/orffinder/. Accessed May, 2018.
40. ExPaSy. TMpred. https://embnet.vital-it.ch/software/TMPRED_form.html. Accessed May, 2018.
41. UCSF. TOPO2. http://www.sacs.ucsf.edu/cgi-bin/open-topo2.py. Accessed May, 2018.
42. Kang YJ, Yang DC, Kong L, et al. CPC2: a fast and accurate coding potential calculator based on sequence intrinsic features. Nucleic Acids Res 2017;45(W1):W12-W16.
43. Wang L, Park HJ, Dasari S, Wang S, Kocher JP, Li W. CPAT: Coding-Potential Assessment Tool using an alignment-free logistic regression model. Nucleic Acids Res 2013;41(6):e74.

44. Fickett JW, Tung CS. Assessment of protein coding measures. Nucleic Acids Res 1992;20(24):6441-6450.
45. Yao J, Hong W, Huang J, Zhan K, Huang H, Hong M. N-Glycosylation dictates proper processing of organic anion transporting polypeptide 1B1. PLoS One 2012;7(12):e52563.
46. Girard H, Levesque E, Bellemare J, Journault K, Caillier B, Guillemette C. Genetic diversity at the UGT1 locus is amplified by a novel 3' alternative splicing mechanism leading to nine additional UGT1A proteins that act as regulators of glucuronidation activity. Pharmacogenet Genomics 2007;17(12):1077-1089.
47. Rouleau M, Roberge J, Bellemare J, Guillemette C. Dual roles for splice variants of the glucuronidation pathway as regulators of cellular metabolism. Mol Pharmacol 2014;85(1):29-36.
48. Bellemare J, Rouleau M, Harvey M, Guillemette C. Modulation of the human glucuronosyltransferase UGT1A pathway by splice isoform polypeptides is mediated through protein-protein interactions. J Biol Chem 2010;285(6):3600-3607.
49. Zhang Y, Boxberger KH, Hagenbuch B. Organic anion transporting polypeptide 1B3 can form homo- and hetero-oligomers. PLoS One 2017;12(6):e0180257.
50. Ni C, Yu X, Fang Z, Huang J, Hong M. Oligomerization Study of Human Organic Anion Transporting Polypeptide 1B1. Mol Pharm 2017;14(2):359-367.
51. Li D, Gaedigk R, Hart SN, Leeder JS, Zhong XB. The role of CYP3A4 mRNA transcript with shortened 3'-untranslated region in hepatocyte differentiation, liver development, and response to drug induction. Mol Pharmacol 2012;81(1):86-96.

SUPPLEMENTAL INFORMATION

Figure S1 Example for splice variant 34 of the design of primers by the identification of unique location F=Forward, R=Reverse, nest=nested primer

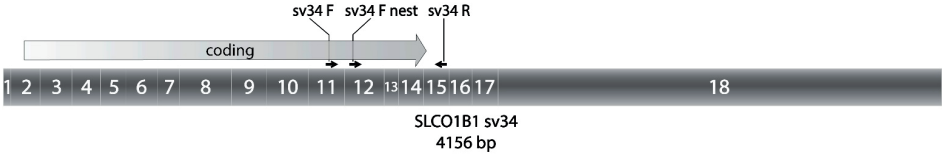

Figure S2 Nested PCR products for different splice variants, analyzed on a 4% agarose gel before subsequent sequencing.

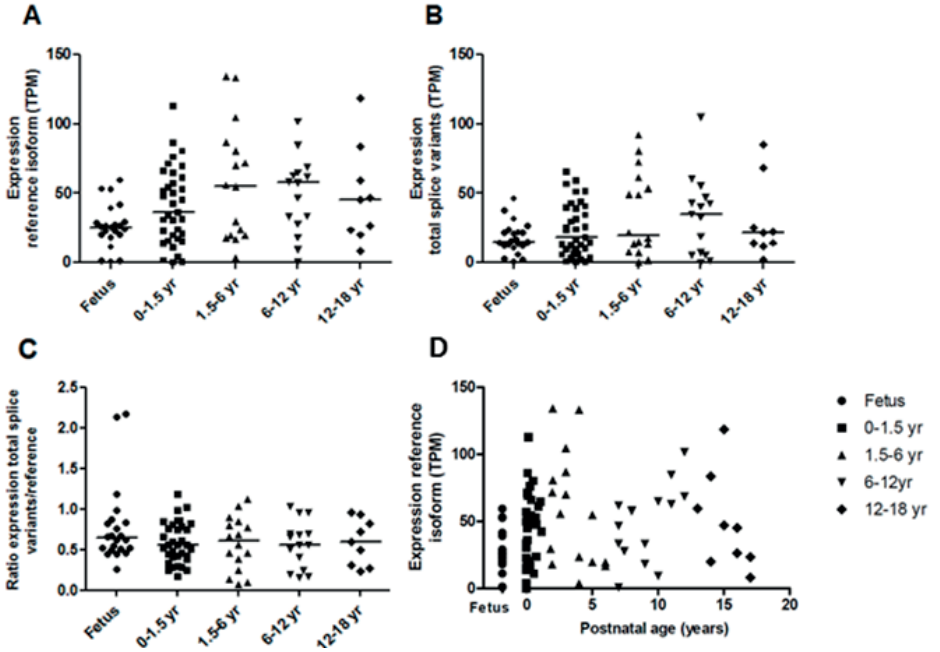

The arrow indicates the band which was excised from the gel; the amplicon was extracted and sequenced. Black indicates correct amplicon size which was confirmed by sequencing. Gray indicated band sizes which were either too large (sv21), too short (sv37) or did not amplify at all. The universal SLCO1B1 primer pair (sv-all) was used for the positive control (+), while an actin primer pair was utilized in the none template control (NTC).

Table S1 Primer sequences to verify the existence of splice variants in our samples by RT-PCR. F=Forward, R=Reverse, nest=nested, sv=splice variant

Primer Name	Sequences (5'-3')	Sv
SLCO1B1 sv21 F	CGGCTTCCATTCAATGATTATG	sv21 and sv30
SLCO1B1 sv21 F nest	GATCGCTAGGAGGTATTCTAGTTCC	sv21
SLCO1B1 sv21 R	CCACTATCTCAGGTGATGCTCTATTG	sv21
SLCO1B1 sv24 F	CAGCTGTGGAGCACGAGG	sv24
SLCO1B1 sv24 F nest	GGCTTGAAGTATCTTCTAGGTATGAGAC	sv24
SLCO1B1 sv24 R	ATCTCCGTTCTATATGAATGATGGAAC	sv24
SLCO1B1 sv26 F	ATGATAGTGGCGTCTGCTCCTA	sv26
SLCO1B1 sv26 F nest	GTGAGAGCAGGATTGTTCAACC	sv26
SLCO1B1 sv26 R	AGCTTTGTTCCAGCCTTAATCATC	sv26
SLCO1B1 sv28 F	TTCAAAATAGCTATTTTGAGGAAACTCATAG	sv28
SLCO1B1 sv28 F nest	GGATAATACCAGAGAACTTCTCAAACTTAGAG	sv28
SLCO1B1 sv28 R	CTGGTATTGATGAAATCCCTCAGTG	sv28
SLCO1B1 sv30 F nest	GAAGAGACATTTTCACCAGTATCTTCTAG	sv30
SLCO1B1 sv30 R	TGATGCTCAGTTTGAAACAATCAC	sv30
SLCO1B1 sv34 F	AACAATGGAATAACTTACATCTCACCC	sv34
SLCO1B1 sv34 F nest	CAGAACAGAAATTACTCAGCCCAT	sv34
SLCO1B1 sv34 R	GATTTAGAACCTACAGCAACTGCAG	sv34 and sv50
SLCO1B1 sv37 F	ATCTAAGGCTAACATCTTATTGGGAGTC	sv37
SLCO1B1 sv37 F nest	ATAACCATACCTATTTTTGCAAGTGG	sv37
SLCO1B1 sv37 R	TGGTACATCTCTATGAGATGTCACTGG	sv37
SLCO1B1 sv38 F	GGGTTTCCACTCAATGGTTATACG	sv38
SLCO1B1 sv38 F nest	GGGCTCTGATTGATACAACGTGTATA	sv38
SLCO1B1 sv38 R	CATCTCTTAAGCCCAGGAAGC	sv38
SLCO1B1 sv44 F nest	CAATGGATTGAAGGAATTTCATAATAC	sv44
SLCO1B1 sv44 R	TGATGATTATGTGTCTTGTGGATGAC	sv44
SLCO1B1 sv48 F	TGCTGTAGGATTCTAAATCCAGGTG	sv48 and sv44
SLCO1B1 sv48 F nest	GAGGCACAACCTTCAGAGAATAAG	sv48
SLCO1B1 sv48 R	TTCCAAATATTGGAGTGAATGTATTCTC	sv48
SLCO1B1 sv50 F	AGCTATTGGGACTGAAGAGACCATAC	sv50
SLCO1B1 sv50 F nest	GGACATAAGAAAGTCTGTTCTAAACTTACAG	sv50
SLCO1B1 sv51 F	CAGCTTTATTGCTAAGACACTAGGTGC	sv51
SLCO1B1 sv51 F nest	GAATTGGAGGTGTTTTGACTGC	sv51
SLCO1B1 sv51 R	TCTTATAGGCAAAGACGTACAGTATATACGTTATAC	sv51
SLCO1B1 sv-all F	CTGGGAAATTGACAGAAAGTACTCTG	all sv
SLCO1B1 sv-all F nest	GGGAAGATAATGGTGCAAATAAAG	all sv
SLCO1B1 sv-all R	CAAAGAAGAATGTCCTTCTTTAGCG	all sv

Table S2 non-relevant splice variants of SLCO1B1 in 97 pediatric liver samples

Splice variant	Abundance of all novel isoforms (%)	Abundance compared to reference isoform (%)	Found in number of samples	Number of exons	Length (nt)	ORF (n AA)	Overlapping number of AA with locus:				Number of TM helices
							ORF SLCO1B1 (% of reference SLCO1B1)	Intron *SLCO1B1*	In between *SLCO1B1* and *SLCO1A2*†	*SLCO-1A2*†	
49	3.81	2.37	24	17	2511	455	443 (64%)	12	-	-	9
43	0.92	0.57	6	10	3826	420	199 (29%)	221	-	-	9
55	0.79	0.49	43	4	10573	107	61 (9%)	42	5	-	2
39	0.64	0.40	61	16	8163	453	443 (64%)	10	-	-	10
54	0.51	0.31	30	2	5898	50	50 (7%)	-	-	-	1
42	3.88	2.41	88	13	13920	347	331 (48%)	16	-	-	6
53	1.50	0.93	55	2	3148	98	98 (14%)	-	-	-	2
47	3.69	2.29	46	16	2394	455	443 (64%)	12	-	-	9
41	0.83	0.51	18	19	13498	691	691 (100%)	-	-	-	12
33	0.67	0.42	18	20	13612	691	691 (100%)	-	-	-	12
35	1.24	0.77	85	18	4697	456	452 (65%)	-	4	-	8
40	1.52	0.94	56	18	3389	659	621 (90%)	-	-	38	12
36	2.11	1.31	16	19	2530	625	621 (90%)	-	4	-	11
45	0.47	0.29	11	16	6316	453	443 (64%)	10	-	-	10
37	8.65	5.37	56	16	2935	455	444 (65%)	11	-	-	9
21	2.56	1.59	53	17	2151	490	452 (65%)	-	-	38	7
48	3.36	2.08	83	3	9877	-	-	-	-	-	-

Table S3 Coding-potential prediction using the Coding-Potential Assessment Tool (CPAT) and Coding Potential Calculator version 2 (CPC2)

	CPAT				CPC2				
Splice variant	**Fickett Score**	**Hexamer Score**	**Coding Probability**	**Coding Label**	**Fickett Score**	**Isoelectric point**	**ORF Integrity**	**Coding Probability**	**Coding Label**
24	0.701	-0.145	0.999	Coding	0.390	8.704	1	1.000	Coding
26	0.659	-0.152	0.999	Coding	0.294	8.852	1	1.000	Coding
28	0.845	0.029	1.000	Coding	0.334	9.696	1	1.000	Coding
30	0.648	-0.146	0.999	Coding	0.324	8.682	1	0.999	Coding
34	0.661	-0.152	0.999	Coding	0.304	8.905	1	1.000	Coding
38	0.841	-0.146	0.999	Coding	0.275	9.185	1	0.999	Coding
44	0.621	-0.284	0.005	Noncoding	0.294	8.864	1	0.089	Noncoding
46	0.845	-0.154	0.924	Coding	0.285	9.026	1	0.972	Coding
50	0.841	-0.146	0.998	Coding	0.271	9.185	1	0.999	Coding
51	0.663	-0.159	0.999	Coding	0.266	8.633	1	0.999	Coding

PART III

- to clinical research

7 Dose-linearity of the pharmacokinetics of an intravenous [^{14}C] midazolam microdose in children

Bianca D van Groen, Wouter H Vaes, B Kevin Park, Elke H J Krekels, Esther van Duijn, Lenne-Triin Kõrgvee, Wiola Maruszak, Grzegorz Grynkiewicz, R Colin Garner, Catherijne A J Knibbe, Dick Tibboel, Saskia N de Wildt, Mark A Turner

Br J Clin Pharmacol 2019 Jul 3; DOI 10.1111/BCP.14047

ABSTRACT

Aims: Drug disposition in children may vary from adults due to age-related variation in drug metabolism. Microdose studies present an innovation to study pharmacokinetics (PK) in paediatrics, however, it should be used only when the PK is dose linear. We aimed to assess dose-linearity of a [^{14}C]midazolam microdose, by comparing the PK of an intravenous (IV) microtracer (a microdose given simultaneously with a therapeutic midazolam dose), with the PK of a single isolated microdose.

Methods: Preterm to two-year-old infants admitted to the intensive care unit received [^{14}C]midazolam IV as a microtracer or microdose, followed by dense blood sampling up to 36 hours. Plasma-concentrations of [^{14}C]midazolam and [^{14}C]1-hydroxy-midazolam were determined by accelerator mass spectrometry. Non-compartmental PK analysis (NCA) was performed and a population PK model was developed.

Results: Of 15 infants (median gestational age 39.4 [range 23.9-41.4] weeks, postnatal age 11.4 [0.6-49.1] weeks), six received a microtracer and nine a microdose [^{14}C] midazolam (111 Bq kg^{-1}; 37.6 ng kg^{-1}). In a two-compartment PK model, bodyweight was the most significant covariate for volume of distribution. There was no statistically significant difference in any PK parameter between the microdose and microtracer, nor in the AUC ratio [^{14}C]1-OH-midazolam/[^{14}C]midazolam, showing the PK of midazolam to be linear within the range of the therapeutic and microdoses.

Conclusion: Our data supports the dose-linearity of the PK of an IV [^{14}C]midazolam microdose in children. Hence, a [^{14}C]midazolam microdosing approach may be used as an alternative to a therapeutic dose of midazolam to study developmental changes in hepatic CYP3A activity.

INTRODUCTION

Drug disposition in children may vary from adults due to age-related variation in the processes governing absorption, distribution, metabolism and excretion.[1,2] This variation is largest in the first years of life and is not directly proportionate to size.[3,4] However, in daily clinical practice drug dosing in paediatrics is often based on bodyweight based corrections, which because of variation arising from development, can result in sub-therapeutic or toxic drug exposure in certain subgroups.[2] Hence, doses used for children cannot simply be extrapolated from adults using a simple bodyweight-based correction.

Phenotyping studies, in which model drugs representative for a certain pathway are studied across the paediatric age range, can be used to elucidate the age-related variation in drug disposition pathways in vivo.[5] However, these studies are faced with ethical, practical and scientific challenges. Children are vulnerable, and so exposing them to (almost) therapeutic doses of drugs for a non-therapeutic reason, as in a phenotyping study, may not be ethically acceptable. Moreover, blood sampling for pharmacokinetic (PK) analyses in children is challenging because of the burden for the individual child, the smaller blood volume that can be taken, as well as the technical difficulties associated with sampling.

Microdosing studies present an attractive alternative to overcome the ethical and analytical challenges of phenotyping studies.[6] A microdose is a very small, sub-therapeutic dose of a drug (<1/100th of the therapeutic dose or <100 µg), that is unlikely to result in pharmacological effects or adverse events.[7,8] A radioactive label [^{14}C] allows ultra-sensitive quantification of extremely low plasma-concentrations by accelerator mass spectrometry (AMS) for which only 10-15 µl plasma is required.[9,10] The radiation dose associated with a [^{14}C]microdose is safe as it is below 1 µSievert. This is much lower than yearly background exposure (2.5 mSievert year^{-1} in The Netherlands), a computed tomography (CT)-scan of the head (1200 µSievert), or chest x-ray (12 µSievert).[6]

Microdosing studies can provide unique information of the PK of drugs in children, and with that valuable information on developmental changes in drug metabolism pathways, as shown successfully before.[6,11-13] Importantly, a prerequisite is that the PK of a microdose are linear to the PK of a therapeutic dose.[14,15] Lack of linearity may occur for example, when a therapeutic dose saturates drug metabolism pathways, plasma protein binding and/or active transporters, which may result in altered PK when studying a microdose.[15] A very elegant approach to study dose-linearity is by comparing the PK parameters of an isolated [^{14}C]microdose with the PK parameters of a [^{14}C]microtracer, where the labelled microdose is administered concurrently or even mixed with a therapeutic drug dose.[12]

Cytochrome P450 (CYP) 3A is a developmentally regulated drug metabolizing enzyme that is abundant in the liver and accounts for nearly 46% of the oxidative metabolism of clinically relevant drugs.[1,2,16-21] As midazolam is a well-established model substrate for CYP3A activity, this drug may be used for phenotyping studies using a microdosing approach to elucidate developmental changes in CYP3A.[5,22-25] To the best of our knowledge, dose-linearity of the PK of a microdose to those of a therapeutic dose of midazolam has been established in adults[14,26,27], but not in children. Yet, the results in adults cannot simply be extrapolated to children due to the development of drug metabolism, hepatic blood flow, protein binding and drug transport.

We therefore aimed to study the dose-linearity of the PK of a [^{14}C]midazolam microdose in children, by studying the PK parameters of midazolam when given as an intravenous (IV) [^{14}C]microdose, and as a [^{14}C]microtracer given simultaneously with a therapeutic midazolam dose.

METHODS

Study design

This study was part of the ERA-NET PRIOMEDCHILD project 'Paediatric Accelerator Mass Spectrometry Evaluation Research Study (PAMPER)'. The two units participating in this study were the Alder Hey Children's NHS Foundation Trust, Liverpool, UK and the Liverpool Women's NHS Foundation Trust, Liverpool, UK. Children were recruited on the paediatric intensive care units (PICUs) of these units. Ethical approval was obtained from the Research Ethics Committees for the hospitals where patients were enrolled. All parents or an adult who carried parental responsibility provided written informed consent for their child to be included prior to any study-specific procedures. No radioactive substance administration approval was required as the administered radioactive dose was below 1 μSievert, the UK Administration of Radioactive Substances Advisory Committee (ARSAC) exemption level.

Subjects

Children were eligible to be included in this study from birth up to two years of age, when they had intravenous lines in place for intravenous administration, and had suitable vascular access for blood sampling. Exclusion criteria were serious hepatic impairment (defined by aspartate-aminotransferase [ASAT] and alanine-aminotransferase [ALAT] > 200 U L^{-1}) or renal impairment (defined by plasma creatinine > 150 μmol), hemofiltration, peritoneal/hemodialysis or extracorporeal membrane oxygenation (ECMO).

Study procedures

A single [^{14}C]midazolam (111 Bq kg^{-1}; 37.6 ng kg^{-1}) dose was administered IV either as a microtracer during therapeutic midazolam infusion or as an isolated microdose (Figure 1). The microtracer was mixed with the first therapeutic loading dose of midazolam given by the treating physician for sedation, and was administered over 30 min. The microdose was administered with a similar infusion rate to ensure similar exposure to [^{14}C]levels. The IV therapeutic midazolam dose was prescribed by the treating physician for clinical purposes according to British National Formulary for Children dosing guidelines. Blood samples were taken before and up to 36 hours after administration of the [^{14}C]midazolam microtracer or microdose. The time points for blood sampling were based on the PK of midazolam in paediatric ICU patients where a median half-life of 5.5 hours was found [28]. To ensure complete sampling of a single dose, at least 5 times the half-life was taken. Moreover, to capture the distribution, metabolism and elimination phase, the sampling times were set on pre-dose, and 0.17, 0.5, 1, 2, 4, 6, 10, 24 and 36 hours post-IV dose. The maximum number of study specific blood samples was limited to 6 per subject. The specific time points for each patient were decided based on discussion between the research team, clinical team and parents to ensure cares were coordinated at this time and with minimal disruption to the patients' routine. The maximum amount of blood could not exceed the guidelines by European Medicines Agency (up to 1% of calculated circulating blood volume).[29] The blood samples were centrifuged and plasma was stored at -80°C until analysed.

Figure 1 Explanation of the terms IV 'microdose' and 'microtracer' midazolam

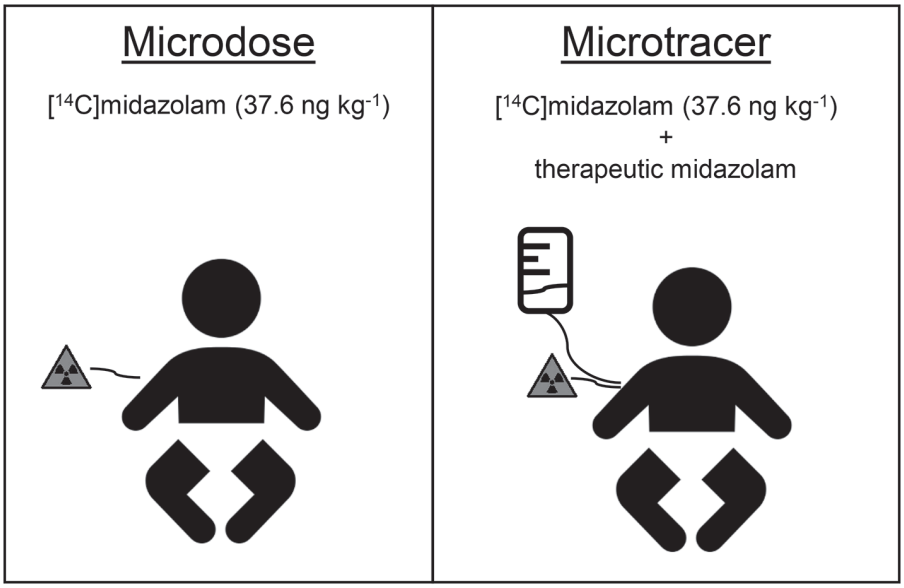

Radiopharmaceutical Preparation

[^{14}C]midazolam was synthesized by Selcia Ltd, United Kingdom at a specific activity of 1072 MBq mmol^{-1} (equal to 2.95 MBq mg^{-1}). The chemical name is 8-chloro-6-(2-fluorophenyl)-1-methyl-^{4}H-[1-^{14}C] imidazo[l,5-a][l,4]benzodiazepine hydrochloride. In the Radiopharmacy Department, Addenbrookes Hospital, Cambridge, United Kingdom under aseptic conditions [^{14}C]midazolam was brought in ethanol 96% solution, the activity was measured and the solution was further diluted 10 000 fold in 5% w/v dextrose solution to the required concentration. The final solution was filter sterilised (pore size 0.2 µm) and batched for intravenous injection. The final [^{14}C]midazolam concentration was 500Bq mL^{-1}.

[^{14}C]midazolam and [^{14}C]1-hydroxy-midazolam plasma concentration analysis

Plasma sample extraction and Ultra Performance Liquid Chromatography (UPLC) Separation

Methanol (10 µL) was added to plasma samples in order precipitate proteins and to extract the test substance using protein precipitation plates. Each run consisted of samples measured once and eight calibrator levels in duplicate plus three different QC levels in duplicate. The extract was evaporated to dryness, re-dissolved and analysed using UPLC. The fraction where midazolam and 1-hydroxy-midazolam eluted from the column was collected for each sample, evaporated to dryness and subsequently analysed using Combustion-CO_2-AMS. Fractions were transferred to a tin foil cup and evaporated to dryness prior to Accelerator Mass Spectrometry (AMS) analysis.

Accelerator Mass Spectrometry analysis

[^{14}C]levels were quantified as described before.[13,30] The UPLC and AMS qualification was performed in accordance with the recommendation of the European Bioanalytical Forum.[31] The tin foil cups (see 5.5.1) were combusted on an elemental analyser (Vario Micro; Elementar, Langenselbold, Germany). Generated CO_2 was transferred to a home-built gas interface, composed of a zeolite trap and syringe.[30] CO_2 was adsorbed to the trap on the interface; and after heating of the trap, the CO_2 was transferred to a vacuum syringe using helium. A final CO_2/helium mixture of 6% was directed to the AMS ion source, at a pressure of 1 bar and a flow of 60 µL min^{-1}. A 1-MV Tandetron AMS (High Voltage Engineering Europe B.V., Amersfoort, The Netherlands)[32] was used. The lower limit of quantification (LLOQ) was 0.31 mBq mL^{-1}.

Patient characteristics

Patient characteristics (age, weight) and patient lab values (creatinine, total bilirubin, ASAT, ALAT) were described using standard statistics, and data was presented as median

(range). Microtracer and microdosing groups were compared using Mann-Whitney test, as data were not distributed normally.

Pharmacokinetic Analysis

Exploration of the data

The data was first explored by visualization of time-concentration profiles of [^{14}C] midazolam and [^{14}C]1-hydroxy-midazolam (GraphPad Prism 5). Next, their area under the curve (AUC) and the ratio AUC [^{14}C]1-hydroxy-midazolam/[^{14}C]midazolam was estimated using a log-linear non-compartmental model (Excel PKSolver add-in software[33]) and compared between microdose and microtracer administration using Mann-Whitney U test.

Nonlinear mixed effects modelling

[^{14}C]midazolam concentration–time data were analysed using the nonlinear mixed effects modelling software NONMEM version 7.4 (ICON; Globomax LLC, Ellicott, MD). Model development was in four steps: (1) selection of a structural model, (2) selection of an error model, (3) covariate analysis, and (4) internal validation of the model. For model selection, we used the objective function value (OFV) and standard goodness of fit plots. For the OFV, a drop of more than 3.84 points between nested models was considered statistically significant, which corresponds to $p<0.05$ assuming a chi-square distribution.[34,35] For the structural and error models, a decrease in OFV of 3.84 points was considered statistically significant ($P<0.05$). For the structural model, one, two and three compartment models were tested. Inclusion of log-normally distributed inter-individual variability (IIV) was tested on all model parameters. For the residual unexplained variability additive, proportional and a combination of additive and proportional error model were tested. The continuous covariates evaluated were postnatal age, postmenstrual age, bodyweight, creatinine, ALAT, ASAT, and total bilirubin. Categorical covariates included treatment arm (i.e. microdosing or microtracer administration) only. All covariates were tested on all model parameters. Potential covariates were evaluated using forward inclusion and backward elimination with a level of significance of less than 0.005 (ΔOFV< -7.9 points) and less than 0.001 (ΔOFV >10.8 points), respectively. In addition, inclusion of a covariate in the model had to result in a decline in unexplained IIV and/or improved goodness of fit plots before it was included in the final model.[36,37] Next, the model was internally validated using bootstrap analysis in Perl-speaks-NONMEM (PsN).

RESULTS

Subjects and data

Fifteen infants (gestational age 39.4 [23.9-41.4] weeks, postnatal age 11.4 [0.6-49.1 weeks]) were included in the study of which nine received a microdose and six a microtracer [^{14}C]midazolam. See Table 1 for the patient characteristics. There were no

Table 1 Characteristics of patients that participated in the study and received a microdose or microtracer [^{14}C]midazolam. Data is presented as median (range). *microdose vs microtracer group

	Total	Microdose	Microtracer	Mann Whitney U (p-value)*
Number of patients	15	9	6	-
Number of samples	67	37	30	-
Samples per patient (n)	5 (2-5)	5 (2-5)	5 (5-5)	-
Gestational age (weeks)	39.4 (23.9-41.4)	39.4 (23.9-41.4)	38.4 (26.7-41.0)	0.15
Postnatal age (weeks)	11.4 (0.6-49.1)	11.4 (0.6-49.1)	13.4 (2.6-42.3)	0.39
Weight (kg)	3.6 (2.6-8.9)	3.5 (2.7-8.9)	3.8 (2.6-6.0)	1.00
Plasma creatinine (μmol L^{-1})	35 (20-51)	41 (29-51)	33 (20-36)	0.07
Total bilirubin (μmol L^{-1})	9 (2-274)	9 (5-274)	9 (2-146)	0.46
ASAT (U L^{-1})	42 (12-93)	41 (12-93)	57 (25-85)	0.39
ALAT (U L^{-1})	17 (7-68)	15 (7-43)	23 (16-68)	0.09

Figure 2 Individual (n=9) semilog plasma concentration-time profiles of [^{14}C]midazolam and [^{14}C]1-hydroxy-midazolam after administration of a [^{14}C]midazolam microdose

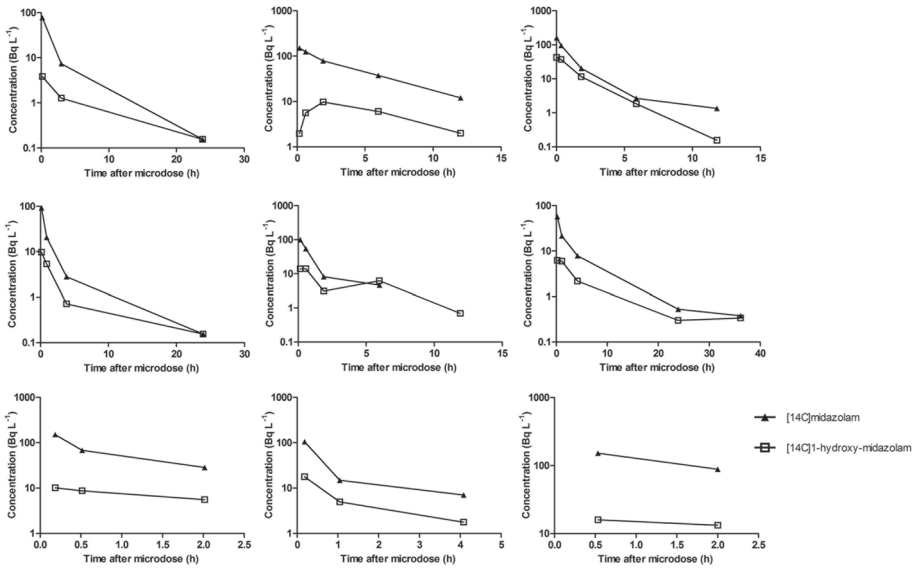

significant differences found between characteristics of the microdose and microtracer group. The complete dataset included data on 67 blood samples. Eight measurements had [^{14}C]midazolam concentrations under the AMS detection limit and were not included in the analysis.[38]

Exploration of the data

The time-concentration profiles of [^{14}C]midazolam and [^{14}C]1-hydroxy-midazolam of the individual subjects are depicted in Figure 2 and 3. In Table 2 the individual AUCs and ratio $AUC_{0\text{-}t}$ [^{14}C]1-hydroxy-midazolam/[^{14}C]midazolam of the microdose and microtracer are presented. There were no significant differences found between the two groups.

Figure 3 Individual (n=6) semilog plasma concentration-time profiles of [^{14}C]midazolam and [^{14}C]1-hydroxy-midazolam after administration of a [^{14}C]midazolam microtracer

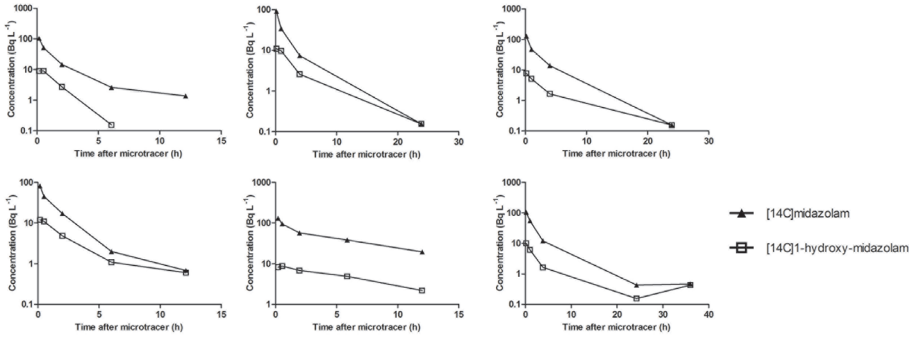

Nonlinear mixed effects modelling

A two-compartment model described the PK of [^{14}C]midazolam best. Inclusion of IIV for clearance improved the model statistically significantly. A combined error model was superior over a proportional error model or an additive error model. Bodyweight was a significant predictor for the central volume of distribution and was therefore included in the model. After inclusion of bodyweight, age and other tested covariates were not found to be statistically significant. There was a trend for a relation between bodyweight and clearance, but this did not reach statistical significance (OFV -4.38). Inclusion of the covariate 'treatment' (e.g. microtracer or microdose) upon inclusion on any of the PK parameters was found to not statistically significantly influence the model fit (OFV >0.01).

The PK parameter estimates of the final model and the bootstrap results are presented in Table 3. Most RSE values of the parameter estimates are well below 50%, suggesting that the estimates are precise. Mean bootstrap values are close to model estimates and

Table 2 Area under the curve (AUC) of [^{14}C]midazolam and [^{14}C]1-hydroxy-midazolam after administration of a microdose or microtracer [^{14}C]midazolam presented as median (range). [a]for one subject this parameter could not be established as there were only 2 plasma samples available. [b]AUC_{0-t} ratio=[^{14}C]1-hydroxy-midazolam AUC_{0-t}/[^{14}C]midazolam AUC_{0-t} *microdose vs microtracer group

	Total (n=15)	Microdose (n=9)	Microtracer (n=6)	Mann Whitney U (p-value)*
[^{14}C]midazolam				
AUC_{0-t} (ng L^{-1} *h)	46.77 (32.42 – 196.77)	46.77 (32.42 – 196.77)	48.28 (39.17 – 81.40)	0.86
AUC_{0-inf} (ng L^{-1} *h)	48.90 (34.15 – 218.80)(n=14[a])	48.90 (34.15 – 218.80)(n=8[a])	49.11 (39.75 – 82.45)	0.66
[^{14}C]1-hydroxy-midazolam				
AUC_{0-t} (ng L^{-1} *h)	10.89 (5.28 – 24.21)	10.19 (5.28 – 24.21)	11.20 (5.84 – 19.93)	0.86
AUC_{0-inf} (ng L^{-1} *h)	12.39 (5.99 – 26.41)(n=14[a])	13.14 (7.40 – 26.41)(n=8†)	12.39 (5.99 – 26.27)	0.95
[^{14}C]1-hydroxy-midazolam / [^{14}C]midazolam				
AUC_{0-t} ratio[b]	0.23 (0.11-0.51)	0.23 (0.11-0.49)	0.21 (0.13-0.51)	0.69

Table 3 Parameter estimates of the pharmacokinetic model for IV [^{14}C]midazolam.

Parameter	Estimate (RSE%)	Bootstrap median (2.5^{th} to 97.5^{th} bootstrap percentile)
Clearance		
CL ($L\ h^{-1}$)	2.06 (24)	2.23 (1.57-3.23)
Inter-compartmental clearance		
Q ($L\ h^{-1}$)	0.79 (44)	0.90 (0.60-2.45)
Volume of distribution		
$V1_i = V1_{4kg} * (WT/4)^{k1}$		
$V1_{4kg}$ (L)	3.81 (8)	3.75 (3.07-4.66)
k1	1.36 (10)	1.34 (0.68-1.68)
V2 (L)	3.19 (18)	3.30 (2.64-6.41)
Inter-individual variability		
ω^2 CL	0.73 (42)	0.62 (0.13-1.41)
Residual error		
Proportional error	0.09 (24)	0.08 (0.05-0.14)
Additional error	0.08 (50)	0.07 (0.01-0.20)

Definition of abbreviations: CL= population predicted clearance; Q= intercompartmental clearance; V1i = individual predicted volume of distribution in the central compartment for individual i; V14kg = population value for volume of distribution in the central compartment at 4 kg; WT= body weight; k1 = exponent to relate body weight to volume of distribution; V2 = volume of distribution in the peripheral compartment; ω2 = variance for the inter-individual variability of the parameter mentioned. The bootstrap was based on 50 resampled datasets.

0 is not in the 95% bootstrap interval, meaning the model is robust. Figure 4 shows the diagnostic plots for the final model and illustrates the predictive value of the model for both the microtracer and microdose group. The figure shows no bias, suggesting that concentrations for both the microdose and the microtracer are accurately predicted by this model, supporting dose-linearity of the microdose.

Figure 4 Diagnostic plots for [^{14}C]midazolam PK model, using different symbols for the different treatments. (A) Observed versus population predicted [^{14}C]midazolam concentrations. (B) Observed versus individually predicted [^{14}C]midazolam concentrations. (C) Weighted residuals versus population predicted [^{14}C]midazolam concentration. (D) Weighted residuals versus time. Solid lines represent the line of unity in A and B, and a value of 0 in C and D. Dotted line represent ±1.96 standard deviation, representing the interval in which 95% of the CWRES values are expected

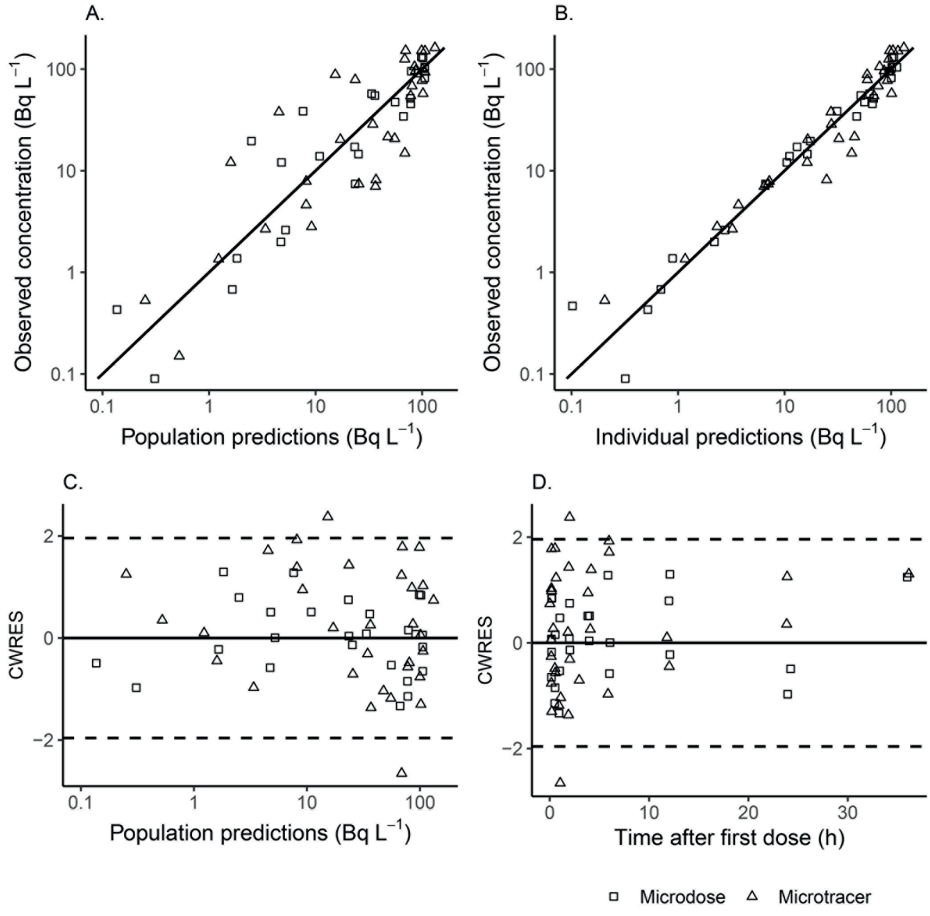

DISCUSSION

Our study shows dose-linearity of the PK of a [^{14}C]midazolam microdose to the therapeutic dose in children, by the finding that none of the PK parameters of midazolam were influenced by the treatment group, i.e. microdose or microtracer [^{14}C]midazolam. A lack of difference in AUC values for [^{14}C]midazolam and [^{14}C]1-hydroxy-midazolam further supports that there is no difference between the PK of a microtracer and microdose.

These results are in line with the findings in adults (n=6), where dose-linearity of a 100 µg [^{14}C]midazolam microdose was assessed in a cross-over design with 3 treatment regimens.[14] The subjects were administered (1) an oral microdose, (2) an IV microdose and (3) a simultaneous dose of an IV microtracer with a therapeutic nonradiolabeled oral dose. Like our results, no difference in IV disposition of midazolam was found when given as a microdose alone or in presence of a therapeutic dose in children.

Previously, studies have reported the midazolam PK in paediatrics after a single IV administration.[39-41] Clearance in our study was found to be 2.06 L h^{-1} for an infant of 4 kg (equal to 8.6 ml kg^{-1} min^{-1}). In preterm infants the clearance was reported to be lower (median 1.8 [range 0.7-6.7] ml kg^{-1} min^{-1})[39] reflecting that CYP3A activity is less mature in preterm infants than in an infant of 4 kg. A study with critically ill children reported a clearance of 1.11 L h^{-1} for an infant of 5 kg (equal to 3.7 ml kg^{-1} min^{-1})[42], which is lower than in our population. This paper concludes that inflammation (reflected by high C-reactive protein concentrations) and/or number of failing organs influenced midazolam clearance, possibly as a result of reduced CYP3A activity.[42] The lower clearance can likely be explained by the fact that this study included patients with a higher inflammation-state and/or more failing organs, as subjects in the current study were only eligible when renal- or hepatic failure was absent. This is further evidenced by two studies investigating a 0.15 mg kg^{-1} dose in healthy children, where clearance was found to be similar (3-10 year old, clearance mean±SD 9.11±1.21 ml kg^{-1} min^{-1} [41]) as or slightly higher (0.5-2 year, clearance 11.3±6.3 ml kg^{-1} min^{-1} [40]) than in our population.

Regulatory authorities have indicated that microdose studies with radioactive labelled compounds are an acceptable component of drug development.[7,43] Yet, to the best of our knowledge this approach has not been used during paediatric drug development, despite this study and previous other studies illustrating feasibility and ethical acceptance in that population.[11-13] For paracetamol the dose-linearity of an oral and IV microdose was successfully assessed in paediatrics.[12] A slightly different approach was taken to study developmental changes in oral disposition of paracetamol and metabolites when an oral microtracer of [^{14}C]paracetamol was administered together

with a therapeutic dose of IV paracetamol.[11,13] The known developmental change from mainly sulfation to glucuronidation was confirmed, and data were added on intestinal and hepatic metabolism of paracetamol in a large paediatric age range. Together with our study, these studies pave the way for microdose studies to be incorporated into paediatric drug development plans to explore PK in this vulnerable population.

This study is limited by the lack of information on the severity of disease and inflammation in these patients and by the wide age range in which extensive development in drug metabolism and transport occurs. The effect of age and disease on CYP3A activity increased the variability in PK of midazolam, possibly obscuring a difference between the PK of a microtracer and a microdose. However, we showed the age range was comparable in both treatment groups, and we assumed the disease severity was similar in the two groups. Another limitation is that the sample size is relatively small. Nevertheless, PK parameters between a microdose and a microtracer were similar and compared with literature values. Moreover, in adults low sample sizes were used to show dose-linearity of midazolam.[14]

A future perspective more specific to this particular study, is that the results indicate that a [^{14}C]midazolam microdose can be used as an alternative to a midazolam therapeutic dose to study CYP3A activity in children. In the case of taking that approach, an attempt can be made in extrapolating the results to other CYP3A-substrates and predict their disposition using a physiology based pharmacokinetic (PBPK) modelling approach. Importantly, whether this may be possible will depend on the characteristics of these substrates, as described by Calvier et al.[44] As a substantial number of clinically relevant drugs used in children are metabolized by CYP3A[16], this has the potential to impact the efficacy and safety of drug dosing in paediatrics through more informed adaptations of dosing regimens to this population.

We conclude that the PK parameters of [^{14}C]midazolam administered as a microdose did not differ significantly in infants from that of a microtracer. This supports the dose-linearity of an IV [^{14}C]midazolam microdose in children, thus a [^{14}C]midazolam microdosing approach as an alternative to a therapeutic midazolam dose can be used to study developmental changes in hepatic CYP3A activity.

REFERENCES

1. Hines RN. The ontogeny of drug metabolism enzymes and implications for adverse drug events. Pharmacol Ther 2008;118(2):250-267.
2. Kearns GL, Abdel-Rahman SM, Alander SW, Blowey DL, Leeder JS, Kauffman RE. Developmental pharmacology--drug disposition, action, and therapy in infants and children. N Engl J Med 2003;349(12):1157-1167.
3. Allegaert K, Rochette A, Veyckemans F. Developmental pharmacology of tramadol during infancy: ontogeny, pharmacogenetics and elimination clearance. Paediatr Anaesth 2011;21(3):266-273.
4. de Wildt SN, Kearns GL, Murry DJ, Koren G, van den Anker JN. Ontogeny of midazolam glucuronidation in preterm infants. Eur J Clin Pharmacol 2010;66(2):165-170.
5. de Wildt SN, Ito S, Koren G. Challenges for drug studies in children: CYP3A phenotyping as example. Drug Discov Today 2009;14(1-2):6-15.
6. Turner MA, Mooij MG, Vaes WH, et al. Pediatric microdose and microtracer studies using 14C in Europe. Clin Pharmacol Ther 2015;98(3):234-237.
7. European Medicines Agency. ICH Topic M3 (R2) Non-Clinical Safety Studies for the Conduct of Human Clinical Trials and Marketing Authorization for Pharmaceuticals. 2008.
8. Food and Drug Administration US Department of Health and Human Services Guidance for Industry Investigators and Reviewers. Exploratory IND Studies. 2006.
9. Salehpour M, Possnert G, Bryhni H. Subattomole sensitivity in biological accelerator mass spectrometry. Anal Chem 2008;80(10):3515-3521.
10. Vuong LT, Blood AB, Vogel JS, Anderson ME, Goldstein B. Applications of accelerator MS in pediatric drug evaluation. Bioanalysis 2012;4(15):1871-1882.
11. Mooij MG, van Duijn E, Knibbe CA, et al. Successful Use of [14C]Paracetamol Microdosing to Elucidate Developmental Changes in Drug Metabolism. Clin Pharmacokinet 2017.
12. Garner CR, Park KB, French NS, et al. Observational infant exploratory [(14)C]-paracetamol pharmacokinetic microdose/therapeutic dose study with accelerator mass spectrometry bioanalysis. Br J Clin Pharmacol 2015;80(1):157-167.
13. Mooij MG, van Duijn E, Knibbe CA, et al. Pediatric microdose study of [(14)C]paracetamol to study drug metabolism using accelerated mass spectrometry: proof of concept. Clin Pharmacokinet 2014;53(11):1045-1051.
14. Lappin G, Kuhnz W, Jochemsen R, et al. Use of microdosing to predict pharmacokinetics at the therapeutic dose: experience with 5 drugs. Clin Pharmacol Ther 2006;80(3):203-215.
15. Bosgra S, Vlaming ML, Vaes WH. To Apply Microdosing or Not? Recommendations to Single Out Compounds with Non-Linear Pharmacokinetics. Clin Pharmacokinet 2016;55(1):1-15.
16. Williams JA, Hyland R, Jones BC, et al. Drug-drug interactions for UDP-glucuronosyltransferase substrates: a pharmacokinetic explanation for typically observed low exposure (AUCi/AUC) ratios. Drug Metab Dispos 2004;32(11):1201-1208.
17. Stevens JC, Hines RN, Gu C, et al. Developmental expression of the major human hepatic CYP3A enzymes. J Pharmacol Exp Ther 2003;307(2):573-582.
18. de Wildt SN, Kearns GL, Leeder JS, van den Anker JN. Cytochrome P450 3A: ontogeny and drug disposition. Clin Pharmacokinet 1999;37(6):485-505.
19. Stevens JC. New perspectives on the impact of cytochrome P450 3A expression for pediatric pharmacology. Drug Discov Today 2006;11(9-10):440-445.

20. Lacroix D, Sonnier M, Moncion A, Cheron G, Cresteil T. Expression of CYP3A in the human liver--evidence that the shift between CYP3A7 and CYP3A4 occurs immediately after birth. Eur J Biochem 1997;247(2):625-634.
21. Leeder JS, Gaedigk R, Marcucci KA, et al. Variability of CYP3A7 expression in human fetal liver. J Pharmacol Exp Ther 2005;314(2):626-635.
22. Watkins PB. Noninvasive tests of CYP3A enzymes. Pharmacogenetics 1994;4(4):171-184.
23. Streetman DS, Bertino JS, Jr., Nafziger AN. Phenotyping of drug-metabolizing enzymes in adults: a review of in-vivo cytochrome P450 phenotyping probes. Pharmacogenetics 2000;10(3):187-216.
24. Chainuvati S, Nafziger AN, Leeder JS, et al. Combined phenotypic assessment of cytochrome p450 1A2, 2C9, 2C19, 2D6, and 3A, N-acetyltransferase-2, and xanthine oxidase activities with the "Cooperstown 5+1 cocktail". Clin Pharmacol Ther 2003;74(5):437-447.
25. Fuhr U, Jetter A, Kirchheiner J. Appropriate phenotyping procedures for drug metabolizing enzymes and transporters in humans and their simultaneous use in the "cocktail" approach. Clin Pharmacol Ther 2007;81(2):270-283.
26. Hohmann N, Kocheise F, Carls A, Burhenne J, Haefeli WE, Mikus G. Midazolam microdose to determine systemic and pre-systemic metabolic CYP3A activity in humans. Br J Clin Pharmacol 2015;79(2):278-285.
27. Halama B, Hohmann N, Burhenne J, Weiss J, Mikus G, Haefeli WE. A nanogram dose of the CYP3A probe substrate midazolam to evaluate drug interactions. Clin Pharmacol Ther 2013;93(6):564-571.
28. de Wildt SN, de Hoog M, Vinks AA, van der Giesen E, van den Anker JN. Population pharmacokinetics and metabolism of midazolam in pediatric intensive care patients. Crit Care Med 2003;31(7):1952-1958.
29. EMA. Guideline on the investigation of medicinal products in the term and preterm neonate. (EMA/PDCO/362462/2016).
30. van Duijn E, Sandman H, Grossouw D, Mocking JA, Coulier L, Vaes WH. Automated combustion accelerator mass spectrometry for the analysis of biomedical samples in the low attomole range. Anal Chem 2014;86(15):7635-7641.
31. Higton D, Young G, Timmerman P, Abbott R, Knutsson M, Svensson LD. European Bioanalysis Forum recommendation: scientific validation of quantification by accelerator mass spectrometry. Bioanalysis 2012;4(22):2669-2679.
32. Klein MV, Vaes WHJ, Fabriek B, Sandman H, Mous DJW, Gottdang AT. The 1 MV multi-element AMS system for biomedical applications at the Netherlands Organization for Applied Scientific Research (TNO). Nucl Instr Meth Phys Res B 2013;294:14-17.
33. Zhang Y, Huo M, Zhou J, Xie S. PKSolver: An add-in program for pharmacokinetic and pharmacodynamic data analysis in Microsoft Excel. Comput Methods Programs Biomed 2010;99(3):306-314.
34. Mould DR, Upton RN. Basic concepts in population modeling, simulation, and model-based drug development-part 2: introduction to pharmacokinetic modeling methods. CPT Pharmacometrics Syst Pharmacol 2013;2:e38.
35. Mould DR, Upton RN. Basic concepts in population modeling, simulation, and model-based drug development. CPT Pharmacometrics Syst Pharmacol 2012;1:e6.
36. Ince I, Knibbe CA, Danhof M, de Wildt SN. Developmental changes in the expression and function of cytochrome P450 3A isoforms: evidence from in vitro and in vivo investigations. Clin Pharmacokinet 2013;52(5):333-345.

37. Krekels EH, Johnson TN, den Hoedt SM, et al. From Pediatric Covariate Model to Semiphysiological Function for Maturation: Part II-Sensitivity to Physiological and Physicochemical Properties. CPT Pharmacometrics Syst Pharmacol 2012;1:e10.
38. Ahn JE, Karlsson MO, Dunne A, Ludden TM. Likelihood based approaches to handling data below the quantification limit using NONMEM VI. J Pharmacokinet Pharmacodyn 2008;35(4):401-421.
39. de Wildt SN, Kearns GL, Hop WC, Murry DJ, Abdel-Rahman SM, van den Anker JN. Pharmacokinetics and metabolism of intravenous midazolam in preterm infants. Clin Pharmacol Ther 2001;70(6):525-531.
40. Reed MD, Rodarte A, Blumer JL, et al. The single-dose pharmacokinetics of midazolam and its primary metabolite in pediatric patients after oral and intravenous administration. J Clin Pharmacol 2001;41(12):1359-1369.
41. Payne K, Mattheyse FJ, Liebenberg D, Dawes T. The pharmacokinetics of midazolam in paediatric patients. Eur J Clin Pharmacol 1989;37(3):267-272.
42. Vet NJ, Brussee JM, de Hoog M, et al. Inflammation and organ failure severely affect midazolam clearance in critically ill children. Am J Respir Crit Care Med 2016;194(1):58-66.
43. Roth-Cline M, Nelson RM. Microdosing Studies in Children: A US Regulatory Perspective. Clin Pharmacol Ther 2015;98(3):232-233.
44. Calvier EAM, Krekels EHJ, Yu H, et al. Drugs Being Eliminated via the Same Pathway Will Not Always Require Similar Pediatric Dose Adjustments. CPT Pharmacometrics Syst Pharmacol 2018;7(3):175-185.

8 The oral bioavailability and metabolism of midazolam in stable critically ill children: a pharmacokinetic microtracing study

Bianca D van Groen, Elke HJ Krekels, Miriam G Mooij, Esther van Duijn, Wouter HJ Vaes, Albert D Windhorst, Joost van Rosmalen, Stan JF Hartman, N Harry Hendrikse, Birgit CP Koch, Karel Allegaert, Dick Tibboel, Catherijne AJ Knibbe, Saskia N de Wildt

Submitted

ABSTRACT

Midazolam is metabolized by the developmentally regulated intestinal and hepatic drug metabolizing enzyme cytochrome P450 (CYP) 3A4/5. It is frequently administered orally to children, yet knowledge is lacking on the oral bioavailability in term neonates up until 1 year of age. Furthermore, the dispositions of the major metabolites 1-OH-midazolam (OHM) and 1-OH-midazolam-glucuronide (OHMG) after oral administration are largely unknown for the entire pediatric age span. We aimed to fill these knowledge gaps with a pediatric [^{14}C]midazolam microtracer population pharmacokinetic study. Forty-six stable, critically ill children (median age 9.8 [range 0.3 – 276.4] weeks) received a single oral [^{14}C]midazolam microtracer (58 [40-67] Bq/kg) when they received a therapeutic continuous intravenous midazolam infusion and had an arterial line in place enabling blood sampling. For midazolam, in a one-compartment model, bodyweight was a significant predictor for clearance (0.98 L/h) and volume of distribution (8.7L) (values for a typical individual of 5 kg). The typical oral bioavailability in the population was 66% (range 25%-85%). The exposures of OHM and OHMG were highest for the youngest age groups and significantly decreased with postnatal age. The oral bioavailability of midazolam, largely reflective of intestinal and hepatic CYP3A activity, was on average lower than the reported 49-92% for preterm neonates, and higher than the reported 21% for children >1 year of age and 30% for adults. As midazolam oral bioavailability varied widely, systemic exposure of other CYP3A-substrate drugs after oral dosing in this population may also be unpredictable, with risk of therapy failure or toxicity.

INTRODUCTION

Midazolam is a short-acting benzodiazepine that is widely used in pediatric hospital practice for various indications, including the induction of anesthesia by oral administration.[1, 2] When an orally administered drug is subject to intestinal and/or hepatic drug metabolism, variation in its metabolism is an important determinant of bioavailability and systemic clearance of that drug.

Oral bioavailability is defined as the fraction of the administered oral dose reaching the systemic circulation unchanged and importantly depends on the absorption and first-pass metabolism by both intestinal and hepatic drug metabolizing enzymes. Cytochrome P450 (CYP) 3A is a drug metabolizing enzyme family, abundant in both the liver and the gut, which contributes to the first-pass metabolism of many orally administered drugs.[3] CYP3A consists of the three main isoforms CYP3A4, -3A5 and -3A7, for which the substrate specificity differs.[3, 4] *In vitro* studies have shown that the CYP3A7 abundance in the liver declines rapidly after birth and that the abundance CYP3A4 in the liver and in the gut increases with increasing age.[5-7] CYP3A5 is polymorphically expressed, with a stable expression from fetus to adult. This developmental pattern of CYP3A4 expression seen in *in vitro* studies is supported by pharmacokinetic (PK) data of CYP3A substrate drugs. The benzodiazepine midazolam is a well-validated CYP3A probe with substrate specificity for CYP3A4/5 and almost none for CYP3A7.[8, 9] In preterm infants (gestational age 26-31 weeks and postnatal age 3-13 days), oral midazolam clearance was markedly lower (0.16 L/h/kg vs 3.0 L/h/kg) and oral bioavailability higher (49-92% vs 21%) than in children beyond 1 year of age.[10-12] These findings suggest developmentally lower intestinal and/or hepatic CYP3A activity in preterm neonates. Midazolam is one of the many CYP3A4/5 substrates frequently administered to children.[3] Hence, this developmental pattern in CYP3A4/5 mediated systemic and pre-systemic metabolism may imply that safe and effective systemic exposure of oral doses of not only midazolam, but also other CYP3A4/5 substrates, may not be reached.

The oral bioavailability of midazolam has been previously studied across the pediatric age span.[10-14] However, there is a distinct knowledge gap for the age group from birth (term born) throughout infancy, i.e. <1-year-old. The classical study design to obtain data on oral bioavailability entails a cross-over study in which an oral and IV dose of a drug are administered alternately, with a wash-out period in between. This design is ethically and practically challenging as children are exposed twice to therapeutic drug doses with extensive blood sampling.

An interesting approach to study oral bioavailability is by a [^{14}C]labelled microtracer, which has been shown practically and ethically feasible to study developmental changes in PK in children.[15-17] A microtracer is defined as '<1/100th of the dose needed to reach the no observed adverse effect level (NOAEL) or <100 µg', concurrently administered with a therapeutic dose.[18, 19] The [^{14}C]label allows quantification of extremely low plasma concentrations by accelerator mass spectrometry (AMS) in only 10-15 µl plasma.[20, 21] A microtracer of an oral [^{14}C]labelled drug is administered simultaneously with therapeutic IV doses of the same unlabeled drug, allowing measuring both the oral and IV disposition in one subject at the same time and, with that, accurately quantifying the absolute oral bioavailability [15, 16], overcoming the limitations of a traditional cross-over design.

Besides the oral bioavailability of midazolam, the systemic exposure to the major metabolites 1-OH-midazolam (OHM) and 1-OH-midazolam-glucuronide (OHMG) after oral dosing is also of interest, since both metabolites are pharmacologically active, although to a lesser extent than midazolam.[22] Also, a better understanding of age-related variation in metabolite disposition provides further insight in developmental pharmacology. OHM is the primary metabolite formed by CYP3A, which is further glucuronidated to OHMG by UDP-glucuronosyltransferase (UGT) 2B4, -2B7 and, to a lesser extent, -1A4.[23, 24] A high systemic exposure to OHMG may result in therapeutic effects of this metabolite despite its lower potency.[25] A report of five critically ill adults with severe renal failure showed accumulation of OHMG after continuous IV infusion of midazolam.[25] This accumulation led to prolonged sedation (assessed by Ramsey score and electroencephalographic [EEG] evaluation) that could be reversed by the use of flumazenil, which is a competitive benzodiazepine antagonist. This finding highlights the importance of knowledge on disposition of the metabolites of midazolam. The metabolism and disposition of midazolam and the primary metabolite OHM after oral dosing have been described in preterm neonates and older children[10, 13, 14, 26, 27], but gaps remain for term neonates to children <2 years old. Most importantly, to the best of our knowledge, data on systemic exposure of OHMG in adults and children after oral dosing are not available.

Given these considerations, we have designed and conducted an oral [^{14}C]midazolam microtracer population PK study in stable, critically ill children from 0-6 years old with the aim to answer two questions: (1) what is the oral bioavailability of midazolam; and (2) what is the systemic exposure to midazolam and its major metabolites OHM and OHMG after oral dosing in this population.

MATERIAL AND METHODS

Setting

This multicenter study was carried out in the level III pediatric intensive care unit (PICU) of the Erasmus MC–Sophia Children's Hospital, Rotterdam, the Netherlands (October 2015-March 2018) and the Radboudumc-Amalia Children's Hospital, Nijmegen, the Netherlands (May 2017-March 2018). The study was approved by the Dutch Central Committee on Research Involving Human Subjects (EudraCT 2014-003269-46). Parental written informed consent was obtained. The radiation exposure of a single microtracer was explained to the parents and legal guardians by a comparison with the yearly mean background exposure of 2.6 mSv in the Netherlands in 2013.[28] The Dutch Nuclear Research and Service Group estimated the radiation exposure for a single microtracer <1 μSv was well below the minimal risk category 1 of the International Commission of Radiological Protection, where a maximum exposure of 100 μSv is allowed. Category 1 risk studies are considered minimal risk and ethically justified in humans when they provide new scientific knowledge.[29]

Population

Children were eligible to participate in the study when aged from birth (post menstrual age >36 weeks) up to 6 years of age, had medical need for sedation with continuous IV midazolam, and had an indwelling arterial or central venous line in place enabling blood sampling. To minimize inter-individual variability due to critical illness or organ failure, exclusion criteria were death anticipated in 48 hours, extra corporeal membrane oxygenation (ECMO) treatment, circulatory failure (defined by the administration of >1 vasopressor drug, or increase of the dose of a vasopressor drug in the last 6 hours), kidney failure (according to the pediatric Risk, Injury, Failure, Loss, End stage renal disease (pRIFLE) criteria 'failure', i.e. estimated creatinine clearance decreased by 75% or an urine output of <0.3 ml/kg/h for 24h or anuria for 12 hours), liver failure (defined by aspartate-aminotransferase [ASAT] or alanine-aminotransferase [ALAT] >2 times the upper limit for age), gastrointestinal disorders, or concomitant administration of co-medication known to interact with midazolam (according to the Flockhart Table™[30]).

Study design

A single [^{14}C]midazolam (20.3 [14.1-23.6] ng/kg; 58 [40-67] Bq/kg; 0.25 ml/kg) dose was administered as an oral microtracer via the enteral feeding tube to ensure delivery in the gastrointestinal tract, followed by either 1-2 mL of saline or food to ensure rinsing of the tube. The IV therapeutic midazolam dose was prescribed by the treating physician for clinical purposes and was adjusted on the guidance of validated sedation scores and according to a standardized sedation titration protocol. According to this

protocol, midazolam bolus doses varied between 0.05-0.2 mg/kg and the continuous infusion rate between 0.05-0.3 mg/kg/h. Blood samples were taken pre-microtracer administration and around 0.5h, 1h, 2h, 4h, 6h, 12h, and 24h after administration of the [^{14}C]midazolam microtracer to ensure that the PK of the oral absorption phase was captured. The maximum number of blood samples for the study was limited to 8 per subject and the maximum amount of blood could not exceed the guidelines by EMA (up to 1% of calculated circulating blood volume).[31] The blood samples were centrifuged and plasma was stored at -80^{o}C until analysis.

Midazolam

Midazolam for therapeutic infusion was manufactured and compounded by the Pharmacy A15 (Gorinchem, NL) under Good Manufacturing Practice (GMP) conditions. [^{14}C]midazolam was synthesized by Selcia Ltd, United Kingdom at a specific activity of 1033 MBq/mmol (equal to 2.85 MBq/mg). The chemical name is 8-chloro-6-(2-fluorophenyl)-1-methyl-^{4}H-[1-^{14}C]imidazo[l,5-a][l,4]benzodiazepine hydrochloride and it was brought in ethanol solution (96%). In the department of Radiology and Nuclear Medicine at the VU University Medical Center (Amsterdam, NL), the solution was further diluted to the required concentration with sodium chloride 0.9% solution (Fresenius Kabi, Zeist, NL) under GMP conditions. The final [^{14}C]midazolam concentration was 210-270 Bq/mL with 1 Bq=0.31 ng [^{14}C]midazolam.

Measurements

[^{14}C]midazolam, [^{14}C]OHM and [^{14}C]OHMG plasma concentration quantification

Plasma sample extraction and Ultra Performance Liquid Chromatography Separation

The Ultra Performance Liquid Chromatography (UPLC) and Accelerator Mass Spectrometry (AMS) (see 3.5.1.2) qualifications were performed in accordance with the recommendation of the European Bioanalytical Forum.[32] Methanol (200 µL, containing unlabeled midazolam, OHM and OHMG) was added to 15 µL plasma samples in order to precipitate proteins and to extract the test substance using protein precipitation plates (Phenomenex). Each run consisted of samples and eight calibrator levels (180, 60, 20, 10, 5, 2.5, 1.25 and 0.625 Bq/L) in duplicate, plus three different QC levels (135, 7.5 and 0.625 Bq/L) in duplicate to quantify midazolam, OHM and OHMG. 30 µL extract was evaporated to dryness, re-dissolved in 30 µl 1 mM ammonium formate in water + 5% AcN and 25 µL was injected on the UPLC. The fractions where midazolam, OHM and OHMG eluted from the column were collected for each sample, transferred to a tin foil cup, evaporated to dryness and analyzed using Combustion-CO_2-AMS. Each series was accompanied by 2 calibrations lines at eight levels, and QCs in triplicate at three levels. Accuracy and precision complied with the EBF criteria of 20% of 2/3 of the QCs.

Accelerator Mass Spectrometry analysis

[^{14}C]levels were quantified as described before.[16, 33] The tin foil cups (see 5.5.1.1) were combusted on an elemental analyser (Vario Micro; Elementar, Langenselbold, Germany). Generated CO_2 was transferred to an in-house developed gas interface, composed of a zeolite trap and syringe.[33] CO_2 was adsorbed to the trap on the interface; after heating of the trap, the CO_2 was transferred to a vacuum syringe using helium. A final CO_2/helium mixture of 6% was directed to the AMS ion source, at a pressure of 1 bar and a flow of 60 µL min^{-1}. A 1-MV Tandetron AMS (High Voltage Engineering Europe B.V., Amersfoort, the Netherlands)[34] was used. The lower limit of quantification (LLOQ) of the LC-AMS was 0.31 Bq/L and the upper limit was 200 Bq/L.

Therapeutic midazolam plasma concentration quantification by liquid chromatography–tandem mass spectroscopy

Midazolam and the major metabolites were quantified by means of a liquid chromatography–tandem mass spectroscopy (LC-MS/MS) with electrospray ionization in the positive ionization mode (Waters) validated according to Food and Drug Administration (FDA) guidance.[35] The LLOQ for midazolam was 2 µg/L, for OHM 3 µg/L and for OHMG 10 µg/L. The upper limit of quantification for midazolam was 2400 µg/L, for OHM 2300 µg/L and for OHMG 3000 µg/L. The internal standard is midazolam-d4. During analysis 3 standards (covering the whole range of linearity) and 4 quality controls are used from different manufacturers, to obtain objectivity. 100 µl sample is used. After sample preparation (e.g. adding internal standard), the supernatant (3 µL) is injected in the system. The runtime is 7.6 minutes per sample.

Data collection

We collected data on the doses of therapeutic midazolam and [^{14}C]midazolam and the respective timings of administration and blood sampling. Patient characteristics and relevant clinical and laboratory measurements were prospectively recorded.

Pharmacokinetic analysis

Population pharmacokinetics to assess the oral bioavailability

The oral bioavailability of a drug was quantified by means of a population PK analysis. All [^{14}C]midazolam and midazolam concentration–time data were analyzed simultaneously using nonlinear mixed effects modeling with NONMEM version 7.4 (ICON; Globomax LLC, Ellicott, MD) after log transformation of the concentration data. [^{14}C]midazolam concentrations under the AMS detection limit (<LLOQ) were discarded.[36] Pirana 2.9.7, R (version 3.4.1), and R-studio (version 1.0.153) were used to visualize the data. Model development was in four steps (see Methods S1 for detailed information): (1) selection of a structural model, (2) selection of an error model, (3) covariate analysis, and (4)

internal validation of the model. The absorption rate constant (ka) for midazolam was fixed at 4.16 h^{-1}, which yields peak concentrations to be reached round 30 min, which is in agreement with the observed tmax in our data and with values reported for children in previous literature.[13]

Non-compartmental analysis to assess the systemic exposure to midazolam and its major metabolites after oral dosing

To calculate the systemic exposure of midazolam and its major metabolites, the concentration-time areas under the curve after oral dosing were determined with non-compartmental analyses. The [^{14}C]midazolam and metabolite concentrations were measured in Bq/L. Values were converted from Bq to ng based on molecular weights ($9.6*10^{-4}$ mol/Bq), where [^{14}C]midazolam was 325.8 g/mol (0.31 ng/Bq), [^{14}C]OHM 341.8 g/mol (0.33 ng/Bq) and [^{14}C]OHMG 517.9 g/mol (0.50 ng/Bq). The AUC from time zero to the last sampling time point ($AUC_{0-tlast}$) was calculated using the log-linear trapezoidal method; the AUC from time zero to infinite time (AUC_{0-inf}) was calculated by extrapolation beyond the last observation.[37] If $AUC_{tlast-inf}$ was larger than 20% of the actual $AUC_{0-tlast}$, then the AUC_{0-inf} was excluded from the analysis, as it would limit the accuracy of the results and hence would introduce unreliable estimation of the AUC_{0-inf}. The first sample below the LLOQ was set on 0.155 Bq/L (0.5 * LLOQ), and any following samples <LLOQ were discarded.

The ratios $AUC_{0-tlast}$ [^{14}C]OHM/[^{14}C]midazolam (OHM/M) and ratio $AUC_{0-tlast}$ [^{14}C]OHM/[^{14}C]OHMG (OHM/OHMG) were calculated with AUC_{0-last} in Bq/L/h and therefore correction of molecular weight was not necessary. All PK parameters derived from individual patients were estimated using the Excel PKsolver add-in software.[37]

The relationships between AUC and AUC ratios and postnatal age were described with Nonparametric Spearman's rank correlation. All statistical tests were two-sided and a significance level of p=0.05 was used.

RESULTS

Population

Between October 2015 and March 2018, ninety-six of 454 screened patients were eligible to participate, and informed consent was obtained from parents of 46 of these children (median gestational age at birth of 39.0 [29.4 – 43.0] weeks and a median postnatal age of 9.8 weeks [2 days – 5.3 years]) (see Figure 1). Three-quarters were 0-6 months old. Table 1 provides the characteristics of these 46 children.

Figure 1 Flowchart of patient recruitment

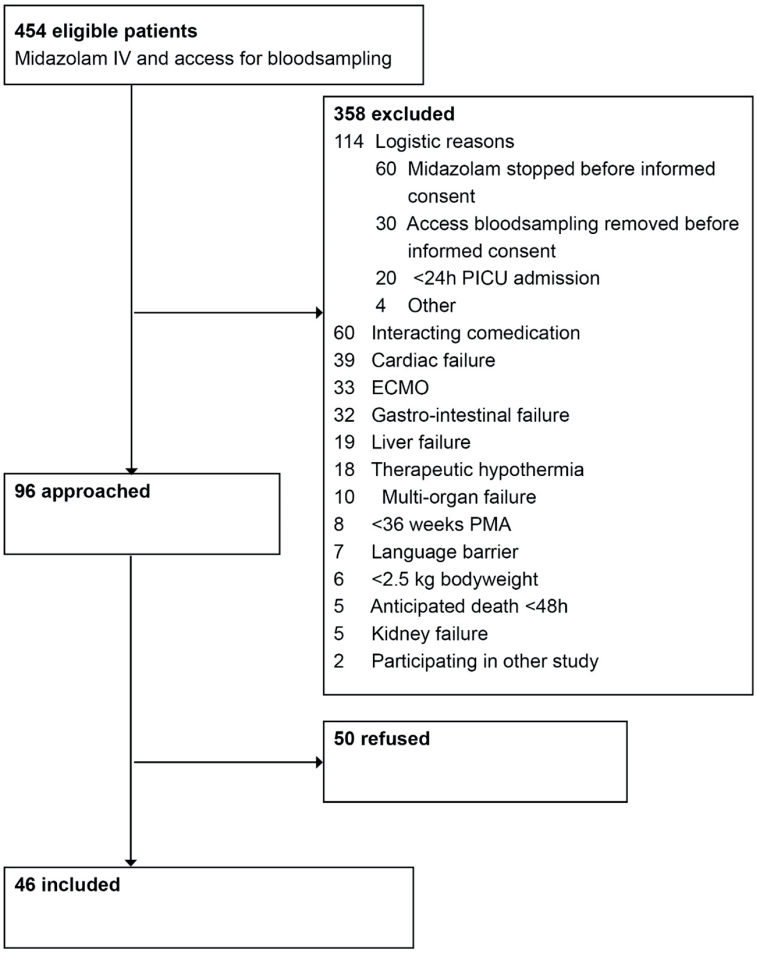

Data of three of these 46 children were excluded from further analysis. In one, extubated shortly after receiving the [^{14}C]midazolam microtracer, no [^{14}C]midazolam concentration could be detected in the plasma samples. The undetectable concentrations can be explained by clinical practice, because immediately before extubation the child's stomach is completely emptied to avoid aspiration. The two others had, in hindsight, received interacting co-medication that induced CYP3A.

Oral bioavailability

In the final population PK model, the typical oral bioavailability in the population was 66% with a high IIV of 0.86; individual bioavailability estimates ranged from 25% to 85%. See Figure 2 for the variability in individual bioavailability. All PK parameter estimates of this model are presented in Table 2.

Table 1 Characteristics of patients included in the analysis presented as median (range) or number

Patient characteristics		
Number of patients (n)	46	
Location (n Erasmus MC/n Radboudumc)	39/7	
Postnatal age (weeks)	9.8 (0.3 – 276.4)	
Postmenstrual age (weeks)	48.9 (38.9 – 316.4)	
Weight (kg)	4.7 (2.8 – 18.0)	
Z-score weight for age*	-0.9 (-3.0 – 2.5)	
Gender (M/F)	29/17	
Ethnicity (Caucasian/other)	41/5	
Reason for admission (n)	Respiratory failure	
	• Pneumonia/bronchiolitis	18
	• Congenital cardiac abnormality	7
	• Pulmonary hypertension	2
	• Traumatic injury to the airways	2
	• Lobar emphysema	2
	• Meconium aspiration	1
	Post cardiac surgery	12
	Status epilepticus	2
Disease severity scores		
PELOD	11 (0-21)	
Number of organs failing on study day	1 (0 – 2)	
PRISM	16 (3 – 32)	
PIM	-2.5 (-4.8 – -0.4)	
Laboratory values at day of administration [^{14}C]midazolam		
Plasma creatinine (μmol/L)	29 (11 – 63)	
ASAT (U/L)	42 (16 – 155)	
ALAT (U/L)	18 (6 – 138)	
CRP (mg/L)	43 (2 – 298)	
Study medication		
Dose [^{14}C]midazolam (Bq)	282.7 (165.0 – 1080.0)	
Dose [^{14}C]midazolam (ng)	87.6 (51.15 – 334.8)	

*PELOD=Pediatric Logistic Organ Dysfunction; PRISM=Pediatric Risk of Mortality; PIM=Pediatric Index of Mortality; ASAT= aspartate-aminotransferase; ALAT=alanine-aminotransferase; CRP=C-reactive protein; *As determined by TNO growth curves*

For this model, a total of 30 [^{14}C]midazolam concentrations under the AMS detection limit (<LLOQ) were discarded.[36] The complete dataset included 326 and 245 radiolabeled and cold midazolam concentrations, respectively, from 43 patients. The final model entails a one-compartment model that best described the PK of oral and IV midazolam. Inclusion of IIV for clearance, volume of distribution, and oral bioavailability improved the model

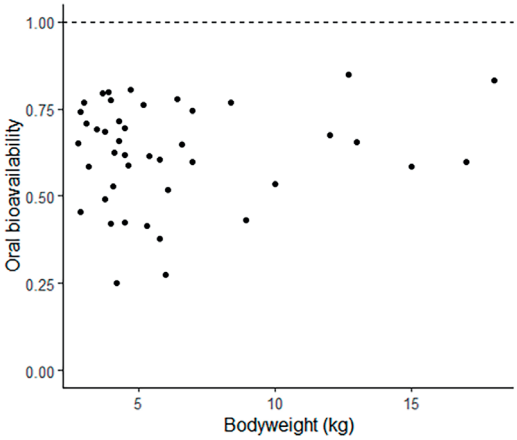

Figure 2 Oral bioavailability of midazolam and its variability versus bodyweight. Bodyweight did not explain the variability in oral bioavailability.

statistically significantly. Bodyweight was the most significant predictor for clearance (ΔOFV -11.11) and volume of distribution (ΔOFV -15.95) in exponential relationships (see Table 2). After this inclusion, both the variance of the IIV for clearance and volume of distribution decreased. Age and other tested covariates were found not statistically significant after inclusion of bodyweight.

All relative standard error (RSE) values of the parameter estimates were below 50%, indicating that the estimates could be obtained from the data with good precision. The diagnostic plots for the final model are presented in Figure S1 (oral data) and in Figure S2 (IV data). Both figures indicate that the model describes the obtained data accurately, upon both oral and IV administration, even though for the oral data more random variability is observed. The robustness of the estimated model parameters was evaluated in a bootstrap analysis. The bootstrap analysis confirmed the precision of parameter estimates of the final model, as the parameter estimates were very similar to the bootstrap medians and within the 95% confidence interval (Table 2). The distribution of the NPDEs indicates that the model can adequately predict both the median trend and the variability in the observed concentrations. This is further supported by the absence of visible trends in NPDE versus time and NPDE versus predictions (see Figure S3 and S4).

Systemic exposure to midazolam and its major metabolites after oral dosing

The systemic exposures, as reflected by the AUCs of midazolam and its major metabolites after administration of the oral [^{14}C]midazolam microtracer are presented in Table 3. The complete dataset included data on 335 plasma samples from 43 patients. A total of 21 (6%), 41 (12%), and 14 (4%) samples were set on 0.5*LLOQ for respectively [^{14}C] midazolam, [^{14}C]OHM and [^{14}C]OHMG. A total of 9 (3%), 93 (28%), and 2 (0.6%) samples were discarded for respectively [^{14}C]midazolam, [^{14}C]OHM and [^{14}C]OHMG. Eight (19%),

Table 2 Parameter estimates of a one-compartmental model.

Parameter	Model parameters estimates (RSE%)	Bootstrap median (2.5th to 97.5th bootstrap percentile
Oral bioavailability		
	$F_i = e^{log(TVF/(1-TVF))} /(1+ e^{log (TVF/(1-TVF))})$	
TVF	0.66 (8%)	0.66 (0.56-0.78)
Absorption rate constant		
ka (h^{-1})	4.16 FIXED	-
Clearance		
	$CL_i = CL_{5kg} * (WT/5)^{k1}$	
CL_{5kg} (L/h)	0.98 (13%)	0.99 (0.78-1.28)
k1	0.92 (31%)	0.93 (0.44-1.59)
Volume of distribution		
	$V_i = V_{5kg} * (WT/5)^{k2}$	
V_{5kg} (L)	8.70 (11%)	8.68 (6.94-10.78)
k2	1.16 (21%)	1.17 (0.79-1.85)
Inter-individual variability		
ω^2 CL	0.65 (19%)	0.61 (0.39-0.87)
ω^2 V	0.40 (24%)	0.37 (0.18-0.58)
ω^2 TVF	0.86 (49%)	0.78 (0.17-1.78)
Residual error		
Additive error oral [^{14}C]midazolam data	0.08 (29%)	0.07 (0.04-0.13)
Additive error IV midazolam data	0.47 (30%)	0.47 (0.25-0.77)

ω^2 = variance for the inter-individual variability of the indicated parameter; CL = clearance; CL_i = predicted clearance of individual i; CL_{5kg} = population-predicted clearance for a subject with a median weight of 5 kg; CV= coefficient of variation; F = absolute oral bioavailability; F_i = predicted absolute oral bioavailability of individual i; k1 = exponent to relate body weight to clearance; k2 = exponent to relate body weight to volume of distribution; RSE = relative standard error; TVF = population parameter in the logit equation for oral bioavailability; V = volume of distribution; V_i = individual predicted volume of distribution for individual i; V_{5kg} = population-predicted volume for a subject with a median weight of 5 kg; WT= body weight

Table 3 Area under the curves of midazolam and its major metabolites 1-OH-midazolam and 1-OH-midazolam-glucuronide and their ratios after administration of an oral [^{14}C]midazolam microtracer (20.3 [14.1-23.6] ng/kg; 58 [40-67] Bq/kg)

		Midazolam	OHM	OHMG
$AUC_{0\text{-}tlast}$	Bq/L/h	162.6 (10.4-898.4) (n=43)	12.0 (1.1-77.0) (n=38)	254.4 (62.6-821.6) (n=43)
	ng/L/h	50.4 (3.2-278.5) (n=43)	4.0 (0.4-25.4) (n=38)	127.2 (31.3-410.8) (n=43)
$AUC_{0\text{-}inf}$	Bq/L/h	160.9 (10.6-753.3) (n=32)	17.9 (3.0-81.7) (n=29)	272.2 (71.6-921.8) (n=22)
	ng/L/h	49.9 (3.3-233.5) (n=32)	5.9 (1.0-27.0) (n=29)	136.1 (35.8-460.9) (n=22)
$AUC_{0\text{-}tlast}$ ratio OHM/M			0.1 (<0.1-1.5) (n=38)	
$AUC_{0\text{-}tlast}$ ratio OHM/OHMG			0.05 (<0.01 – 0.20) (n=38)	

Data is presented as median (range). n= number of patients. M=midazolam, OHM=1-OH-midazolam, OHMG=1-OH-midazolam-glucuronide, AUC=Area Under the Curve. See 4.3 for explanation on the patient numbers.

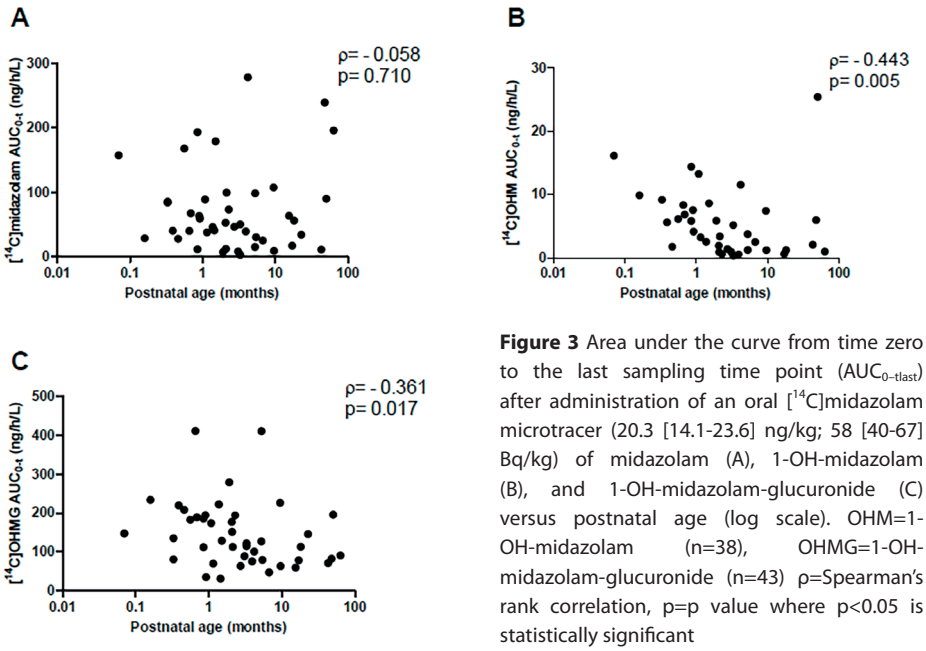

Figure 3 Area under the curve from time zero to the last sampling time point ($AUC_{0-tlast}$) after administration of an oral [^{14}C]midazolam microtracer (20.3 [14.1-23.6] ng/kg; 58 [40-67] Bq/kg) of midazolam (A), 1-OH-midazolam (B), and 1-OH-midazolam-glucuronide (C) versus postnatal age (log scale). OHM=1-OH-midazolam (n=38), OHMG=1-OH-midazolam-glucuronide (n=43) ρ=Spearman's rank correlation, p=p value where p<0.05 is statistically significant

9 (21%), and 21 (49%) patients were excluded from AUC_{0-inf} analyses of respectively [^{14}C]midazolam, [^{14}C]OHM and [^{14}C]OHMG as the $AUC_{tlast-inf}$ was larger than 20% of the actual $AUC_{0-tlast}$. For another 3 patients (7%) the AUC_{0-inf} of [^{14}C]midazolam could not be calculated. For 2 patients, only one plasma sample taken after the absorption phase was available due to loss of the arterial catheter, and in one patient the plasma concentration-time profile had no apparent log-linear slope, for which no explanation was found. For 5 patients (12%) the $AUC_{0-tlast}$ and AUC_{0-inf} of OHM could not be calculated as most plasma concentrations were <LLOQ.

Figure 3 shows the $AUC_{0-tlast}$ of [^{14}C]midazolam, [^{14}C]OHM, and [^{14}C]OHMG versus postnatal age after administration of the oral [^{14}C]midazolam microtracer. The AUC of [^{14}C]OHM and [^{14}C]OHMG were the highest for the youngest age groups, even though the AUC of [^{14}C]midazolam was similar across age. Analysis of the data revealed a statistically significant negative correlation for both [^{14}C]OHM $AUC_{0-tlast}$ and AUC_{0-inf} and [^{14}C]OHMG $AUC_{0-tlast}$ and AUC_{0-inf} with postnatal age (see Figure 3B and C for $AUC_{0-tlast}$, results for AUC_{0-inf} not shown). No significant relationship was identified between postnatal age and [^{14}C]midazolam $AUC_{0-tlast}$ (see Figure 3), [^{14}C]midazolam AUC_{0-inf}, OHM/M AUC ratio, and OHM/OHMG ratio (data not shown).

DISCUSSION

To study the oral bioavailability of midazolam and the systemic exposure to midazolam and its major metabolites in children, we designed a prospective oral [^{14}C]midazolam microtracer population PK study in children receiving midazolam for clinical purposes. Our main observations were that (1) the median oral bioavailability of midazolam was 66% and varied greatly with a range of 25-85% and (2) the systemic exposure (AUC) of the major metabolites 1-OHM formed by CYP3A and 1-OHMG formed out of 1-OHM by UGT2B4, -2B7 and -1A4 were highest for the youngest age ranges, despite weight normalized midazolam doses.

Our study design has previously been applied to investigate the oral bioavailability of paracetamol and the systemic exposure to its metabolites in children[15, 17] and has now shown to be successful for midazolam. The informed consent rate of 50% was in agreement with the consent rate of other non-therapeutic studies in pediatric intensive care. Moreover, our population PK model results were in agreement with reported values on oral PK parameters for midazolam, confirming the feasibility of the [^{14}C] midazolam microtracer approach. The median CL of 0.20 L/h/kg in our study was in line with literature values of 0.26 L/h/kg in children 0-18 year in the IC.[38] Our median V of 1.7 L/kg lies in the range of 0.2-3.5 L/kg as found in critically ill children with an age between 8 days and 16 years.[39]

More specifically, for the oral bioavailability in our patients, of whom three-quarters were 0-6 months old, the median of 66% is lower than the reported median value of 92% (range 67 to 95%) in 37 preterm neonates with a gestational age of 26-34 weeks[11] and higher than the reported median value of 21% (range 2 to 78%) in 264 older children of 1-18 years.[12] Also the reported mean ±SD of 28±7% in adults is lower than in our population.[40] These latter findings can be explained by the expected CYP3A ontogeny, as older children and adults are thought to have a higher CYP3A activity in both the gut wall and liver, resulting in a lower oral bioavailability[3] than found in our patients, and *vice versa* for preterm neonates. Statistically significant covariate relationships that could explain part of the inter-individual variability in oral bioavailability were not found. However, a highly variable oral bioavailability was also found in previous pediatric PK studies[10-12], particularly in preterm neonates[10, 11], and we can conclude it is independent of the microtracer-design. The higher variability in oral bioavailability in our study may be due to the nature of the studied population: stable, critically ill patients instead of healthier patients. A previous study from *Vet et al.* found a significant impact of organ failure on midazolam clearance [38], with the greatest impact on midazolam clearance in the presence of ≥3 failing organs and inflammation as reflected by CRP.[38] We were

not able to identify these covariates in our data, likely because children with severe circulatory, kidney or liver failure were excluded, and the number of failing organs in our study ranged from 0 to 3 per child. CRP values in our study were comparable to those in the previous study from *Vet et al.;* i.e., (median [range] 43 [2 – 298] vs 32 [0.3–385] mg/L, resp.). However, we only included 6 patients with a CRP > 100 mg/L, whereas the previously reported cohort consisted of more patients with CRP > 100 mg/L.

The variability in oral bioavailability as observed in our study leads to unpredictable systemic exposure to midazolam, and potentially also other CYP3A-substrates, after oral dosing in (critically ill) children. These children may be at risk of subtherapeutic or toxic exposure after oral dosing of other CYP3A-substrates.

In addition, the systemic exposures of the main metabolites OHM and OHMG were highest in the youngest age ranges at similar exposure of midazolam across age. This observation can most likely not be attributed solely to CYP3A ontogeny, but to other developmental changes as well, as the exposure of each metabolite is dependent on various factors. First, the CYP3A activity drives the formation of 1-OHM. Second, the reported age-related changes in UGTs may increase the glucuronidation of 1-OHM over age.[41] The age-related decrease in AUC of 1-OHMG can be partly explained by the fact that the OHMG metabolite is excreted renally and considering that children's renal function increases over age[42-44] This explanation is supported by a reported postconceptional age-related increase in urinary excretion of OHMG in preterm neonates.[45] A metabolic shift, as seen for paracetamol where a switch from mainly sulphation to glucuronidation is seen in the first of years life is less likely. As in the case of midazolam this would mean decreased formation of another metabolite than 1-OHMG in the younger age group compared to older children than adults. But as no other major metabolite for midazolam, in addition the minor metabolites 4-OHM(G) and MG have been identified in adults, this seems unlikely.[46, 47] Third, the distribution volume of the metabolites may change with age, impacting the total systemic exposure of the metabolites.[48] Considering the case-reports on the association between OHMG accumulation and prolonged sedation[25], clinicians should be aware that the systemic exposure to OHMG may be higher in neonates than in older children, potentially also contributing to its sedative effect.

The following limitations of the study need to be addressed. First, our innovative study design limits the inclusion of pharmacodynamic (PD) data as the extremely low dose of the microtracer midazolam is not expected to have pharmacological effects. Hence, we can speculate that the variability in oral availability of midazolam and the higher systemic exposure to OHMG may lead to subtherapeutic or toxic exposure. The real impact of this variability on pharmacodynamics parameters should be assessed in future studies.

Second, data of 21 patients were excluded from $AUC_{0\text{-}inf}$ analyses of OHMG because the elimination of this metabolite was not complete after 24h. In retrospect, longer sampling time would have benefited this analysis. Third, the absorption of midazolam may be influenced by food intake as food in the gastrointestinal tract may alter the gastrointestinal physiology, including the motility patterns, intestinal transit time, and the local blood flow.[49] However, information on food was not collected and the study was not powered to detect an effect of food on midazolam absorption but may have contributed to the variability in our data. Also, dose linearity of the PK of an oral microdose to those of a therapeutic dose of midazolam has been established in adults.[50-52] We made the assumption that this also accounts for children, further supported by dose-linearity of IV midazolam in children[53], but not been formally established.

This study presents some future opportunities. Recently, a framework was published for between-drug extrapolation of covariate models[54] which was used by *Brussee et al* to study whether scaling with a pediatric covariate function from midazolam will lead to accurate clearance values of other CYP3A-substrates.[55] Clearances of drugs were accurately scaled when they were mainly eliminated by CYP3A-mediated metabolism with, for example, high protein binding to albumine (> 90%) and a low-to-intermediate extraction ratio of < 0.55 in adults. However, the covariate relationship for clearance was based on data from children >1 year of age. As our population consists of infants mainly <1 years of age, our data now present a unique opportunity to test the proposed framework for this younger age group. Also, this study design is promising for drugs under development. When there is interest to, besides an IV administration, study the drug as an oral administration, an oral [^{14}C] labelled microtracer can be added without setting up a new pediatric cohort, or *vice versa*. Lastly, a microdose pediatric study can be used to obtain information on the PK for drugs with high toxicity, like oncology agents, and clear PK/PD relationship followed by the determination of an effective dose based on the PK profile.

In conclusion, the results of this population PK study added data on oral bioavailability of midazolam as a marker for CYP3A in an age range where data was missing. It shows that children may be at an increased risk of subtherapeutic or toxic exposure of midazolam and potentially also of other CYP3A-substrates when dosed orally. The study design with an oral [^{14}C]microtracer was shown successful for safely studying the oral bioavailability of midazolam in children. To ultimately improve the safety and efficacy of pediatric drug therapy, we recommend to consider study designs with microdoses for minimal risk PK studies and [^{14}C]microtracer studies to elucidate oral bioavailability.

REFERENCES

1. Notterman, D.A. Sedation with intravenous midazolam in the pediatric intensive care unit. Clin Pediatr (Phila) 1997;36(8):449-54.
2. Liacouras, C.A., Mascarenhas, M., Poon, C. & Wenner, W.J. Placebo-controlled trial assessing the use of oral midazolam as a premedication to conscious sedation for pediatric endoscopy. Gastrointest Endosc 1998;47(6):455-60.
3. de Wildt, S.N., Kearns, G.L., Leeder, J.S. & van den Anker, J.N. Cytochrome P450 3A: ontogeny and drug disposition. Clin Pharmacokinet 1999;37(6):485-505.
4. Williams, J.A. et al. Comparative metabolic capabilities of CYP3A4, CYP3A5, and CYP3A7. Drug Metab Dispos 2002;30(8):883-91.
5. Stevens, J.C. et al. Developmental expression of the major human hepatic CYP3A enzymes. J Pharmacol Exp Ther 2003;307(2):573-82.
6. Fakhoury, M. et al. Localization and mRNA expression of CYP3A and P-glycoprotein in human duodenum as a function of age. Drug Metab Dispos 2005;33(11):1603-7.
7. Johnson, T.N., Tanner, M.S., Taylor, C.J. & Tucker, G.T. Enterocytic CYP3A4 in a paediatric population: developmental changes and the effect of coeliac disease and cystic fibrosis. Br J Clin Pharmacol 2001;51(5):451-60.
8. Streetman, D.S., Bertino, J.S., Jr. & Nafziger, A.N. Phenotyping of drug-metabolizing enzymes in adults: a review of in-vivo cytochrome P450 phenotyping probes. Pharmacogenetics 2000;10(3):187-216.
9. de Wildt, S.N., Ito, S. & Koren, G. Challenges for drug studies in children: CYP3A phenotyping as example. Drug Discov Today 2009;14(1-2):6-15.
10. de Wildt, S.N., Kearns, G.L., Hop, W.C., Murry, D.J., Abdel-Rahman, S.M. & van den Anker, J.N. Pharmacokinetics and metabolism of oral midazolam in preterm infants. Br J Clin Pharmacol 2002;53(4):390-2.
11. Brussee, J.M. et al. First-Pass CYP3A-Mediated Metabolism of Midazolam in the Gut Wall and Liver in Preterm Neonates. CPT Pharmacometrics Syst Pharmacol 2018;7(6):374-83.
12. Brussee, J.M. et al. Characterization of Intestinal and Hepatic CYP3A-Mediated Metabolism of Midazolam in Children Using a Physiological Population Pharmacokinetic Modelling Approach. Pharm Res 2018;35(9):182.
13. Reed, M.D. et al. The single-dose pharmacokinetics of midazolam and its primary metabolite in pediatric patients after oral and intravenous administration. J Clin Pharmacol 2001;41(12):1359-69.
14. Payne, K., Mattheyse, F.J., Liebenberg, D. & Dawes, T. The pharmacokinetics of midazolam in paediatric patients. Eur J Clin Pharmacol 1989;37(3):267-72.
15. Mooij, M.G. et al. Successful Use of [14C]Paracetamol Microdosing to Elucidate Developmental Changes in Drug Metabolism. Clin Pharmacokinet 2017;DOI: 10.1007/s40262-017-0508-6
16. Mooij, M.G. et al. Pediatric microdose study of [(14)C]paracetamol to study drug metabolism using accelerated mass spectrometry: proof of concept. Clin Pharmacokinet 2014;53(11):1045-51.
17. Kleiber, N. et al. Enteral Acetaminophen Bioavailability in Pediatric Intensive Care Patients Determined With an Oral Microtracer and Pharmacokinetic Modeling to Optimize Dosing. Crit Care Med 2019;DOI: 10.1097/CCM.0000000000004032
18. European Medicines Agency. ICH Topic M3 (R2) Non-Clinical Safety Studies for the Conduct of Human Clinical Trials and Marketing Authorization for Pharmaceuticals. 2008;

19. Food and Drug Administration US Department of Health and Human Services Guidance for Industry Investigators and Reviewers. Exploratory IND Studies. 2006;
20. Salehpour, M., Possnert, G. & Bryhni, H. Subattomole sensitivity in biological accelerator mass spectrometry. Anal Chem 2008;80(10):3515-21.
21. Vuong, L.T., Blood, A.B., Vogel, J.S., Anderson, M.E. & Goldstein, B. Applications of accelerator MS in pediatric drug evaluation. Bioanalysis 2012;4(15):1871-82.
22. Tuk, B., van Oostenbruggen, M.F., Herben, V.M., Mandema, J.W. & Danhof, M. Characterization of the pharmacodynamic interaction between parent drug and active metabolite in vivo: midazolam and alpha-OH-midazolam. J Pharmacol Exp Ther 1999;289(2):1067-74.
23. Heizmann, P. & Ziegler, W.H. Excretion and metabolism of 14C-midazolam in humans following oral dosing. Arzneimittelforschung 1981;31(12a):2220-3.
24. Seo, K.A., Bae, S.K., Choi, Y.K., Choi, C.S., Liu, K.H. & Shin, J.G. Metabolism of 1′- and 4-hydroxymidazolam by glucuronide conjugation is largely mediated by UDP-glucuronosyltransferases 1A4, 2B4, and 2B7. Drug Metab Dispos 2010;38(11):2007-13.
25. Bauer, T.M. et al. Prolonged sedation due to accumulation of conjugated metabolites of midazolam. Lancet 1995;346(8968):145-7.
26. Johnson, T.N., Rostami-Hodjegan, A., Goddard, J.M., Tanner, M.S. & Tucker, G.T. Contribution of midazolam and its 1-hydroxy metabolite to preoperative sedation in children: a pharmacokinetic-pharmacodynamic analysis. Br J Anaesth 2002;89(3):428-37.
27. Salman, S. et al. A novel, palatable paediatric oral formulation of midazolam: pharmacokinetics, tolerability, efficacy and safety. Anaesthesia 2018;73(12):1469-77.
28. RIVM. Stralingsbelasting in Nederland. https://www.rivm.nl/stralingsbelasting-in-nederland (2013). Accessed 10 April, 2019.
29. International Commission on Radiological Protection. 1990 Recommendations of the International Commission on Radiological Protection. Ann ICRP 1991;21(1-3):1-201.
30. Indiana University. Drug Interactions Flockhart Table. https://drug-interactions.medicine.iu.edu/Main-Table.aspx. Accessed 10 April, 2019.
31. EMA. Guideline on the investigation of medicinal products in the term and preterm neonate. (EMA/PDCO/362462/2016).
32. Higton, D., Young, G., Timmerman, P., Abbott, R., Knutsson, M. & Svensson, L.D. European Bioanalysis Forum recommendation: scientific validation of quantification by accelerator mass spectrometry. Bioanalysis 2012;4(22):2669-79.
33. van Duijn, E., Sandman, H., Grossouw, D., Mocking, J.A., Coulier, L. & Vaes, W.H. Automated combustion accelerator mass spectrometry for the analysis of biomedical samples in the low attomole range. Anal Chem 2014;86(15):7635-41.
34. Klein, M.V., Vaes, W.H.J., Fabriek, B., Sandman, H., Mous, D.J.W. & Gottdang, A.T. The 1 MV multi-element AMS system for biomedical applications at the Netherlands Organization for Applied Scientific Research (TNO). Nucl Instr Meth Phys Res B 2013;294(14-7.
35. Food and Drug Administration. Guidance for Industry: Bioanalytical Methods Validation. . 2001;
36. Ahn, J.E., Karlsson, M.O., Dunne, A. & Ludden, T.M. Likelihood based approaches to handling data below the quantification limit using NONMEM VI. J Pharmacokinet Pharmacodyn 2008;35(4):401-21.
37. Zhang, Y., Huo, M., Zhou, J. & Xie, S. PKSolver: An add-in program for pharmacokinetic and pharmacodynamic data analysis in Microsoft Excel. Comput Methods Programs Biomed 2010;99(3):306-14.

38. Vet, N.J. et al. Inflammation and organ failure severely affect midazolam clearance in critically ill children. Am J Respir Crit Care Med 2016;194(1):58-66.
39. Nahara, M.C., McMorrow, J., Jones, P.R., Anglin, D. & Rosenberg, R. Pharmacokinetics of midazolam in critically ill pediatric patients. Eur J Drug Metab Pharmacokinet 2000;25(3-4):219-21.
40. Brill, M.J. et al. Midazolam pharmacokinetics in morbidly obese patients following semi-simultaneous oral and intravenous administration: a comparison with healthy volunteers. Clin Pharmacokinet 2014;53(10):931-41.
41. Rowland, A., Miners, J.O. & Mackenzie, P.I. The UDP-glucuronosyltransferases: their role in drug metabolism and detoxification. Int J Biochem Cell Biol 2013;45(6):1121-32.
42. Rhodin, M.M. et al. Human renal function maturation: a quantitative description using weight and postmenstrual age. Pediatr Nephrol 2009;24(1):67-76.
43. Faa, G. et al. Morphogenesis and molecular mechanisms involved in human kidney development. J Cell Physiol 2012;227(3):1257-68.
44. Heizmann, P., Eckert, M. & Ziegler, W.H. Pharmacokinetics and bioavailability of midazolam in man. Br J Clin Pharmacol 1983;16 Suppl 1(43S-9S.
45. de Wildt, S.N., Kearns, G.L., Murry, D.J., Koren, G. & van den Anker, J.N. Ontogeny of midazolam glucuronidation in preterm infants. Eur J Clin Pharmacol 2010;66(2):165-70.
46. Klieber, S. et al. Contribution of the N-glucuronidation pathway to the overall in vitro metabolic clearance of midazolam in humans. Drug Metab Dispos 2008;36(5):851-62.
47. Hyland, R. et al. In vitro and in vivo glucuronidation of midazolam in humans. Br J Clin Pharmacol 2009;67(4):445-54.
48. Kearns, G.L., Abdel-Rahman, S.M., Alander, S.W., Blowey, D.L., Leeder, J.S. & Kauffman, R.E. Developmental pharmacology--drug disposition, action, and therapy in infants and children. N Engl J Med 2003;349(12):1157-67.
49. Abuhelwa, A.Y., Williams, D.B., Upton, R.N. & Foster, D.J. Food, gastrointestinal pH, and models of oral drug absorption. Eur J Pharm Biopharm 2017;112(234-48.
50. Lappin, G. et al. Use of microdosing to predict pharmacokinetics at the therapeutic dose: experience with 5 drugs. Clin Pharmacol Ther 2006;80(3):203-15.
51. Hohmann, N., Kocheise, F., Carls, A., Burhenne, J., Haefeli, W.E. & Mikus, G. Midazolam microdose to determine systemic and pre-systemic metabolic CYP3A activity in humans. Br J Clin Pharmacol 2015;79(2):278-85.
52. Halama, B., Hohmann, N., Burhenne, J., Weiss, J., Mikus, G. & Haefeli, W.E. A nanogram dose of the CYP3A probe substrate midazolam to evaluate drug interactions. Clin Pharmacol Ther 2013;93(6):564-71.
53. van Groen, B.D. et al. Dose-linearity of the pharmacokinetics of an intravenous [(14) C]midazolam microdose in children. Br J Clin Pharmacol 2019;10.1111/bcp.14047
54. Calvier, E.A.M. et al. Drugs Being Eliminated via the Same Pathway Will Not Always Require Similar Pediatric Dose Adjustments. CPT Pharmacometrics Syst Pharmacol 2018;7(3):175-85.
55. Brussee, J.M. et al. A Pediatric Covariate Function for CYP3A-Mediated Midazolam Clearance Can Scale Clearance of Selected CYP3A Substrates in Children. AAPS J 2019;21(5):81.
56. Mould, D.R. & Upton, R.N. Basic concepts in population modeling, simulation, and model-based drug development. CPT Pharmacometrics Syst Pharmacol 2012;1(e6.
57. Ince, I., Knibbe, C.A., Danhof, M. & de Wildt, S.N. Developmental changes in the expression and function of cytochrome P450 3A isoforms: evidence from in vitro and in vivo investigations. Clin Pharmacokinet 2013;52(5):333-45.

58. Krekels, E.H. et al. From Pediatric Covariate Model to Semiphysiological Function for Maturation: Part II-Sensitivity to Physiological and Physicochemical Properties. CPT Pharmacometrics Syst Pharmacol 2012;1(e10.
59. Comets, E., Brendel, K. & Mentre, F. Computing normalised prediction distribution errors to evaluate nonlinear mixed-effect models: the npde add-on package for R. Comput Methods Programs Biomed 2008;90(2):154-66.

SUPPLEMENTARY INFORMATION

Methods S1 Population pharmacokinetic model development to assess the oral bioavailability

Model selection

For model selection, we used the objective function value (OFV) and standard goodness of fit (GOF) plots. For the OFV, a drop of more than 3.84 points between nested models was considered statistically significant, which corresponds to $p<0.05$ assuming a chi-square distribution.[56] For the structural model, one, two, and three compartment models were tested. For the error model an additive error model in the log-domain was used. Inclusion of log-normally distributed inter-individual variability (IIV) was tested on all model parameters. For bioavailability, a logit transformation with a normal distribution for inter-individual variability was used to avoid individual bioavailability estimates outside the 0%-100% range. The absorption rate constant (ka) for midazolam was fixed at 4.16 h^{-1}, which yields peak concentrations to be reached round 30 min, which is in agreement with the observed tmax in our data and with values reported for children in previous literature.[13]

Covariate analysis

The correlation with PK parameters was evaluated for the following continuous covariates: postnatal age, postmenstrual age, bodyweight, creatinine, urea, alanine aminotransferase (ALAT), aspartate aminotransferase (ASAT), alkaline phosphatase (AF), Gamma-glutamyltransferase (γ-GT), C-reactive protein (CRP), leukocytes count, Pediatric Risk of Mortality (PRISM) score, and Pediatric Index of Mortality (PIM) score. Categorical covariates included gender, Pediatric Logistic Organ Dysfunction (PELOD) score, and organ failure as determined by the PELOD score.

Potential covariates were evaluated using forward inclusion and backward elimination with cut-off values of $p<0.005$ (OFV -7.9 points) and $p<0.001$ (OFV -10.8 points), respectively. In addition, for a covariate to be retained in the model, its inclusion had to result in a decline in unexplained variability and/or improved goodness of fit plots.[57, 58]

Model evaluation

The model was internally validated using a bootstrap analysis in Perl-speaks-NONMEM (PsN), for which five hundred datasets were resampled with replacement from the original datasets and refitted to the model. The obtained parameter values from these 500 model fits were summarized as median values and 95% confidence intervals, which were compared to the values obtained in the original model fit.

Normalized prediction distribution errors (NPDE) were calculated with the NPDE package in R.[59] For this method, the data set used for model development was simulated a thousand times with inclusion of inter-individual and residual variability. The distribution of obtained NPDE values in the overall dataset as well as the distribution of NPDE values versus time and predicted concentrations was assessed. The analysis was stratified for oral administration and for IV administration.

Figure S1 Goodness-of-fit plots of the oral [^{14}C]midazolam data for the final model. A. Log-value of observed plasma concentrations vs. log-value of population predicted concentrations. B. Log observed plasma concentrations vs. log individual predicted concentrations. C. Conditional weighted residuals (CWRES) versus log population predictions. D. CWRES versus time after dosing.

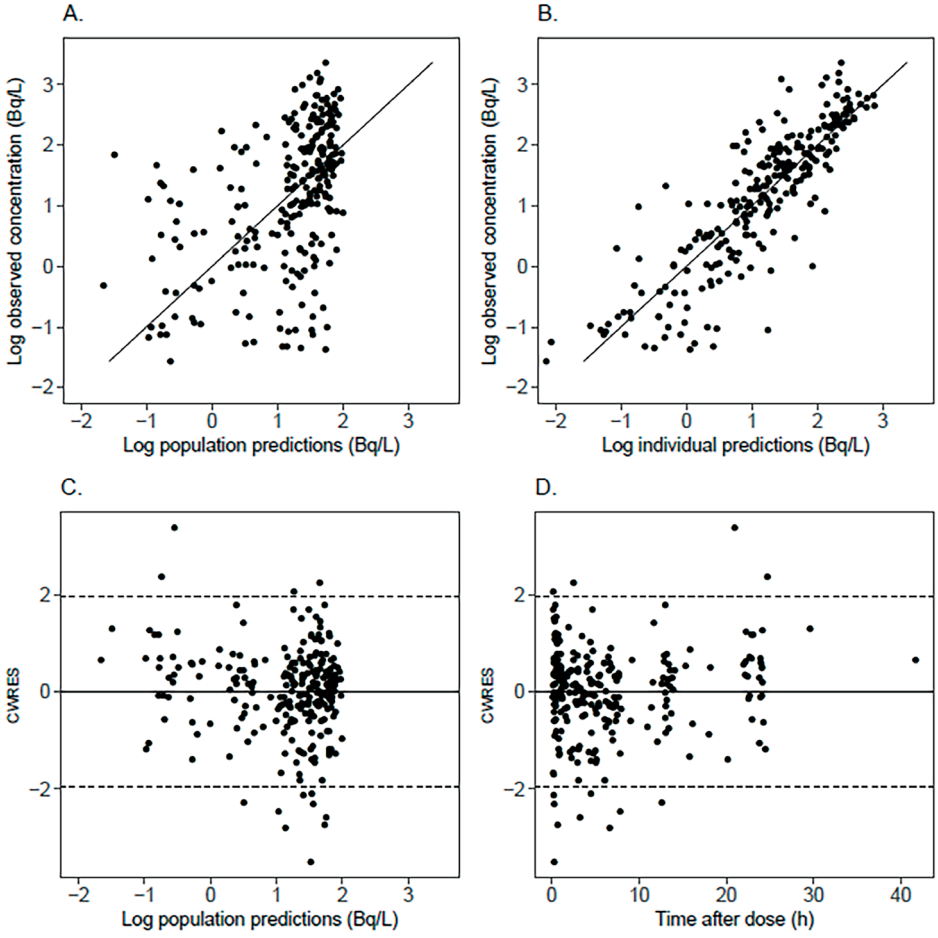

Figure S2 Goodness-of-fit plots of the intravenous midazolam data for the final model. A. Log observed plasma concentrations vs. log population predicted concentrations. B. Log observed plasma concentrations vs. log individual predicted concentrations. C. Conditional weighted residuals (CWRES) versus log population predictions. D. CWRES versus time after first dose.

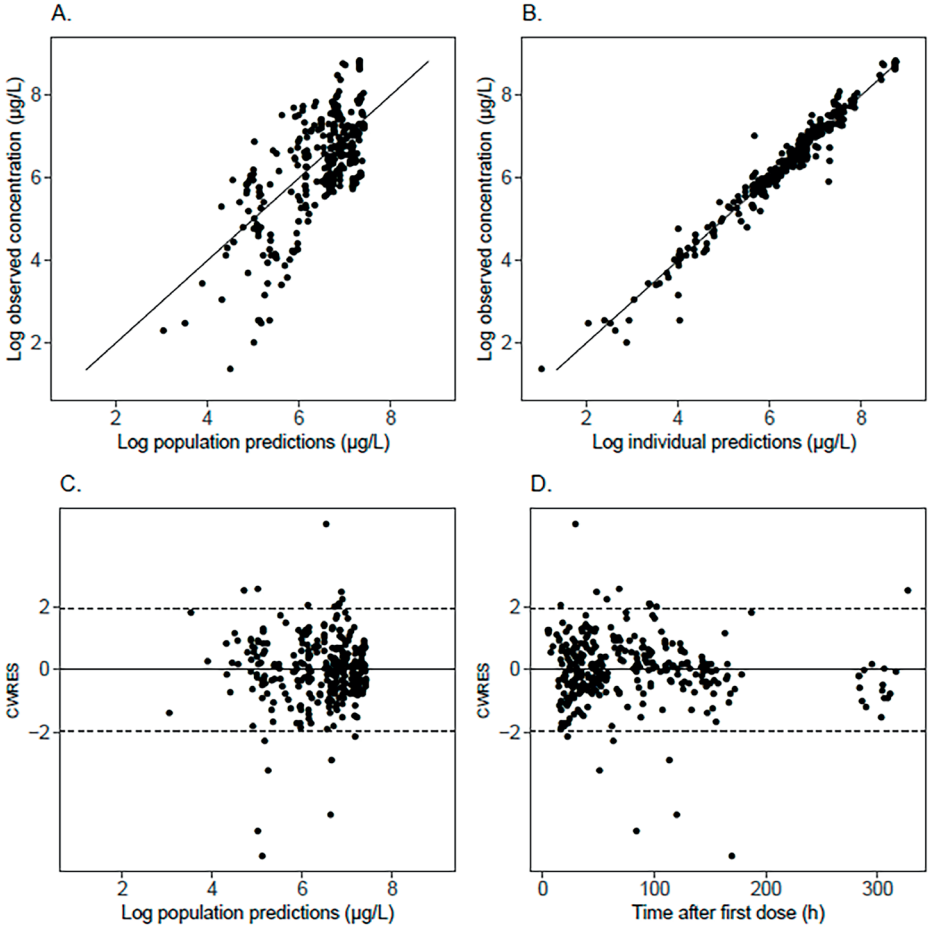

Figure S3 Normalized prediction distribution error (NPDE) of the final model for oral [^{14}C]midazolam. A. Quantile-quantile plot of NPDE versus the expected standard normal distribution. B. The histogram of NPDE with the observed frequency of sample quantiles of the NPDE (white bars), overlaid with the density of the standard normal distribution (grey bars). C. NPDE versus time, with the NPDE for each observation (dots) and the lines indicating the mean (light grey middle line) and the 90% percentiles (light grey upper and lower line) of the NPDE, and the shaded areas are the simulated 90% confidence intervals of the NPDE median (light grey middle box) and 95% percentiles (light grey upper and lower box). D. NPDE versus predicted concentration, with dots and lines as described for C.

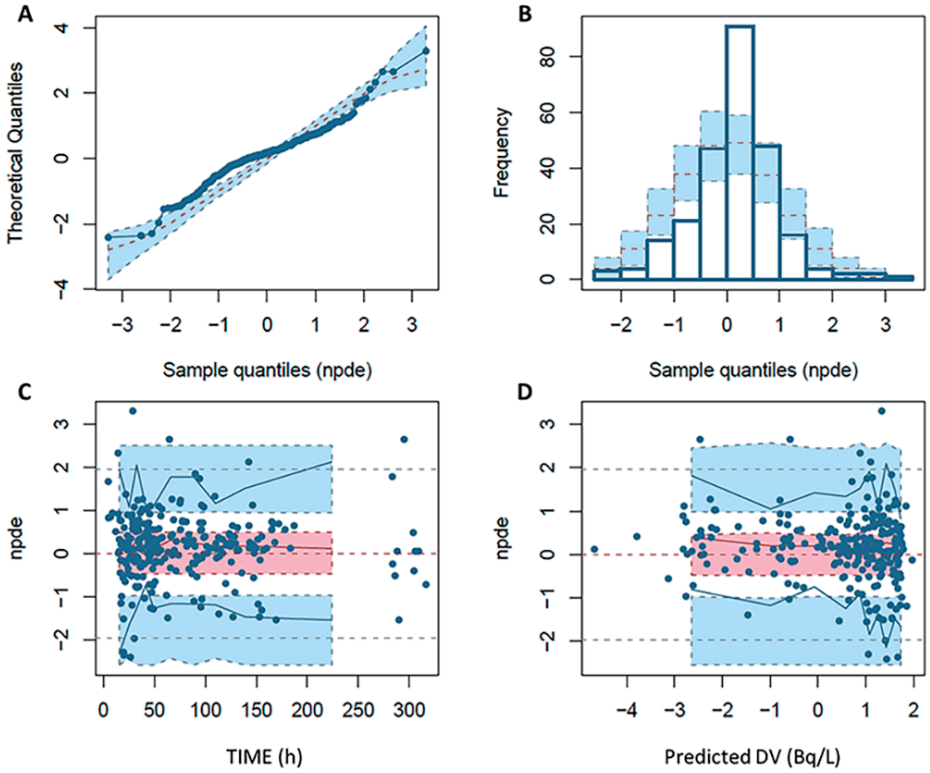

Figure S4 Normalized prediction distribution error (NPDE) of the final model for intravenous midazolam. A. Quantile-quantile plot of NPDE versus the expected standard normal distribution. B. The histogram of NPDE with the observed frequency of sample quantiles of the NPDE (white bars), overlaid with the density of the standard normal distribution (grey bars). C. NPDE versus time, with the NPDE for each observation (dots), and the lines indicate the mean (light grey middle line) and the 90% percentiles (light grey upper and lower line) of the NPDE, and the shaded areas are the simulates 90% confidence intervals of the NPDE median (light grey middle box) and 95% percentiles (light grey upper and lower box). D. NPDE versus predicted concentration, with dots and lines as described for C.

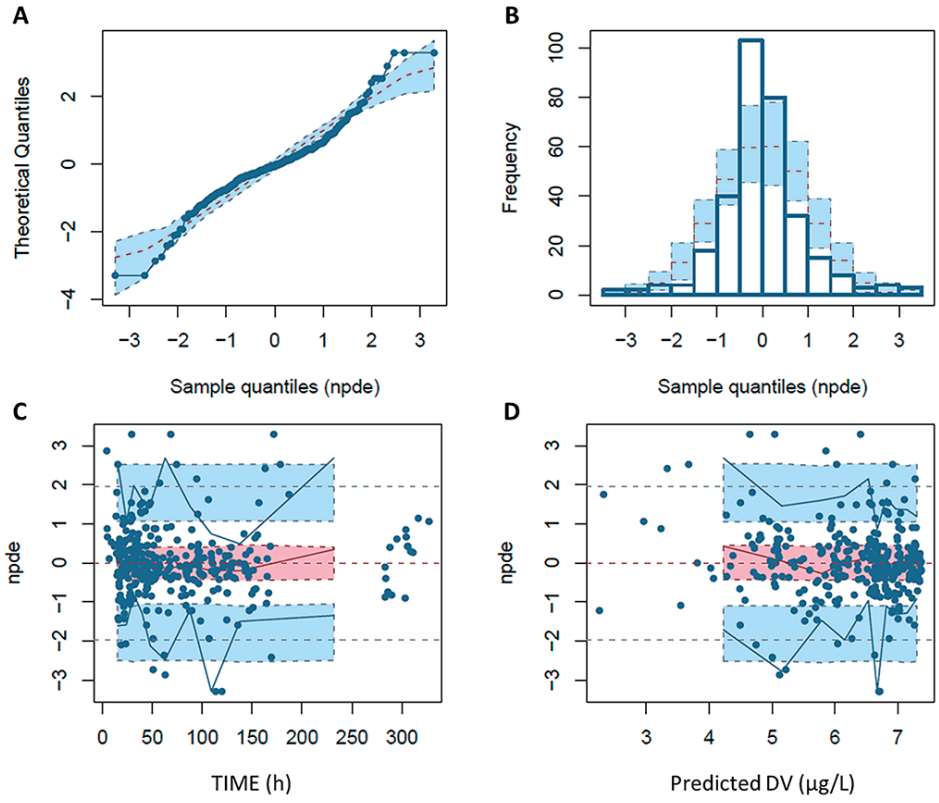

9 Proof of concept: first pediatric metabolite in safety testing (MIST) study using an oral [^{14}C] midazolam microtracer

Bianca D van Groen, Esther van Duijn, Arjan de Vries, Miriam G. Mooij, Dick Tibboel, Wouter HJ Vaes*, Saskia N de Wildt*

**Contributed equally to this work*

Submitted

ABSTRACT

Introduction: Growth and development affect drug metabolizing enzyme activity thus could alter the metabolic profile of a drug. Traditional metabolite in safety testing (MIST) studies are used to create metabolite profiles and study the routes of excretion but are unethical in children due to the high radioactive burden. To overcome this challenge, we aimed to show the feasibility of a MIST study using a [^{14}C]midazolam microtracer as proof of concept in children.

Methods: Twelve stable, critically ill children received an oral [^{14}C]midazolam microtracer (20 ng/kg; 60 Bq/kg) while receiving intravenous therapeutic midazolam. Blood was sampled up to 24h after dosing. A Hamilton-pool per patient was prepared reflecting the mean area under the curve (AUC_{0-t}) plasma level, and subsequently one pool for each age group (0-1 months, 1-6 months, 0.5-2 years and 2-6 years). Plasma extracts were injected on a UPLC and the effluent was split into a fraction collector for [^{14}C]level quantification by AMS (off-line), and to a Q-Exactive hrMS (in-line) for metabolite identification. Urine and feces (n=4) were collected up to 72h and [^{14}C]levels were quantified by AMS.

Results: The approach resulted in sufficient sensitivity to quantify individual metabolites in chromatograms. [^{14}C]1-OH-midazolam-glucuronide was most abundant in all but one age group, followed by unchanged [^{14}C]midazolam and [^{14}C]1-OH-midazolam. The small proportion of unspecified metabolites <10% of the total drug related exposure most probably includes [^{14}C]midazolam-glucuronide and [^{14}C]4-OH-midazolam. Excretion was mainly in urine; the total recovery in urine and feces was 77-94%.

Conclusion: This first pediatric MIST pilot study makes clear that using a [^{14}C]midazolam microtracer is feasible and safe to generate metabolite profiles and study recovery in children. This approach is promising for first-in-child studies to delineate age-related variation in drug metabolite profiles, while fewer juvenile animal studies are needed.

INTRODUCTION

Drug development consists of several stages, including establishing the absorption, distribution, metabolism and excretion (ADME), as well as the efficacy and safety of the drug. Importantly, metabolites of the parent drug may also contribute to efficacy and safety.[1] A general approach to study these aspects is by performing a mass balance and metabolite in safety testing (MIST) study to obtain information on the routes and extent of excretion and to create metabolite profiles.

In 2008, the U.S. Food and Drug Administration recommended that regarding the non-clinical safety of drug metabolites the exposure threshold for further metabolite characterization for an individual metabolite must be >10% of the estimated *parent-drug* exposure. In 2009, the International Conference on Harmonisation (ICH) M3 guideline (R2) altered this threshold significantly to >10% of the estimated *total-drug* exposure, which was included in the FDA guideline in 2016.[2,3]

The disposition of a drug is driven by processes such as drug metabolism, drug transport, glomerular filtration and body composition. These processes are subject to age-related changes reflecting growth and maturation along the pediatric continuum.[4,5] Most drug metabolizing enzymes and drug transporters act differently in neonates than in older children or adults, and the maturational patterns are isoform-dependent.[4,6-10] Children's metabolism may not only be slower or faster than that of adults but may also use different compensatory pathways. The resulting metabolite profiles could contain metabolites that have not yet been identified or are ≤10% of the total drug exposure in adults, yet are present, disproportionately present or even represent >10% of the total drug exposure in children. This mechanism is most obvious for paracetamol, whose metabolism switches from mainly sulfation to glucuronidation from birth to 12 years of age.[11] Glucuronidation is underdeveloped in newborns; hence, sulfation is used as a compensatory pathway. In newborns, the exposure to paracetamol-sulfate is higher than that to paracetamol-glucuronide, whereas in adults this is the other way around. Similarly, the metabolite pattern of sirolimus differs between children and adults. Studies have found that di-demethylated and hydroxy-desmethyl metabolites were not present in children but were present in adults, most likely due to maturation of cytochrome P450 (CYP) 3A.[12,13] Lastly, the demethylation of caffeine by CYP1A2 increases with age, as in newborns caffeine is almost completely excreted by renal clearance of the parent drug, while in adults caffeine is many metabolically cleared.[14,15] As in general the metabolites differ in terms of efficacy and toxicity[16], knowledge on metabolite profiles in children is crucial for applying effective and safe pediatric drug therapy.

Metabolite profiles are typically generated by human radiolabeled ADME studies, one of the possible MIST studies, by analyzing plasma, urine or feces samples with liquid chromatography with fraction collectors, followed by offline radioactivity detection using liquid scintillation counting.[16] For this latter technique, a high radioactive dose of 100 µCi in humans is needed. Just recently, advances mainly in analytical technology have enabled new approaches to MIST studies with less radioactivity exposure.[16,17] By using [^{14}C]microtracers concurrently administered with a therapeutic dose, metabolites can be identified and quantified by accelerator mass spectrometry (AMS) with a radioactivity exposure of even less than 0.1 µCi.[18,19]

The amount of radiolabeled dose that is ethically justified to be administered to human volunteers participating in clinical trials has been risk classified by the International Commission on Radiological Protection (ICRP) (Table 1).[20] The use of [^{14}C]labeled microtracers with AMS quantification not only justifies earlier radioactive exposure during drug development, but may also serve to derive metabolite profiles for vulnerable populations like newborns, for which 100 µCi levels would not be ethically acceptable, even in a late stage of drug development. Various pediatric microtracer studies to study the PK of [^{14}C]labelled compounds have already been successfully conducted.[11,21-24] Yet, to the best of our knowledge, pediatric MIST microtracer studies with [^{14}C]labelled compounds to create complete metabolite profiles have not yet been performed.

Midazolam is a drug with well-known metabolism in adults and is widely used as a marker for CYP3A4/5 activity, a developmentally regulated phase 1 metabolizing enzyme, with lower activity in neonates than in adults.[25] We hypothesized that using an oral [^{14}C] midazolam microtracer as an example-compound in children receiving therapeutic intravenous midazolam for clinical needs, would permit to generate metabolite profiles of midazolam in children and study routes of excretion. Therefore, we aimed to explore, as a proof of concept, the feasibility of a MIST microtracer study with an oral [^{14}C] midazolam microtracer in children in the 0-6 years age range.

Table 1 The International Commission on Radiological Protection (ICRP) classification and justification of radiolabeled doses to be administered to human volunteers participating in clinical trials[20]

ICRP risk category	Radioactive dose		Justified for	Drug developmental stage	Ethically allowed in children?
	µSv	µCi			
I	100	0.1-1 but preferably lower	An increase of knowledge	At any stage in drug development	Yes
IIa	1000	10-100	An increase of knowledge and health benefit	At the end of phase 2 in drug development, after radiological dosimetry using tissue distribution data from animals and demonstration of efficacy of a drug in humans	No

MATERIAL AND METHODS

Study design

This study (EudraCT 2014-003269-46) was part of the ZonMw Priority Medicines for Children project 'Pediatric microdosing: elucidating age-related changes in oral absorption to guide dosing of new formulations', described in previous publications.[11,21,26] The study was approved by the Dutch Central Committee on Research Involving Human Subjects (The Hague, The Netherlands). All parents or legal guardians provided prior to any study-specific procedures written informed consent for their child to be included. The Dutch Nuclear Research and Service Group estimated the radiation exposure for a single microtracer of 60 Bq/kg (equivalent to an adult study of 0.1 μCi) and <1 μSv and are allowed in this population according to the ICRP (Table 1).[20,27] We explained the parents and legal guardians that the radiation exposure of a single microtracer is almost negligible compared with the yearly mean background exposure 2600 μSv in the Netherlands in 2013.[28]

Subjects

Patients admitted to the pediatric intensive care unit of the Erasmus MC-Sophia Children's Hospital were considered for inclusion. The following inclusion criteria applied: age from birth (post menstrual age >36 weeks) up to 6 years of age, bodyweight >2.5kg, clinical need for intravenous midazolam, and an indwelling arterial line in place enabling blood sampling. Exclusion criteria were the following: anticipated death in 48 hours, extra corporeal membrane oxygenation (ECMO) treatment, circulatory failure (defined by the administration of ≥1 vasopressor drug, or increase of a vasopressor drug in the last 6 hours), kidney failure (according to the Pediatric Risk, Injury, Failure, Loss, End stage renal disease score (pRIFLE) criteria, i.e. estimated creatinine clearance decreased by 75% or an urine output of <0.3 ml/kg/h for 24h or anuria for 12 hours), liver failure (defined by aspartate-aminotransferase [ASAT] or and alanine-aminotransferase [ALAT] >2 times the upper limit for age), gastrointestinal disorders, or co-medication known to interact with midazolam (according to the Flockhart Table™[29]).

Study procedures

A single [^{14}C]midazolam dose was administered as an oral microtracer via the enteral feeding tube. Intravenous (IV) exposure was at therapeutic levels in the context of clinical care, which allowed identification of metabolites by high resolution mass spectrometry (hrMS). The IV therapeutic midazolam dose was prescribed by the treating physician for clinical purposes and was adjusted on the guidance of validated sedation scores and according to a standardized sedation titration protocol. According to this protocol, midazolam bolus doses varied between 0.05-0.2 mg/kg and the continuous infusion

rate between 0.05-0.3 mg/kg/h. Blood samples were taken pre-dose and up to 24 hours after administration of the [^{14}C]midazolam microtracer. The maximum number of study-specific blood samples was limited to 8 per subject and the maximum amount of blood could not exceed the EMA guidelines (maximum of 1% of the total blood volume at any time and a maximum 3% during a period of four weeks where the total volume of blood is estimated at 80-90 ml/kg).[30] The blood samples were centrifuged and plasma was stored at -80ºC until analysis. Urine was collected from patients with a urinary catheter in place for clinical reasons. It was collected with a maximum of 72h after [^{14}C]midazolam administration or until the urinary catheter was removed. The nurses noted the urine volumes in the clinical electronic patient record. One sample (2 mL) was stored at -80 °C until analysis. As long as urine was collected, also diapers were collected for the purpose of studying the recovery in feces. The diapers were stored at -80 °C until analysis.

Radiopharmaceutical preparation

Non-good manufacturing practice (non-GMP) [^{14}C]midazolam was synthesized and the quality characterized by Selcia Ltd, United Kingdom at a specific activity of 1033 MBq/mmol (equal to 2.85 MBq/mg). The chemical name is 8-chloro-6-(2-fluorophenyl)-1-methyl-^{4}H-[1-^{14}C]imidazo[l,5-a][l,4]benzodiazepine-hydrochloride, and it was brought in ethanol solution (96%). In the department of Radiology and Nuclear Medicine at the VU University Medical Center (Amsterdam, NL) the solution was further diluted to the required concentration with sodium chloride 0.9% solution (Fresenius Kabi, Zeist, NL) to provide a GMP drug product. The final [^{14}C]midazolam concentration was 210-270 Bq/mL, with 1 Bq being equivalent to 0.31 ng [^{14}C]midazolam.

Metabolite profiles

Subjects and plasma samples

We created four age groups: 0-28 days; 1-6 months; 6 months-2 years; 2-6 years. First a time-averaged pool per patient ($AUC_{0\text{-}t}$ where t is the last sampling time point) was prepared according to the Hamilton method [31,32], after which age group pools were generated by equi-volumetric pooling. A time-averaged pool consists of aliquots from individual samples that form one composite sample. The volume of the aliquot taken from each individual plasma sample was determined by the time interval between drawing of the samples. The final time-averaged pool reflects the mean plasma level of the testing period (0-≈24h).

Identification of metabolites and quantification [14C]levels

In total, 150 µl of the plasma pool was added to 600 µL methanol and centrifuged. The supernatant was evaporated to dryness and redissolved in 80 µL 95/5 1 mM ammonium formate in MilliQ + 5% ACN / ACN. The plasma extracts were injected on a

UPLC (20 µL/injection) with a gradient runtime of 30 min, allowing absolute metabolite separation. The flow was split directly after UPLC separation diverting one line coupled to a Q-Exactive hrMS (in-line) for metabolite identification and one line to a fraction collector (90 fractions in 30 min) for subsequent AMS (off-line) (1MV Tandetron) [^{14}C] level quantification. For each time-averaged pool, 90 fractions were collected (0-20 min 4 fractions/min; 20-30 min 1 fraction/min) and transferred to a tin foil cup and evaporated to dryness prior to [^{14}C]level quantification.

Quantification [^{14}C]levels with AMS

[^{14}C]levels were quantified as described before.[32] In brief, the tin foil cups were combusted on an elemental analyzer (Vario Micro; Elementar, Langenselbold, Germany). Generated CO_2 was transferred to a home-built gas interface, composed of a zeolite trap and syringe.[32] CO_2 was adsorbed to the trap on the interface; and after heating of the trap, the CO_2 was transferred to a vacuum syringe using helium. A final CO_2/helium mixture of 6% was directed to the AMS ion source, at a pressure of 1 bar and a flow of 60 µL min^{-1}. A 1-MV Tandetron AMS (High Voltage Engineering Europe B.V., Amersfoort, the Netherlands)[33] was used. To determine the true amount of radioactivity in each fraction, the measured [^{14}C]/[^{12}C] ratios were multiplied by the corresponding total carbon measurement of the elemental analyzer.

hrMS metabolite identification

A Q-exactive high resolution mass spectrometer (Thermo Fisher) was used for metabolite identification. The Q-exactive mass spectrometer was operated in positive ion mode at a resolution of 35000 in MS and 17500 in MS2. The used mass range was from 100 to 850 m/z. For data dependent MS2, an isolation window of 2.0 m/z was used. The collision voltage was set at 35 eV. For mass measurement of metabolites, the mass range was from 200 to 2000 m/z. The minimum automatic gain control was set at 5E3 and the intensity threshold at 1E5. Compound Discoverer was used for data processing.

Mass balance

With regard to the mass balance part, routes of excretion were studied by determining the recovery of the administered [^{14}C]midazolam dose in urine and feces. Total [^{14}C]levels in urine were measured by AMS as described in chapter *Quantification [14C]levels with AMS*. Recovery in urine was calculated by multiplying the [^{14}C]levels by the total urine volume. Diapers were extracted using ethanol:water (25:75). To optimize extraction, the diapers were first inverted with the inside facing out. The diapers were individually transferred to a bucket and one liter of the extraction solvent was added. With lid closed, the bucket was placed on a horizontal shaker for 7 days during which the analytes were

extracted. After completion, the samples were homogenized with an Ultra-Turrax and a small part of the sample was transferred to a tin foiled cup for direct AMS analysis.

RESULTS

Subjects

For the original study (see 3.1) 96 patients were eligible based on the in- and exclusion criteria, of which parents of 46 patients consented to let their child participate in the study. For this sub-study, the samples of the first 12 included patients were selected, which had a median (range) age of 13.1 (1.3 – 218.6) weeks and bodyweight of 5.6 (3.1 – 17.0) kg were analyzed. In Table 2 the patient characteristics can be found, and the detailed characteristics per individual patient in Table S1. The age groups/time-averaged pools 0-28 days, 1-6 months, 6 months-2 years and 2-6 years consisted of 4, 5, 1 and 2 patients, respectively. Each received an oral [^{14}C]midazolam dose of 59.6 (55.7-66.3) Bq/

Table 2 Characteristics of patients included in the analysis; data are presented as median (range) or number

Patient characteristics		
Number of patients (n)	12	
Postnatal age (weeks)	13.1 (1.3 – 218.6)	
Weight (kg)	5.6 (3.1 – 17.0)	
Gender (M/F)	8/4	
Reason for admission (n)	Respiratory failure	
	· Pneumonia/bronchiolitis	3
	· Congenital cardiac abnormality	2
	· Pulmonary hypertension	1
	Post cardiac surgery	5
	Status epilepticus	1
Disease severity scores		
PELOD	6.5 (0-20)	
Number of organs failing on study day	1 (0-2)	
PRISM	18 (11-28)	
PIM	-3.1 (-4.7 – -0.6)	
Laboratory values at day of administration [^{14}C]midazolam		
Plasma creatinine (µmol/L)	38 (25-63)	
ASAT (U/L)	53 (16-309)	
ALAT (U/L)	17 (7-114)	
CRP (mg/L)	21 (3-123)	

PELOD=Pediatric Logistic Organ Dysfunction; PRISM=Pediatric Risk of Mortality; PIM=Pediatric Index of Mortality; ASAT= aspartate-aminotransferase; ALAT=alanine-aminotransferase; CRP=C-reactive protein

kg, equal to 18.7 (17.5-20.8) ng/kg, in addition to therapeutic continuous IV midazolam, for which the doses were determined by the treating physician, according to the PICU sedation protocol (0.05-0.2 mg/kg bolus and 0.05-0.3mg/kg/h continuous infusion).

Metabolite profiles

We were able to identify metabolite profiles for each age group (Figure 1 and Table 3). Two prominent peaks and some smaller peaks were present in the AMS radio chromatogram for each group (Figure 1), showing the amount of radioactivity for [^{14}C] labelled compounds/metabolites. All MS/MS spectra were consistent with those of the available reference standards. In the three youngest age groups, [^{14}C]1-OHMG was the most abundant, followed by the unchanged [^{14}C]midazolam. In the age group 2-6 years,

Figure 1 Metabolite profiles as presented by the radio chromatogram of [^{14}C] levels after administration of an oral [^{14}C]midazolam microtracer to children.

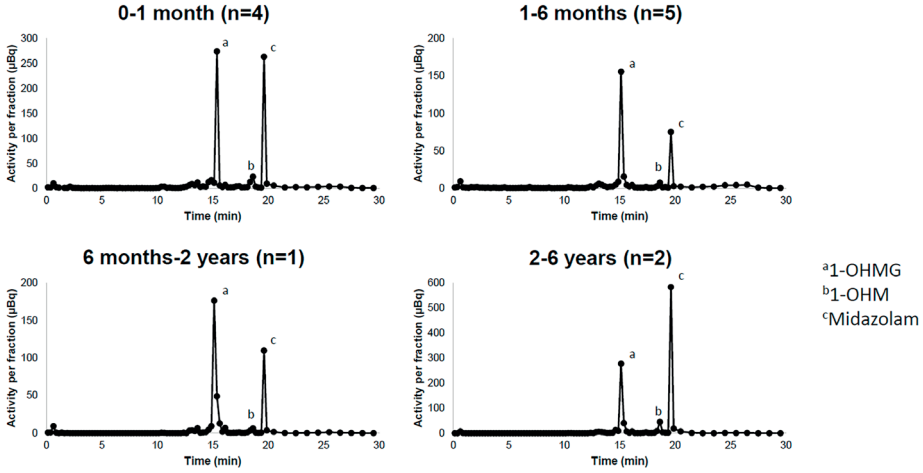

The population was divided in four age groups/Hamilton pools: 0-1 month, 1-6 months, 6 months-2 year and 2-6 year. [^{14}C]levels were quantified with Accelerator Mass Spectrometry. 1-OHMG=1-OH-midazolam-glucuronide; 1-OHM=1-OH-midazolam. The corresponding high resolution mass spectrometry retention times can be found in Table 4.

Table 3 The parent and metabolite exposures in percentage of the total drug related exposure of an oral [^{14}C]midazolam microtracer in four age groups

	Midazolam	1-OHM	1-OHMG	Unspecified
0 – 1 month	40.7%	5.0%	42.7%	11.5%
1 – 6 months	26.2%	2.5%	63.0%	8.3%
6 months – 2 years	27.0%	2.5%	59.2%	11.3%
2 – 6 years	56.1%	5.6%	32.0%	6.3%

the unchanged [^{14}C]midazolam was most abundant, followed by [^{14}C]1-OHMG. For all age groups, the quantities of [^{14}C]1-OHM were much lower than [^{14}C]midazolam and [^{14}C]1-OHMG. For all age groups, there was a small proportion of unspecified metabolites of which individual peaks were <10% of the total drug related material.

Table 4 Mass balance results after oral administration of an oral [^{14}C]midazolam microtracer

Subject	Sampling time	Urine		Feces		Total fraction of the administered dose recovered in urine and feces
		Total recovery (Bq)	Fraction of administered dose	Total recovery (Bq)	Fraction of administered dose	
1	20h	155	0.74	6.21	0.03	0.77
2	48h	124	0.74	31.5	0.19	0.93
3	48h	81	0.49	64.1	0.39	0.88
4	71h	330	0.92	7.12	0.02	0.94

Mass balance

Table 4 presents the mass balance results of urine samples and diapers of four patients. The main route of excretion was renal, resulting in a recovery of 49-72%. The total recovery of the [^{14}C]midazolam dose in urine and feces was 77-94%.

DISCUSSION

With this proof-of-concept study, we have shown that it is feasible to perform a MIST study using a [^{14}C]microtracer study design in pediatric patients. We used an oral [^{14}C] midazolam microtracer concurrently administered with therapeutic IV midazolam as an example-compound, and successfully created metabolite profiles and studied routes of excretion by the use of AMS and hrMS. The metabolite profiles differed per age group and consisted of the parent drug, two major metabolites 1-OHM and 1-OHMG, and small proportions of unspecified fraction of metabolites that were <10% of the total drug related exposure. The recovery of the administered dose in urine and feces was 77-94%.

Our finding that in the three youngest age groups the systemic exposure to 1-OHMG was most abundant, followed by midazolam and 1-OHM, is in line with literature and supports the feasibility of our microtracer MIST approach. *De Wildt et al* have shown that after up to 6 hours after oral administration of midazolam in preterm neonates the fraction of urinary excreted midazolam, 1-OHM and 1-OHMG was median (range) 0.11% (0.02–0.59%), 0.02% (0.00–0.10%) and 1.69% (0.58–7.31%), , respectively.[34] Those data indirectly reflect that, similarly to our results, the systemic exposure to 1-OHMG was

the highest, followed by midazolam and 1-OHM. Also in adults, the major metabolite found in urine was 1-OHMG – accounting for 60-80% of the administered dose.[35] Based on literature, we expect that the small portion of unspecified fraction included known midazolam metabolites, such as midazolam-glucuronide and 4-OH-midazolam.[36,37] For adults, nearly 90% urinary recovery after oral dosing of midazolam has been found [38], which is in concordance with our findings that recovery was highest in urine, and the total recovery in urine and feces was 77-94%. More specifically for our results, the lowest recovery of 77% was found for a patient whose urinary catheter had been removed after 20h. A longer sampling time could have resulted in a higher recovery as the excretion may not yet have been complete. While the relative distribution of systemic exposure to metabolite and parent drug was similar in the three youngest age groups, the absolute distribution was not similar. The sample size of this pilot/proof-of-concept study is too small, however, to draw conclusions about age-related changes in the absolute metabolite profiles, as for example the age group 6 months-2 year is underrepresented with only one patient.

The introduction of MIST studies with [^{14}C]microtracers in drug development has resulted in an improvement in drug development for adults, with earlier human metabolism studies increasing the safety as well as efficacy of drugs.[16] Finding a unique human metabolite at a late stage in drug development, that had not at all or at a disproportional level been detected in animals during non-clinical drug evaluation introduces safety and toxicity concerns, as human volunteers may be exposed to this metabolite whose characteristics are not known.[17] In addition, this may cause considerable delay in drug registration because addition of toxicological assessments might be required. Current regulatory guidelines for drug development also mandate scientists to submit a pediatric drug development program to the regulators.[39] Although for midazolam no unique metabolite was found in children, we can speculate that this may not be true for other drugs. Thus, conducting a MIST study with a [^{14}C]microtracer is a potentially valuable addition to pediatric drug development that may secure drug safety and efficacy, and avoiding delay in drug registration. Also, MIST studies may lead to a reduction in animal radiolabel studies.[16] Currently, juvenile animals are often used to predict drug disposition and metabolism in children. Besides the fact that findings in juvenile animals cannot be directly translated human children as they differ widely in terms of drug disposition[40], pediatric MIST studies may also reduce the need of animal studies. Subsequently, metabolic profiles in other vulnerable populations whose drug metabolism and disposition differ from those in healthy adults can be studied using a MIST study, such as elderly and pregnant women.[41,42]

To conclude, with this study we have shown that it is feasible to use a [^{14}C]microtracer MIST approach in pediatrics. By simultaneous identification of metabolites and quantification of [^{14}C]levels, we were able to safely generate metabolite profiles of midazolam and study the routes of excretion in children. This approach is promising to improve safety and efficacy of drug therapy for children and other vulnerable populations.

REFERENCES

1. Leclercq, L., Cuyckens, F., Mannens, G.S., de Vries, R., Timmerman, P. & Evans, D.C. Which human metabolites have we MIST? Retrospective analysis, practical aspects, and perspectives for metabolite identification and quantification in pharmaceutical development. Chem Res Toxicol 2009;22(2):280-93.
2. International Conference on Harmonization. Guidance for Industry. M3(R2) Nonclinical Safety Studies for the Conduct of Human Clinical Trials and Marketing Authorization for Pharmaceuticals. https://www.fda.gov/media/71542/download (2010). Accessed June 14, 2019.
3. US Food and Drug Administration. Guidance for Industry. Safety Testing of Drug Metabolites https://www.fda.gov/media/72279/download (2016). Accessed June 14, 2019.
4. van den Anker, J., Reed, M.D., Allegaert, K. & Kearns, G.L. Developmental Changes in Pharmacokinetics and Pharmacodynamics. J Clin Pharmacol 2018;58 Suppl 10(S10-S25.
5. Brouwer, K.L. et al. Human ontogeny of drug transporters: review and recommendations of the pediatric transporter working group. Clin Pharmacol Ther 2015;98(3):266-87.
6. van Groen, B.D. et al. Proteomics of human liver membrane transporters: a focus on fetuses and newborn infants. Eur J Pharm Sci 2018;124(217-27.
7. Prasad, B. et al. Ontogeny of hepatic drug transporters as quantified by LC-MS/MS proteomics. Clin Pharmacol Ther 2016;100(4):362-70.
8. Mooij, M.G. et al. Ontogeny of human hepatic and intestinal transporter gene expression during childhood: age matters. Drug Metab Dispos 2014;42(8):1268-74.
9. Mooij, M.G. et al. Proteomic analysis of the developmental trajectory of human hepatic membrane transporter proteins in the first three months of life. Drug Metab Dispos 2016;44(7):1005-13.
10. Wun Kathy Cheung, K. et al. A comprehensive analysis of ontogeny of renal drug transporters: mRNA analyses, quantitative proteomics and localization. Clin Pharmacol Ther 2019;10.1002/cpt.1516
11. Mooij, M.G. et al. Successful Use of [14C]Paracetamol Microdosing to Elucidate Developmental Changes in Drug Metabolism. Clin Pharmacokinet 2017;DOI: 10.1007/s40262-017-0508-6
12. Filler, G., Bendrick-Peart, J., Strom, T., Zhang, Y.L., Johnson, G. & Christians, U. Characterization of sirolimus metabolites in pediatric solid organ transplant recipients. Pediatr Transplant 2009;13(1):44-53.
13. Ying, H., Qiao, C., Yang, X. & Lin, X. A Case Report of 2 Sirolimus-Related Deaths Among Infants With Kaposiform Hemangioendotheliomas. Pediatrics 2018;141(Suppl 5):S425-S9.
14. Pons, G. et al. Maturation of caffeine N-demethylation in infancy: a study using the 13CO2 breath test. Pediatr Res 1988;23(6):632-6.
15. Salem, F., Johnson, T.N., Abduljalil, K., Tucker, G.T. & Rostami-Hodjegan, A. A re-evaluation and validation of ontogeny functions for cytochrome P450 1A2 and 3A4 based on in vivo data. Clin Pharmacokinet 2014;53(7):625-36.
16. Schadt, S. et al. A Decade in the MIST: Learnings from Investigations of Drug Metabolites in Drug Development Under the "Metabolites in Safety Testing" Regulatory Guidances. Drug Metab Dispos 2018;DOI: 10.1124/dmd.117.079848
17. Yu, H., Bischoff, D. & Tweedie, D. Challenges and solutions to metabolites in safety testing: impact of the International Conference on Harmonization M3(R2) guidance. Expert Opin Drug Metab Toxicol 2010;6(12):1539-49.
18. European Medicines Agency. ICH Topic M3 (R2) Non-Clinical Safety Studies for the Conduct of Human Clinical Trials and Marketing Authorization for Pharmaceuticals. 2008;

19. Food and Drug Administration US Department of Health and Human Services Guidance for Industry Investigators and Reviewers. Exploratory IND Studies. 2006;
20. International Commission on Radiological Protection. 1990 Recommendations of the International Commission on Radiological Protection. Ann ICRP 1991;21(1-3):1-201.
21. Mooij, M.G. et al. Pediatric microdose study of [(14)C]paracetamol to study drug metabolism using accelerated mass spectrometry: proof of concept. Clin Pharmacokinet 2014;53(11):1045-51.
22. Turner, M.A. et al. Pediatric microdose and microtracer studies using 14C in Europe. Clin Pharmacol Ther 2015;98(3):234-7.
23. Garner, C.R. et al. Observational infant exploratory [(14)C]-paracetamol pharmacokinetic microdose/therapeutic dose study with accelerator mass spectrometry bioanalysis. Br J Clin Pharmacol 2015;80(1):157-67.
24. Burt, T. et al. Phase 0, including microdosing approaches: Applying the Three Rs and increasing the efficiency of human drug development. Altern Lab Anim 2018;46(6):335-46.
25. Genome Reference Consortium. Genome Reference Consortium Human Build 37. https://www.ncbi.nlm.nih.gov/assembly/GCF_000001405.13/. Accessed May, 2018.
26. Kleiber, N. et al. Enteral Acetaminophen Bioavailability in Pediatric Intensive Care Patients Determined With an Oral Microtracer and Pharmacokinetic Modeling to Optimize Dosing. Crit Care Med 2019;DOI: 10.1097/CCM.0000000000004032
27. Netherlands Commission on Radiation Dosimetry. Human Exposure to Ionising Radiation for Clinical and Research Purposes: Radiation Dose & Risk Estimates. 2016;
28. RIVM. Stralingsbelasting in Nederland. https://www.rivm.nl/stralingsbelasting-in-nederland (2013). Accessed 10 April, 2019.
29. Indiana University. Drug Interactions Flockhart Table. https://drug-interactions.medicine.iu.edu/Main-Table.aspx. Accessed 10 April, 2019.
30. EMA. Guideline on the investigation of medicinal products in the term and preterm neonate. (EMA/PDCO/362462/2016).
31. Hamilton, R.A., Garnett, W.R. & Kline, B.J. Determination of mean valproic acid serum level by assay of a single pooled sample. Clin Pharmacol Ther 1981;29(3):408-13.
32. van Duijn, E., Sandman, H., Grossouw, D., Mocking, J.A., Coulier, L. & Vaes, W.H. Automated combustion accelerator mass spectrometry for the analysis of biomedical samples in the low attomole range. Anal Chem 2014;86(15):7635-41.
33. Klein, M.V., Vaes, W.H.J., Fabriek, B., Sandman, H., Mous, D.J.W. & Gottdang, A.T. The 1 MV multi-element AMS system for biomedical applications at the Netherlands Organization for Applied Scientific Research (TNO). Nucl Instr Meth Phys Res B 2013;294(14-7.
34. de Wildt, S.N., Kearns, G.L., Murry, D.J., Koren, G. & van den Anker, J.N. Ontogeny of midazolam glucuronidation in preterm infants. Eur J Clin Pharmacol 2010;66(2):165-70.
35. Heizmann, P., Eckert, M. & Ziegler, W.H. Pharmacokinetics and bioavailability of midazolam in man. Br J Clin Pharmacol 1983;16 Suppl 1(43S-9S.
36. Swart, E.L., Slort, P.R. & Plotz, F.B. Growing up with midazolam in the neonatal and pediatric intensive care. Curr Drug Metab 2012;13(6):760-6.
37. Hyland, R. et al. In vitro and in vivo glucuronidation of midazolam in humans. Br J Clin Pharmacol 2009;67(4):445-54.
38. Heizmann, P. & Ziegler, W.H. Excretion and metabolism of 14C-midazolam in humans following oral dosing. Arzneimittelforschung 1981;31(12a):2220-3.

39. US Food and Drug Administration. Best Pharmaceuticals for Children Act and Pediatric Research Equity Act. https://www.fda.gov/science-research/pediatrics/best-pharmaceuticals-children-act-and-pediatric-research-equity-act. Accessed June 11, 2019.
40. Soellner, L. & Olejniczak, K. The need for juvenile animal studies--a critical review. Regul Toxicol Pharmacol 2013;65(1):87-99.
41. Isoherranen, N. & Thummel, K.E. Drug metabolism and transport during pregnancy: how does drug disposition change during pregnancy and what are the mechanisms that cause such changes? Drug Metab Dispos 2013;41(2):256-62.
42. Klotz, U. Pharmacokinetics and drug metabolism in the elderly. Drug Metab Rev 2009;41(2):67-76.

Table S1 Individual characteristics of patients included in the analysis

Subject	Postnatal age (weeks)	Bodyweight (kg)	Gender (M/F)	Dose microtracer (Bq)	Dose microtracer (ng)
1	1.7	3.1	M	178.4	55.95
2	3.7	4.1	M	257	80.6
3	3.6	4.7	M	308.4	96.71
4	1.3	4.3	F	264	82.79
5	9.2	5.4	M	301	94.39
6	14.2	6.6	M	368	115.4
7	14.1	6.0	M	385.5	120.89
8	12.1	4.2	F	257	80.6
9	22.9	5.8	M	360	112.9
10	100.7	10	F	580	181.89
11	209.3	15	M	870	272.83
12	218.6	17	F	986	309.21

PART IV

Discussion and summary

11 Summary / samenvatting

SUMMARY

Drug disposition in children is impacted by developmental changes in drug absorption, distribution, metabolism and excretion. This mandates the need for dosing regimens specifically tailored to children. Yet, there are gaps in the knowledge on these developmental changes, for example regarding hepatic and renal drug transport and cytochrome P450 (CYP)3A metabolism, putting children at risk for subtherapeutic or toxic drug exposure. Pediatric drug research is faced with ethical and analytical challenges. This thesis addresses these knowledge gaps and challenges by using innovative study designs.

Chapter 1 provides the background and aims of the studies presented in this thesis. It contains a general introduction to ontogeny of drug metabolism and transport and describes the current knowledge gaps.

Part I From literature research –

The current stage of knowledge for ontogeny of hepatic transporters, phase 1 and phase 2 metabolism is reviewed in **Chapter 2.** More specifically for transporters, **Chapter 3** shows our current knowledge on developmental changes in transporters in the liver, kidney and intestine in human. It also illustrates the utility of incorporating this information in predicting drug exposure of tazobactam in children. These reviews add to understanding the age-related changes in transporter expression, but also revealed important knowledge gaps and challenges. These include, but are not limited to, the fact that non-hepatic transporter expression in newborns is understudied, that the clinical relevance of developmental changes in transporter expression remain unknown, and that practices in study designs and methods differ from lab to lab and should be harmonized.

Part II – to bench –

Developmental changes in mRNA and protein expression of hepatic and renal transporters are studied in **Chapter 4** and **Chapter 5**. In Table 1 and Table 2, the developmental patterns are presented for liver and kidney respectively, showing transporter- and organ dependent rates and patterns of maturation. Furthermore, we found maturational differences between mRNA expression and protein expression as well as correlations between the expression levels of various transporters. For hepatic transporters specifically, the impacts of single nucleotide polymorphisms (SNPs) on transporter expression were studied, but no genotype-protein expression relationship was detected. For renal tissue we found that, using immunohistochemistry, the MRP4 localization at the apical side of the proximal tubule in pediatric samples was similar to that in adult samples.

Table 1 Developmental changes in hepatic protein expression in the perinatal period **(Chapter 4)**

Transporter *gene*/protein	**Hepatic protein expression***
ATP1A1/ ATP1A1	Stable
ABCG2/BCRP	Stable
ABCB11/BSEP	Lower in fetuses than in term newborns and adults.
SLC2A1/GLUT1	Higher in fetuses than in term newborns, pediatrics and adults.
SLC16A1/MCT1	Stable
ABCB1/MDR1	Lower in fetuses than in adults.
ABCC1/MRP1	Lower in fetuses and term newborns than in adults.
ABCC2/MRP2	Lower in fetuses and term newborns than in adults.
ABCC3/MRP3	Lower in fetuses and term newborns than in adults.
SLC10A1/NTCP	Lower in fetuses than in term newborns, pediatrics and adults. Lower in preterm newborns than in adults.
SLCO1B1/OATP1B1	High in fetuses, low in term newborns
SLCO1B3/OATP1B3	Stable
SLCO2B1/OATP2B1	Stable
SLC22A1/OCT1	Lower in fetuses and term newborns than in adults.

* *Determined in post-mortem hepatic tissue of fetuses (n=36), preterm newborns (n=12), term newborns (n=10), pediatrics (n=4) and adults (n=8)*

One of the underlying mechanisms of age-related changes in transporter expression and/or activity may be by developmentally regulated alternative splicing. The hepatic influx transporter OATP1B1 (gene name SLCO1B1) plays an important role in the disposition of endogenous substrates and drugs prescribed to children. In **Chapter 6,** alternative splicing of this transporter in pediatric liver tissue is studied. We found that two splice variants code for reference OATP1B1 protein, and eight code for truncated proteins. The expression of eight isoforms was associated with age. It was concluded that alternative splicing of SLCO1B1 occurs frequently in children. Although the functional consequences remain unknown, the data raise the possibility of a regulatory role for alternative splicing in mediating developmental changes in drug disposition.

In conclusion, these transporter- and organ specific maturation patterns suggest that hepatic and renal handling of substrates likely change with age.

Part III – to clinical research

Most drugs are administered to children orally; hence oral bioavailability is an important determinant for systemic exposure. CYP3A4 is abundant in both the intestine and liver and contributes to the first-pass metabolism of many orally administered drugs, including the well-validated CYP3A4 probe midazolam. Traditional study designs for

Table 2 Developmental changes in renal mRNA and protein expression **(Chapter 5)**

Transporter *gene*/protein	**Renal mRNA expression**	**Renal protein expression***
ABCG2/BCRP	Higher in term neonates than in children, adolescents and adults[α]	Stable
SLCA2/GLUT2	Stable[α]	Stable
SLC47A1/MATE1	Stable[β]	Stable
SLCO47A2/MATE2-K	Lower in term newborns than in adults[β]	Stable
ABCB1/MDR1	Increase over the entire age span[β]	Increased with age with TM_{50} approximately 1 month
ABCC2/MRP2	Stable[γ]	-
ABCC4/MRP4	Stable[γ]	-
SLC22A6/OAT1	Lower in preterm newborns than in infants and children[β]	Increased with age. TM_{50} was approximately 5 months.
SLC22A8/OAT3	Lower in preterm newborns than in infants, children and adults; lower in term newborns than in children[β]	Increased with age. TM_{50} was approximately 8 months.
SLC22A2/OCT2	Lower in preterm newborns than in infants, children and adults; lower in term newborns than in children[β]	Increased with age. TM_{50} was approximately 1 month.
SLC22A12/URAT1	Lower in term newborns than in infants and children[α]	Lower in term newborns than in adults

* *Determined in post-mortem renal tissue of term newborns (n=1), infants (n=30), children (n=16), adolescents (n=5) and adults (n=10);*

[α] *Determined in post-mortem renal tissue of term newborns (n=11), infants (n=60), children (n=31), adolescents (n=10) and adults (n=10);*

[β] *Determined in post-mortem renal tissue of preterm newborns (n=9), term newborns (n=19), infants (n=81), children (n=38), adolescents (n=10) and adults (n=27);*

[γ] *Determined in post-mortem renal tissue of preterm newborns (n=9), term newborns (n=8), infants (n=21), children (n=7) and adults (n=17); TM_{50}: age at which half of the adult value is reached*

pediatric drug research are ethically and practically challenging. Using an innovative microdosing/microtracing study design with [^{14}C]labelled substrates overcomes these challenges. In **Chapter 7,** the dose-linearity of the PK of an intravenous [^{14}C]midazolam microdose was studied in 15 infants (median gestational age 39.4 [range 23.9-41.4] weeks, postnatal age 11.4 [0.6-49.1] weeks). By comparing the PK of a microtracer (a microdose given simultaneously with a therapeutic midazolam dose), with the PK of a single isolated microdose, dose-linearity from microdose to therapeutic dose can be supported. **Chapter 8** presents the results of a [^{14}C]midazolam microtracer population PK study aimed to determine the bioavailability of midazolam. In 46 stable, critically ill children (median age 9.8 [range 0.3 – 276.4] weeks), the typical oral bioavailability varied widely with a median of 66% and a range of 25-85%. The exposures of the major metabolites 1-OH-midazolam (OHM) and 1-OH-midazolam-glucuronide (OHMG) were

also studied to give further insight in the ontogeny of glucuronidation and kidney function involved in the metabolism to OHM and OHMG, respectively. OHM and OHMG exposure was highest for the youngest age groups and significantly decreased with postnatal age, which is likely a combined result of ontogeny of CYP3A, glucuronidation and kidney function. As midazolam oral bioavailability varied widely, systemic exposure of other CYP3A-substrate drugs and their metabolites after oral dosing in this population may also be unpredictable, with risk of therapy failure or toxicity.

Due to developmental changes in drug metabolism, metabolic profiles of a drug can change. Metabolite in safety testing (MIST) studies using [^{14}C]microtracers are used to create metabolite profiles and study the routes of excretion, but had not been conducted before in children. **Chapter 9** presents the first pediatric MIST study. Using a [^{14}C]midazolam microtracer approach as a sub-study of chapter 8, we showed that it is feasible and safe to generate metabolite profiles and study recovery in children. This approach is promising for first-in-child studies in drug development to delineate age-related variation in drug metabolite profiles.

Part IV General discussion

In **Chapter 10** we discuss our main findings, compare them with current literature and provide recommendations for future research to further improve pediatric drug therapy.

Specifically for the study designs used and the data generated in this thesis, we recommend the following:

- The influences of other potential factors on transporter expression should be studied, such as the use of co-medications, inflammation and genotype
- *Ex vivo* transporter data should be validated by e.g. *in vivo* pharmacokinetic data
- Practices for proteomic studies need to be harmonized
- Pediatric [^{14}C]microtracer and MIST studies are an interesting opportunity to increase efficacy and safety in pediatric drug development and for drugs already used in clinical practice
- The intestinal and hepatic intrinsic CYP3A-mediated clearance of midazolam should be studied using the data generated in this thesis
- It should be studied whether the midazolam-data presented in this thesis can be extrapolated to other CYP3A-substrates

These recommendations are supplemented with the following more general recommendations on future studies/approaches and on how to use our current knowledge to create impact on in clinical practice:

- International biobanks, collaborations, datasharing-platforms and pediatric clinical trial networks/infrastructures will aid in accelerating pediatric drug research

- To validate and further study transporter ontogeny, study approaches with exosomes, organoids, endogenous substrates and metabolomics may be of value
- Physiologically based PK (PBPK) modeling helps us understand drug metabolism and transport pathways, and the impact of a change in a certain pathway
- As knowledge gaps on ontogeny remain, routine use of PBPK modeling in prediction of pediatric drug disposition should be done carefully until these knowledge gaps are filled
- Integrating population PK and PBPK models in clinical practice can be accelerated by creating electronic systems to use complex dosing regimens in clinical care parallel to the electronic health care system

SAMENVATTING

De dispositie van een geneesmiddel wordt beïnvloed door leeftijdsafhankelijke veranderingen in de absorptie, verdeling, metabolisme en excretie van het geneesmiddel. Daarom dienen doseringsschema's voor kinderen op maat te zijn gemaakt. Echter, er zijn hiaten in onze kennis over de leeftijdsafhankelijke veranderingen van onder andere geneesmiddeltransport in de lever en de nieren en geneesmiddelmetabolisme door cytochroom P450 (CYP)3A. Hierdoor hebben kinderen een grote kans op subtherapeutische of toxische blootstelling aan geneesmiddelen. Geneesmiddelonderzoek bij kinderen wordt bemoeilijkt door ethische en praktische uitdagingen. Met behulp van innovatieve onderzoeksmethoden hebben we onderzocht welke de leeftijdsafhankelijke veranderingen in geneesmiddeltransport en geneesmiddelmetabolisme zijn

Hoofdstuk 1 beschrijft de achtergrond en de doelen van de diverse onderzoeken. Er wordt een introductie gegeven over de ontogenie van geneesmiddelmetabolisme en -transport, en een beschrijving van de huidige hiaten in onze kennis.

Deel I Van literatuur –

Door middel van literatuuronderzoek is in **hoofdstuk 2** de huidige kennis beschreven over de ontogenie van hepatische transporters, fase 1 en fase 2 metabolisme. **Hoofdstuk 3** geeft een overzicht van de leeftijdsafhankelijke veranderingen in transporters in de lever, nieren en darmen in de mens. Ook is er een casus opgenomen waarin informatie over ontogenie van transporters is gebruikt om blootstelling van het geneesmiddel tazobactam in kinderen te voorspellen. Deze twee hoofdstukken dragen bij aan het begrijpen van leeftijdsafhankelijke veranderingen in transporterexpressie. Het literatuuronderzoek heeft belangrijke hiaten en uitdagingen in onze huidige kennis geïdentificeerd. Dit omvat onder andere dat extra-hepatische transporterexpressie in pasgeborenen nog niet voldoende is opgehelderd, dat de klinische relevantie van leeftijdsafhankelijke veranderingen in transporterexpressie nog onduidelijk blijft, en dat er tussen laboratoria grote verschillen zijn in studieopzetten en methoden.

Deel II – tot het lab –

Leeftijdsafhankelijke veranderingen in mRNA en eiwit expressie van transporters in de lever en nieren zijn onderzocht in **hoofdstuk 4** en **hoofdstuk 5**. In Tabel 1 en Tabel 2 zijn de maturatiepatronen terug te vinden voor respectievelijk de lever en de nieren. Deze patronen zijn zowel transporter- als orgaanafhankelijk. Daarnaast hebben we verschillen in maturatie gevonden tussen mRNA-expressie en eiwitexpressie, maar ook verbanden tussen de expressie van verschillende transporters. Voor transporters in de lever is er is

Tabel 1 Leeftijdsafhankelijke veranderingen in eiwit expressie van lever transporters **(hoofdstuk 4)**

Transporter *gen*/eiwit	**Eiwit expressie***
ATP1A1/ ATP1A1	Stabiel
ABCG2/BCRP	Stabiel
ABCB11/BSEP	Lager bij foetussen dan bij a terme neonaten en volwassenen
SLC2A1/GLUT1	Hoger bij foetussen dan bij a terme neonaten, kinderen en volwassenen
SLC16A1/MCT1	Stabiel
ABCB1/MDR1	Lager bij foetussen dan bij volwassenen
ABCC1/MRP1	Lager bij foetussen en te vroeg geboren neonaten dan bij volwassenen
ABCC2/MRP2	Lager bij foetussen en a terme neonaten dan bij volwassenen
ABCC3/MRP3	Lager bij foetussen en a terme neonaten dan bij volwassenen
SLC10A1/NTCP	Lager bij foetussen dan bij a terme neonaten, kinderen en volwassenen. Lager bij te vroeg geboren neonaten dan bij volwassenen.
SLCO1B1/OATP1B1	Hoger bij foetussen dan bij a terme neonaten
SLCO1B3/OATP1B3	Stabiel
SLCO2B1/OATP2B1	Stabiel
SLC22A1/OCT1	Lager bij foetussen en a terme neonaten dan bij volwassenen

* *Bepaald in post-mortem leverweefsel van foetussen (n=36), te vroeg geboren neonaten (n=12), a terme neonaten (n=10), kinderen (n=4) en volwassenen (n=8)*

geen relatie tussen genotype en eiwitexpressie gevonden. Voor nierweefsel hebben we via immunohistochemie gevonden dat de MRP4 locatie in niertubuli van kinderen dezelfde was als bij volwassenen.

Eén onderliggend mechanisme van leeftijdsafhankelijke veranderingen in transporter expressie en/of activiteit zou kunnen zijn dat *alternative splicing* wordt gereguleerd door groei en ontwikkeling. De levertransporter OATP1B1 (gen naam *SLCO1B1*) is belangrijk in de dispositie van endogene substraten en geneesmiddelen die voor kinderen worden voorgeschreven. In **hoofdstuk 6** is *alternative splicing* van SLCO1B1 onderzocht in leverweefsel van kinderen. We vonden dat twee *splice variants* coderen voor de gehele OATP1B1 transporter, en dat er acht coderen voor kortere eiwitten. De expressie van acht *splice variants* was geassocieerd met leeftijd. We hebben geconcludeerd dat *alternative splicing* van SLCO1B1 vaak voorkomt in kinderen; we weten nog niet wat de functionele consequenties hiervan zijn, maar stellen dat *alternative splicing* wellicht bijdraagt aan leeftijdsgerelateerde veranderingen in geneesmiddeldispositie.

Concluderend, deze transporter- en orgaanafhankelijke maturatiepatronen suggereren dat de verwerking van substraten in de lever en de nieren kan veranderen met leeftijd.

Tabel 2 Leeftijdsafhankelijke veranderingen in mRNA- en eiwitexpressie van niertransporters **(hoofdstuk 5)**

Transporter *gen*/eiwit	**mRNA-expressie**	**Eiwitexpressie***
ABCG2/BCRP	Hoger bij a terme neonaten dan bij kinderen, adolescenten en volwassenen[α]	Stabiel
SLCA2/GLUT2	Stabiel[α]	Stabiel
SLC47A1/MATE1	Stabiel[β]	Stabiel
SLCO47A2/MATE2-K	Lager bij a terme neonaten dan bij volwassenen[β]	Stabiel
ABCB1/MDR1	Neemt toe over de hele leeftijdsspanne[β]	Neemt toe met leeftijd. TM_{50} van ongeveer 1 maand.
ABCC2/MRP2	Stabiel[γ]	-
ABCC4/MRP4	Stabiel[γ]	-
SLC22A6/OAT1	Lager bij te vroeg geboren neonaten dan bij zuigelingen en kinderen[β]	Neemt toe met leeftijd. TM_{50} van ongeveer 5 maanden.
SLC22A8/OAT3	Lager bij te vroeg geboren neonaten dan bij zuigelingen, kinderen en volwassenen; lager bij a terme neonaten dan bij kinderen[β]	Neemt toe met leeftijd. TM_{50} van ongeveer 8 maanden.
SLC22A2/OCT2	Lager bij te vroeg geboren neonaten dan bij zuigelingen, kinderen en volwassenen; lager bij a terme neonaten dan bij kinderen[β]	Neemt toe met leeftijd. TM_{50} van ongeveer 1 maand.
SLC22A12/URAT1	Lager bij a terme neonaten dan bij zuigelingen en kinderen[α]	Lager bij a terme neonaten dan bij volwassenen

* *Bepaald in post-mortem nierweefsel van a terme neonaten (n=1), zuigelingen (n=30), kinderen (n=16), adolescenten (n=5) en volwassenen (n=10);*

[α] *Bepaald in post-mortem nierweefsel van a terme neonaten (n=11), zuigelingen (n=60), kinderen (n=31), adolescenten (n=10) en volwassenen (n=10);*

[β] *Bepaald in post-mortem nierweefsel van te vroeg geboren neonaten (n=9), a terme neonaten (n=19), zuigelingen (n=81), kinderen (n=38), adolescenten (n=10) en volwassenen (n=27);*

[γ] *Bepaald in post-mortem nierweefsel van te vroeg geboren neonaten (n=9), a terme neonaten (n=8), zuigelingen (n=21), kinderen (n=7) en volwassenen (n=17); TM_{50}: leeftijd waarop de helft van de volwassenhoeveelheid is bereikt.*

Deel III – tot klinisch onderzoek

De meeste geneesmiddelen worden oraal toegediend aan kinderen. Orale biologische beschikbaarheid is daarom belangrijk voor de systemische blootstelling. CYP3A is aanwezig in de darmen en lever en draagt significant bij aan het first-pass metabolisme van veel orale geneesmiddelen, waaronder de gevalideerde CYP3A-marker midazolam. Geneesmiddelonderzoek bij kinderen kent ethische en praktische uitdagingen. Deze uitdagingen kunnen overwonnen worden via een innovatieve microdosing/microtracing studieopzet met een [^{14}C]gelabelde substraat. In **hoofdstuk 7** is de dosis-lineariteit van de PK van een intraveneuze [^{14}C]midazolam microdosis bestudeerd in 15 zuigelingen

(mediaan zwangerschapsduur 39.4 [range 23.9-41.4] weeks, postnatale leeftijd 11.4 [0.6-49.1] weken). De PK van een microtracer (een microdosis tegelijk gegeven met een therapeutische midazolam dosis) werd vergeleken met de PK van een eenmalige geïsoleerde microdosis; het resultaat van de studie lijkt het bestaan van dosis-lineariteit bij kinderen te ondersteunen. **Hoofdstuk 8** presenteert de resultaten van een [^{14}C] midazolam microtracer populatie PK studie die als doel had de orale biologische beschikbaarheid van midazolam te bepalen. In 46 stabiel kritisch zieke jonge kinderen (mediaan leeftijd 9.8 [spreiding 0.3 – 276.4] weeks) was er een grote spreiding in de typische orale biologische beschikbaarheid: de mediaan was 66% en de spreiding was 25%-85%. De systemische blootstelling aan de belangrijkste metabolieten 1-OH-midazolam (OHM) en 1-OH-midazolam-glucuronide (OHMG) was ook bestudeerd. Dit gaf verder inzicht in de maturatie van glucuronidering en de nierfunctie, die respectievelijk betrokken zijn bij de omzetting van OHM naar OHMG en renale klaring. Blootstelling aan OHM en OHMG was het hoogst voor de jongste leeftijdsgroepen en daalde significant met stijgende leeftijd. Dit is hoogstwaarschijnlijk een gecombineerd resultaat van ontogenie van CYP3A, glucuronidering en nierfunctie. De grote spreiding in de orale biologische beschikbaarheid van midazolam maakt de systemische blootstelling aan CYP3A-substraten en de metabolieten na orale toediening onvoorspelbaar, met risico op falen van geneesmiddeltherapie of op toxiciteit.

Door leeftijdsafhankelijke veranderingen in geneesmiddelmetabolisme, zoals in CYP3A4, kunnen metabolietprofielen van een geneesmiddel veranderen. *Metabolite in safety testing* (MIST) studies met [^{14}C]microtracers kunnen gebruikt worden om metabolietprofielen te maken en de routes van excretie te bestuderen, maar zijn niet eerder uitgevoerd bij kinderen. **Hoofdstuk 9** laat de eerste MIST studie in kinderen zien. Door toepassing van een [^{14}C]midazolam microtracer konden we aantonen dat het haalbaar en veilig is om metabolietprofielen te genereren en na te gaan hoeveel er van de dosis terug te vinden is in urine en feces. Deze aanpak is veelbelovend voor *first-in-child* studies.

Deel IV Algemene discussie

In **hoofdstuk 10** bespreken we onze belangrijkste bevindingen, vergelijken deze met de huidige literatuur en doen de volgende aanbevelingen om farmacotherapie bij kinderen verder te optimaliseren.

Specifiek voor de onderzoeksmethoden en de data verkregen in dit proefschrift, bevelen we het volgende aan:

- De invloed van andere potentiele covariaten op de transporterexpressie moet bestudeerd worden, zoals het gebruik van co-medicatie, het optreden van ontsteking, en genotype
- *Ex vivo* transporter data moet gevalideerd worden met behulp van bijvoorbeeld *in vivo* farmacokinetiek data
- De huidige aanpak voor *proteomic* studies moet geharmoniseerd worden
- [^{14}C]microtracer en MIST studies bij kinderen zijn een interessante mogelijkheid om effectiviteit en veiligheid in de geneesmiddelontwikkeling en huidige farmacotherapie voor kinderen te verbeteren
- De intrinsieke CYP3A-gemedieerde klaring van midazolam in de darmen en lever moet bestudeerd worden met behulp van de data gegeneerd in dit proefschrift
- Het moet bestudeerd worden of de in dit proefschrift gepresenteerde midazolam-data geëxtrapoleerd kan worden naar andere CYP3A-substraten

Deze aanbevelingen worden aangevuld met de volgende meer algemene aanbevelingen voor toekomstige studies/benaderingen, en voor hoe onze huidige kennis gebruikt kan worden in de klinische praktijk:

- Internationale biobanken, samenwerkingsverbanden, platforms voor het delen van data, en netwerken/infrastructuren voor klinische onderzoek bij kinderen kunnen geneesmiddelonderzoek bij kinderen helpen versnellen
- Studies met exosomen, organoïden, endogene substraten en *metabolomics* kunnen een belangrijke bijdrage leveren aan het valideren van transporter ontogenie
- *Physiologically based PK* (PBPK) modelleren helpt ons om geneesmiddelmetabolisme en -transport te begrijpen, evenals de impact van een verandering in deze processen
- Totdat de hiaten in de kennis over ontogenie zijn weggenomen, moet men voorzichtig zijn met routinegebruik van PBPK modelleren om geneesmiddelblootstelling in kinderen te voorspellen
- Populatie PK en PBPK modellen kunnen in de klinische praktijk sneller worden geïntegreerd door het ontwikkelen van elektronische systemen die complexe doseringsschema's kunnen integreren. Deze systemen kunnen dan parallel aan het elektronisch patiëntendossier gebruikt worden.

PART V

Appendices

LIST OF ABBREVIATIONS

^{14}C	Carbon 14
AF	Alkaline phosphatase
ALAT	Aspartate-aminotransferase
AMS	Accelerator mass spectrometry
ARSAC	Administration of Radioactive Substances Advisory Committee
ASAT	Alanine-aminotransferase
ATP	ATPase Na+/K+ Transporting
AUC	Area Under the Curve
$AUC_{0\text{-}inf}$	Area Under the Curve from time zero to infinity
$AUC_{0\text{-}t}$	Area Under the Curve from time zero to last observed timepoint
BCRP (ABCG2)	Breast Cancer Resistance Protein
BPCA	Best Pharmaceuticals for Children Act
Bq	Becquerel
BSEP (ABCB11)	Bile Salt Export Pump
Ci	Curie
CL	Clearance
CL/F	Oral clearance
$CL_{Biliary}$	Biliary clearance
CL_R	Renal clearance
C_{max}	Maximum concentration
CO_2	Carbon dioxide
COMT	Catechol-O-Methyltransferase
CRP	C-Reactive Protein
CYP	Cytochrome P450
DDI	Drug-Drug Interaction
DHEA	Dehydroepiandosteron
DME	Drug metabolizing enzyme
DNA	Deoxyribonucleic acid
DT	Drug transporter
ECMO	Extra Corporeal Membrane Oxygenation
EMA	European Medicines Agency
ENT	Equilibrative Nucleoside Transporter
FDA	US Food and Drug Administration
FEUA	Fractional Excretion of Uric Acid
GA	Gestational Age
GAPDH	Glyceraldehyde 3-phosphate dehydrogenase
GFR	Glomerular Filtration Rate

GLUT	Glucose Transporter
GMP	Good Manufacturing Practice
GOF	Goodness Of Fit
GST	Glutathione–S–transferase
HEK	Human embryonic kidney
HNF	Hepatic nuclear factor
HPLC	Ultra-performance liquid chromatography
HRMS	High resolution mass spectrometer
ICH	International Conference on Harmonization
IHC	Immunohistochemistry
IIV	Inter-individual variability
IRB	Independent Review Boards
IV	Intravenous
LC	Liquid Chromatography
LC-MS/MS	Liquid Chromatography with tandem Mass Spectrometry
LLOQ	Lower Limit Of Quantification
MATE (SLC47A)	Multidrug And Toxin Extrusion protein
MCT1	Monocarboxylate transporter 1
MDCK	Madin-Darby Canine Kidney
MDR	Multi-Drug Resistance
MDR1 (P-gp; ABCB1)	Multi-Drug Resistance 1; P-glycoprotein
MeSH	Medical Subject Headings
MIDD	Model informed drug development
MIST	Metabolite In Safety Testing
mRNA	Messenger RNA
MRP (ABCC)	Multidrug Resistance-associated Protein
NAT	N-acetyltransferase
NDA	New Drug Application
NOAEL	No observed adverse effect level
NONMEM	Nonlinear mixed effects modelling
NPDE	Normalized prediction distribution errors
NTCP (SLC10A1)	Na+ -Taurocholate Cotransporting Polypeptide
OAT (SLC22A)	Organic Anion Transporter
OATP (SLCO)	Organic Anion Transporting Polypeptide
OCT (SLC22A)	Organic Cation Transporter
OCTN (SLC22A)	Organic Cation/ergothioneine Transporter
OFV	Objective Function Value
ORF	Open Reading Frame
PAH	P-aminohippurate

PAMPER	Paediatric Accelerator Mass Spectrometry Evaluation Research
PBPK	Physiologically Based Pharmacokinetics
PCR	Polymerase Chain Reaction
PD	Pharmacodynamics
PDUFA	Prescription Drug User Fee Act
PEDMIC	PEDiatric MICrodosing
PELOD	Pediatric Logistic Organ Dysfunction;
PEPT	Peptide Transporter
PICU	Pediatric Intensive Care Unit
PIM	Pediatric Index of Mortality
PK	Pharmacokinetics
PMA	Postmenstrual age
PNA	Postnatal age
PREA	Pediatric Research Equity Act
PRISM	Pediatric Risk of Mortality
PXR	Pregnane X Receptor
qRT-PCR	Quantitative Reverse Transcription Polymerase Chain Reaction
RIN	RNA integrity number
RNA	Ribonucleic acid
RNA-Seq	RNA-Sequencing
RNAse	Ribonuclease
RSE	Relative Standard Error
SCN	Neuronal sodium channel
SD	Standard Deviation
SLC	Solute Carrier
SLCO	Solute Carrier Organic anion
SNP	Single-Nucleotide Polymorphism
SRM	Selective Reaction Monitoring
SULT	Sulfotransferase
Sv	Sievert
t1/2	Elimination half-life
TM	Transmembrane
TM_{50}	The age at which half of adult level is reached
T_{max}	Time at maximum concentration
TPM	Transcripts Per Million
UA	Uric Acid
UGT	Uridine 5'-diphospho-glucuronosyltransferase
UPLC	Ultra-Performance Liquid Chromatography

UPLC-MS/MS	Ultra-Performance Liquid Chromatography tandem Mass Spectrometry
URAT1 (SCL22A12)	Urate Transporter 1
US	United States of America
V	Volume of distribution
V_{SS}/F	Apparent volume of distribution
γ-GT	Gamma-glutamyltransferase

AFFILIATIONS CO-AUTHORS*

*At the time the studies were conducted

Karel Allegaert	Department of Development and Regeneration, KU Leuven, Leuven, Belgium Department of Pharmacy and Pharmaceutical Sciences, KU Leuven, Leuven, Belgium Department of Clinical Pharmacy, Erasmus MC, Rotterdam, The Netherlands
Pieter Annaert	Department of Pharmaceutical and Pharmacological Sciences, Drug Delivery and Disposition, KU Leuven, Leuven, Belgium
Justine Badée	Department of PK Sciences, Novartis Institutes for BioMedical Research, 4002 Basel, Switzerland
Chengpeng Bi	Division of Clinical Pharmacology, Toxicology & Therapeutic Innovation, Department of Pediatrics, Children's Mercy Kansas City, Kansas City, MO, USA
Marjolein D van Borselen	Department of Pharmacology and Toxicology, Radboud Institute of Health Sciences, Radboud University Medical Center, Nijmegen, the Netherlands
Adrianus CJM de Bruijn	Department of Pediatrics, Erasmus MC-Sophia Children's Hospital, Rotterdam, the Netherlands
Gilbert J Burckart	Office of Clinical Pharmacology, Office of Translational Sciences,Center for Drug Evaluation & Research,US Food and Drug Administration,Silver Spring, MD, USA
Kit Wun Kathy Cheung	Department of Bioengineering and Therapeutic Sciences, University of California-San Francisco, San Francisco, CA, USA Office of Clinical Pharmacology, Office of Translational Sciences, Center for Drug Evaluation & Research, U.S. Food and Drug Administration, Silver Spring, MD, USA Oak Ridge Institute for Science and Education (ORISE Fellow), Oak Ridge, TN, USA
Steven Van Cruchten	Department of Veterinary Sciences, Faculty of Pharmaceutical, Biomedical and Veterinary Sciences, University of Antwerp, 2610 Wilrijk, Belgium
Esther van Duijn	TNO, Zeist, the Netherlands
Roger Gaedigk	Division of Clinical Pharmacology, Toxicology & Therapeutic Innovation, Department of Pediatrics, Children's Mercy Kansas City, Kansas City, MO, USA
R Colin Garner	Garner Consulting, York, United Kingdom
Kathleen M Giacomini	Department of Bioengineering and Therapeutic Sciences, University of California-San Francisco, San Francisco, CA, USA
Grzegorz Grynkiewicz	Pharmaceutical Research Institute, Warsaw, Poland
Stan JF Hartman	Department of Pharmacology and Toxicology, Radboud Institute of Health Sciences, Radboud University Medical Center, Nijmegen, the Netherlands
N Harry Hendrikse	Department of Radiology and Nuclear Medicine, Amsterdam UMC, location VUmc, Amsterdam, The Netherlands.
Shiew-Mei Huang	Office of Clinical Pharmacology, Office of Translational Sciences, Center for Drug Evaluation & Research, U.S. Food and Drug Administration, Silver Spring, MD, USA
Catherijne AJ Knibbe	Department of Clinical Pharmacy, St. Antonius Hospital, Nieuwegein, The Netherlands Division of systems biomedicine and pharmacology, Leiden Academic Center for Drug Research, Leiden University, Leiden, The Netherlands
Birgit CP Koch	Department of Clinical Pharmacy, Erasmus MC, Rotterdam, The Netherlands
Barbara AE de Koning	Division of Pediatric Gastroenterology, Erasmus MC-Sophia Children's Hospital, Rotterdam, the Netherlands
Lenne-Triin Kõrgvee	University of Tartu, Tartu, Estonia

Elke HJ Krekels	Division of systems biomedicine and pharmacology, Leiden Academic Center for Drug Research, Leiden University, Leiden, The Netherlands
Anton C Kuik	Division of systems biomedicine and pharmacology, Leiden Academic Center for Drug Research, Leiden University, Leiden, The Netherlands
J Steven Leeder	Division of Clinical Pharmacology, Toxicology & Therapeutic Innovation, Department of Pediatrics, Children's Mercy Kansas City, Kansas City, MO, USA
Marola MH van Lipzig	TNO, Zeist, the Netherlands
Wiola Maruszak	Pharmaceutical Research Institute, Warsaw, Poland
Miriam G Mooij	Department of Pediatrics, Leiden University Medical Centre, Leiden, The Netherlands
Johan Nicolaï	Development Science, UCB BioPharma SRL, B-1420 Braine-l'Alleud, Belgium
B Kevin Park	University of Liverpool, Liverpool, United Kingdom
Els van Peer	Department of Veterinary Sciences, Faculty of Pharmaceutical, Biomedical and Veterinary Sciences, University of Antwerp, 2610 Wilrijk, Belgium
Joost van Rosmalen	Department of Biostatistics, Erasmus MC, Rotterdam, the Netherlands
Janneke N Samsom	Department of Pediatrics, Erasmus MC-Sophia Children's Hospital, Rotterdam, the Netherlands
Luc De Schaepdrijver	Nonclinical Safety, Janssen R&D, B-2340 Beerse, Belgium
Ron HN van Schaik	Department of Clinical Chemistry, Erasmus MC, University Medical Center, Rotterdam, the Netherlands
Stephan Schmidt	Department of Pharmaceutics, Center for Pharmacometrics and Systems Pharmacology, College of Pharmacy, University of Florida, Orlando, FL, USA
Ytje Simons-Oosterhuis	Department of Pediatrics, Erasmus MC-Sophia Children's Hospital, Rotterdam, the Netherlands
Bart Smeets	Department of Pathology, Radboudumc, Nijmegen, the Netherlands
Anne Smits	Department of Development and Regeneration KU Leuven, Leuven, Belgium; Neonatal intensive care unit, University Hospitals Leuven, Leuven, Belgium
Edwin Spaans	CDTS consulting BV & SDD consulting BV, Etten-Leur, the Netherlands
Vincent S Staggs	Health Services and Outcomes Research, Children's Mercy Kansas City, School of Medicine, University of Missouri-Kansas, Kansas City, MO, USA
Evita van de Steeg	TNO, Zeist, the Netherlands
Dick Tibboel	Intensive Care and Department of Pediatric Surgery, Erasmus MC-Sophia Children's Hospital, Rotterdam, the Netherlands
Mark A Turner	University of Liverpool, Liverpool, United Kingdom
Wouter HJ Vaes	TNO, Zeist, the Netherlands
Robert M Verdijk	Department of Pathology, Erasmus MC, Rotterdam, the Netherlands
Arjan de Vries	TNO, Zeist, the Netherlands
Saskia N de Wildt	Department of Pharmacology and Toxicology, Radboud Institute of Health Sciences, Radboud University Medical Center, Nijmegen, the Netherlands Intensive Care and Department of Pediatric Surgery, Erasmus MC-Sophia Children's Hospital, Rotterdam, the Netherlands
Albert D Windhorst	Department of Radiology and Nuclear Medicine, Amsterdam UMC, location VUmc, Amsterdam, The Netherlands.
Heleen M Wortelboer	TNO, Zeist, the Netherlands
Lei Zhang	Office of Research and Standards, Office of Generic Drugs, Center for Drug Evaluation & Research, U.S. Food and Drug Administration, Silver Spring, MD, USA

LIST OF PUBLICATIONS

This thesis

van Groen BD, Nicolaï J, van Peer E, Kuik A, Smits A, Schmidt S, de Wildt SN, Allegaert K, van Cruchten S, de Schaepdrijver L, Annaert P, Badée J
Ontogeny of hepatic drug metabolizing enzymes and transporters in human and nonclinical species: a quantitative review
[Submitted]

van Groen BD, van Duijn E, de Vries A, Mooij MG, Tibboel D, Vaes WHJ, de Wildt SN.
Proof of concept: first pediatric metabolite in safety testing (MIST) study using an oral [^{14}C]midazolam microtracer
[Submitted]

van Groen BD, Krekels EHJ, Mooij MG, van Duijn E, Vaes WHJ, Windhorst AD, van Rosmalen J, Hartman SJF, Hendrikse NH, Koch BCP, Allegaert K, Tibboel D, Knibbe CAJ, de Wildt SN.
The oral bioavailability and metabolism of midazolam in stable critically ill children: a pharmacokinetic microtracing study.
[Submitted]

van Groen BD, Bi C, Gaedigk R, Staggs VS, Tibboel D, de Wildt SN, Leeder JS.
Alternative splicing of the SLCO1B1 gene: an exploratory analysis of isoform diversity in pediatric liver
Clin Transl Sci. 2020 Jan 9. doi: 10.1111/cts.12733.

van Groen BD*, Cheung KWK*, Spaans E, van Borselen MD, de Bruijn ACJM, Simons-Oosterhuis Y, Tibboel D, Samsom JN, Verdijk RM, Smeets B, Zhang L, Huang SM, Giacomini KM, de Wildt SN. *Contributed equally
A Comprehensive Analysis of Ontogeny of Renal Drug Transporters: mRNA Analyses, Quantitative Proteomics, and Localization.
Clin Pharmacol Ther. 2019 Nov;106(5):1083-1092. doi: 10.1002/cpt.1516.

van Groen BD, Vaes WH, Park BK, Krekels EHJ, van Duijn E, Kõrgvee LT, Maruszak W, Grynkiewicz G, Garner RC, Knibbe CAJ, Tibboel D, de Wildt SN, Turner MA.
Dose-linearity of the pharmacokinetics of an intravenous [^{14}C]midazolam microdose in children.
Br J Clin Pharmacol. 2019 Oct;85(10):2332-2340. doi: 10.1111/bcp.14047.

Cheung KWK, **van Groen BD**, Burckart GJ, Zhang L, de Wildt SN, Huang SM.
Incorporating Ontogeny in Physiologically Based Pharmacokinetic Modeling to Improve Pediatric Drug Development: What We Know About Developmental Changes in Membrane Transporters.
J Clin Pharmacol. 2019 Sep;59 Suppl 1:S56-S69. doi: 10.1002/jcph.1489.

van Groen BD, van de Steeg E, Mooij MG, van Lipzig MMH, de Koning BAE, Verdijk RM, Wortelboer HM, Gaedigk R, Bi C, Leeder JS, van Schaik RHN, van Rosmalen J, Tibboel D, Vaes WH, de Wildt SN.
Proteomics of human liver membrane transporters: a focus on fetuses and newborn infants.
Eur J Pharm Sci. 2018 Nov 1;124:217-227. doi: 10.1016/j.ejps.2018.08.042.

Other manuscripts

van Groen BD, Pilla Reddy V, Badee J, Olivares-Morales A, Johnson T, Nicolai J, Annaert P, de Wildt SN, Knibbe CAJ, de Zwart L.
Pediatric pharmacokinetics and dose predictions: a report of a satellite meeting to the 10th Juvenile Toxicity Symposium
[Submitted]

Bestebreurtje P, Koning BAE, Knibbe CAJ, Tibboel D, van Sorge AA, **van Groen BD**, van de Ven CO, Plötz FB, de Wildt SN.
Randomized controlled trial on rectal versus oral omeprazole treatment of gastroesophageal reflux disease in infants with congenital birth defects.
[Submitted]

Smits TA, Gresnigt FMJ, **van Groen BD**, Franssen EJF, Attema-de Jonge ME
A prospective investigation of the performance of two gamma-hydroxybutyric acid (GHB) tests: DrugCheck GHB Single Test and Viva-EGHB immunoassay.
Ther Drug Monit. 2019 Jul 15. doi: 10.1097/FTD.0000000000000677.

Mooij MG, van de Steeg E, van Rosmalen J, Windster JD, de Koning BA, Vaes WH, **van Groen BD**, Tibboel D, Wortelboer HM, de Wildt SN.
Proteomic Analysis of the Developmental Trajectory of Human Hepatic Membrane Transporter Proteins in the First Three Months of Life.
Drug Metab Dispos. 2016 Jul;44(7):1005-13. doi: 10.1124/dmd.115.068577.

Mooij MG, de Koning BE, Lindenbergh-Kortleve DJ, Simons-Oosterhuis Y, **van Groen BD**, Tibboel D, Samsom JN, de Wildt SN.
Human Intestinal PEPT1 Transporter Expression and Localization in Preterm and Term Infants.
Drug Metab Dispos. 2016 Jul;44(7):1014-9. doi: 10.1124/dmd.115.068809.

van Groen BD, Gombert-Handoko KB.
Vergelijking van botuline-A-toxine-preparaten voor off-label-indicaties.
PW Wetenschappelijk Platform. 2015;9:a1546. [Dutch]

Societal impact

Gene versus protein expression in children.
Medicines 2018 Aug; 9: 49.

van Groen BD.
International Profile.
Clin Pharmacol Ther 2017 Dec; 102:891.

Interview **van Groen BD**.
'Safe drug dosing in children'.
Monitor 2017 Jun; 46: 20-22. [Dutch]

PHD PORTFOLIO

Name PhD student	Bianca D. van Groen
Erasmus MC Department	Intensive Care and Department of Pediatric Surgery
PhD period	Feb 2016 – Jan 2020
Promotors	Prof. Dr. D. Tibboel
	Prof. Dr. S.N. de Wildt
	Prof. Dr. K. Allegaert

	Year	ECTS
Cursus		
Scientific integrity	2016	0.3
NIHES - Biostatistical methods 1: basic principles CCO2	2016	5.7
Biomedical English writing and communication	2016-2017	3.0
Basic Course Rules & Organization Clinical Researchers (BROK)	2016	1.0
Stralingsbescherming deskundigheidsniveau 5B	2016	0.6
Erasmus MC trial IT - introduction to open clinica	2016	0.1
Systematic literature search and Endnote	2016	0.6
Teach the teacher course (NVKFB)	2016	0.5
NIH principles of pediatric pharmacology lectures	2016-2017	2.0
Training laboratory technique DNA	2016	1.0
Lareb introduction day and adverse events day	2016	0.3
College ter Beoordeling van Geneesmiddelen (CBG) dag	2016	0.3
Molmed - Research management for PhD students	2017	1.0
Paul Janssen Future Lab - Clinical Development online	2017	1.0
NONMEM course for beginners, Cologne	2017	0.9
Symposia/national conferences		
Pump your career NWO	2015	0.3
NVT sections pharmaceutical and reproduction toxicology	2016	0.3
Sophia Research day	2016	0.3
Erasmus MC klinische farmacologie dag	2016	0.3
NVKFB mededelingendag	2016	0.3
Sophia Research Day - *oral*	2017	1.0
NVKFB mededelingendag - *2x poster*	2017	2.0
Figon Dutch Medicines Days - *oral*	2017	1.0
Leiden&Rotterdam research day - *oral*	2017	1.0
NNPM symposium: *oral* **(best oral presentation award)**	2018	1.0
Figon Dutch Medicines Days - *poster*	2018	1.0
RIMLS Kidney Theme lunchmeeting Radboudumc - *oral*	2018	1.0
Farewell symposium D Tibboel	2018	0.3
Sophia Research Day - *oral* **(best oral presentation award)**	2019	1.0

NVKFB mededelingendag – *poster*	2019	1.0
Erasmus MC ACE – Pharmacology & Therapeutics symposium	2019	0.3

International conferences		
Preconference International Transporter Consortium - *poster*	2017	1.0
ASCPT Annual Meeting Washington - *2x poster, 2x oral* **(presidential trainee award)**	2017	4.0
ESDPPP Leuven - *2x oral*	2017	2.0
Training Course: Medicines in children – what you need to know? Leuven	2017	0.3
UNGAP meeting Leuven - *poster*	2018	1.0
ASCPT Annual Meeting Orlando - *poster*	2018	1.0
IATDCMT congress Brisbane- *poster*	2018	1.0
ASCPT Annual Meeting Washington - *poster*	2019	1.0
Pediatric PK and dose predictions Janssen Beerse - *2x invited speaker*	2019	2.0
ESDPPP Basel – *oral*	2019	1.0
Local research meetings		
Pediatric Clinical Pharmacology meetings (weekly)	2016-2020	1.0
Clinical Pharmacology meetings (weekly)	2016-2020	1.0
Teaching		
Presenter webinar 'Ontogeny of human hepatic transporters' ASCPT	2016	1.0
Presenter webinar 'How to learn more about the ontogeny of transporters' – Simcyp transporter working group	2019	1.0
Supervising master's thesis A. Kuik – Leiden University	2019	
Professional societies		
Board member Sophia Researchers Representation	2017-2018	1.0
Board member Special Populations Community - ASCPT	2018-2020	1.0
Reviewer scientific proposals ASCPT Annual Meeting 2019&2020	2018-2019	0.3
Organizing committee symposium ACE – Pharmacology & Therapeutics	2019	1.0
Other		
Fellowship Clinical Pharmacology	2016-2019	
TULIPS PhD curriculum	2018-2020	1.1

ABOUT THE AUTHOR

Bianca D. van Groen was born on September 8th 1990 in Barendrecht, the Netherlands. In 2008 she received her Gymnasium degree. That same year, she started studying Pharmacy at the Utrecht University. As part of her master's program, she performed research for six months at Imperial College London, United Kingdom, to investigate the effect of novel epigenetic inhibitors on inflammatory responses in Chronic obstructive pulmonary disease (COPD). In 2015 she received her master's degree in Pharmacy (PharmD).

After working as a pharmacist at the hospital pharmacy of the OLVG hospital for six months, Bianca started her PhD program in February 2016 at the Intensive Care and Pediatric Surgery of the Erasmus MC – Sophia Children's Hospital in Rotterdam, the Netherlands, under supervision of Prof. dr. D. Tibboel, Prof. Dr. S.N. de Wildt and Prof. Dr. K. Allegaert. In the third year of her PhD research Bianca was awarded with the Ter Meulen grant by the Royal Netherlands Academy of Arts & Sciences, which enabled her to conduct a research project at the Children's Mercy Hospital in Kansas City, USA, under supervision of Prof. dr. J.S. Leeder.

Alongside her PhD she started her training in clinical pharmacology, and became a board certified clinical pharmacologist of the Dutch Society for Clinical Pharmacology & Biopharmacy in February 2019. Also, she was selected for the Training Upcoming Leaders in Pediatric Science (TULIPS) PhD curriculum. Lastly, she has been actively involved in the American Society for Clinical Pharmacology & Therapeutics (ASCPT) as chair of the Special Populations Community.

After her PhD project, Bianca has been given the opportunity to continue her career as a scientist at Roche in Basel, Switzerland.

DANKWOORD

De afgelopen jaren heb ik met veel plezier aan dit proefschrift gewerkt. De samenwerking met velen heb ik als zeer waardevol ervaren; zonder deze samenwerkingen had dit proefschrift niet tot stand kunnen komen. Naast dat ik het grootste gedeelte van mijn tijd als PhD-student in het Erasmus MC-Sophia (Rotterdam) ben geweest, heb ik de kans gehad om een aantal maanden door te brengen in het Children's Mercy Hospital (Kansas City, MO, USA), LACDR (Leiden) en Radboudumc (Nijmegen). Ofwel; een hele hoop mensen hebben bijgedragen aan dit proefschrift of aan mijn tijd als promovenda. En die wil ik graag allemaal bedanken!

Allereerst heel veel dank aan de patiënten en ouders die aan de PedMic studie hebben meegedaan, ondanks de onzekere tijden tijdens opname op de Intensive Care Kinderen (ICK). Het vertrouwen en de bereidheid om belangeloos bij te dragen aan verbetering van geneesmiddeltherapie bij kinderen is bewonderenswaardig. Ook alle medewerkers van de ICK wil ik bedanken voor hun inzet bij het uitvoeren van de PedMic studie.

Beste prof.dr. Tibboel, beste Dick, dank voor uw waardevolle begeleiding de afgelopen jaren. Uw bijzondere gave om het hoofddoel van een project of een paper niet uit het oog te verliezen, heeft een hoop pagina's tekst voor dit proefschrift bespaard. Uw gedrevenheid voor onderzoek heb ik erg gewaardeerd. Ik hoop dan ook dat u nog mooi onderzoek kunt blijven doen; zowel in de kindergeneeskunde als wellicht nog een zijstap richting de geschiedenis van geneeskunde of zelfs in de kunst.

Lieve prof.dr. de Wildt, lieve Saskia, wat mag ik in mijn handjes knijpen met een begeleider zoals jij. Je hebt met ongelooflijk veel geleerd op gebied van het doen van onderzoek, klinische farmacologie, kindergeneeskunde en CV building. Het was even schrikken dat je vrij snel na mijn start naar het Nijmeegse vertrok, maar dit heeft goed uitgepakt door jouw onuitputtelijke energie en het feit dat je àltijd bereikbaar bent geweest. Naast onze inhoudelijke discussies, heb ik genoten van onze uitstapjes in Washington (sightseeën, tripje naar Baltimore en basketbal), Orlando (zwemmen en shoppen), Amsterdam (VIVA!) en Nijmegen (BOMmen en wijn). Ooit hoop ik een net zo mooie garderobe als jij te mogen bezitten. En je moet me toch echt nog eens uitleggen hoe die Harry Potter koffer van je werkt;)

Beste prof.dr. Allegaert, beste Karel, ik kan mij blijven verbazen over je enorme parate kennis die je met een snufje Vlaamse humor op een onvergetelijke wijze weet over te brengen. Ook de snelheid waarmee je stukken voorziet van kritisch commentaar is indrukwekkend. Wat ik erg gewaardeerd heb, is dat je deur heeft altijd open gestaan

voor overleg ondanks je overvolle agenda; of het nou ging over mijn promotietraject, opleiding tot klinisch farmacoloog of mijn toekomstige carrière. Het ga je goed in Leuven!

De leden van de kleine promotiecommissie, prof.dr. van Schaik, prof.dr. Leeder, en prof. dr. Knibbe, wil ik hartelijk danken voor het beoordelen van mijn proefschrift. Dr. Koch en dr. Vaes wil ik hartelijk danken voor het plaats nemen in de grote commissie.

Alle co-auteurs wil ik bedanken voor de prettige samenwerking de afgelopen jaren. In het bijzonder onze samenwerkingspartners van TNO; dr. Wouter Vaes, dr. Esther van Duijn en dr. Evita van de Steeg. Maar liefst de helft van de manuscripten in dit proefschrift zijn door deze samenwerking tot stand gekomen. Het gaf mij altijd veel energie om langs te komen in Zeist of met elkaar te brainstormen op congressen over hoe we de pediatrische microdosing kunnen integreren in de huidige praktijk. Hopelijk hebben we nu genoeg bewijs geleverd dat het veilig en zinvol is om pediatrische microdosing/MIST studies te doen! Our colleagues at UCSF; prof.dr. Giacomini, thank you so much for giving me the opportunity to collaborate with you and Kathy. Your drive to work together rather than to compete is very inspiring. Dear Kathy, you have been my partner in crime for exploring career options. I am so happy that we are (sort of) direct colleagues now that you work at Genentech and I work at Roche. Please promise me to stay loyal to your *Sunday funday*! The HESI consortium; we never thought that this manuscript would end up to be such an enormous project. Thank you all for the perseverance to make this journey a success.

For three months I was given the opportunity to spend time at Childrens' Mercy Hospital under the supervision of prof.dr. J. Steven Leeder and dr. Charlie Bi. Dear Steve, already in my first year as a PhD-student I met you and Donna in Amsterdam over brunch. Who would have thought that I ended up in Kansas City for a couple months! I cannot put in words what an incredible mentor you are. You have taught me to take the time to think about and interpret data, and to see opportunities in literally everything without losing the clinical relevance out of sight. Once again thank you for travelling all the way to the Netherlands to be part of my PhD-committee. Charlie, our collaboration was the perfect example of two people with an entirely different background being complimentary to make a project work. Thank you for supervising me and teaching me all the bio-informatic knowledge. Dear Jean and Chelsea, you have made me feel like home in Kansas City. Thank you for taking me out to lunch, inviting me over for wine+knitting and have Friday night drinks. Tina, brunch and yoga! Do I need to say more?! Let's make brunches at conferences a tradition, please! Matt, you have the special gift to make people laugh. Maybe that is why your surname is McLaughlin?! Jen, thank

you for picking me up to go to the hospital and introducing me to your neighborhood. Also, thanks for warning to not go to *Save a Lot* after 8pm, which has probably saved me a lot, e.g. my life;)

Heb je het over *modelling and simulation* van pediatrische PK data dan kun je niet anders dan aan de onderzoeksgroep van prof.dr. Catherijne Knibbe denken! Grote dank aan de gehele groep voor de hulp en gezelligheid tijdens mijn uitwisseling. Beste Catherijne, ik ben erg dankbaar dat ik heb mogen leren modelleren in jouw groep. Bedankt voor je begeleiding van en het brainstormen over de microdosing data. Het is bewonderenswaardig hoe jij de tijd neemt elk project tot een goed einde te brengen, ondanks je drukke agenda als professor en ziekenhuisapotheker. Lieve Elke, van jou heb ik het echte modelleren geleerd op technisch vlak maar nog meer over hoe de data geïnterpreteerd kan worden. Zat ik al een week te ploeteren op een fout in het model, wist jij het in één oogopslag op te lossen. Je betrokkenheid op zowel inhoudelijk als persoonlijk vlak zullen mij altijd bij blijven. Jantine, midazolam en kids; daar weet jij meer dan genoeg vanaf! Dank voor je hulp vanuit Zwitserland. Dear Danica, we started around the same time with our 'modelling-career' and shared the fun but also the frustration on learning to work with the complex software. Thank you so much for all the good talks, you have made my Leiden-time unforgettable! Sinzi, thank you for teaching me how to perform dose simulations. I am sure we will run into each other in the drug development world.

Lieve Joke, al meerdere keren heb ik verzucht wat ik toch zonder jou had gemoeten afgelopen jaren. Je hebt me het reilen en zeilen van klinisch onderzoek laten zien, stond altijd klaar met een kop koffie en een luisterend oor, en hebt me laten gieren van het lachen door je gevatte opmerkingen. Hopelijk houden we contact en kom je een keer met Hans langs in Basel. Je bent een topper! Ko, bedankt dat je mijn manuscripten hebt voorzien van mooie vloeiende Engelse zinnen. Marjolein, ook al was ik betrokken van een afstand, jij bent mijn eerste student geweest die ik heb mogen begeleiden. Leuk dat we elkaar hebben gezien in San Francisco én Basel. Anton, fantastisch hoe jij je kan verliezen in data en programma's maar een overzichtelijk eindproduct weet te creëren. Blijf vooral je creatieve brein gebruiken!

Mijn medepromovendi uit Erasmus MC hebben de afgelopen 4 jaar onvergetelijk gemaakt. Lieve Annelieke, we begonnen als de twee dwarrels in het feutenhoekje. Ondertussen ben jij getrouwd én gepromoveerd en zijn we toch echt volwassen! Lieve Tanja, àltijd bereid om te helpen, koffie te drinken of te borrelen. Brisbane was fantastisch! Lieve Shelley, het laatste half jaar hebben we veel frustraties gedeeld. Er komt echt een einde aan en dan kan je weer lekker fulltime de kliniek in. Manuel, wat

een eer dat ik je paranimf heb mogen zijn. Jammer dat onze Nijmegen-tijd net langs elkaar liep maar hopelijk heb je je plekje daar gevonden. Frank en Willem, bedankt voor alle gezellige borrels. Ben erg benieuwd waar jullie over een aantal jaar terecht gaan komen! Norani, altijd in voor gezelligheid, succes met je 1000 projecten! Chantal, wat een harde werker ben je toch met het combineren van onderzoek en kliniek. Renate, eindelijk komt je terug op de kamer en nu ben ik weg!:(Miriam, bedankt dat je je projecten vol vertrouwen aan me over hebt gedragen. Wie weet kunnen we nog eens een microdosing-trial opzetten! Raisa, Esther, Marlous, Lisette, Kitty, Dorian; bedankt voor alle tips over 'hoe overleef ik het promoveren'. Denise, Stephanie, Joppe, Sophie, Sophie, Arnout, Karlien, Lorenzo en Anne-Fleur; bedankt voor de gezelligheid de laatste maanden op de kamer. De ICK-poule met o.a. Özge, Gerdien en Nienke; bedankt voor het waarnemen van de PedMic.

Tijdens mijn PhD-tijd heb ik de tijd gekregen om een aantal extra-curriculaire activiteiten te doen. Allereerst de opleiding tot klinisch farmacoloog. Veel dank aan mijn opleiders dr. Birgit Koch en prof.dr. Karel Allegaert om deze tijd tot een succes te maken. Birgit, ik heb zelden iemand ontmoet die zo efficiënt is als jij. Bedankt voor je betrokkenheid en gezelligheid, met de basketbalwedstrijd in Washington als kers op de taart. Prof.dr. Teun van Gelder, je energie en creativiteit zijn aanstekelijk en wat hebben we een lol gehad in Brisbane. Brenda, hoe druk je ook was, je had altijd tijd om te overleggen of even bij te praten. Jorie, je passie voor klinische farmacologie is overduidelijk! Sinno en Robert, wat een drive hebben jullie voor onderzoek! Jullie zijn ontzettend goede mentors. Bedankt voor alle inspirerende en motiverende gesprekken over o.a. carrièrekeuzes. Mijn mede-klinisch farmacologen i.o.: Rixt, zo leuk om Brisbane met je te ontdekken; Sanne, jij als arts in de apotheek en ik als apotheker in de kliniek! Je wordt ongetwijfeld een fantastische kinderpsychiater; Laura en Fleur, het was leuk om op de valreep nog een ACE pharmacology & therapeutics symposium met jullie te organiseren; Paola, hopelijk heb je het naar je zin als AIOS ziekenhuisfarmacie in het oosten!; Florine, wat een hilarisch dominator-avontuur hebben we meegemaakt. Ook heb ik deel mogen nemen aan het PhD-curriculum van TULIPS. Dank aan de 'ronde gaten' voor het delen van ervaringen rondom het promotie-traject, de nuttige bijeenkomsten maar bovenal de gezellige borrels/weekenden/etentjes. I also would like to thank Paulien, Pooja and Violette for the great years as part of the leadership of the ASCPT – Special Populations Community.

Bedankt aan iedereen van de Farmacologie en Toxicologie afdeling van het Radboudumc voor het opnemen van mij als outsider in jullie groep. In het bijzonder wil ik Prof.dr. Frans Russel bedanken voor de mogelijkheid om een aantal maanden onderdeel te zijn van uw afdeling. Stan, super dat je de PedMic studie uitgevoerd hebt in het Radboudumc.

Geniet ervan dat je onlangs papa bent geworden van Noortje! Jelle, veel plezier met je avontuur in Engeland. Laurens, Jolien en Gaby; hou vol, het einde komt ook voor jullie in zicht. Rick, dank voor de gesprekken in de wandelgangen. Margret, het is een hele klus om Saskia haar agenda onder controle te houden, maar bedankt dat je altijd een gaatje wist te vinden om afspraken met haar in te plannen.

Naast fijne collega's wil ik ook mijn vrienden en familie enorm bedanken voor de ontspanning die ik soms hard nodig heb gehad! Lieve Nienke, vriendinnetjes voor altijd! Lieve Annemarie, wat heerlijk om een tijdje bij je om de hoek in Den Haag te wonen en veel quality time te hebben. Lieve Spamily, lieve Marieke, Corné, Anne, Paulien, Tielke, Maartje, Eline/Poot, Isabelle, Yvette en Simone, ik hoop dat we nog velen avonturen met elkaar gaan beleven. Lieve lichting 26, lieve Sophie, Laura, Veerle, Leonie en Nienke, ook al zijn we verspreid over de hele wereld, hoop ik dat we voor altijd mosselen blijven eten, Herman in eer blijven behouden en mooie ervaringen blijven delen. Lieve Mirjam, onze (korte) tijd als huisgenootjes was heel bijzonder! Cathelijne, hopelijk binnenkort allebei in Zwitserland! Renske en de knorrenboefjes; allemaal apotheker maar allemaal ons eigen carrière pad. Laten we veel blijven borrelen!

Lieve Noor en Nori, ik ben zo blij dat jullie aan mijn zijde zullen staan als paranimfen! Noor, ruim 10 jaar geleden is onze vriendschap ontstaan in Utrecht. In de tussentijd hebben wij beiden veel tijd in het buitenland doorgebracht, wat onze vriendschap alleen maar hechter heeft gemaakt. Ook al zijn we totaal verschillend; we begrijpen elkaar en kunnen daardoor uren praten over alles wat in de wereld en in ons eigen leven afspeelt. Voor jou het liefst tijdens een veel te lang durende hardloopsessie, yoga om 7u 's ochtends of in de keuken waar we letterlijk àlles zelf maken;) Lieverd, ik hoop dat we samen nog heel veel kattenkwaad gaan uithalen! Nori, ook al kennen we elkaar nog niet zolang, je hebt een belangrijk plekje in mijn hart veroverd. Onze lunchwandelingen, pottenbakken, hardlopen (want atletisch lichaam!) heeft er in no-time voor gezorgd dat we elkaar niet laten uitpraten en alles aan elkaar kwijt kunnen. Hopelijk kom je ècht op den duur in Zwitserland wonen zodat we samen de bergen kunnen ontdekken!

Lieve pap en mam, ik weet niet waar ik moet beginnen met jullie bedanken. Jullie zijn er altijd voor mij, zijn altijd geïnteresseerd en hebben altijd in mijn kunnen geloofd. Dat waardeer ik enorm! Het was heerlijk om zo nu en dan tot rust te komen bij jullie; samen sporten, met Mila wandelen, en tranen met tuiten lachen onder het genot van een wijntje/biertje. Lieve zusjes, wat ben ik trots op jullie! Eline, jij zit heerlijk op je plek in Frankrijk en jouw onvoorwaardelijke loyaliteit aan o.a. de brandweer is ontzettend bijzonder. Hopelijk kun je binnenkort settelen boven op de berg! Anne-lyke, jij staat altijd klaar om te helpen. Jongste zusje maar als eerste een huis gekocht, wat jullie

prachtig hebben opgeknapt. Geniet van de ruimte om je heen! Lieve Tony en Monika, bedankt voor alle weekenden die we bij jullie hebben doorgebracht. Ik kan me geen fijnere schoonfamilie wensen!

Lieve Rikkert, mijn rots in de branding. Wat zal jij blij zijn als er PhD achter mijn naam staat en dit traject eindelijk is afgerond! Met jouw positieve en optimistische kijk heb jij me afgelopen jaren met beiden benen op de grond gehouden. Ik weet dat dit niet altijd makkelijk was, maar hier ben ik je wel eeuwig dankbaar voor! We hebben al zoveel avonturen beleefd en kan niet wachten om deze lijst verder aan te vullen. Te beginnen met ons avontuur in Zwitserland. Ben zo benieuwd wat de toekomst voor ons in petto heeft!

Bianca